Potentials of CD36 in sensing apoptotic cells and modulating hemin mediated immune response from macrophages

A thesis submitted in partial fulfilment of the requirement for the degree of

Doctor of Philosophy

by

Sooram Banesh

156106009

Dept. of Biosciences and Bioengineering,
Indian Institute of Technology-Guwahati,
Guwahati, Assam, 781039
India

TH-2507_156106009

Dedicated to my parents, thesis advisors and friends

Sooram Banesh

TH-2507_156106009

Indian Institute of Technology Guwahati.
Department of Biosciences and Bioengineering.

Statement

I hereby declare that the matter embodied in this thesis entitled "**Potentials of CD36 in sensing apoptotic cells and modulating hemin mediated immune response from macrophages**" is a cumulative account of investigations carried out in the Department of Biosciences and Bioengineering, Indian Institute of Technology, Guwahati, India, under the joint supervision of **Prof. Vishal Trivedi** and **Prof. Vibin Ramakrishnan**.

In keeping with the general practice of reporting scientific observations, due acknowledgements have been made wherever the work of other investigators are referred.

Dec, 2020

(**Sooram Banesh**)
Roll No. 156106009

Indian Institute of Technology Guwahati.
Department of Biosciences and Bioengineering.

Certificate

This is to certify that the work incorporated in this thesis entitled "**Potentials of CD36 in sensing apoptotic cells and modulating hemin mediated immune response from macrophages**", by **Mr. Sooram Banesh** (Roll no. 156106009), submitted to Indian Institute of Technology, Guwahati, India, for the award of the degree of Doctor of Philosophy, is an authentic record of results obtained from the research work carried out under our joint supervision at the Department of Biosciences and Bioengineering, Indian Institute of Technology, Guwahati, Assam, India. We further certify that this work has not been submitted to any other University or Institution in part or full for the award of any degree or diploma. Research material obtained from other sources has been duly acknowledged in the thesis. Any text, illustration, table etc., used in the thesis from other sources, have been duly cited and acknowledged.

Prof. Vishal Trivedi
(Supervisor)

Prof. Vibin Ramakrishnan
(Co-Supervisor)

Acknowledgements

Before finishing my journey as a Ph.D student at this institute it's my pleasure to mention and thanks the people who backed me throughout my research work, supported me at every stage.

Firstly, I would like to express my sincere gratitude to my advisors Prof. Vishal Trivedi and Prof. Vibin Ramakrishnan for their continuous support, patience, motivation, and immense knowledge during my Ph.D research work. They helped me a lot professionally as well as personally.

I would also like to thank to rest of the doctoral committee members: Prof. Rakhi Chaturvedi, Dr. Sachin Kumar and Dr. Debasis Manna for their advice and encouragement.

I would also like to thank my past and present lab members Dr. Suman Jyoti Deka, Dr. S.N.Balaji, Mr. Ankur Mishra, Mr. Anil Kumar D, Mr. Alok Kumar Pandey, Mr. Rafi Uzzama Khan, Mr. Siddharth Neog, Mr. Rajendra Prasad, Mr. Rakesh Kumar Singh, Mr. Umesh, Ms. Shikha Jha, and Ms. Vimee Raturi.

I would also like to thank friends from other labs Dr. Vikky Rajulapati, Dr. Sudhir, Ms. Sunanda Chettry, Dr. Gaurav Jerath and Dr. Ruchika Goyal.

I would also like to thank Prof. Uttam Chand Banerjee, my M.Tech supervisor who encouraged me to join here at IIT. I would also like to thank Dr. Bharat Prasad Dwivedee, Dr. Neeraj Singh Thakur, Dr. Mahesh D Patil, Dr. Gopal Patel, Dr. Kiran Bilare, Dr. Suyog Madhav Amrutkar, Dr. Saptarshi Ghosh, Dr. Seema Kirar, Dr. Surbi Soni, Dr. Umesh Bihade for their encouragement during my early days of PhD. I would also like to thank Mr. Mohd Hameed, Mr. Pastam naresh, Mr. Naresh Nayak, Mr. Darla Bala kishor, Mr. M. Ravi for their support and encouragement during my ups and downs.

I would extend my thanks to Dept. of Biosciences and Bioengineering, Central instrumentation facility for providing analytical instruments for my research work.

I would like to thank Indian institute of Technology for providing the financial assistance.

I thank my parents for their support throughout time and believing in me.

Finally, I am ever grateful to God, the creator and guardian and to whom I owe my very existence.

(**Sooram Banesh**)

TH-2507_156106009

Table of contents

TH-2507_156106009

TH-2507_156106009

List of Figures

TH-2507_156106009

List of Tables

TH-2507_156106009

Abbreviations

AGE	Advanced glycation end products
BSA	Bovine serum albumin
CD36	Clusters of differentiation 36
DAB	3, 3'-Diaminobenzidine
DMEM	Dulbecco's modified eagles medium
FITC	Fluorescein isothiocyanate
GA	Gallic acid
GM-CSF	Granulocyte macrophage Colony stimulating factor
HEPES	(4-(2-hydroxyethyl)-1-piperazine ethanesulfonic acid
ICAM1	Intercellular cell adhesion molecule 1
IFN-γ	Interferon gamma
IPTG	Isopropyl β- d-1-thiogalactopyranoside
LCFAs	Long chain fatty acids
LPS	Lipopolysaccharide
Lyn	Lck/Yes novel tyrosine kinase
MAPK	Mitogen activated protein kinase
MCP-1	Monocyte chemoattractant 1
MDM	Monocyte derived macrophages
PCR	Polymerase chain reaction
PDB	Protein databank
PfEMP-1	Plasmodium falciparum erythrocyte membrane protein 1
PPAR-γ	Peroxisome proliferator-activated receptor gamma
IRBC	Infected RBC
PA	Phosphatidic acid
PC	Phosphatidylcholine
PE	Phosphatidylethanolamine
PG	Phosphatidylglycerol
PS	Phosphatidylserine
PVDF	Polyvinylidene difluoride
RANTES	Regulated on Activation, Normal T Cell Expressed and Secreted
ROS	Reactive oxygen species
SiRNA	Small interfering RNA
STAT	Signal transducer and activator of transcription
TLR	Toll like receptor
TNF-α	Tumour necrosis factor alpha
SDS	Sodium dodecyl sulphate
NAFLD	Non-alcoholic fatty liver disease
NF-κB	Nuclear factor kappa-light-chain-enhancer of activated B cells
NLRP3	NLR family pyrin domain containing 3
oxiLDL	Oxidized low density lipoprotein
oxiPS	Oxidized phosphatidylserine
PAGE	Polyacrylamide gel electrophoresis
PBS	Phosphate buffered saline
FBS	Fetal bovine serum

TH-2507_156106009

Units

Å	Angstrom
°C	Degree Celsius
mL	millilitre
L	litre
mg	milligram
M	molar
mM	millimoles
µM	micromole
kDa	kilodaltons
µg	microgram
hr	hour
min	Minutes
nm	nanometer

TH-2507_156106009

Chapter-I

Therapeutic potentials of Scavenger receptor CD36 mediated innate immune responses against infectious and non-infectious diseases.

TH-2507_156106009

1.1. Introduction

The cell-cell communication is crucial for growth, metabolism, and defense purposes in multicellular organisms (Trosko and Ruch, 1998). To achieve this, the cells use various receptors present on the cell surface or inside the cells (intracellular receptors) such as nuclear receptors (Schlessinger, 2000). The surface receptor expression varies from cell type to cell type. For instance, the T cells express T cell receptors that are required for antigen presentation (Kubo et al., 1989). Most of the cell surface receptors contain an external ligand-binding domain and an internal response or communication domain (Kiessling et al., 2006). The cells involved in the immune system express various cell surface receptors that recognize, uptake, and process the threats from endogenous (damage-associated molecular patterns, DAMPs) and exogenous (pathogens) threats (Rudd et al., 1999). The receptors that are involved in recognizing the exogenous or endogenous threats are called pattern recognition receptors and serves as a defense mechanism against various infectious and non-infectious diseases (Takeuchi and Akira, 2010). The recognition of threats or non-threats is not only required for pathogen dissemination but also for metabolism, development, and maintaining a healthy host (Blander and Sander, 2012). The sensing of biological molecules is not only required for pathogen dissemination but also metabolism, development, and maintaining a healthy host. The innate sensing of various pathogenic or endogenous molecules such as damage associated molecular patterns (DAMP) is essential to maintain homeostatic balance in host (Radoshevich and Dussurget, 2016). The innate sensing of microbes such as bacteria, fungi, virus or parasite requires immune cells expressing pattern recognition receptors (Meylan et al., 2006). Various immune cells such as monocytes/macrophages, lymphocytes express PRRs on their cell surface (Gazzinelli et al., 2014). The innate immune cell PRRs sensing of pathogen associated molecular patterns (PAMPs) triggers inflammatory cytokine secretion which can alter tissue homeostasis (Medzhitov, 2008). The PRRs are classified into two categories, such as membrane bound PRRs and cytosolic PRRs (Gallo et al., 2014). The examples for membrane-bound PRRs is toll-like receptors (TLRs), C-type lectin receptors (CLRs), receptor for advanced glycation end products (RAGE) and scavenger receptors (SRs) (Altenbach and Robatzek, 2007; Krieger, 1997). The cytosolic pattern recognition receptors involved in sensing nucleic acids (Gallo et al., 2014). The first member of toll like receptors (TLR) has been identified in *Drosophila* with similarities of cytosolic domain with IL-1 receptor in

TH-2507_156106009

humans (Gay and Keith, 1991; Hashimoto et al., 1988). The TLRs contain ectodomain with leucine rich repeats and a cytosolic domain with Toll or IL-1 receptor like domain (TIR) (Medzhitov et al., 1997). The intracellular domain of TLRs involved in signal transduction. The TLRs can activate downstream signalling via two routes such as MyD88 dependent pathway or IFN-β dependent pathway and induce pro-inflammatory cytokine production (Akira and Takeda, 2004). So far 10 TLR receptors (TLR1- TLR10) have been identified in human. In mice there is 13 TLRs identified till date (Du et al., 2000; Tabeta et al., 2004). The TLRs senses PAMPs such as LPS (lipopolysaccharide), LTA (lipoteichoic acid), lipoarabinomannan, zymosan, unmethylated CpG DNA, dsRNA from viruses, RSV F protein, and HSP60 (Janssens and Beyaert, 2003). The TLR4, after ligand binding translocated into cytosolic domain to initiate intracellular signalling. In similar mechanism, TLR4 recognizes pneumolysin from Streptococcus pneumoniae, F protein of respiratory syncytial virus, and glycoinositol phosphate from trypanosoma (Kurt-Jones et al., 2000). The TLR2 sense PAMPs from bacteria, virus, fungi and mycoplasma. TLR2 forms heterodimers with TLR-1 or TLR-6 to initiate signalling. Various accessory molecules or co-receptors such as CD36, and CD14 are required for TLR2 mediated pattern recognition (Akira et al., 2006; Hoebe et al., 2005). The other class of receptors (FcRs) express on hematopoietic cells play crucial role in identification and elimination of pathogens. The FcγRs belong to immunoglobulin family and important for opsonized phagocytosis of microbes (Fridman, 1991). The scavenger receptors are predominantly expressed on granulocytes and monocytes and tasked in a wide range of biological functions, such as cell adhesion, lipid transport, endocytosis, antigen presentation, and sensing of pathogens and their removal from circulation (Yu et al., 2015b). The scavenger receptors classified into class A to J and involved in recognition of ligands from diverse origin. Each class has specificity towards similar group or class of ligands (PrabhuDas et al., 2017). The Class A scavenger receptors sense the dsRNA of virus, cell wall components of gram positive and gram negative bacteria, heat shock proteins, modified lipoproteins such as oxiLDL and amyloid β (PrabhuDas et al., 2017; Vo et al., 2019). Most prominent receptor in Class B is scavenger receptor CD36. The SR-B1 of this class B scavenger recognizes HDL (high density lipoprotein), unmodified LDL, and anionic phospholipids (Acton et al., 1994; Rigotti et al., 1995). The scavenger receptors class D and E involved in recognition of modified lipids, sensing of bacteria and apoptotic cells

(Wilkinson and El Khoury, 2012). The other class of scavenger receptors involved in detection of phospholipids, advanced glycation end products and modified lipids. The scavenger receptor CD36 has been reported to be involved in recognition of lipids, apoptotic cells, lipoproteins, fatty acids and various DAMPS. The CD36 acquired much attention due to its new role in development of pathology during various diseases thus it is prudent to study how CD36 regulates the immune response.

1.2. Scavenger receptor CD36

The scavenger receptors initially thought of binding and internalizing LDL but the current understanding is that they bind to ligands from diversified sources (Zani et al., 2015). The receptors contain a large group of integral membrane proteins classified and divided into A-J groups (PrabhuDas et al., 2014). The receptors are placed in different classes based on their sequence similarity, structural topology, and detection of similar kinds of ligands (Zani et al., 2015). Class B scavenger receptors contain two cytosolic domains, two transmembrane domains, and one large extracellular domain (Kiefer et al., 2002). This class of receptors generally 450-500 residue proteins and divided into three groups such as SR-B1, SR-B2 and SR-B3. The large ectodomain is highly glycosylated and involved in ligand recognition. The cytosolic domains have been predicted for their role in intracellular signaling. The SR-B1 gene located on chromosome 12 in humans whereas the SR-B2 and SR-B3 located on chromosome 4 and chromosome 7 respectively. The scavenger receptor CD36 is a classical class B (SR-B2) scavenger receptor involved in homeostasis, metabolism and angiogenesis (Acton et al., 1994). The scavenger receptor CD36 interacts with a wide variety of ligands such as oxiLDL, thrombospondin-1, apoptotic cells, long chain fatty acids (LCFAs), and bacterial cell wall components. The interaction of CD36 with apoptotic cells, and diacylglycerols are implicated in the secretion of pro-inflammatory cytokines and host pathology (Tserentsoodol et al., 2006).

1.2.1. Expression and regulation of CD36

The human CD36 gene encoded in 17 exons spanned in ~36 kb in chromosome 7 q11.2 and can generate four isoforms through alternative splicing (https://www.ncbi.nlm.nih.gov/gene/948). The extracellular ectodomain is encoded by 11 exons and the transmembrane domain is by 1 exon (Figure 1.1). The N and C terminal domains

TH-2507_156106009

of CD36 protein is encoded by exon 3 and exon 14, respectively, whereas the exons 1, 2 and 15 are non-coding (Rać et al., 2007). While exon 1 and 2 were non coding but deletion of exons 1, 2, and 3 results in loss of CD36 expression (Gautam et al., 2011). The CD36 exons lack the TATA boxes and the CpG islands. The CD36 expression was controlled by alternative splicing and various tissue-specific upstream promoters. A recent study suggested the CD36 promoter containing STAT binding GAS elements (Sp et al., 2018), which is consistent with fact that STAT family member proteins regulate CD36 expression in various tissues (Hosui et al., 2017). The alternative splicing of pre-sliced mRNA provides functional diversity in CD36. The transcription starts 289 bases upstream of the translation initiation site. The 5' flanking region contains several cis-regulatory elements that might involve in the regulation of CD36 transcription (Armesilla and Vega, 1994). The CD36 expression is regulated in response to various surrounding molecules such as insulin, glucose, LPS, and various cytokines. The CD36 gene expression is regulated by PPAR-γ. The core binding factor (CBF), CCAAT/enhancer binding protein alpha (C/EBPα) controls the CD36 gene promoter translation (Niculite et al., 2019).

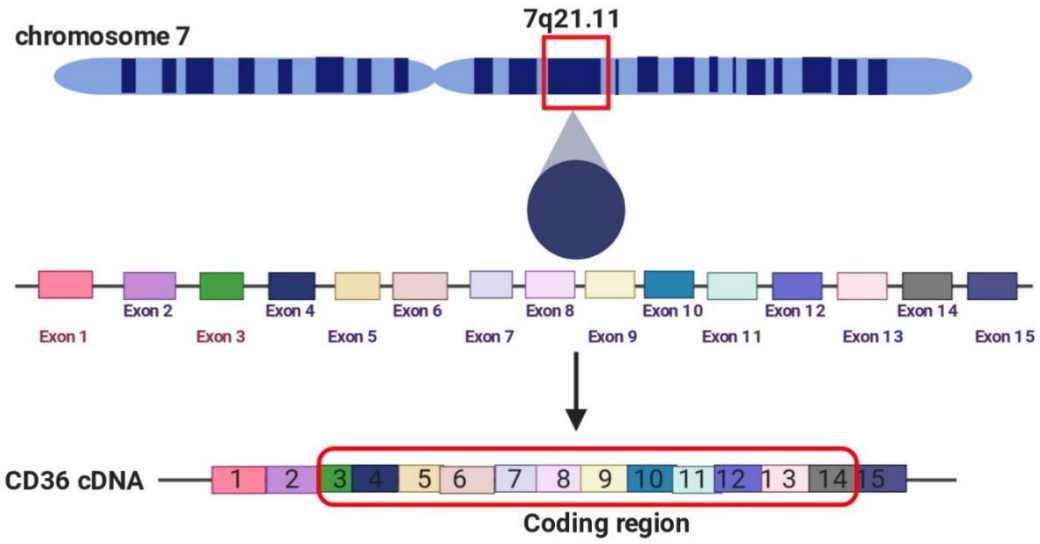

Figure 1.1. Gene organization of scavenger receptor CD36. The CD36 gene is located on 7q21.11. The cDNA of CD36 consists of coding region containing 3-14 exons.

CD36 expressed in wide variety of cells. The CD36 express on adipocytes and cardiomyocytes, macrophages, platelets, capillary endothelial cells and mammalian epithelial cells (Coburn et al., 2000), https://www.proteinatlas.org/ENSG00000135218-CD36. The

CD36 shows highest expression in adipose tissue and placental tissue (Bonen et al., 2009) (Figure 1.2). The heart, liver and spinal cord also shows the CD36 expression (Koonen et al., 2007). The regulation of tissue-level CD36 expression and its implications in various disease conditions will be discussed in upcoming sections. The CD36 expressed on multiple organs of the humans most prominently in heart muscle, adipose tissue, bone marrow, breast skin, duodenum, colon, epididymis and skeletal muscle (Cai et al., 2012) (Figure 1.2). The CD36 expressed but not significantly on brain, eye, lung, pancreas and urinary bladder. In addition, the sensory neurons in olfactory epithelium express the CD36, and some researchers believe that CD36 expression could be involved in sensing and taste of lipids (Sayed et al., 2015).

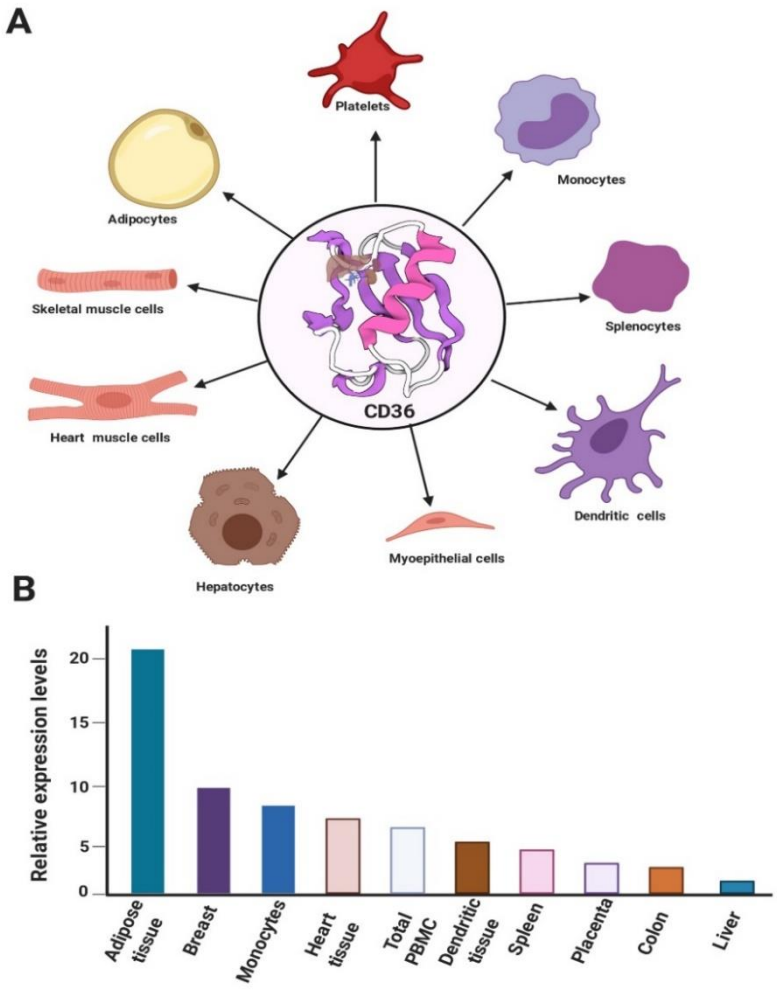

Figure 1.2. CD36 expression on various tissues and organs. **(A)** CD36 expression on various cells and tissue. **(B)** The relative expression of CD36 on various organs (plot is based on protein atlas database mRNA levels of CD36). The adipose tissue has highest expression whereas liver has lowest.

The scavenger receptor CD36 dynamically traffic between cytosol and plasma membrane based on the ligand stimulus (Schwenk et al., 2010). The basic function of CD36 is to recognize the pathogenic or endogenous ligands and facilitate their capture by macrophages. It has been shown that in rat hepatoma cells, the CD36 localization to plasma membrane and uptake of fatty acids is dependent on C-terminal domain of CD36. Further the study highlighted that the C-terminal domain has the ability to dictate the CD36 to plasma membrane (Eyre et al., 2007). The CD36 translocated from membrane to cytosol in TLR-4 dependent manner in oxiLDL+β2/aβ2 treated THP-1 cells (He et al., 2019). The macrophages needed CD36 on plasma membrane for sensing various ligands. The uptake of oxidized lipids by macrophages is mostly dependent on the membrane bound CD36 and its association with tetraspanin CD9. The CD36 localization on plasma membrane influence the fatty acid uptake and lipid metabolism (Huang et al., 2011). The extent of CD36 present on cell membrane is governed by the level of glycosylation. The CD36 with high glycosylation trafficked to membrane whereas less glycosylated CD36 stay in subcellular compartment of secretory pathway (Alessio et al., 1996). In cardiomyocytes, the uptake of fatty acids and glucose is mediated through CD36 and GLUT4 respectively. During heavy workout or increased plasma insulin concentration, the CD36 and GLUT4 translocated to sarcolemma. In insulin resistant type-2 diabetes, the translocated CD36 stays at sarcolemma but the GLUT4 reverted back to cytosol (Steinbusch et al., 2011). The CD36 function is intensely regulated by the tissue or subcellular distribution of CD36. The transcription factor FoxO1 is activated when the insulin levels are low, which activates the AMP-activated protein kinase, and muscular contraction which recruits the muscle CD36 from the cytosol store to the cell membrane leads to increased uptake of fatty acids (Bastie et al., 2005). The CD36 trafficking and the signal which directs it was mostly unclear. Some studies have highlighted the role of the GTPase Rab11a and its effector proteins. CD36 trafficking also believed to be regulated by modification of its ubiquitination state leads to its protein interactions, subcellular localization, and its turnover. CD36 ubiquitination on K469 and K472 in the C-terminal domain is repressed by insulin and enhanced by Fatty acids (Rodrigue-Way, 2011).

1.2.2. Structure and functions of CD36

CD36 is a 55 kDa heavily glycosylated protein with 3 distinct structural parts (Figure 1.3). The CD36 structurally similar to the lysosomal integral membrane protein-I (Pepino et al.,

2014). Residues 35-439 forms a large extracellular ectodomain, where the ligands can interact. The ectodomain consists of three disulfide linkages between Cys 242-310, Cys271-332 and Cys 312-321 residues (Pepino et al., 2014). The ectodomain is glycosylated on residues 79, 102, 134, 163, 205, 220, 235, 247, 321 and 417. The residue 93 and 237 are phosphorylated and implicated in binding of thrombospondin to CD36. The post-translational modifications has been linked to the functional roles of CD36. The residues from 1-9 and 466-472 are the cytosolic N-terminal and C-terminal domains respectively. During signaling event started at cell surface via CD36-ligand interaction, this region provides docking site for a particular set of adaptor proteins to relay the signal for functional outcomes. Ectodomain and cytosolic (N-terminal or C-terminal) part of protein is connected by trans-membrane regions ranging from 9-35 and 442-466(Heit et al., 2013). The basic role of CD36 is transport the LCFAs to the cytosolic side of the cell for metabolism. The ectodomain consists of two hydrophobic tunnels which will allow the passage of LCFAs (Figure 1.3).

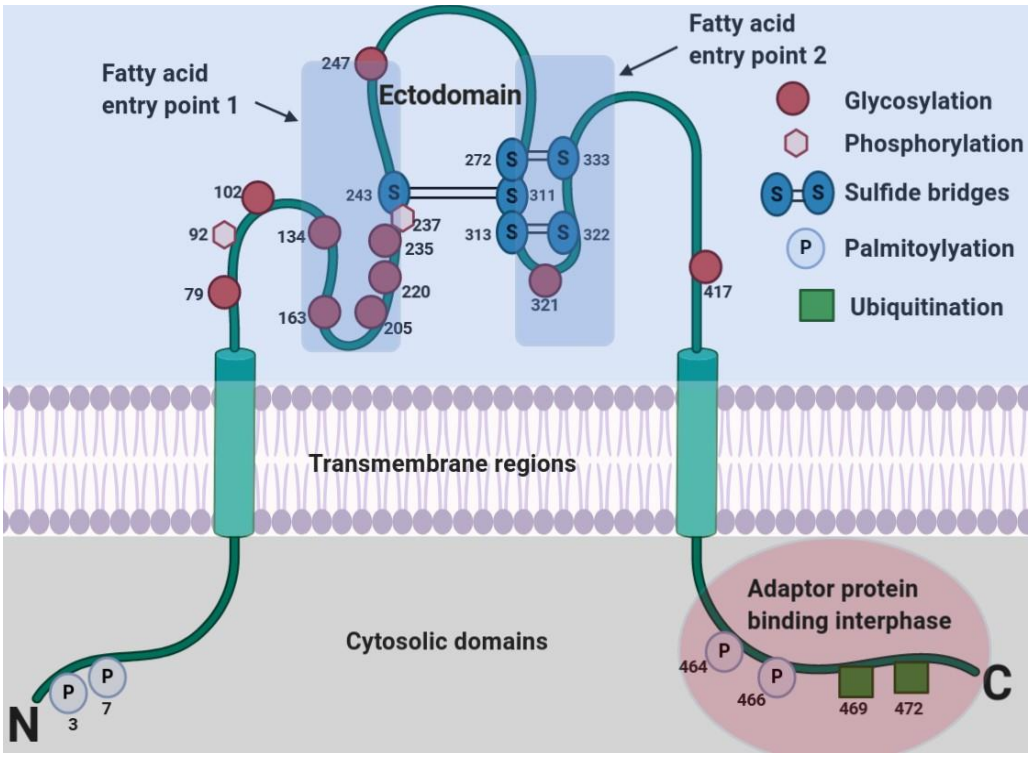

Figure 1.3. Structural organization of scavenger receptor CD36. The CD36 contains large ectodomain, two cytosolic and transmembrane regions. The glycosylation and phosphorylation sites positions presented in figure. The C-terminal known to be involved in intracellular signaling. The information and model is based on a representation by (Moon et al., 2020).

The CD36 has shown to be involved in transport the un-esterified fatty acids across plasma membrane in heart and muscle cells (Abumrad et al., 1981; Bonen et al., 2006). Further, the null mutation or reduced expression in CD36 resulted in complete abolishment fatty acid uptake or decreased uptake of fatty acid in myocytes (Bonen et al., 2006). The mechanistic studies on how fatty acid pass through the CD36 revealed that a distinct cavity spanned throughout the CD36 which is similar to CD36 homolog LIMP II. The lining of this cavity is predominantly covered with hydrophobic residues which allow the passage of fatty acids (Hsieh et al., 2016). Previous reports suggested the entry location of fatty acid lies near to K164 residue. Still, the recent study proved that it contains two fatty acid entry sides and one of the entry site contains K164 residues (Thylur et al., 2017). The study provides unequivocal evidence that CD36 is involved in fatty acid transport. CD36 regulates the lipid metabolism through its ability to recognize the oxidized LDL and fatty acid sensing. Its role as fat perception receptor has been widely studies and acquired sustained attention from research community. The taste buds express the CD36 and when the fatty acid comes in contact with taste buds, the CD36 senses the fat and a several complex cell signaling events takes place and ultimately provides central fat perception (Zhao et al., 2018) (Figure 1.4). The CD36 belongs to the scavenger receptor family SR-B2 (Zani et al., 2015). The CD36 involved in fatty acid uptake and lipid metabolism. The scavenger receptor known for its ability to accept ligands from endogenous as well as exogenous sources (Zani et al., 2015). It interacts with various lipid molecules from diverse sources and is implicated in inflammation, metabolism, and homeostatic balance (Zani et al., 2015). Recent crystal structure shed light onto how the receptor take up the fatty acids and the binding domains responsible interaction (Hsieh et al., 2016). The clearance of aged/dead cells from circulation is crucial to prevent pathological complications (Hsieh et al., 2016). During senescence or apoptosis, the cells express the phosphatidylserine (PS) on their external surface (Fadok et al., 2001) (Figure 1.4). The externalized phosphatidylserine can be used as a marker for detection of apoptotic cells and removed by macrophages (Fadok et al., 2001). Various receptors detect the PS and phagocytose them for further processing. The bacterial LTA or diacylated lipopeptide detection ability of CD36 abolished due to a nonsense mutation in CD36 suggests the non-redundant role of CD36 in detection of bacterial lipids or lipopeptides through TLR2 dependent manner (Hoebe et al., 2005). The oxidized PS interactions with macrophage CD36

TH-2507_156106009

is essential for uptake of apoptotic cells (Greenberg et al., 2006). CD36 not only involved in disease biology but also recognizes variety of biological molecules. Recent studies have highlighted that oxidized phosphatidylcholines ($oxPC_{CD36}$) act as high affinity ligand for CD36. The region spanning from 157-171 of CD36 provides the binding site for $oxPC_{CD36}$. The $oxPC_{CD36}$ are involved in macrophage foam cell formation and platelet hyper-reactivity (Kar et al., 2008). The primary function of macrophage CD36 is to scavenge the apoptotic cells or cell debris. It has been widely accepted that the scavenger receptor interactions with oxidized phosphatidylserine (oxiPS) is crucial for uptake of apoptotic cells by macrophages. The sensing of oxiPS is crucial to prevent unwanted complications in host (Greenberg et al., 2006). The CD36 family sensory neuron membrane protein 1 (SNMP-1) in drosophila senses the pheromones in insect (Gomez-Diaz et al., 2016) (Figure 1.4).

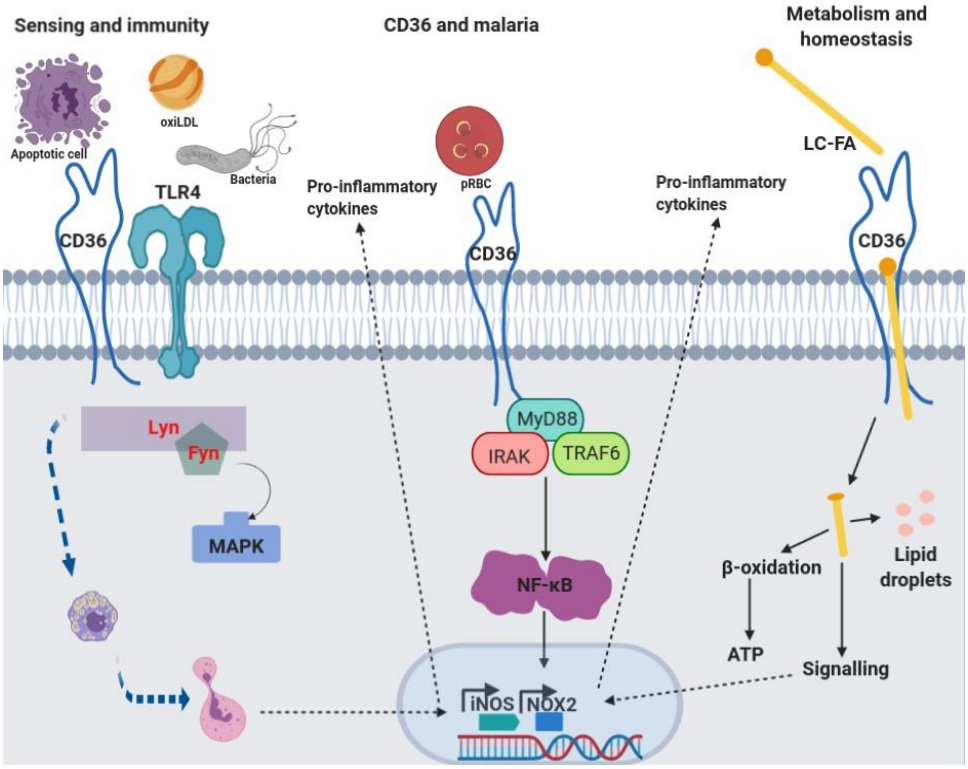

Figure 1.4. Sensing and metabolic functions of CD36. The scavenger receptor CD36 is involved in recognition of apoptotic cells, oxiLDL, bacteria. Parasitized RBC, LC-FA. The receptor is also involved in lipid metabolism.

Role of CD36 in immune responses: Recognition of phagocytic objects and engulfing them for clearance are essential roles of macrophages during infection (Erdman et al., 2009). CD36, is expressed in a variety of cell types including macrophages and interacts with a diverse array

of ligands. CD36 has been shown to participate in the phagocytosis of a number of particles, including β-amyloid , oxiLDL, bacteria, apoptotic cells, and Plasmodium falciparum infected erythrocytes (Febbraio et al., 2001). The monocytes exposed to IRBC showed clustering of CD36 in cytosol. The clustered CD36 is colocalized with IRBC and suggests the membrane bound CD36 play crucial role in non-opsonic phagocytosis (Lagassé et al., 2016). In addition, contrary to involvement of αvβ3 or TSP-1 in non-opsonic phagocytosis of IRBC, the CD36 functioning alone; and does not require the αvβ3 or TSP-1. Further, the non-opsonic phagocytosis is dependent on CD36 mediated intracellular signaling (Lagassé et al., 2016). The phagocytosis of *Staphylococcus aureus* and *Streptococcus pneumoniae* requires scavenger receptor CD36 in mammals. The transfection of HEK293T cells with murine cDNA increased binding and internalization of staphylococcus or E.coli to 3 fold (Stuart et al., 2005a). The macrophages with $CD36^{-/-}$ showed a marked reduction of internalization of bacteria and pro-inflammatory cytokines suggests the CD36 role in pathogens phagocytosis. It is interesting to note that the influenza infected human monocyte derived macrophages showed reduced phagocytosis of *Streptococcus pneumoniae* and down regulation of scavenger receptor CD36 (Cooper et al., 2016). The internalization of LTA (lipoteichoic acid) or bacteria requires the C-terminal domain of CD36. The C-terminal motif residues Y463 and C464 are crucial for activation of TLR2/6 signaling (Stuart et al., 2005a). The scavenger receptor CD36 is also implicated in the uptake of amyloid-β fragments by microglia (Coraci et al., 2002). The CD36 mediated uptake of amyloid-β activates the microglia and results in the production of pro-inflammatory cytokines TNFα, MCP-1, MIP-1α and IL-1β. The CD36 deficient mice macrophages failed to uptake or be stimulated by amyloid-β (El Khoury et al., 2003a).

The scavenger receptor CD36 is involved in the production of pro-inflammatory cytokines during atherosclerosis, Alzheimer's, bacterial infections, parasite infections and dyslipidemias (Gowda et al., 2013). The glycosylphosphatidylinositol (GPIs) of malaria parasite have been shown to prompted pro-inflammatory cytokines TNF-α, IL-6 and IL-1 in macrophages and produce nitric oxide by endothelial cells through activation of TLR2 (Kumar et al., 2012). The CD36 acts as a co-receptor for TLR2 and modulate the GPI mediated pro-inflammatory cytokine secretion in dendritic cells (Kumar et al., 2012). Besides, CD36 also involved in the clearance of P.falciparum infected RBC by targeting them for phagocytosis which decreases the parasite burden in the system (Davis et al., 2012). During the infection, the pro-

TH-2507_156106009

inflammatory cytokine release is regulated by CD36 by interacting with co-receptor TLR-2 (Erdman et al., 2009). The foam cell formation is a critical step in atherosclerosis. The migration of monocytes to arteries is the first step in forming senile plaques in atherosclerosis where the monocytes are developed into macrophages. The oxLDL of long chain fatty acids will bind to CD36 expressing macrophages and get internalized. The internalized oxLDL acts as a ligand for PPAR-γ related nuclear hormone receptors. This will up regulate the CD36 expression on macrophages and eventually more oxLDL internalization which fuel the pro-inflammatory cytokine secretion by macrophages. The whole process makes the onset worst by pro-inflammatory cytokine release, leading to pathological consequences (Zhao et al., 2018). Besides the iRBC, various products of parasite and host are shown to be bind to the CD36. The scavenger receptor CD36 is also involved in the production of LTB4, PGE2 induced IL-1β in immune cells in response to the venom of scorpion *Tityus serrulatus*. The CD36 coordinate with CD14 to induce IL-1β (Zoccal et al., 2018). The scavenger receptor CD36 is involved in phagocytosis of pathogens and contributes to oxidative stress generation in cells and organs. The OmpU, of *Vibrio cholerae*, activates the CD36 and the activation induces the ROS generation (Prasad et al., 2019). The vascular smooth muscle cells stimulated with oxidized lipids show down-regulation of the antioxidant factor (Nrf2) in CD36 dependent manner (Li et al., 2010). The mechanistic studies revealed that the CD36 signaling in vascular smooth muscle cells involved down-regulation of Nrf2 through phosphorylation of Src family kinase Fyn (Chen et al., 2008; Ishii et al., 2004). Further the Fyn was shown to associate with CD36 upon recognizing DAMP in endothelial cells (Ishii et al., 2004). The Nrf2 functions as promoter of peroxiredoxin-2 transcription. The peroxiredoxin 2 is involved in peroxide detoxification. The downregulation of Nrf2 leads to reduced peroxiredoxin 2 and increased oxidative stress in cells (Ishii et al., 2004). Further, the $CD36^{-/-}$ vascular smooth muscle cells showed reduced levels of ROS comparing to wildtype suggests the CD36 mediates the ROS generation and is dependent on ligand-CD36 interactions. The microvascular endothelial cells (MVEC) express CD36 on their surface. The CD36 plays a crucial role in the functioning of endothelial cells. The anionic PS binding to the CD36 on MVEC activates intracellular signaling, which involves the recruitment of Fyn to the CD36, activation of NADPH oxidase, and ROS generation (Ramakrishnan et al., 2016). In cells, the NADPH oxidase (NOX) is the primary source of free radicals. The CD36 has been shown to

be involved in improper activation of platelets, thrombosis, and associated cardiovascular risk (Magwenzi et al., 2015). In platelets, the recognition of oxiLDL by CD36 activates the Src family kinase proteins and phosphorylation of Syk. The phosphorylated Syk activates the PLCγ2 (Qiao et al., 2018). The activated PLCγ2 coordinates with TRAF4 and Lyn in platelets which promotes the phosphorylation of p47 thox subunit of NOX2 (Qiao et al., 2018). The activated NOX2 is responsible for the ROS generation in platelets and arterial thrombosis. The CD36 deficient platelets showed no ROS generation confirms CD36 regulates the ROS production in platelets.

1.2.3. CD36 recognizes ligands from diversified sources

The CD36 ectodomain is a broad platform to provide a docking site for ligands of diversified origin (Figure 1.5 and Table 1.1). The region of ectodomain relevant for molecular interactions with different ligands are given in (Figure 1.5). Characterization of oxiLDL binding domain on CD36 unveiled the stretch of 155-171 amino acids which is responsible for interaction with ligand (Pepino et al., 2014). The K_D value of oxiLDL for CD36 was reported as 10.44 ± 0.08 μg/mL (Martin et al., 2007). The primary function of CD36 is to transfer the fatty acids to cytosol and CD36 perform this function by providing two entry points to fatty acids on an apex region of the CD36 ectodomain. Both the sites are rich in hydrophobic amino acids and have a tunnel-like shape which accommodates the LCFA (Hsieh et al., 2016). The other ligand PfEMP-1, a parasite protein involved in malaria pathology has binding site overlapping with the binding region of the oxiLDL. The interaction between the PfEMP-1 and CD36 is made by F153 residue present on the apex region of ectodomain and L664 of the PfEMP-1 domain. The binding studies suggested that the interaction between these two molecules is strong with a dissociation constant K_D of 12 nM (Hsieh et al., 2016). CD36 and thrombospondin-1 interactions play a significant role in phagocytosis of apoptotic or senescence cells, cell adhesion (Yesner et al., 1996). The stretch of 93-120 amino acids of CD36 ectodomain has a role in TSP-1 binding with K_D of 8.6±3.6 nM (Pearce et al., 1995) (Figure 1.5). Hexarelin, a growth hormone releasing peptide was found to interact with CD36 (Bodart et al., 2002). The binding site for hexarelin is 132-177 stretch of amino acids, and it overlaps with oxiLDL binding site (Demers et al., 2004). The oxidised phospholipids present on plasma membrane interact with CD36 to perform various molecular recognition processes such as detection of apoptotic cells. The CD36 has been implicated in sensing the

TH-2507_156106009

phosphatidylserine present on the external side of plasma membrane (Greenberg et al., 2006; Lee et al., 2015). Interaction studies of oxidized phosphatidylcholine (oxiPC) and CD36 revealed that the binding position of oxiPL has a region of 157-171 and the lysine in this region K164, K166 are crucial for the binding (Greenberg et al., 2006) (Figure 1.5). The bacterial cell wall component LTA interacts with CD36 through phosphocholine moiety. The affinity for phosphocholine towards CD36 was estimated as 6.5 ± 0.5 μM. Acute phase protein Serum amyloid-α was found in various pathophysiological processes. Recent reports suggested that CD36 interacts with serum amyloid-α with K_D = 8.1 μg/ml (Baranova et al., 2010). The advanced glycation end products (AGEs) formed during various pathophysiological conditions, damage associated molecular patterns (DAMP) reported interacting with CD36. A little bit is known about AGEs and DAMPs and their association with CD36 (Miller et al., 2011). A thorough investigation into the impact of these two classes of ligands with CD36 could be useful to understand the CD36 mediated pathology during disease conditions.

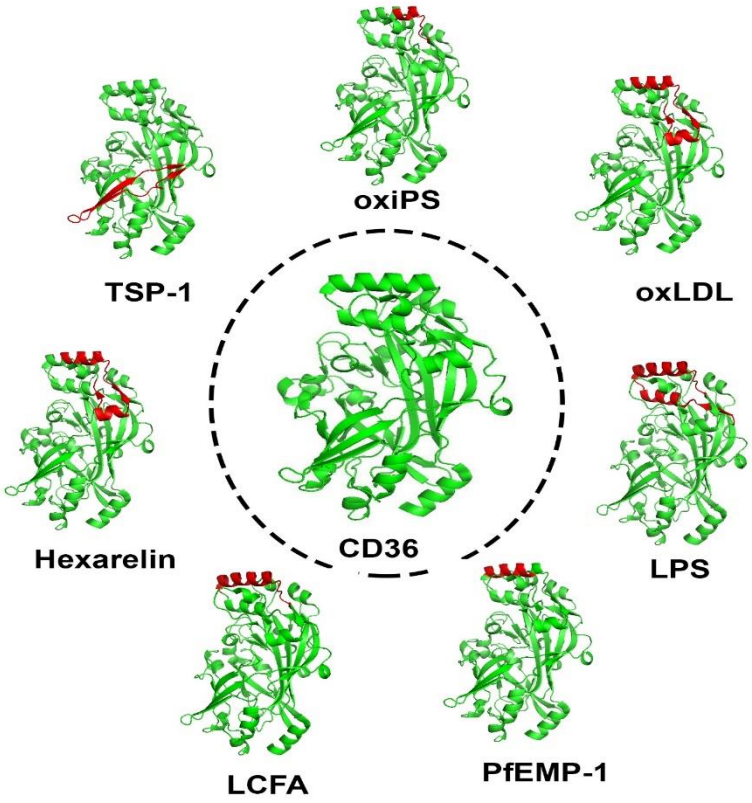

Figure 1.5. CD36 ligands and their binding sites. The ligands binding site highlighted in red color. Most of the ligands binding site overlapping with oxiLDL binding site.

TH-2507_156106009

Table 1.1. CD36 accepts ligands of diversified origins to generate a cellular response

S.No	Ligand	Target cells	Interacting residues	K_D towards CD36	Implications	References
1	LCFA	Multiple cell types	150-168 stretch	0.1mM	Obesity, insulin resistance	(Ibrahimi and Abumrad, 2002), (Ahmed et al., 1997)
2	TSP	Multiple cell types	Stretch of 93-120 amino acids	8.6±3.6 nM	Anti-angiogenesis	(Pearce et al., 1995)
3	OxiLDL, mLDL	Adipocytes	155-171 stretch	10.44±0.08 µg/ml	Sterile inflammation	(Pepino et al., 2014)
4	Amy-β	Glial cells	ND	0.8 µM	Alzheimer's	(El Khoury et al., 2003b)
5	DAMP	Macrophages	ND	ND	Phagocytosis	(Miller et al., 2011)
6	OxiPS	Macrophages	157-171 stretch, K164, K166 are crucial	ND	Non-opsonic phagocytosis	(Greenberg et al., 2006)
7	LPS	Macrophages	132-169	ND	Pneumonia and other bacterial infections	(Baranova et al., 2010),(Sharif et al., 2013)
8	Hexarelin	Macrophages	132-177	0.95±0.26 µM	Anti-atherosclerotic	(Demers et al., 2004)
9	PfEMP1	Macrophages	146-164 stretch and F153	12 nM	Malaria	(Hsieh et al., 2016), (Baruch et al., 1999)
10	Sequestrin	Macrophages	ND	ND	Malaria	(Ockenhouse et al., 1991)
11	Phosphocholine	Macrophages	157-171 stretch	4.81 ± 1.25 µM	Pneumonia and other bacterial infections	(Sharif et al., 2013)

TH-2507_156106009

1.3. CD36 and Downstream signaling

CD36 involvement in fatty acid transport, lipid metabolism and immune response was well documented (Febbraio et al., 2001). CD36 is crucial for fatty acid uptake in muscle cells or myocytes and regulates lipid metabolism and homeostasis (Zhao et al., 2018). The macrophages expressing CD36 on their surface, scavenges the dead or apoptotic cells through non-opsonic phagocytosis. Besides, CD36 is also involved in NLRP3 inflammasome, foam cell formation and inflammation (Ackers et al., 2018) Figure 1.6. The scavenger receptor is crucial for the regulation of immune response during pathological condition. The CD36 mediated immune response is mostly dependent on the ligand binding. Various ligands act as modulators for the CD36 downstream signaling process. Among the ligands iRBCs, parasites GPIs, oxPL (oxidized phospholipids), β-amyloids mediated downstream signaling well explored (Cho, 2012). The downstream signaling is initiated by adaptor protein binding, phosphorylation, and target protein regulation (Duronio et al., 1998). The CD36 uses ectodomain as a recognition element and transmit a signal through cytosolic domains. Also, the ectodomain of CD36 may function as an anchor to assembling the signaling complex in macrophages and other cells (Yang and Silverstein, 2019). The N-terminal cytoplasmic domain is concise and most likely associated with the plasma membrane (Silverstein et al., 2010). The C-terminal domain, which is a 12-13 amino acids length, contains a CXCX5K motif which is homologous to a region from the intracellular domains of CD4 and CD8 which are studied previously, to interact with signaling molecules (Primo et al., 2005). This 13 residue length peptide was tagged with the GST used in affinity purify the proteins from monocytes. The proteins identified to interact with GST tagged CXCX5K motif are MAP kinases, MEKK2 and Src family Lyn protein (Primo et al., 2005). The adaptor proteins identified downstream to the CD36 in various instances are from Src family kinase proteins. In recent past researchers have explored CD36 mediated downstream signaling associated with atherosclerosis pathology. The binding of oxiLDL to CD36 activates the signaling machinery where the Src family kinases are docked to the C-terminal domain of the CD36 (Silverstein et al., 2010). The Src family kinases serves as the immediate adaptor proteins in CD36 mediated signal transduction (Wang and Aikawa, 2015) (Figure 1.6). The recruitment and phosphorylation of Lyn downstream to the CD36 activates mitogen activated kinases

TH-2507_156106009

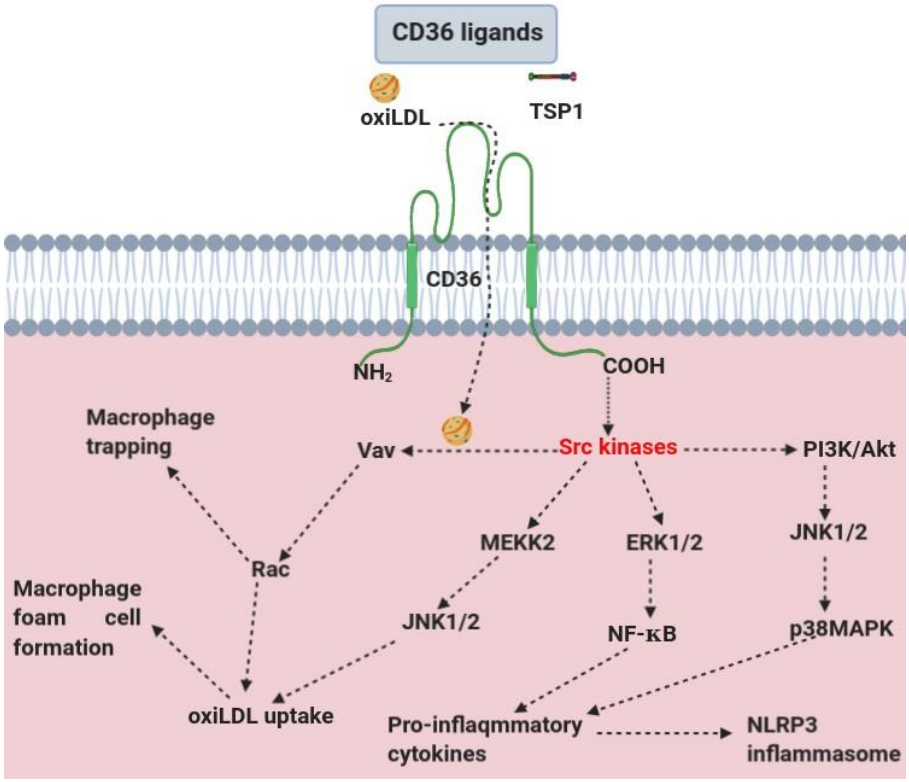

Figure 1.6. CD36 mediated downstream signaling. The CD36 utilizes C-terminal domain to interact with adaptor proteins and regulate the physiological response. Most prominent adaptor proteins that found to interact with CD36 C-terminal domain is Src family kinases. Cd36 mediated downstream signaling responsible for macrophage foam cell formation and pro-inflammatory cytokine secretion.

JNK1/2 (Geng et al., 2018). The JNK kinases upregulate the oxiLDL uptake and enhance the macrophage foam cell formation. Recent evidence suggests another adaptor protein Vav also involved in CD36 mediated atherosclerosis pathology (Silverstein et al., 2010). The Vav is a guanine nucleotide exchange factor activated by Src family kinases. The activation leads to the recruitment and activation of Rac and Rho. The Vav protein through dynamin regulates the oxiLDL uptake. The binding of oxiLDL to the CD36 also activates the p38 MAPK and ERK ½ (Yun et al., 2009a). The activation of p38 MAPK and ERK1/2 leads to activation of NF-κB (Figure 1.6). The NF-κB activation leads to the transcription regulation and pro-inflammatory cytokine secretion (Niu et al., 2018). Several studies have indicated that the receptor acts in coordination with other innate sensing receptors like TLRs or other surface receptors integrins (Kennedy et al., 2011). The studies on CD36 signaling shown that a multimolecular signalling complex consisting β1/β2 integrins, CD9/CD81 tetraspanins

involved in the linking CD36 to the adaptor FcRγ (Heit et al., 2013). This linkage enables the CD36 complex to engage with Src family kinases which contain ITAM and able to internalize and transduce signals (Heit et al., 2013).

Further, the inhibition of Src kinases Lyn, Fyn using small molecule inhibitors blocked the downstream signaling (Moore et al., 2002). The CD36 mediated internalization specifically phosphorylated MAP kinases JNKs which have not observed in CD36 null mice (Rahaman et al., 2006). CD36 in response to diacylglycerols negatively charged molecules shown to activate the MyD88 signaling cascade (Jimenez-Dalmaroni et al., 2009). The anti-angiogenic activity of CD36 was involved in the activation of Src-family tyrosine kinase, Fyn, and a specific mitogen-activated serine/threonine (MAP) kinase family member, p38 (Li et al., 2013).

1.4. Role of CD36 during infectious and non-infectious diseases

Infectious organism surface antigens are recognized by several cell surface receptors present on immune or non-immune cells in host (Mogensen, 2009). The sole purpose of these pathogen pattern recognition (PRRs) receptors is to capture pathogen to control the infection through down-stream cellular responses (Palm and Medzhitov, 2009). Class B scavenger receptor CD36 is one of the receptors involved in non-opsonic phagocytosis of the endogenous and exogenous material and triggers the downstream signaling cascade of pro-inflammatory or anti-inflammatory cytokine secretion pathway. This cellular response potentially could control infection, but inappropriate responses could lead to damage to the target tissue site or organ.

1.4.1. Role of CD36 in Tuberculosis: Tuberculosis is caused by *Mycobacterium tuberculosis* (Mtb), and it spread through aerosol droplets containing the pathogen (Falkinham III, 2003). The Mtb infection is a global burden as day by day the new resistant strains evolving which are unable to treat with the current drugs, and there is need of new multidrug-resistant Mtb targeting drugs (Müller et al., 2013). Exploring potential targets from host and pathogen may leave new therapeutic target sources. After entry of the pathogen into the host, the alveolar macrophages are first cells to interact with bacterium cells through scavenger receptor CD36. It helps in recognizing Mtb and phagocytosis of the bacterium to clear the infection from circulation. The phagocytosis of Mycobacterium by macrophages triggers the immune

TH-2507_156106009

responses involving the cytokines production, targeting the phagocytes by secreting the antimicrobial agents, recruiting the PMNs to the site of infection. This will allows immobilizing the bacteria by forming the granuloma (Ndlovu and Marakalala, 2016). Granulomas formed by infiltrating macrophages and immobilized Mtb generates an oxidative stress to kill immobilized bacteria. The oxidative stress initiates the production of oxiLDL and advanced glycation end products (AGEs) which are also ligands for CD36. The recognition and uptake of these products may involve in the inflammation and over-expression of CD36 on macrophages (Ohgami et al., 2002; Zhu et al., 2012). Contrary to its role in controlling infection, CD36 was also reported in promoting the intracellular growth of Mtb (Dodd et al., 2016). CD36 is known to facilitate lipid uptake in cells (Pepino et al., 2014). The lipid uptake can be the source of carbon which facilitates the growth. The macrophages pre-treat with surfactant lipids was found to increase the CD36 transcript levels and induced the CD36 translocation from the cytosol to membrane (Dodd et al., 2016). Knockdown of CD36 revealed that the growth of Mtb decreased significantly. Another independent study on the role of scavenger receptor during Mtb infection revealed that the $CD36^{-/-}$ mice showed a reduced level of inflammatory mediators, the density of granuloma and the burden of Mtb in liver and spleen. The viable bacteria inside macrophages from $CD36^{-/-}$ was also found to be reduced (Hawkes et al., 2010). The basis of the recognition of Mtb was may be due to cell wall containing mannosylated lipoarabinomannan (ManLAM) (Figure 1.7). The blockage of the scavenger receptor CD36 with neutralising anti-CD36 antibody reduced the TNF-α levels. The study suggests that ManLAM may be a ligand or interacting molecule for CD36 and it mediates the TNF-α secretion in LPS stimulated macrophages (Józefowski et al., 2011). Single nucleotide polymorphisms in CD36 revealed that the risk of pulmonary tuberculosis is decreased in SNPs due to the reduced ability of CD36 to recognize the Mtb pattern recognition molecules (Lao et al., 2017). The Mtb engulfed by macrophages also serves as a hiding place for bacteria (Palanisamy et al., 2012). The reports available to date demonstrates the indispensable role for CD36 during tuberculosis.

1.4.2. CD36 is involved in regulating the inflammatory response during Pneumonia: The lungs are the primary organs affected by pneumonia infection which involves inflammation in air sacs. When the bacteria enter into lungs, they are detected, captured and phagocytosed by the alveolar macrophages. The binding and detection of the Pneumococcal pneumonia are

TH-2507_156106009

mediated by the bacterial component such as LTA (lipoteichoic acid). The LTA consists of phosphocholine residue (PC) which is the key molecule involved in recognition (Han et al., 2003) (Figure 1.7). One of the CD36 natural ligand is oxidized low-density lipoprotein (oxiLDL) which mimics the PC at the molecular level. The investigation into the recognition mechanism by macrophages suggested that the PC is being detected by the CD36 and the

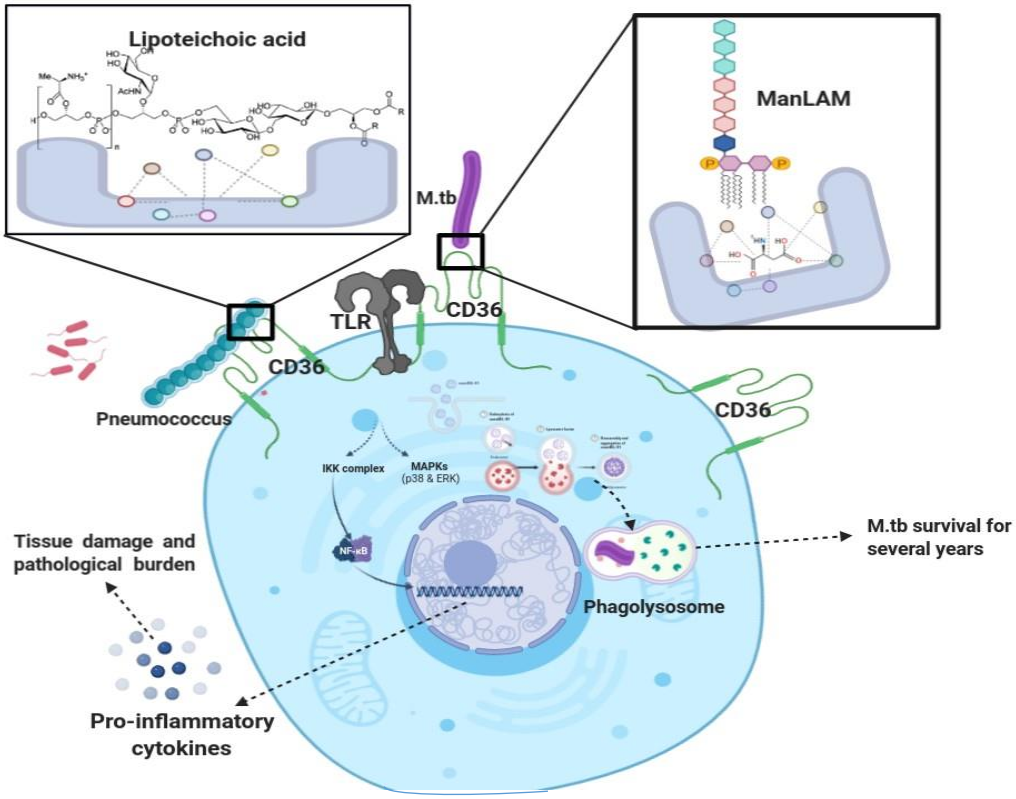

Figure 1.7. Role of CD36 during bacterial infections. The scavenger receptor CD36 detects gram positive and gram negative bacteria cell wall components such as LPS, LTA and ManLAM. The CD36 mediated detection of bacteria leads to phagocytosis of pathogens by macrophages and clear pathogens from circulation. Not always CD36 mediated phagocytosis is helpful sometimes it is involved in pathology and microbe escape from immune response.

blockage of the CD36 with anti-CD36 antibody decreased the uptake of bacteria. The study established PC as a ligand for CD36. It also revealed that at the early stage of infection the levels of inflammatory cytokines levels are very high and later stages the levels are significantly decreased compared to initial stage in $CD36^{-/-}$ mice. Another study on CD36 involvement in inflammation during Pneumonia highlighted the early infection in $CD36^{-/-}$ mice showed elicited inflammation (Sharif et al., 2013). The double knockdown of the

scavenger receptor A and CD36 were found to be beneficial to host during peritoneal infection. Apart from these, the CD36 levels were down-regulated during influenza virus-mediated pneumonia conditions (Cooper et al., 2016). To add further, during *Klebsiella pneumoniae* infection, the absence of CD36 in host make it more vulnerable to infection which states CD36 mediated phagocytosis is necessary for clearance of bacteria (Cooper et al., 2016). The mechanistic study of internalization of S*taphylococcus aureus* by phagocytic cells has revealed that the cytoplasmic domain of the CD36 receptor is required for the phagocytosis. The residues of cytoplasmic domain Y463 and C464 were crucial and involved in TLR 2/6 signallingandCD36 is lacking macrophages are failed to clear the bacteria and showed a defect in secretion of TNF-α and IL-16 (Stuart et al., 2005b).

1.4.3. Scavenger receptor and its role in leishmaniasis: Leishmaniasis caused by the Leishmania a protozoan parasite which is transmitted through sand-fly (Clem, 2010). Like Mtb, it is also intracellular pathogen and survives inside the phagocytic cells by escaping the immune response from the host. Macrophages and dendritic cells are the primary defenders of this infection. The recognition of Leishmania is more complicated as there have been several receptors involved in this process (Gupta et al., 2013). The engagement of the host cells with Leishmania induces innate immune response such as phagocytosis of parasite and secretion of cytokine molecules. A recent study on the role of scavenger receptors in a Drosophila model revealed that CD36 levels are very high at the parasitophorous vacuole where the parasite contacts the phagolysosome. Further, the $CD36^{-/-}$ cells showed a decrease in the size of parasitophorous vacuole (Okuda et al., 2016). How it recognizes the parasite contact points yet to be explored.

1.4.4. Role of CD36 in viral infections: Viruses are devoid of cellular machinery to replicate, so they infect the other cells and hijacks its cellular machinery. They took control over cell by integrating the genetic material into the host cell genetic material and subsequently produced viral encoded proteins helps in replication of virus (Cohen, 2016). During viral infections, the attachment is the limiting step for virus replication (Cherry and Perrimon, 2004). The attachment of virus-mediated through the virus pattern recognition molecules and interaction with the host cell receptors (Baranowski et al., 2001; Cliver, 2009; Shayakhmetov et al., 2010). Several reports stated that Hepatitis C virus, CMV, influenza and HIV infections may found

TH-2507_156106009

linked to the CD36 expression (Baranowski et al., 2001; Carlquist et al., 2004; Meroni et al., 2005; Staples et al., 2015). Hepatitis C virus attachment and replication is mediated by the HCV protein E1 interactions with host cell receptor CD36 (Figure 1.8). Further, the replication is reduced by blocking the CD36 with anti-CD36 antibody (Shalygina et al., 1989). The CD36 expression during HBV infection found to correlate with the virus replication in a hepatocyte cell line (HepG2.2.15). The genome-wide transcriptome analysis showed that there is a link between the CD36 over-expression and HBV metabolism (Shalygina et al., 1989). HBV is regarded as metabolo viruses it depends solely on host metabolism for propagation. The replication of HBV inside the host cells needs viral protein Hbx. The protein Hbx is required to induce cell cycle arrest at a G1 phase in hepatocytes (Gearhart and Bouchard, 2010).

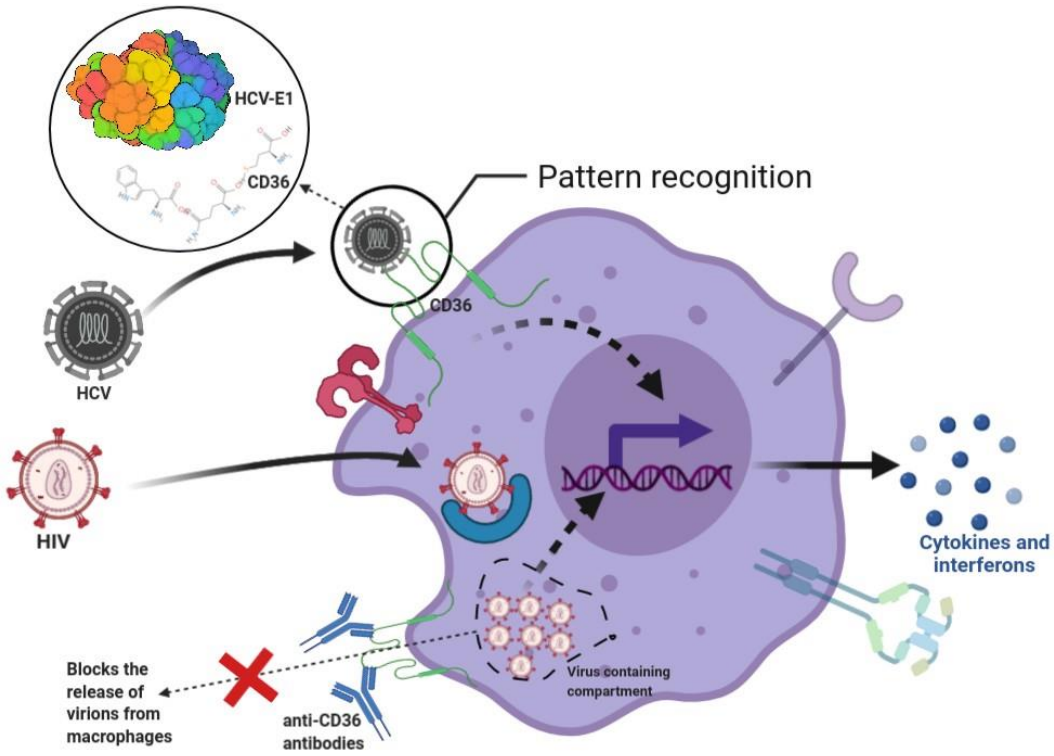

Figure 1.8. CD36 and viral infections. The CD36 detects HCV E1 protein and induce pro-inflammatory cytokines secretion. During HIV the CD36 mediates the release of virions into circulation which may induce inflammation and the blocking of CD36 prevents the virion

The functioning of hepatitis B virus protein Hbx, cytosolic calcium is required (Casciano et al., 2017). CD36 is involved in the operation of store-operated Ca^{2+}channel mediated by Src-kinases mediated signaling pathway (Huang et al., 2017) which facilitate the HBV replication.

TH-2507_156106009

During influenza infection, the CD36 levels (at the cell surface and mRNA level) are significantly decreased in monocyte-derived macrophages. Still, there is a void on how the HBV and influenza infections are linked to CD36 and which ligand is involved in mediating CD36 down-stream signaling during these conditions. Apart from its contribution to infection mediated pathology, it is also involved in reducing the virus burden. The CD36 detects the PS exposed on the surface of influenza-infected cells and subjects them for phagocytosis by macrophages (Shiratsuchi et al., 2000). The CD36 also play a crucial role in spreading HIV-1 infection (Figure 1.8).

The infected macrophages act as reservoirs to accumulate newly generated virions in specific virus-containing compartments. The virus-containing compartments from infected macrophages showed co-localization of viral gag protein with the host protein CD36. The molecular mechanism behind the recruitment of gag to CD36 containing VCC is still not clear. Interestingly, the scavenger receptor blockage using soluble anti-CD36 antibodies inhibited the release of the virions from infected macrophages and spreading the infection to CD4+ cells (Berre et al., 2013). During HIV-1 infection, the levels of CD36 expression on the membrane of macrophages were decreased which is down-regulated the mRNA levels of CD36. The biochemical study revealed that virus Nef protein involved in the impairment of CD36. The Nef-mediated down-regulation of CD36 affected the phagocytosis of the infected cells and contributed to the pathology of the host. The study also suggested that the TNF-α, a pro-inflammatory cytokine secretion mediated by Nef-CD36 interactions (Olivetta et al., 2014). So in summary CD36 play a significant role during viral infections and modulating CD36 mediated response may be useful in controlling infection and the associated pathology.

1.4.5. CD36 and diabetes: The diabetes mellitus is a group of disorders characterized by increased plasma glucose concentration (Guthrie and Guthrie, 2004). The diabetes mellitus is classified into two categories viz., type-1 and type-2. The type-1 diabetes mellitus is associated with the destruction of pancreatic β islets cells (Guthrie and Guthrie, 2004). The destruction of pancreatic β cells is largely mediated through autoimmune response. The type 2 diabetes mellitus is not dependent on insulin levels in plasma (Guthrie and Guthrie, 2004). The analysis of large group of patients with type-2 diabetes suggested the soluble CD36 levels in plasma increased to several folds (Handberg et al., 2009). The adipocytes and macrophages exposed to oxiLDL activated c-JUN kinases and affected insulin signalling (Kennedy et al.,

TH-2507_156106009

2011). In addition the CD36 knockdown reduced c-JUN activation and improved insulin signalling (Kennedy et al., 2011). The pancreatic β cells isolated from obese and type-2 diabetic patients showed elevated levels of CD36, reduced insulin secretion. The CD36 involved in downregulation of Insulin receptor substrate-1 (IRS-1) downregulation which will affect the PI3K/Akt insulin signalling pathway (Nagao et al., 2020) (Figure 1.9). The ceramides levels in plasma positively regulates the generation of oxidative stress and inflammation in β cells. The ceramide exposed β cells presented with redoxosome formation in CD36 dependent manner. The redoxosome activated JNK and transcription of NF-κB. The activated JNK induced the phosphorylation of P66Shc serine 36 an hyper oxidation of peroxiredoxin-3. The oxidized peroxiredoxin-3 involved in β cell apoptosis and mitochondrial dysfunction (Karunakaran et al., 2019). The inhibition of CD36 prevented **β** cell destruction and potentiated insulin secretion (Karunakaran et al., 2019). The CD36 mediated β cell destruction and its association in obese patients established it as a target for testing potential therapeutic molecules. Further, the soluble CD36 levels in patients with type-2 diabetes can also be used as biomarker for detection of early onset of disease.

1.4.6. CD36 and liver disorders: The liver is the largest organ of the body involved in metabolism, synthesis, storage and immunity (Hernandez-Gea and Friedman, 2011). Among the chronic liver diseases, Non-alcoholic fatty liver disease (NAFLD) is the most common in world population (Rada et al., 2020). The animal studies and patient case studies indicate NAFLD is induced by excessive fatty acid uptake by hepatocytes (Nguyen et al., 2008). In patients with non-alcoholic steatohepatitis, the soluble CD36 (sCD36) levels were elevated. Moreover the disease severity is correlating with the sCD36 levels in plasma (Rada et al., 2020). The CD36 expression on hepatocytes is low but during lipid rich diet and NAFLD the expression levels will go high (Greco et al., 2008). The CD36 overexpression is induced by different stimulus such as high fatty acid intake, insulin levels and lipid metabolites (Bechmann et al., 2010). The CD36 enhanced expression induce apoptosis of hepatocytes in steatohepatitis condition (Bonen et al., 2007). The CD36 mediated free fatty acid transport in hepatocytes is regulated by the PPAR-γ, unknown receptors of liver (Silverstein and Febbraio, 2009). The immunohistochemistry with liver sections of steatohepatitis patients showed that the CD36 localized to the plasma membrane of hepatocytes. In healthy adults very low CD36 levels were observed in cytoplasm (Figure 1.9). The study indicate the CD36 expression on

hepatocytes is crucial for development of steatohepatitis pathology (Miquilena-Colina et al., 2011). Further, the hepatic CD36 knockdown in mice fed with high fat diet, significantly reduced the triglycerides and inflammatory markers (Wilson et al., 2016). On contrary to the CD36 role in steatohepatitis, CD36 overexpression glycogen homeostasis, and attenuated the steatohepatitis (Garbacz et al., 2016). Briefly, the CD36 is not only a biomarker for liver NAFLD but also a potential target for drug discovery process.

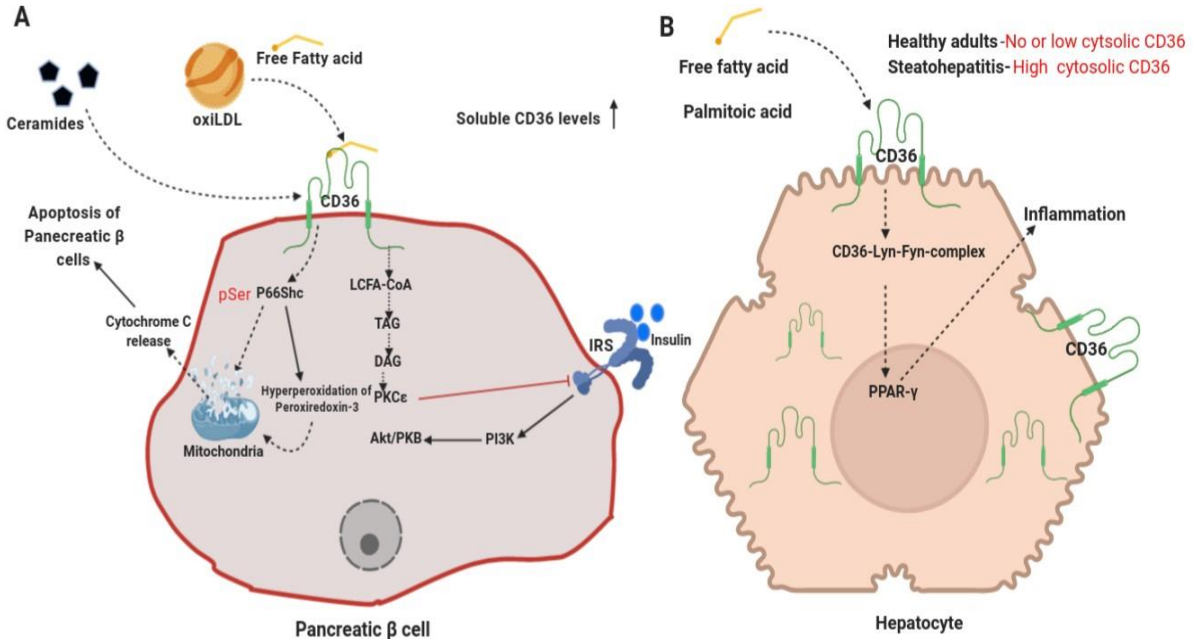

Figure 1.9. Role of CD36 in diabetes and fatty liver. (A) The scavenger receptor CD36 take up the free fatty acids and the downstream signaling blocks the Insulin release signling through blocking akt/PkB pathway. The ceramides are also involved in pancreatic β cell destruction through mitochondrial apoptosis and cytokine c release. CD36 not only disrupt insulin signaling but also destroy insulin producing cells through apoptosis. **(B)** The fatty acid bound CD36 activated downstream signaling involving src family kinase recruitment and production of pro-inflammatory cytokines. Further, the cytosolic levels of CD36 was modulated during steatohepatitis.

1.4.7. CD36 and brain disorders: The stroke induced brain injury is a multifactorial pathological condition. The brain stroke involves production of pro-inflammatory cytokines, oxidative stress, activation of necrosis or apoptosis pathways in brain cells and vascular dysfunction (Cho, 2012). The constant presence of immune cells in brain induces the oxidative stress and secretion of pro-inflammatory cytokines (Cho and Kim, 2009). The high fat fed mice after 3 days after ischemic stroke showed elevated levels of CD36, MCP-1 and CCR2 proteins (Kim et al., 2012). In normal condition the CD36 expression levels are low in brain

TH-2507_156106009

cells but during ischemic stroke the levels are upregulated. In addition the hyperlipidemia amplifies the ischemic stroke condition and causes more damage in CD36 mediated manner (Kim et al., 2012). The bone marrow chimeras study in mice indicated that the mice (CD36-/-) transplanted with wildtype (CD36) had smaller infarcts in brain whereas the wild type mice receiving bone marrow cells from CD36-/- showed pattern of wildtype. The study suggests the CD36 expression in brain cells (microglia and endothelial cells) is responsible for post-ischemic stroke but not the cells originating in and carried by blood (Garcia-Bonilla et al., 2015). The CD36 functioning largely controlled or mediated by the ligand interactions but the ligands involved in pathology of post-ischemic stroke remains to be identified (Cho et al., 2005).

CD36 recognizes β-Amyloid fibrils and contributes to pathology: Alzheimer's disease is a neurodegenerative disease, with histopathological features of soluble oligomeric amyloid-β or insoluble plaques in cerebral cortex and microglia (Bali et al., 2010). Similar to other neurodegenerative diseases, it is also a multifactorial ailment involving genetic and non-genetic causes (St George-Hyslop and Petit, 2005). The neuropathological hallmarks include cerebral amyloid angiopathy, neurofibrillary tangles, neuronal loss (Muller-Hill and Beyreuther, 1989; Serrano-Pozo et al., 2011). The clinical symptoms include the loss of cognitive skills such as thinking and memory (Swerdlow, 2007). The β-Amyloid fibrils stimulate the microglia which secretes the chemo-attractants. The starting point of pathology during Alzheimer's is very complicated as so many receptors are involved in this process such as integrins, Clusters of differentiation molecules which serves in accepting the β-Amyloid as ligand (Ho et al., 2005). The expression analysis of different receptor molecules involved in Alzheimer's patient's cerebral cortex, microglia suggested that the CD36 expression is very high as compared to the control. The neuronal cells exposed to β-Amyloid after 24h exhibits increased several folds CD36 expression (Ricciarelli et al., 2004). The interaction between CD36 and β-Amyloid fibrils induced the production of oxidant molecules from microglia whereas $CD36^{-/-}$ subject's microglia and macrophages exhibit reduced levels of ROS (El Khoury et al., 2003b; Ricciarelli et al., 2004). The oxidative stress during Alzheimer's was mediated by NADPH oxidases which are the result of the Aβ binding to CD36 (Park et al., 2011). CD36 also contributes into a generation of H_2O_2 during Alzheimer's disease as blockage of CD36 with specific antibodies inhibited H_2O_2 production in human fetal microglia

and N9-immortalized mouse microglia (Coraci et al., 2002). The role of CD36 is to recruit circulating macrophages to the site of plaque deposition in microglia or brain capillaries and inflammation (Coraci et al., 2002). The recruitment of macrophages and microglia to the brain site was found less in CD36 null mice receiving an intra-cerebral injection of the β-Amyloid fibrils (El Khoury et al., 2003b). It was found that the leukocyte CD36 expression levels in Alzheimer's patients are very high as compared to healthy subjects with no mild cognitive

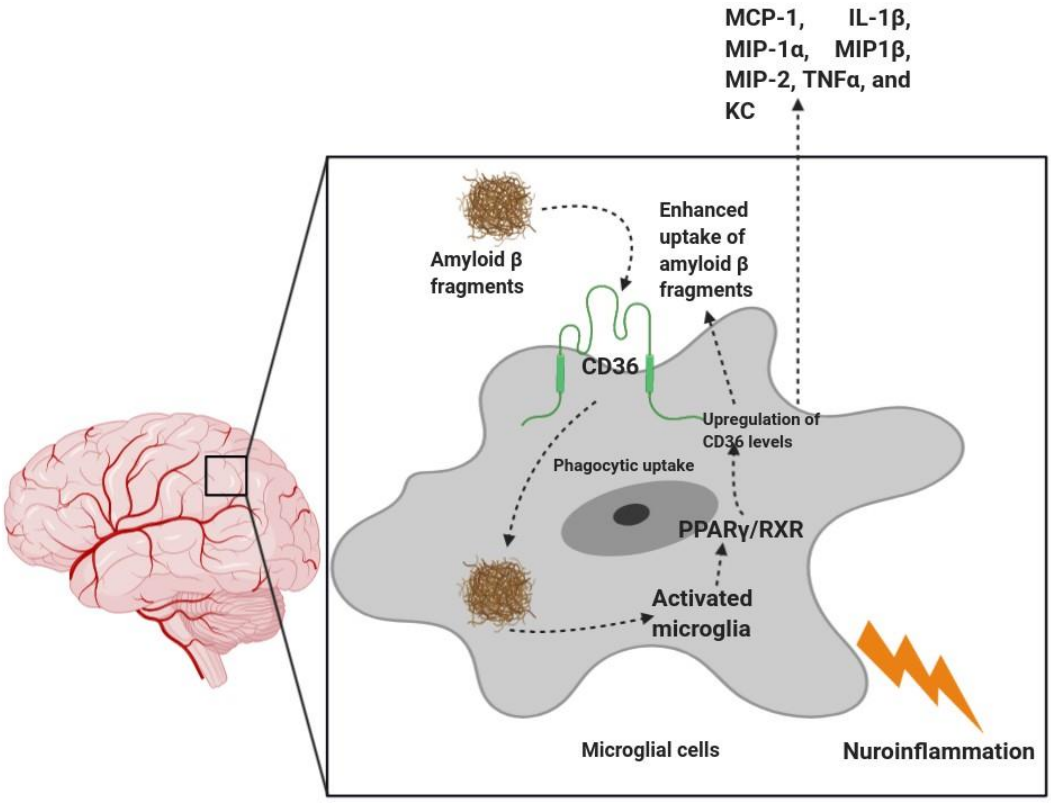

Figure 1.10. Role of CD36 in Alzheimer's. CD36 involved in uptake of amyloid fibrils which activates the cytokine signaling. The secretion of pro-inflammatory cytokines induce neuro-inflammation.

impairment (Giunta et al., 2007). The interaction of β-Amyloid with CD36 induces downstream signaling through MAPK involving Src family kinases such as Lyn and Fyn. The MAPK signaling pathway mediated by β-Amyloid-CD36 engagement resulted in the production of ROS by macrophages which are not found in CD36 null macrophages (Moore et al., 2002). The therapeutic potential of CD36 and β-Amyloid interaction blockers found to be useful in controlling the inflammation associated with the disease (Figure 1.10). Further

TH-2507_156106009

refinement of small molecule inhibitors may be utilized in the treatment of Alzheimer's disease.

1.4.8. CD36 and atherosclerosis: There are several complications involved with this disease including the pro-inflammatory cytokine secretion and infiltration of immune cells to the area of plaque deposition (Spence, 1989). Various reports highlighted the role of different proteins involved in the development of atherosclerosis (van der Vorst et al., 2015). As the development of the disease is mainly due to the lipid deposition, the role of CD36 was explored, as it is involved in fatty acid metabolism. CD36 has been reported to interacting with advanced-glycation end products (AGEs) generated during various cellular processes (Vlassara, 1996). AGEs were produced during diabetes-associated atherosclerosis condition (Singh et al., 2014; Vlassara, 1996) found to interact with scavenger receptor CD36 (Vlassara and Uribarri, 2014; Xu et al., 2018) (Figure 1.11).

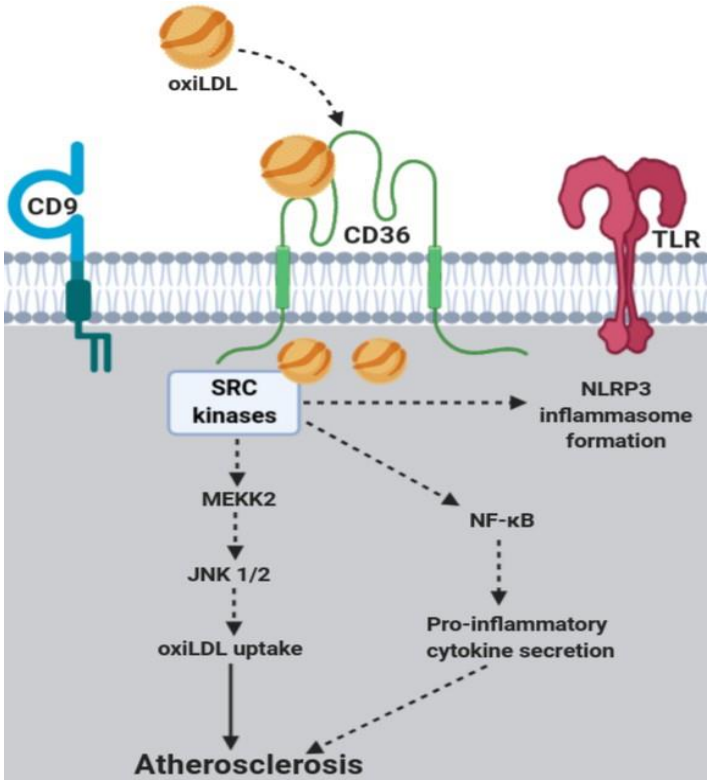

Figure 1.11. CD36 and atherosclerosis. CD36 mediates foam cell formation and NLRP3 inflammasome. The oxiLDL uptake by macrophages incuce cytokine secretion and involved in pathological progression of atherosclerosis.

Moreover, the uptake of advanced glycation end products such as Nε-(carboxyethyl)lysine has been implicated in pathological consequences during diabetes-associated atherosclerosis condition (Ahmed et al., 1997). The mechanism of chemical mediator triethylamine N-oxide in the pathogenesis of atherosclerosis revealed that it promotes atherosclerosis in CD36-dependent MAPK/JNK pathway. The chemical molecule increased the cytokine expression such as TNF-α, IL-6 and ICAM-1. The treatment of molecule to peritoneal macrophages also enhanced the expression of CD36 and attenuated the effect by knockdown of CD36 using si-RNA (Geng et al., 2018). Wnt5a, a member of Wnt family involved in embryogenesis and developmental process. The Wnt5a expressed significantly in advanced atherosclerosis lesions comparing to less advanced lesions. The Wnt5a expression increased the CD36 expression levels in these lesions, and the inhibition of the Wnt5a averted CD36 expression and lipid accumulation (Ackers et al., 2018). Electro-acupuncture is one of the treatment method used to alleviate the symptoms associated with atherosclerosis (Ackers et al., 2018). Although the mechanism behind the treatment is not clear but during the treatment period, it reduces the CD36 mRNA levels in a rabbit model of atherosclerosis (Cheng et al., 2018). The reports available so far tells that CD36 is involved in the development of atherosclerosis along with other molecules and contributes to the inflammation.

1.4.9. CD36 and cancer: Cancer is a second leading cause of mortality worldwide. The tumor is either benign or malignant. The cancer cells have the capability to migrate to other sites within the body to spread cancer (Sudhakar, 2009). During pancreatic adenocarcinoma, the microarray and pathological conditions revealed that the CD36 expression was down-regulated in transformed cells and it is correlating with the prognosis (Jia et al., 2018). It was also found that the ovarian cancer cells co-cultured with adipocytes showed progressive metastasis. The study says the CD36 drives the bioenergetic adaptation of cancer cells and regulates their plasticity. Further, blocking of the CD36 with antibody prevented metastasis progression (Ladanyi et al., 2018). Targeting CD36 positive cells with anti-CD36 antibodies kill chronic myeloid leukemia and this approach could be advantageous as these cells are less sensitive to anticancer drug imatinib (Landberg et al., 2017). The children with CD36 positive B-lymphoblastic leukemia are involved in poor outcome (Newton et al., 2017). Obesity is a crucial factor to predispose a person for cancer especially breast cancer. In chronic diet-induced obesity mice model, lysophosphatidic acid/protein kinase D1 (LPA/PKD-1)-

TH-2507_156106009

CD36signalling promoted ER-positive breast cancer. The cancer progression was driven by CD36 mediated microvascular remodeling (Dong et al., 2017). A recent study, in human oral carcinomas, contains $CD44^{bright}$cells with no mesenchymal genes expression but very high levels of CD36 expression. The high-fat diet fed NSG mice presented larger metastatic lymph nodes in a CD36 dependent manner. The knockdown of CD36 inhibited the expression of genes associated with metastasis whereas its over-expression up-regulated the metastatic genes (Pascual et al., 2017). In breast cancer cells, the lipid metabolism is not only regulated by de-novo synthesis but also by the exogenous lipids uptake. The fat from an external source can be up-taken by cancer cells through the fatty acid translocase which drives the progression of breast cancer cells. This study provides insights into the CD36 targeting in cancer therapy (Zhao et al., 2017). Blocking of CD36 with neutralizing antibodies stopped the progression of metastasis (Pascual et al., 2017). In summary, although there is no clear experimental evidence to correlate CD36 with metastatic cancer progression but existing literature suggest that CD36 conclusively play a significant role in cancer progression (Figure 1.12).

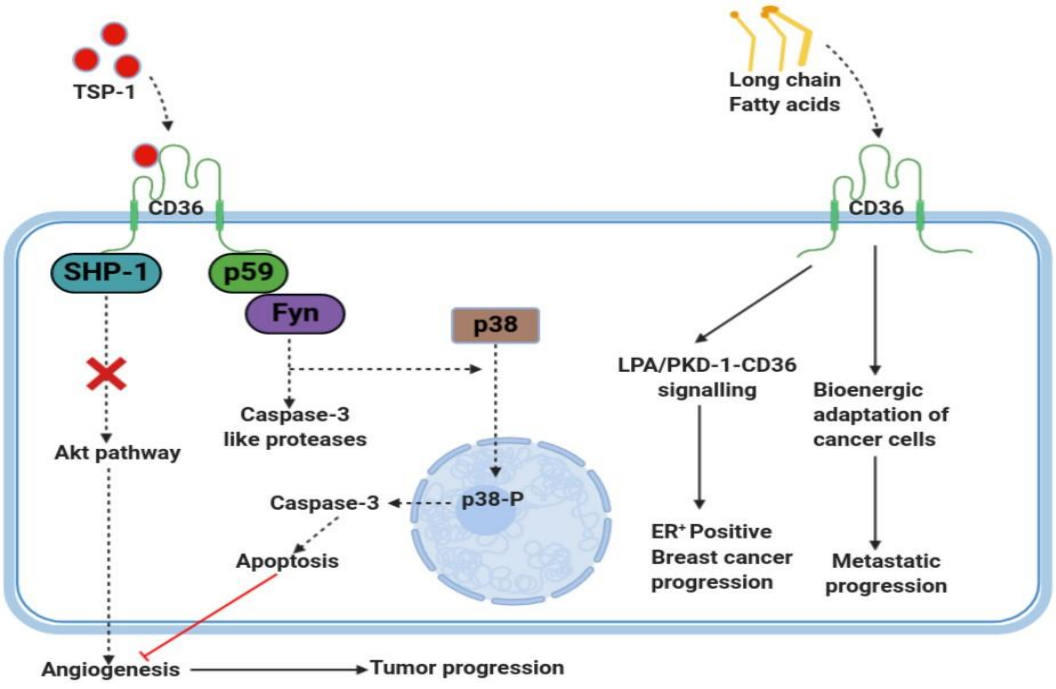

Figure 1.12. Role of CD36 in cancer progression. CD36 and TSP-1 interaction could be beneficial and protects cells from cancer progression by inducing apoptosis. The CD36 is also involved in progression of cancer through fatty acid uptake which fuels the cancer cell

1.5. Small molecule blockers targeting CD36

CD36 plays a significant role in the pathology of the host by regulating the innate immune response. Targeting CD36 with synthetic molecules could be an approach to control the pathology associated with CD36. By summarizing the research on CD36 available to date, it is very clear that targeting the CD36 may be utilized in imparting protection to host. Some bioactive agents are reported for their ability to disrupt the CD36-ligand interaction and downstream events. The CD36 targeting therapeutic molecules are chemically categorized into Protein/peptide molecules, synthetic molecules and phytochemicals. The structural features of each category of molecules and their intervention in regulating/correcting the immune response induced by CD36 will be discussed in the following section (Table 1.2) (Figure 1.13).

1.5.1. Protein/peptide based molecules: A series of synthetic amphipathic helical peptides tested on scavenger receptor molecules showed that they are specifically interacting with CD36. The treatment with peptides especially synthetic amphipathic helical peptide L-37pA significantly reduced infiltrating neutrophils levels and the IL-8 in a LPS mediated acute lung injury (Bocharov et al., 2016). LPS is one of the major marker of gram-negative bacterial infections, known to interact with CD36. The scavenger receptor CD36 and LPS interactions may contribute to the release of pro-inflammatory cytokines thus facilitating host homeostasis imbalanced. The peptide L-37pA mimics the apolipoprotein A-I (Apo A-I), a known molecule to interact with CD36 (Navab et al., 2006). The experimental evidence suggested that the L-37pA peptide acts as an antagonist for CD36 to block LPS uptake in THP-1 monocyte cells and inhibits the LPS induced inflammation (Bocharov et al., 2016),(Bocharov et al., 2004). Apart from ELK sequence based peptides ELK-B and ELK-B1 are found to be blocking very selectively CD36 and not any other scavenger receptors. These peptides inhibited IL-8 secretion in Hela cells transfected with CD36 and stimulated with LPS/E.coli bacteria. It was also noted that the Apo A-I involved in enhancing anti-inflammatory activity of HDL in rabbits infused with Apo A-I (Patel et al., 2010). CD36 plays an important role in metabolism and inflammation during cardiovascular and kidney diseases (Souza et al., 2016). Another Apo A-I mimicking amphipathic helical peptide 5A was reported for therapeutic role in the chronic kidney disease, inflammatory bowel disease in mice, inhibiting oxidative stress in rabbit carotids and preventing atherosclerosis in mice. The investigation into the interactions

TH-2507_156106009

between 5A peptide with scavenger receptor has revealed that, the peptide competes for the oxiLDL binding site on CD36 with a Ki value of 1.45 µM (Amar et al., 2010; Nowacki et al., 2016; Tabet et al., 2010). Internalization of oxiLDL through CD36 activates macrophages involving Src family kinase Lyn and MAP kinase kinase 2 (Yokoi and Yanagita, 2016). CD36 specific antagonistic peptide 5A down-regulate the inflammatory signaling pathway but molecular mechanism is not fully understood (Pennathur et al., 2015). Although the reports available till date uses the structural amphipathic helical peptides in ameliorating inflammation in experimental model of disease by targeting CD36, there is a wide scope for them in treatment of various infectious diseases which needs attention of research community. The scavenger receptor CD36 also contributes to the cerebral ischemia pathology. The treatment of ischemic stroke mice with SS31, a cell-permeable peptide down-regulated the CD36 levels and correlating with the neuroprotective properties but no effect was observed in CD36 null mice. Further the treatment of mouse peritoneal macrophages with SS31 attenuated the oxiLDL induced CD36 expression and foam cell formation (Cho et al., 2007). The CD36 is also involved in regulating the pathology during Alzheimer's disease. During Alzheimer's disease oxidative stress is pronounced and play crucial factors involved in neuronal degeneration. The antioxidant peptide SS31 targeting the mitochondria may be utilized as tool to slow down the cognitive impairment (Jia et al., 2016). SS31 peptide was also reported in protecting the retinal ganglion cells during glaucoma by scavenging the reactive oxygen species (Yu et al., 2015a). During malaria, cyto-adherence is crucial for binding of the PRBC to endothelial cells and represent a potential target to control the pathology associated with infection (Davis et al., 2012). The cyto-adherence during malaria can be an effective target to control pathology. Various research groups are explored to designing the cyto-adherence blocking peptides by targeting ICAM-1:PfEMP binding site (Mehra et al., 2015) and CD36:PfEMP interactions (Baruch et al., 1999). The CiDRα domain of PfEMP-1 binds to CD36 leads to the recognition of parasite and internalization by macrophages. The peptide PpMC-179 which corresponds to the minimal CD36-interacting domain taken from PfEMP-1 used in blocking the PfEMP-1 binding and inhibiting the cyto-adherence of Plasmodium falciparum (Yipp et al., 2003a). The engagement of PpMC-179 with CD36 induces ERK1/2 and MAPK phosphorylation which is involved in regulating the cyto-adherence of parasitized RBC to endothelial cells (Yipp et al., 2003b). Similarly two peptides representing extended

TH-2507_156106009

immune-dominant region of CD36 (145-171 and 156-184) were used in inhibiting the parasitized RBC adhesion to CD36 which provides insights into therapeutic potential of these truncated peptides in treating malaria (Baruch et al., 1999). Obesity is one of the complication associated with diabetes (Serrano, 1998). CD36 is also associated with obesity in type-II diabetic patients (Bonen et al., 2006). An antimicrobial peptide Su2065 (cathelicidin) targeting CD36 inhibited the obesity in diabetes-induced obesity model of mice (Tran et al., 2016). Lipid accumulation is observed in diabetes-induced obesity (Goodpaster and Wolf, 2004). The fatty acid receptors such as free fatty acid receptor-2 and 3, CD36 are reported for their involvement in lipid accumulation in adipocytes (Hara et al., 2013). The CD36 expression on plasma membrane is regulated by ERK1/2 signaling pathway (Turcotte et al., 2005). The cathelicidin treatment inhibited the CD36 expression by blocking the ERK1/2 signaling (Tran et al., 2016). Apart from this, protein IMD (Intermedin), a calcitonin gene-related family has reduced the oxiLDL uptake and cholesterol accumulation in RAW 264.7 macrophages and also decreased the CD36 expression which represents a potential therapeutic agent in treatment of obesity associated with diabetes (Wang et al., 2014). A Growth hormone releasing peptide hexarelin was also reported for its application in atherosclerosis by targeting the CD36 (Bodart et al., 2002). CD36 acts as a regulator of lipid homeostasis (Zhao et al., 2018) by promoting the macrophage cholesterol efflux (Rodrigue-Way et al., 2014) and uptake of oxiLDL, which is involved in atherosclerotic plaque formation (Choromańska et al., 2017). The treatment of hepatocytes (HepG2 cells) with hexarelin was rapidly phosphorylated at Ser-872 position on HMG Co-A reductase, resulting in inactivation of rate-limiting step in cholesterol synthesis. Further the HMG Co-A reductase degradation increased by hexarelin treatment by recruiting anchor proteins Insig1 and Insig2. This study explored the potential of CD36 ligand hexarelin in controlling the atherosclerotic plaque formation by modulating the HMG Co-A reductase and Insig-1/2 expression in CD36 mediated pathway (Rodrigue-Way et al., 2014). Hexarelin was earlier reported for attenuating the cardiac fibrosis in rat (Xu et al., 2012), protecting against myocardial infarction in mice (Mao et al., 2014) and improving cardio myocyte function in streptozocin-induced diabetic rats (Zhang et al., 2018). EP 80317, another peptide derived from growth hormone releasing peptide group with no growth hormone releasing activity, was reported for its potential roles in anti-atherosclerotic (Marleau et al., 2005) and disrupting Amyloid-β-CD36 interactions (Bulgarelli et al., 2009). The

TH-2507_156106009

treatment with EP 80317, a selective inhibitor of CD36 in macrophages significantly decreased the oxiLDL uptake and interfered the cholesterol metabolism by targeting Peroxisome proliferator-activated receptor gamma-Liver X receptor alpha-ATP binding cassette (PPARγ-LXRα-ABC) transporter pathway (Marleau et al., 2005). The recruitment of the mononuclear phagocytic cells to lesion was modulated by CD36. The treatment of EP 80317 in mice reduced the number of phagocytic cells to plaque area, and the area of plaque is also reduced by 43%. The treatment reduced the phosphorylation of PyK2 in a Src kinase-dependent manner. The oxiLDL stimulation in macrophages involved Src family kinases recruitment. Hence, it was concluded that the EP 80317 acts through CD36 in protecting from atherosclerosis (Harb et al., 2009). Taken together, targeting the CD36 with peptide molecules has potential in correcting the pathology associated with CD36 in infectious and non-infectious diseases.

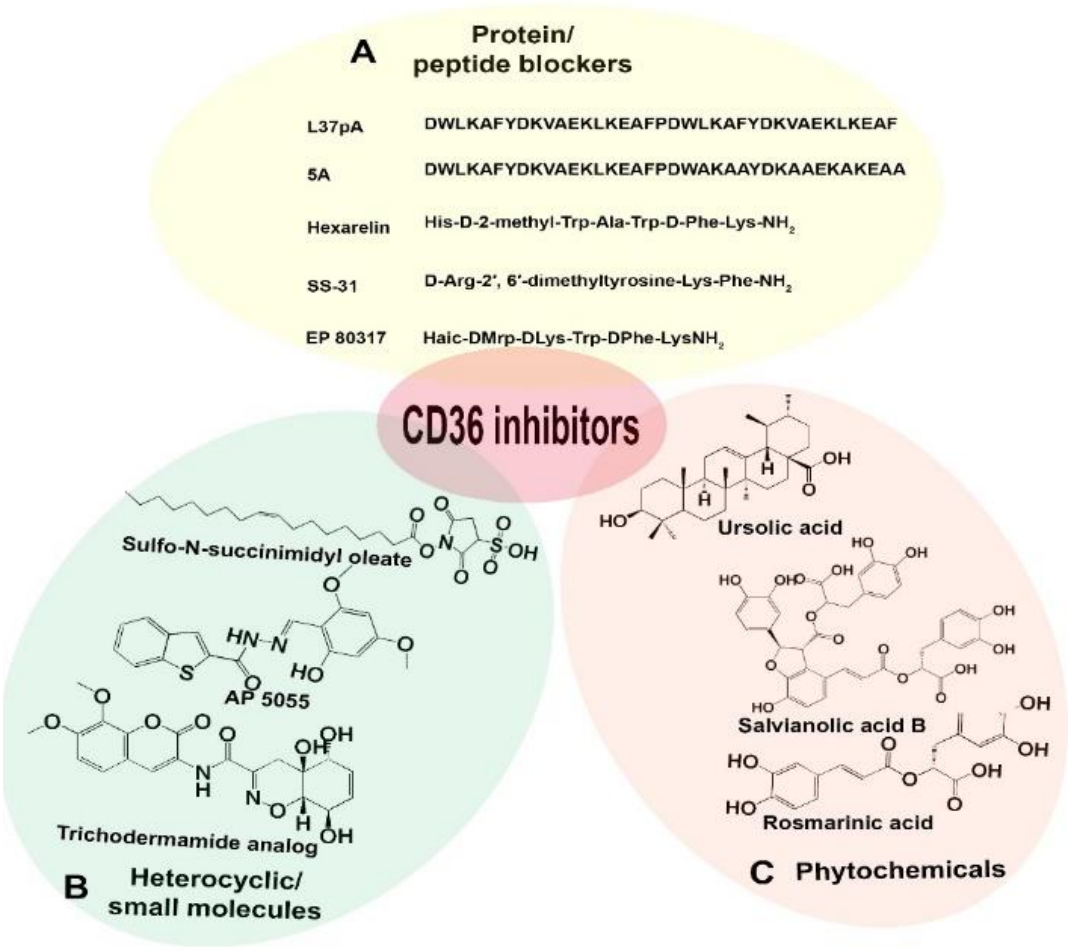

Figure 1.13. Diversity of CD36 blockers.

TH-2507_156106009

1.5.2. Small synthetic heterocyclic molecules: Various heterocyclic and small molecule inhibitors have been explored for their therapeutic potentials in CD36 mediated pathology. An oleic acid derivative sulfo-N-succinimidyloleate (SSO) has been reported for its effectiveness during atherosclerosis. During atherosclerosis lipid uptake and its oxidation provokes the inflammation (Insull Jr, 2009) and it is mainly regulated by the scavenger receptor CD36 also known as fatty acid translocase (Park, 2014). The free fatty acid uptake by the cells is inhibited upon treatment with SSO (Kuda et al., 2013). The SSO and LCFA binding regions are similar. The SSO irreversibly binds to the K164 of CD36 and blocks the binding of the LCFA. It interferes the intracellular calcium signaling to ultimately abrogating CD36 mediated down-stream signaling events (Coort et al., 2002). In cell-based assay, the treatment of macrophages with 25 µM of SSO inhibited the oxiLDL uptake by 50% (Xu et al., 2010). The selective inhibition of CD36 with SSO also implicated in mitigated the hepatocellular carcinoma and correcting the metabolism in diabetic heart (Nath et al., 2015). During HCV infection the treatment of Huh7.5 cells with SSO inhibited the attachment of the virus to cells. The direct blocking of HCV E1 protein-CD36 interaction might be the reason for attachment of virus (Cheng et al., 2016). Another molecule W-9 was also showed effective against HCV infection in Huh7.5 cells. However, the selective activity of the W-9 compound was found to be less compared to the SSO. The results suggests the binding of the molecules to CD36 domain could be different but could be a potential molecule if the potential groups which impart this activity can be highlighted through derivatization (Cheng et al., 2016; Mansor et al., 2017).

The vitamin α-Tocopherol has been reported to inhibit the CD36 expression in monocyte-derived macrophages (MDMs), monocytes, aortic smooth muscle cells and in hypercholesterolemic rabbits (Devaraj et al., 2001). In MDMs, the treatment with α-Tocopherol reduced expression of CD36 and SR-A and inhibited the Ac-LDL, Dil-LDL uptake (Munteanu et al., 2006). It is not very clear how the vit-E inhibiting CD36 expression, but according to one report, the PPAR-γ mediated pathway might be targeted (Özer et al., 2006; Ricciarelli et al., 2000). By summing up the effects mediated by Vit-E, it is inferred that it would be a possible therapeutic molecule for treating atherosclerosis but further research needed. A series of heterocyclic compounds AP5055, AP5156, AP5258 were also protected diabetic dyslipidemia and atherosclerosis by inhibiting the CD36 (Geloen et al., 2012). The AP5055 was also found to be active against the HCV infection with an EC50 of

TH-2507_156106009

0.39 ± 0.16 µM (Munteanu et al., 2006). The 3-cinnamoyl indole has been found in a high throughput screening assay to inhibit lipid uptake by CD36 and can be a therapeutic molecule in Atherosclerosis (Xu et al., 2010).

Table 1.2. CD36 targeting molecules with therapeutics outcomes

S.No	Molecule	Target disease	Dissociation constant (K_D)	References
1	L37pA	Acute lung injury, Inflammation	ND	(Bocharov et al., 2016)
2	5A	Inflammation, renal injury	1.45 µM	(Nowacki et al., 2016; Tabet et al., 2010)
3	SS31	Alzheimer's	ND	(Cho et al., 2007; Jia et al., 2016)
4	PpMC-179	Malaria	ND	(Yipp et al., 2003a)
5	IMD	Atherosclerosis	ND	(Wang et al., 2014)
6	Su2065	Obesity	ND	(Tran et al., 2016)
7	Hexarelin	Atherosclerosis	0.95±0.26 µM	(Bodart et al., 2002; Demers et al., 2004)
8	EP 80317	Atherosclerosis	1.7±0.14 µM	(Demers et al., 2004; Marleau et al., 2005)
9	SSO	Hepatocellular carcinoma	25 µM	(Kuda et al., 2013)
10	Vitamin E	Atherosclerosis	ND	(Ricciarelli et al., 2000)
11	AP5055	Atherosclerosis	1±0.1 µM	(Geloen et al., 2012)
12	AP5258	Atherosclerosis	5±1 µM	(Geloen et al., 2012)
13	3-cinnamoyl indole	Atherosclerosis	ND	(Xu et al., 2010)
14	Trichodermamide analogs	Alzheimer's	11 to 43 µM	(Doens et al., 2017)
15	Ursolic acid	Alzheimer's	82.9 ± 10.9 µM	(Doens et al., 2017; Wilkinson et al., 2011)
16	13-pentyl berberine	Atherosclerosis	ND	(Xu et al., 2010)
17	Salvianolic acid B	Atherosclerosis	3.74 µM	(Wang et al., 2010)
18	Rosmarinic acid	Atherosclerosis	25.1 µM	(Wang et al., 2010)
19	Sodium danshenshu	Atherosclerosis	37.8 µM	(Wang et al., 2010)
20	Nobiletin	Cancer	ND	(Sp et al., 2018)
21	ELK-B, ELK-B1	Bacterial infections	ND	(Bocharov et al., 2004)
22	W-9	atherosclerosis	ND	(Cheng et al., 2016)
23	K-134	cancer	ND	(Ikenoya et al., 2007)

TH-2507_156106009

In Alzheimer's disease, scavenger receptors role is predominant and contributes to inflammation. Researchers tried to block the interaction between β-amyloid with CD36 using trichodermamide analogues (Doens et al., 2017). Seven derivatives of trichodermamide were found to binding at the hydrophobic tunnel on CD36. Moreover, the treatment of the peritoneal macrophages (pre-stimulated with amyloid-β fragments) with these analogues inhibited the production of TNF-α, IL-1β and IL-6 which will show their potential in treating the Alzheimer's disease (Doens et al., 2017). During Arterial thrombotic disease the increased platelet activation leads to pathology and associated complications. Current medications are focused on anti-platelet agent such as Aspirin if only the patients have high cardiovascular risk and controlled blood pressure (Gkaliagkousi et al., 2010; Rajagopalan et al., 2007). But the risks associated with this treatment in low-risk hypertensive patient's forces to discover new agent's suits for strengthening the heart and anti-platelet activity. As CD36 is associated with fatty acid uptake and involved in cardiovascular diseases and platelet activation some of the studies explored to block collagen binding region on CD36 and found that they are useful and can be used as anti-platelet agents. It was well established that CD36 is a major collagen receptor for platelet activation (Kehrel et al., 1998). The quinolinone derivative K-134 (((–)-6-[3-[3-cyclopropyl-3-[(1R,2R)-2-hydroxycyclohexyl]ureido]-propoxy]-2(1H)-quinolinone) has been found to be effective in competing for collagen binding region. The interaction between K-134 and CD36 need to be studied further before using it in clinical investigations (Ikenoya et al., 2007). The nonapeptide analogue of thrombospondin, ABT-510 has potential to inhibit the CD36 and can be utilized in anti-angiogenesis (Isenberg et al., 2008). Although the molecules reviewed in this section focused on non-infectious diseases, it can be possible to explore these molecules in correcting the pathology associated with a CD36-ligand binding in infectious diseases as well.

1.5.3. Plant-derived phytochemicals: Ursolic acid, a triterpenoid compound from fruits used in daily life has been reported for its ability to disrupt the interaction between β-amyloid and CD36. The treatment of ursolic acid has inhibited the production of ROS in a dose-dependent manner in Chinese hamster ovary (CHO) cells. Ursolic acid at 20 µM causes maximum 64% inhibition of Amyloid-β interaction with CD36 (Wilkinson et al., 2011). On contrary to the above observations the aggregated ursolic acid has partly detected by CD36 and causes IL-1β secretion, inflammation and ROS generation by activating macrophages (Ikeda et al., 2007) .

TH-2507_156106009

Apart from this the Ursolic acid was also reported for its diverse biologicals roles such as anti-inflammatory, anti-oxidant and ameliorating atherosclerotic plaques (Ikeda et al., 2008) especially hepatic steatosis in high-fat diet induced non-alcoholic fatty liver disease (NAFLD) in rats. During NAFLD the expression levels of CD36 along with other lipid metabolism associated genes has found to be increased. The treatment of ursolic acid in the NAFLD rats significantly decreased the levels of CD36 and improved the condition (Li et al., 2014). It could be possible to treat atherosclerosis by targeting CD36 with ursolic acid. The uptake of the lipids by macrophages/endothelial cells during atherosclerosis is considered to be an aggravating situation and the targeting the uptake may be beneficial (SHARMA et al., 2010). In an HTS assay, 13-pentyl berberine identified as the CD36 antagonist and it repressed the Ac-LDL uptake which is useful in the treatment of atherosclerosis (Xu et al., 2010). There are other phytochemicals salvianolic acid B (SAB), rosmarinic acid and sodium danshenshu were reported in antagonizing the CD36 and their ability to block the LDL uptake (Wang et al., 2010). Scavenger receptor CD36 plays crucial role in visceral fat accumulation following obesity and obesity induced diabetes as described in disease pathology section. The treatment with salvianolic acid B to BDNF mice showed reduced levels of visceral fat deposition and the insulin resistance improved (Yang et al., 2018). The molecules such as Sab, sodium dansheu, 13-pentyl berberine has been patented for their ability to reduce body weight and fat accumulation, improving insulin sensitivity by antagonizing CD36 receptor (Cho et al., 2016). Numerous research publications explored the role of CD36 in tumorogenesis. The scavenger receptor CD36 is involved in angiogenesis and promoting tumor growth. Recent research activity on discovering therapeutic agents for blocking CD36 and ultimately targeting the cancer revealed that a citrus peel harboring flavonoid Nobiletin, found to be active against the cancer in CD36 dependent manner. The CD36 role in tumor development in linked to the fatty acid metabolism in which CD36 is a crucial receptor. The nobiletin flavonoid inhibited the angiogenesis and migration of the tumor cells to other parts. The mechanistic study showed that this molecule acts through CD36 mediated STAT3/Nf-kB signaling pathway to inhibit the angiogenesis and tumor spheroid formation. This study also suggested that 200 μM of nobiletin completely inhibited the CD36 expression and abolished it's binding to thrombospondin. The molecule experimentally tested and need to be further taken up for clinical trials (Sp et al., 2018).

1.5.4. Molecules modulating CD36 expression:

Apart from direct CD36 interacting molecules there are other molecules reported to regulating CD36 expression indirectly and could be used as therapeutics. Statins are well known for their ability to inhibit HMG-CoA enzyme and their effect in lipid lowering. The treatment with atorvastatin and simvastatin significantly reduced the platelet CD36 levels and the uptake of ox-LDL. During atherosclerosis ox-LDL uptake and the higher CD36 expression causes whole damage to the host and acts as pro-atherogenic. The statins can be used as anti-atherogenic molecules by suppressing the CD36 expression could be useful and re-purposed for treatment of atherosclerosis (Bruni et al., 2005). Non-alcoholic steatohepatitis is aggressive form of NAFLD and currently there is no therapeutic molecules has been developed. The liver and non-liver mortalities are very high in this particular NAFLD. The drug development strategies focused on lipid metabolism and inflammation in hepatocytes (Patel and Siddiqui, 2018). For treatment of NAFLD mediated inflammation and fat accumulation PEGylated-curcumin has been evaluated in recent studies. Curcumin itself well studies for its ability to reduce inflammation, atherosclerosis and obesity (Zingg et al., 2017). But the therapeutic effects of curcumin are limited because of bioavailability problems. The polyethylene glycol conjugated curcumin PEGylated curcumin (PEG-curcumin) has tested for its therapeutic effects in NAFLD steatosis. The treatment of high fat diet (HFD) fed mouse (C57BL/6J) with PEG-curcumin reduced overexpression of CD36 induced by HFD. The mechanistic studies revealed that the PEG-curcumin cAMP response binding protein. The cAMP response binding protein negatively regulates the PPAR-γ/CD36 pathway (Liu et al., 2017). The treatment with artemisinin a sesquiterpene isolated from *artemisia annua* has been found to be effective in reducing hepatocellular lipid accumulation in SMMC-7721 cells. This method can be extrapolated to treatment of Non-alcoholic hepaticsteatosis but further studies needed to repurpose this drug (Wang et al., 2017). Cilostazol a quinolinone derivative has been suggested for its anti-atherogenic effects but it is unclear how it regulates the atherogenic plaque formation. During atherosclerosis the lipid peroxidation takes place which could lead to generation of various byproducts which in turn acts on the receptors and substantiates the inflammation. During this process 4-hydroxynonenal (HNE) was derived and acts on enhancing the CD36 expression which is well documented for its role in atherosclerosis plaque formation and associated pathology. Cilostazol treatment attenuates HNE mediated

scavenger receptor CD36 expression thereby bringing the lipid accumulation down. It was also noted that cilostazol also known to inhibit ROS generation (Yun et al., 2009b).

1.6. Role of CD36 in malaria like condition

Malaria is a burden on humanity as it evident from the number of cases reported in 2018. According to world malaria report, 228 million new cases and 0.4 million deaths were reported globally. Malaria is a parasitic infection caused by the Plasmodium species. The infection transmitted through the mosquito bite which releases sporozoites into host bloodstream. The sporozoites migrate to the liver and infect hepatocytes. At this point, they differentiate into schizont harboring thousands of merozoites (Figure 1.14). The merozoites released into bloodstream infects RBC where they start erythrocytic stage of lifecycle (Soulard et al., 2015). Binding of the parasite to RBC involves various host-parasite interactions including the adhesion molecules from host cells and their counterparts from parasite (Jenkins et al., 2007). The invasion of the parasite into RBC changes the structural integrity of the RBCs (Cooke et al., 2001). Maturing the parasite inside the RBC produces >320 different proteins in which some of them are directed to the cytoplasm and some of them to the plasma membrane of RBC (Hiller et al., 2004). Among the parasitized RBC surface proteins, PfEMP-1 is involved in sequestration of infected RBC to vasculature (Cooke et al., 2006). CD36 involved in recognition of PfEMP1 which facilitates the binding of PRBC to endothelial receptors. The tethering of PRBC to endothelial receptors prevents the destruction and splenic clearance of PRBC. The CiDRα2 domain of the PfEMP1 interacts with CD36 ectodomain at 151-163 region in which the residue F153 is crucial for interactions(Hsieh et al., 2016). The CD36 plays a crucial role in phagocytosis of PRBC (Patel et al., 2004; Smith et al., 2003). It was also found that the uptake of oxidized heme polymer is toxic to the phagocytic cells and induce apoptosis (Deshmukh and Trivedi, 2014). It also acts as sequestration element for the parasite which supports parasite growth (Fonager et al., 2012). The sequestrin, a 270 kDa protein from PRBC could be a ligand recognized by the CD36 and the adhesion of the PRBC to macrophages is inhibited by blocking the CD36-specific monoclonal antibody, OKM8 (Ockenhouse et al., 1991). Apart from this, the study of the molecular interactions that leads to the binding of PRBC to the macrophages revealed that the process of binding is mediated by the CD36 redox-dependent mechanism. The reduction of the CD36 with reducing agents

TH-2507_156106009

abolished the binding of the PRBC to CD36. The CD36 re-oxidization restores cytoadherence of PRBC to CD36 states that the CD36 is necessary for the internalization of PRBC (Gruarin et al., 2001). The role of the TLR during malaria infection inevitable but CD36 mediated internalization of PRBC does not need TLRs. Pretreatment of macrophages with TLR agonists such as Pam3CSK4, FSL-1 was found to increase the secretion of pro-inflammatory cytokine levels (Erdman et al., 2009). The opsonization of PRBCs brings the macrophages to engulf and induce an innate immune response by secreting IL-10, IL-12, IL-18, TNF-α, and IFN-γ cytokines (Zhou et al., 2012). IFN -γ and IL-18 are crucial for the early clearance of parasite burden. To add further, CD36 also contributes the regulation of parasite burden during early blood stage infection, and pro-inflammatory cytokine secretion by dendritic and natural killer cells (Thylur et al., 2017).

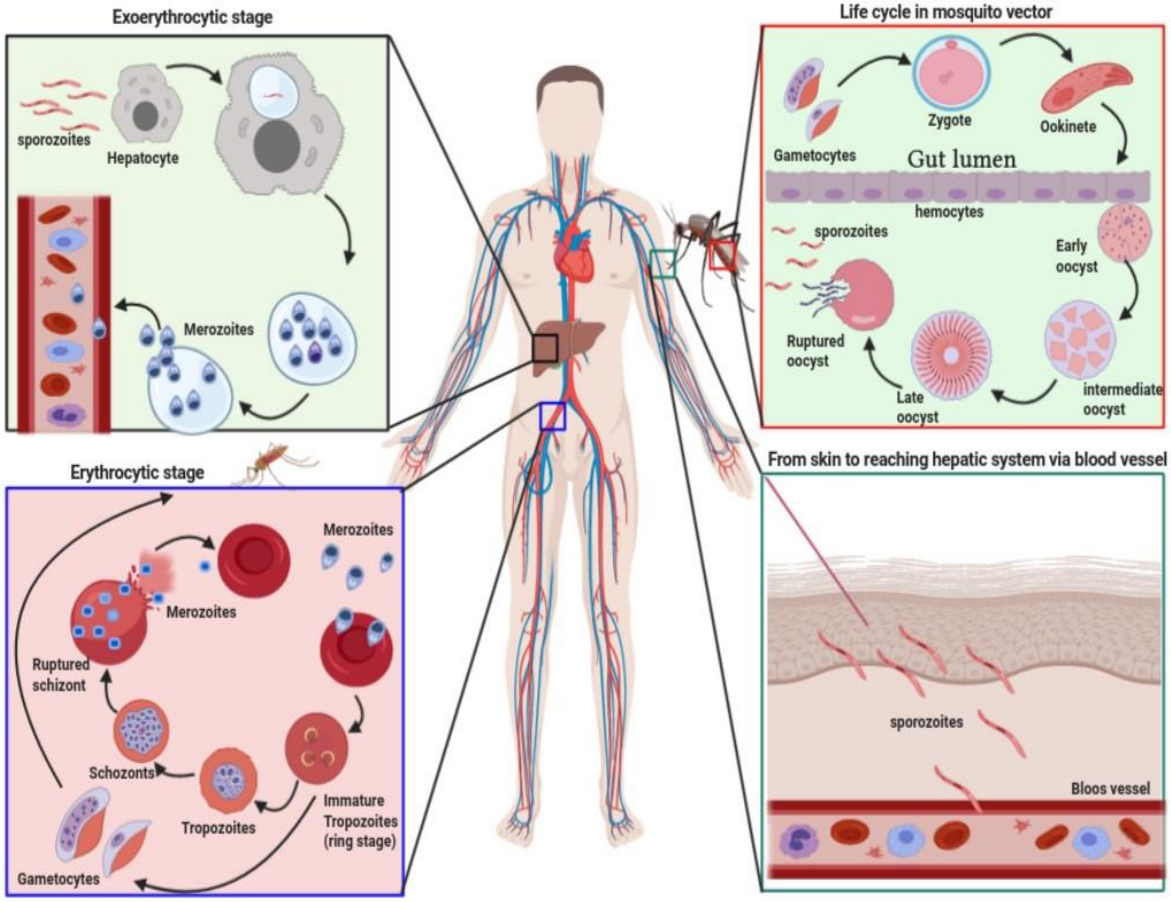

Figure 1.14. Malaria parasite life-cycle. The figure represents the asexual lifecycle in human and sexual lifecycle in mosquito.

Malaria like condition: During RBC rupture, the merozoites along with several host and parasite metabolic/waste products released into blood stream. The molecules act as pro-oxidants and contribute to the pathology. The role of such pro-oxidant molecules summarized below (Figure 1.15).

Haemozoin: During malaria, the malaria parasite digests the hemoglobin into proteinaceous part globin and non-protein prosthetic part free heme (Klonis et al., 2011). The globin part of protein utilized as source of amino acids by parasite since it has limited capacity to synthesize amino acids through de-novo pathway (Wrenger et al., 2005). The free heme is toxic to parasite so the parasite converts it into non-toxic haemozoin through apohaemozoin peptide (Ashong et al., 1989). The haemozoin is also called as malaria pigment due to its appearance in late blood stages of malaria. The evidence suggests that the haemozoin responsible for the immune-dysfunction in macrophages (Scorza et al., 1999). The macrophages fed with haemozoin exhibit phagocytic depression, production of oxidative burst and impaired bactericidal activity (Prada et al., 1996). Further the haemozoin stimulated macrophages to secrete pro-inflammatory cytokine TNF-α, MCP-1, MIP-1α, MIP-1β, and chemokines CXCL-1, CXCL-9, CCL2, and CCL3 (Jaramillo et al., 2005).

Methemoglobin: The hemoglobin released into blood stream readily forms the methemoglobin. During malaria the increased levels of methemoglobin, causes RBC susceptible to the osmotic pressure (Chang et al., 2003). It has been shown that the RBCs exposed to methemoglobin, show oxidative stress. The oxidative stress in RBC causes PS externalization and aggregation of RBCs which could be involved in clogging of microvasculature (Balaji and Trivedi, 2013; Kaul et al., 1991). The RBCs with exposed PS recognized by macrophages and taken up by phagocytosis. The phagocytosis of free hemoglobin by macrophages causes apoptosis in macrophages (Ren et al., 2003). The methemoglobin also activates the endothelial cells and the activated endothelial cells produces the cytokines. The prolonged deposition of methemoglobin in body is toxic to brain, neurons, heart and lungs (Carmona-Fonseca et al., 2009). The methemoglobin mediated cytokine secretion, oxidative stress and cellular or organ toxicity is implicated in the cerebral malaria pathology (Deshmukh and Trivedi, 2013).

Hemin: Hemin is a prosthetic group in heme proteins and involved in various cellular biological functions. In various hemolytic events or pathological conditions the free heme is

released and oxidized. The hemin is a hydrophilic molecule and easily incorporated into membrane bilayers (Shaklai et al., 1985). The hemin intercalation into RBCs shown to have role in oxidative stress generation, PS externalization, loss of potassium ions from cells and enhanced RBC lysis and anaemia (Schmitt et al., 1993). It has been shown that the enhanced erythrophagocytosis of RBCs by macrophages reduced the viability of macrophages through hemin (Cambos and Scorza, 2011). The internalized RBCs release hemin inside the macrophages and the hemin cause oxidative stress in macrophages. During malaria the continuous release of hemin and prolonged stay in circulation causes inflammation.

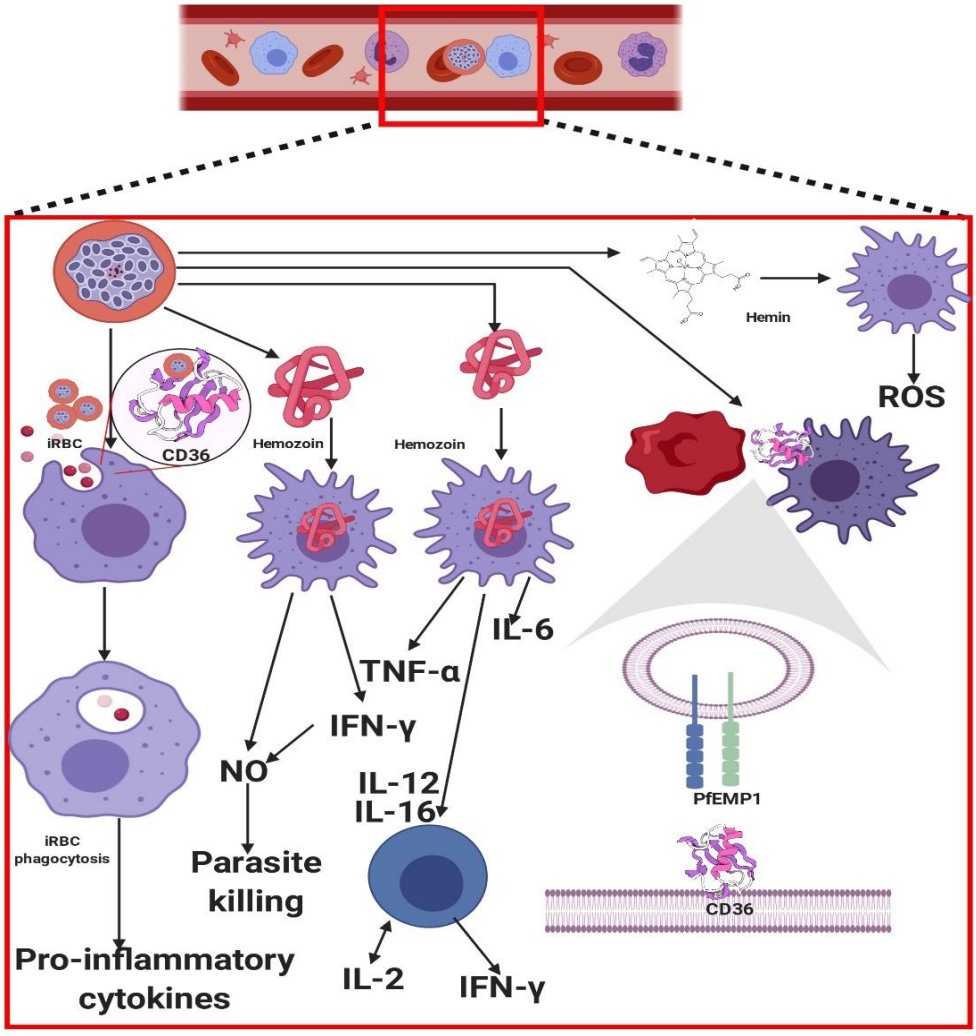

Figure 1.15. Pro-oxidant molecules induced inflammation during malaria. During malaria various pro-oxidant molecules generated and has potent pro-oxidant affects. The hemozoin, hemin were involved in various pathological consequences during malaria.

1.7. Role of CD36 in pathophysiology of the different organ in malaria like condition

The pathological conditions with malaria are complicated which is starts from parasite harbouring to leading new infection. Parasitemia generally exceeds and go beyond 50,000 infected RBCs for each microliter of blood. A variety of host and parasitic products such as hemin, methemoglobin and other cellular contents are released upon infected RBC lysis which is correlative with malaria symptoms including fever and lethargy. The parasitic infection of RBC will change the RBC membrane protein expression and utilizes the host cell machinery (Nash et al., 1989). Among the proteins expressing on surface of RBC PfEMP1 is studied broadly. PfEMP1s is binds to the variety of ligands on different cells and functions in sequestering the iRBC into various tissues, which saves the entering iRBC into the spleen. The PfEMP1-mediated sequestration of iRBCs into different tissues has been implicated in the pathogenesis of severe malaria (Pasternak and Dzikowski, 2009). Apart from PfEMPs Intracellular parasites digest the haemoglobin which results in formation of polarized crystal hemozoin. The hemozoin stored in parasite food vacuole. The parasites obtain energy beginning anaerobic glycolysis of glucose to the lactic acid, which implicated in clinical findings of hypoglycemia and lactic acidosis. Besides the parasites reduce the RBC membrane deformability which is a key event in secondary infection to new RBC. After the 48 h duration of lifecycle in RBC the schizonts are released into blood stream by rupturing the RBC membrane. The consequence of this event is anaemia which is fatal in case of thalassemia patients. The crystal studies are evident that the CIDRα domain is binds to phenylalanine residues which are harbours in the hydrophobic pocket (Hsieh et al., 2016). The other complication includes the impaired erythropoiesis which directly leads to anaemia. The uptake of infected RBCs by macrophages may result in activates the cytokine release which will eventually leads to the sterile inflammation in atherosclerosis, brain stroke and tissue injury (Stewart et al., 2010). Infected RBCs are sequestered into vascular endothelium and enters the brain, kidney where they adhere to the cells, disrupt the vascular endothelial cells. This leads to the fatal pathophysiological condition cerebral malaria (Newbold et al., 1997). The pathogenesis of malaria is complicated and involved various host and parasite factors. All types of malaria exhibits similar symptoms such as fever with chills. Based on the severity, malaria divided into uncomplicated malaria and severe malaria. The complications of malaria associated pathology includes the anaemia, liver failure, pulmonary oedema, and acute renal

TH-2507_156106009

failure.

1.7.1. Anaemia: The apparent pathological outcome from plasmodium infection is the lysis of RBC resulting anaemia (Ekvall, 2003). The RBCs are major site for parasite growth and development. The children and pregnant women faces difficulty because of developed anaemia during malaria (Rogerson et al., 2000). With repeated lysis cycles the hemoglobin levels will decrease and this will severely affect the host oxygen carrying capacity. Further, during malaria the scavenger receptor CD36 facilitate the infected RBC as well as non-infected RBC by non-opsonic phagocytosis may also contribute to the anemia. The degree of hemolysis depends on the parasitemia, and duration of infection. Enhanced splenic clearance of IRBCs as well as uninfected RBCs, dysregulated erythropoiesis in the bone marrow, and drug induced hemolysis also contributes to the anaemia during malaria infection (Price et al., 2001) (Figure 1.16).

1.7.2. Splenomegaly: Spleen is an important organ and play crucial role in the destroying senescent RBCs and pathogens such as plasmodium parasite. During early infection, the spleen is the main organ involved in developing immune response against parasite (Engwerda et al., 2005). The deformed and infected RBCs passed to sinusoidal spleen and impairment in clearing traps the RBCs in spleen which results in enlarged spleen also known as splenomegaly (Wyler et al., 1981). The altered rheological properties of RBCs is the major determining factor for splenomegaly (Wyler et al., 1981). The splenectomized patients showed higher parasitemia and during P. falciparum infection suggests the crucial role spleen plays during malaria infection (Scherf et al., 2008). Further the CD36 mediated sequestration of IRBC into spleen may leads to overcrowding of parasite and enlarged spleen (Fonager et al., 2012). Sometimes the rapid enlargement of spleen due to over parasite and RBC entrapment leads to splenic rupture which is a serious pathological outcome associated with malaria (Mackintosh et al., 2004) (Figure 1.16).

1.7.3. Liver pathology: The most common features of severe malaria is the hepatic dysfunction. After passing the hepatic sinusoid the sporozoites attach and enter into hepatocytes. The sporozoites developed into merozoites in liver (Viriyavejakul et al., 2014). Due to the parasite activity the liver function compromises and results in jaundice. The

TH-2507_156106009

apoptosis and necrosis of hepatocytes was observed and the discoloration or black color spots were found on liver. The hepatic dysfunction associated with malaria is characterized by elevated levels of bilirubin, transaminases and alkaline phosphatase enzymes. In patients with recurrent malaria condition the liver also found to be enlarged (Scaccabarozzi et al., 2018) (Figure 1.16). The sporozoites injected into human by anopheles mosquito eneter the liver after crossing several barriers. The circumsporozoite protein molecular interaction with HSPGs allow the parasite to enter the hepatocytes (Frevert et al., 1993). The hepatocytes also express the CD36 on their surface and responsible for parasite uptake by hepatocytes (Liu et al., 2018). Further, the kupffer cells, the resident macrophages of liver trigger immune response against the parasite. The kupffer cells expressing CD36 on their surface may recognizes the parasite and primes the non-opsonic phagocytosis, generation of oxidative stress and pro-inflammatory cytokine secretion to kill the parasite (Lagassé et al., 2016). The CD36 mediated cytokine secretion may involve in pathology of liver.

1.7.4. Renal failure: The acute renal failure is more common with P.falciparum infections compared to the other variants of parasite (Barsoum, 2000). The renal failure attributed to the mechanical obstruction of tubules by infected RBCs. The infected RBCs also responsible for fluid loss and attracting immune cells to the site. Besides the intravascular hemolysis is also responsible for the renal failure. The oliguria is the characteristic feature of renal failure during malaria (Trang et al., 1992) Figure 1.16.

1.7.5. Cerebral malaria: The most severe form of malaria associated with mortality in human beings. According to world health organization, 2013 report, 1% of the sub Saharan African children developed cerebral malaria whereas in adults 50% of deaths are due to cerebral malaria (CM) (Murphy and Breman, 2001). The etiology and causes behind the developing of CM is not clear so far. The common symptoms in patients with CM is seizures, convulsions, neurological abnormalities, delirium and coma in few cases (Murphy and Breman, 2001).Currently available evidence suggests the sequestration of IRBC into brain capillaries and microvasculature is characteristic feature of CM (MacPherson et al., 1985). The sequestration of IRBC is also detected in heart, lungs, kidneys, and intestine (Milner Jr et al., 2013). The infected RBC express various cell adhesion molecules such as PfEMP-1 and attach to receptors present on endothelial cells (Armah et al., 2005). The attachment of IRBC to the

TH-2507_156106009

endothelial receptors such as ICAM-I and VCAM activates the endothelial cells (Turner et al., 2013). Recent evidence suggests the scavenger receptor CD36 is also involved in CM development by facilitating IRBC binding to the endothelial cells (Hsieh et al., 2016). The IRBC attachment to endothelium clogs the blood flow in microvasculature. More-over the cytokines released during the IRBC interaction with glial cells, the resident macrophages in brain contribute to the blood brain barrier (BBB) integrity loss (Maneerat et al., 1999) (Figure 1.16).

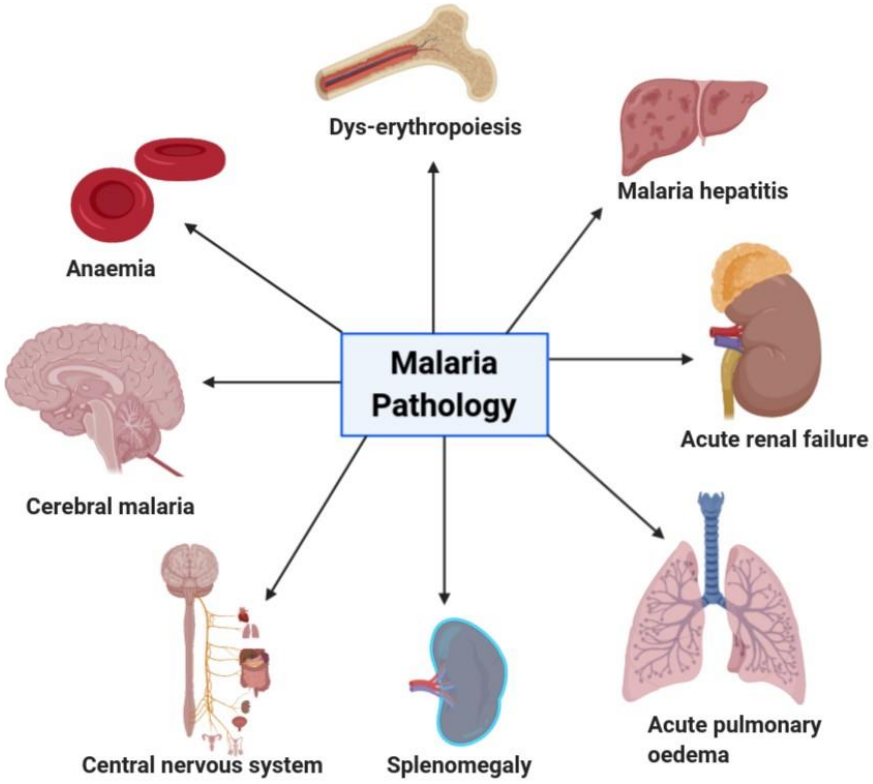

Figure 1.16. Malaria pathology. The malaria infected RBCs sequestration to various organs is the prime reason for malaria associated organ dysfunction.

1.8. Objectives

Based on the problems stated above we hypothesized that PS interacts with CD36 in a precise location and helps to regulate the apoptotic cell count in circulation. Hemin may be acting through the CD36 since the CD36 has a large and diverse ligand repertoire and tends to scavenge the small molecules and regulates the immune response. Based on the hypothesis, we formulated the following objects for study.

TH-2507_156106009

1. Identification of PS recognition region on scavenger receptor CD36.

a). Cloning, over-expression and purfication of human CD36 ectodomain.

b). Biochemical characterization of the purfied CD36 ectodomain.

c). Affnity studies of purified CD36 ectodmain with PS.

d). Elucidation of PS biophore.

e). Investigation into molecular features that enable PS binding to CD36.

2. Exploring potentials of fluorophore conjugated CD36 ectodomain as an apoptosis detection probe.

a). Staining of healthy or apoptotic cells using FITC labelled CD36 ectodomain.

b). Evaluation of the ability of CD36 ectodomain to detect apoptotic cells in nucleated or non-nucleated mammalian cells.

c). Robustness analysis of CD36 ectodomain to detect apoptotic cells in presence of biological fluids.

3. Investigation of role of CD36 in hemin mediated immune dys-function in macrophages.

a). Identification and characterization of hemin binding region on CD36 ectodomain.

b). Study the intracellular signaling downstream to CD36 in hemin stimulated macrophages.

c). Identification of adaptor proteins downstream to CD36 in hemin treated macrophages.

d). Role of identified adaptor proteins and their impact on macrophage immune-dysfunction.

4. Identification of suitable hemin-CD36 interaction blockers and study their utility in Correcting macrophage immune-dysfunction.

a). Screening of phytochemicals or FDA approved drugs against hemin binding pocket on CD36.

b). Identification of high affinity molecules towards CD36 using affinity profiling.

c). Testing the blockers in mitigating the immune dysfunction in macrophages.

1.9. Aims and scope of the study

The overall literature review underlined that CD36 performs various immunological as well as sensing functions. The scavenger receptor CD36 acts as a sensor of lipid molecules, including phospholipids. The phospholipids such as phosphatidylserine (PS), phosphatidylcholine (PC), phosphatidylethanolamine (PE) were fundamental constituents of mammalian cell membranes and during cell senescence phase or apoptotic stage the PS which exists primarily on inner leaflet get externalized. Several reports highlighted the role of CD36 in detection and facilitation of phagocytosis of dead/aged cells through detection of PS, but the mechanistic details with regards to how CD36 interacts with PS remain elusive.

Apart from sensing functions, CD36 is also involved in clearing the malaria parasite from circulation by detecting the infected RBCs. During severe malaria, the cytokine secretion is very high and directly contributes to the pathology. It has been shown that the small chemical entities released from lysed RBCs due to parasite metabolic activity may contribute to the inflammation in host cells. The hemoglobin degradative product hemin released into the blood stream during lytic stage can be a potential molecule involved in the severe malaria pathology but how it interacts with immune cells and regulates the pathophysiology of the host is unknown.

By studying how CD36 interacts with PS and how hemin is involved in immune dysfunction can provide crucial information on how to exploit the CD36-PS interaction for science advancement and how to control hemin mediated pathology.

References: Please refer to the Bibliography section at the end of the thesis.

TH-2507_156106009

Chapter-II

Mapping of Phosphatidylserine recognition region on CD36 Ectodomain.

TH-2507_156106009

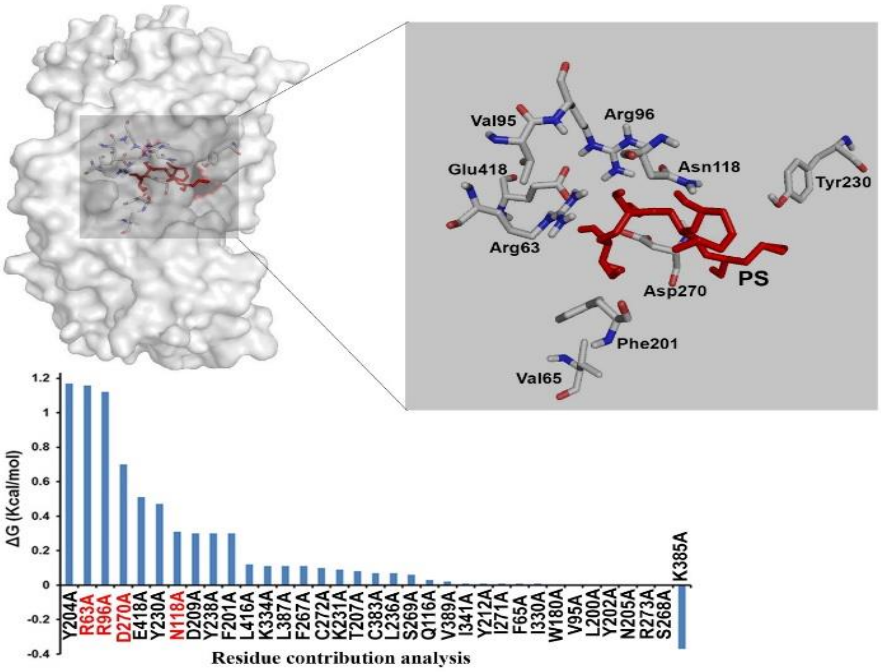

Summary

In this chapter we have investigated PS recognition region on CD36. To explore and map the PS binding region on CD36, we have cloned, over expressed and purified human CD36 ectodomain from bacterial expression system. The dot blot assay, Isothermal titration calorimetry studies of PS vesicles with CD36_ecto indicated the strong binding between PS and CD36 with K_D of 53.7 ± 0.48 μM. The PS biophore was elucidated using computational tools and a molecular model of CD36-PS was generated. Analysis of CD36-PS molecular model showed that the residues R63, R96, N118, D270 and E418 were forming hydrogen bonds with PS. Molecular dynamics simulations indicate that R63 mutation has disrupted the integrity of biophoric constituents, directly affecting the hydrogen bonding from R96, N118 and D270. Further, the affinity studies of mutant protein with PS vesicles indicate complete loss of binding with R63A and very low affinity of PS vesicles with D270A. These finding may help to design suitable agents mimicking PS biophore with potentials in diagnostics of apoptotic cells and cardiovascular intervention.

Key words: Apoptosis, PS, Affinity, Biophore Fingerprint, Molecular dynamics

***Content of this chapter has been published**

Banesh, S., Ramakrishnan, V. and Trivedi, V., 2018. Mapping of phosphatidylserine recognition region on CD36 ectodomain. *Archives of biochemistry and biophysics*, *660*, pp.1-10.

TH-2507_156106009

2.1. Introduction

Phosphatidylserine (PS) is an integral part of the plasma membrane of the mammalian cells (Verkleij et al., 1973). The PS is the major lipid present on the cytosolic side of the plasma membrane in a healthy cell (Kay et al., 2012; Op den Kamp, 1979; Tanaka and Schroit, 1983). As the cell becomes old and follow senescence pathway to undergo apoptosis, the membrane lipid composition and arrangement changes, resulting into the expression of PS on the outer side of the plasma membrane (Borisenko et al., 2003). The externalisation or presence of PS on the outer surface of plasma mem-brane in the cells is the hallmark signal to tag dead/aged/apoptotic cells (Shiratsuchi et al., 1998). The damaged or senescent cells are required to remove from the systemic circulation to avoid inflammation and tissue injury (Haanen and Vermes, 1995). Macrophages are professionally trained to identify and engulf aged/ dead/senescent cells from the circulation to maintain the body homeostasis (Deshmukh and Trivedi, 2014). Phosphatidylserine present on the cell surface is recognized by the scavenger receptor CD36 expressed on professional phagocyte macrophage (Baranova et al., 2008; Borisenko et al., 2003; Greenberg et al., 2006; Helming et al., 2009). CD36 is a transmembrane protein belonging to the scavenger receptor class B family, expressed in most of the immune cells (Hsieh et al., 2016). The protein has three regions; a large extracellular ectodomain, two short cytosolic domains and two transmembrane regions. The apex region of the ecto-domain is identified as the binding site for thrombospondin (Leung et al., 1992; Yesner et al., 1996), long chain fatty acids (Pepino et al., 2014), oxiLDL (Jay et al., 2015), oxiPS (Greenberg et al., 2006), iRBC (Gruarin et al., 2001) and LPS (Hoebe et al., 2005). All these cell surface ligands have well-defined structure, biochemical properties and charge distribution and need distinct features on ectodomain to bind CD36. The amino acids stretch 155–171 is responsible for the binding of oxiLDL to CD36 (Pepino et al., 2014). This region is also act as binding interphase for various ligands such as PfEMP-1, Hexarelin, oxiPL. The PfEMP-1 and CD36 interactions play a crucial role in pathogenesis of malaria. The binding of PfEMP-1 to CD36 is influenced by the phenylalanine residue (F153) found at the membrane distal tip of CD36. The mutation in this residue abolishes the interaction (Hsieh et al., 2016). Another key ligand of CD36 is thrombospondin which is involved in inhibition of the vascular endothelial growth factor (VEGF) signalling (Chu et al., 2013), phagocytosis of apoptotic cells (Yesner et al., 1996). The binding domain of thrombospondin on CD36 is different from the other ligands binding domain and

TH-2507_156106009

corresponds to the stretch of 93–120 amino acids (Pearce et al., 1995). The oxidised phospholipids present on plasma membrane interact with CD36 to perform various molecular recognition processes such as detection of apoptotic cells. The CD36 has been implicated in sensing the oxidised phosphatidylserine present on the external side of plasma membrane (Lee et al., 2015). PS present on cell surface is an important ligand as it has crucial role in giving signal to the cellular machinery for clearance of apoptotic cells through its interaction with CD36. PS in-teracts with CD36, but crucial interactions (or molecular properties) for recognition of PS is never known or explored so far. It is first time, CD36 ectodomain was over-expressed in bacterial expression system and purified to homogeneity. The protein was monomer and present in the native conformation. The dot-blot analysis shows the CD36_ecto selectively binds to the PS vesicles blotted on nitrocellulose membrane. PS binds strongly to CD36_ecto with a dissociation constant K_D of 53.7 ± 0.48 μM. The pharmacophore model for PS was generated after taking structural and physio-chemical information from previously available crystal structures of proteins-PS complexes from protein data bank. The residues Aspartic acid (D), Asparagine (N), Arginine (R) and Tryptophan (W) were found to be the key constituents of the PS pharmacophore. PS was docked on predicted pharmacophoric region on CD36 ecto-domain using Autodock 4.1. The stability of CD36_ecto-PS complex was analysed in molecular dynamics simulation studies. MD analysis indicate that the CD36_ecto-PS complex is stable within the experimental conditions. There are several key residues involved in making interaction between CD36_ecto and PS. The residues R63, N118 and D270 residues are interacting with the PS atoms through hydrogen bonding whereas the residue R96 was found to be forming a salt bridge with PS. Based on the interaction analysis, key residues R63, R96, N118 and D270 were mutated, and the affinity of CD36_ecto to PS was determined. The predicted change in binding energy upon mutating R63, R96 and D270 to alanine showed significant change in binding energy (ΔG) comparative to wild-type. It indicates importance of these residues in CD36 interaction with PS. Mutational analysis indicate that the residues R63, N118 and D270 are crucial for the binding of PS to CD36. These finding may help to design suitable agents mimicking PS biophore with potentials in diagnostics of apoptotic cells and cardiovascular intervention.

CD36 as sensor of biomolecules:

The scavenger receptor CD36 is a classical sensor of long chain fatty acids (LCFAs) and modified lipids. The LCFAs interact with CD36 at a tunnel like shape (stretch of 127-279

TH-2507_156106009

residues) surrounded by hydrophobic residues. The hydrophobicity of tunnel facilitates the passage of LCFAs inside cell. The sensing of LCFAs is crucial for fat metabolism and synthesis of bioactive eicosanoids (Pepino et al., 2014). The CD36 also recognizes the oxiLDL and involved in development of atherosclerosis pathology (Jay et al., 2015). Further, the CD36 is only recognizes lipid part but not the protein part suggests the selectiveness of CD36 towards lipids. The crucial function of CD36 is to detect pathogen derived lipids or lipopeptides. The macrophages with a non-sense mutation in CD36 are insensitive to bacterial lipopeptide and the mice carrying same mutation were severely immunocompromised and their system failed to clear the staphylococcus infection (Hoebe et al., 2005). A recent report suggests that CD36 homolog in insects detect the pheromones (Gomez-Diaz et al., 2016). Recent studies on phospholipid recognition by CD36 revealed that a novel oxidized phosphatidylcholine that possess sn-2 acyl ($oxPC_{CD36}$) serves as high affinity ligand for CD36 (Podrez et al., 2002a). The oxidized phosphatidylcholine with conserved structural motif promotes the binding of phospholipid to CD36 (Podrez et al., 2002b). However the binding location of oxidized phospholipids on CD36 is not clear. The scavenger receptor CD36 is also involved in sensing the apoptotic cells with externalized PS and various studies suggested the CD36 and oxidized PS (phosphatidylserine) interactions are crucial for recognition of apoptotic cells (Greenberg et al., 2006). The previous reports suggests that PS interact with CD36 but the molecular interactions that facilitate the binding of PS to CD36 and PS binding domain on CD36 is not known.

2.2. Experimental procedures

2.2.1. Reagents: LB media, dialysis membrane-70, skim milk, ampicillin, tween-20, and NaCl were procured from HiMedia, India. IPTG, nickel sulfate, ethidium bromide were purchased from Sigma-Aldrich, India. Ni-NTA (Qiagen, Hilden, Germany), primers (Bioserveindia, India). Restriction enzymes (XhoI, NheI), 1 kb DNA ladder, were purchased from New England Biolabs, USA. Dual colour proteins standards purchased from Biorad, California, USA. T4 DNA ligase was purchased from genetics, India. Dream Taq PCR master mix (2x) purchased from Fermantas, India. EZ-run protein marker purchased from Fisher Scientific, USA. PD-10 column was purchased from GE life sciences, India. Human CD36 gene, mApple-CD36-C-10 was a gift from Michael Davidson (Addgene plasmid # 54874), pET23a vector, BL21-(DE3), DH5α bacterial strains were from novagen. Mouse polyclonal anti-6xHis antibody purchased from Sigma-

TH-2507_156106009

Aldrich, India. anti-CD36 antibody and Rabbit HRP con-jugated secondary antibody were procured from Santa Cruz Biotechnology, USA. The POPS (16:0/18:1(9Z)) (cat# 840034C-10 mg), POPC: (16:0–18:1(9Z)) cat#. 850457C-25 mg, POPA: (16:0–18:1(9Z)) cat#. 840857C-25 mg, POPG: (16:0–18:1(9Z)) cat#. 840457C-25 mg, POPE: (16:0–18:1(9Z)) cat#. 850757P-25 mg were procured from Avanti polar lipids (Alabama, USA).

2.2.2. Cloning and Over-expression of Human CD36 ecto-domain: CD36 ectodomain was PCR amplified from mApple-CD36-C-10 vector using site-specific primers hCD36Ecto_F1:5′-AGCGCTAGCCTGC TTATCCAGAAGAC-3′ and hCD36Ecto_R2: 5′-ATCTCGAGGCCAAGGAG GTT-3′, verified the size on 0.8% agarose gel electrophoresis. The band corresponding to the CD36 ectodomain was excised, gel purified and ligated into the pGEM-T easy vector. Subsequently, pGEM-T-hCD36_ecto was double digested with NheI/XhoI and fragment was cloned into the expression vector pET23a. The bacterial colonies containing clone was confirmed by colony PCR, restriction digestion and sequencing. pET23a-hCD36_ecto was transformed into BL21(DE3), and over-expression was confirmed by SDS-PAGE and Western blot using anti-His antibodies. The BL21(DE3) cells carrying pET23a-hCD36_ecto clone was grown for 3 h at 200 RPM at 37 °C until to reach OD600 0.2–0.3. The soluble expression of protein is achieved by following slow induction at different temperature. The induction temperature was decreased to 8 °C and kept for 5 h. In the subsequent step, induction was done using 0.1 mM IPTG and kept for another 5 h. In next step the temperature was increased to 13 °C and maintained culture for 12 h. Subsequently, the temperature increased to 18 °C and followed by incubation for another 15 h. In the final step, temperature was increased to 23 °C kept for 15 h. In between each temperature, ampicillin was added, and finally, bacterial culture brings to 4 °C and pelleted down at 10,000 RPM for 10 min. The pellet is stored at −80 °C until next use.

2.2.3. Site-directed mutagenesis: The traditional PCR amplification method as described (Liu and Naismith, 2008) was used to introduce mutation in pET23a-hCD36_ecto at R63 (R63A) and D270 (D270A) positions using site directed primer (Table 2.1). The long range PCR reaction was performed in 50 µL volume containing 15 ng of pET23a-hCD36_ecto as template, 15 pM mutagenic primers, 200 µM dNTPs and 1 U Pfu-Turbo DNA polymerase (Agilent technologies, Santaclara-CA, USA). The PCR amplification was done by initial denaturation of 4 min at 94 °C, followed by 16 cycles of

denaturation at 94 °C for 30 s, annealing at 60 °C for 1 min and extension at 68 °C for 7 min. The amplified products were PCR cleaned up and eluted in 20 µL of nuclease free water. From the eluted product, 18 µL is Dpn-I digested for 1 h at 37 °C and the resulting product was transformed into NEB 5-alpha competent cells (New England Biolabs, Ipswich-MA, USA). The transformed colonies were picked, cultured and plasmid was isolated. For confirmation of mutation (D270A), an internal restriction site of MspI was introduced. Mutation was finally confirmed by sequencing of mutant clones as well.

Table 2.1. List of primers used in site-directed mutagenesis

S.No.	Primer ID	Sequence
1	R63A_FP	5′-gcacatcaaagatccaaaactgtgcgtaaacttctgtgcctgttttaa-3′
2	R63A_RP	5′-ttaaaacaggcacagaagtttacgcacagttttggatctttgatgtgc-3′
3	D270A_FP	5′-agcatagattgacctgcaaatag**ccgg**aagaaaagaactgcaatac-3′
4	D270A_RP	5′-gtattgcagttcttttcttctgctatttgcaggtcaatctatgct-3′

2.2.4. Purification: The bacterial pellet was re-suspended in lysis buffer (Tris.HCl pH 8.8–50 mM, NaCl-500 mM, glycerol-10%) and sonicated (6 cycles on, 6 cycles off) using probe sonicator. The lysate was clarified by centrifugation at 10,000 RPM for 20 min at 4 °C. The supernatant containing CD36 Ecotodomain was incubated with Ni-NTA agarose beads for 4hrs with intermittent shaking in cold. The beads were poured into the column and washed 2 column volume with the wash buffer-1 (Tris.HCl pH 8.8–50 mM, NaCl-500 mM, 20 mM imidazole). It was again washed 2 column volume with wash buffer-2 (Tris.HCl pH 8.8–50 mM, NaCl-500 mM, 50 mM imidazole), wash buffer-3 (Tris.HCl pH 8.8–50 mM, NaCl-500 mM, 100 mM imidazole) and wash buffer-4 (Tris.HCl pH 8.8–50 mM, NaCl-500 mM, 200 mM imidazole). Finally, hCD36_ecto was eluted with elution buffer (Tris.HCl pH 8.8–50 mM, NaCl-500 mM, 500 mM imidazole, glycerol-20%). The purity of protein was verified with SDS-PAGE and western blotting using anti-His anti-bodies. Fractions containing single band pooled together and dialysed against buffer 50 mM Tris.Hcl, pH 7.4 containing 300 mM NaCl. Similar purification protocol followed for purification of mutant protein.

2.2.5. Size exclusion chromatography: The size exclusion chromatography column Superose 12HR column was used to determine oligomeric status of the purified hCD36_ecto. Gel filtration column was equilibrated with 50 mM Tris.HCl, 300 mM NaCl

TH-2507_156106009

pH 7.4 at a Flow rate of 0.3 ml/min. Dialyzed hCD36_ecto or mutant proteins (R63A, D270A) were loaded onto superose 12 column, and chromatographic elution was monitored at A280 using UV-detector. Under the identical running condition, Superose 12 was calibrated using LMW gel filtration kit (GE Healthcare). The elution volume (V_e) is been used to calculate partition coefficient K_{av} and correlation between logM. Wt to partition coefficient is been used to calculate the molecular weight taking elution volume of CD36_ecto.

2.2.6. Liposomes preparation: The phospholipids were dried under Nitrogen, and dried lipids were hydrated with the Phosphate buffered saline, pH 7.4 and vesicles were prepared as described previously (Trivedi et al., 2006).

2.2.7. Dot-blot: Different phospholipids liposomes vesicles (PS, PC, PA, PG, PE) were applied on the nitrocellulose membrane as dot and air dried with the help of hair dryer. After drying, the membrane is blocked with 6% skimmed milk in PBS containing 0.05% Tween-20 for 1 h at room temperature. The membrane was incubated with purified hCD36_ecto for 2 h at 37 °C, and washed 3 times with wash buffer containing 25 mM Tris pH 7.4, 150 mM NaCl, and 0.05% Tween-20 pH 7.4. Subsequently, the blot was incubated with anti-CD36 antibodies followed by HRP-conjugated secondary antibody to detect presence of hCD36_ecto on membrane. Dot blot was developed using DAB (10 mg/ml) as chromogenic substrate. To test the ability of mutant protein (R63A or D270A) to binds PS, the PS vesicle probed strips were incubated with wild type or mutant (R63A or D270A) protein solution for 2 h at 37 °C. Subsequent steps were performed as described before to develop the blot.

2.2.8. Isothermal titration calorimetry (ITC): The MicroCal iTC200 system (GE Healthcare, Piscataway, NJ, USA) was used to measure affinity of PS liposomes towards hCD36_ecto. The hCD36_ecto or mutant protein (R63A, D270A) (0.025 mM) in a total volume of 200 µL was loaded into the ITC titration cell. The PS liposome solution 40 µL (stock concentration 0.25 mM) was loaded into syringe and introduced into the ITC titration cell. A total of 35 injections were carried out for titrations starting from 0.4 µL of initial injection and 1.16 µL in subsequent injections. To correct the heat values produced by buffer or PS liposomes alone, another titration was carried with buffer and PS liposomes in the absence of hCD36_ecto. Annexin V or BSA was titrated against PS liposomes under identical experimental conditions. Raw data obtained in titration were analysed using

TH-2507_156106009

ORIGIN7 analysis software (Origin Lab, USA) and fitted with sequential binding mode to calculate the dissociation constant, K_D of PS for hCD36_ecto, mutant proteins (R63A, D270A).

2.2.9. Circular dichroism spectroscopy: The Circular Dichroism spectra of purified 1 μM hCD36_ecto or mutant protein (R63A or D270A) in Phosphate buffer, pH 7.4, in the absence or presence of POPS vesicles (1:100 ratio) were recorded on JASCO J-1700 CD spectrophotometer. The scanning range is from 250 to 190 nm with a scan speed of 100 nm/min. A total of eight accumulations were recorded with a data pitch of 0.5 nm and slit width of 1 nm. All the scans were recorded in 1 mm path length cuvet. The CD spectra were analysed by CDpro suite and plotted using ORIGIN7 analysis software (Origin Lab, USA). Under similar conditions, POPS vesicles CD spectrum was recorded and used to correct the contribution of POPS in CD36-POPS CD36 spectrum.

2.2.10. Biophore fingerprinting of phosphatidylserine: To predict the biophore fingerprint of the PS, we analysed the biophore constituents from the PS bound proteins deposited in protein data bank. The PS co-crystalized proteins (1DSY, 2HJ6, 3BIB, 3KAA, 2JG6 and 4B2Z) were downloaded from protein databank. The immediate binding environment of PS with the Protein has been characterized using ContPro webserver (Firoz et al., 2010). We have identified 14 recurring amino acids in the binding site, and among them, Asp, Asn, Trp and Arg are the most consistent ones across six complexes analysed. A matrix (109 X 24) has been constructed with PS and Protein atoms to deduce an interaction fingerprint of PS association with different proteins. The distance between interacting atoms has been colour coded (in VIBGYOR scale with violet minimum and red maximum) with distance as the scaling criterion.

2.2.11. Molecular docking: To validate the biophore, docking study has been performed with Autodock 4.0 software (Morris et al., 2009). The CD36 ectodomain crystal structure (PDB ID: 5LGD) was downloaded from protein data bank and energy minimized. The structure for PS was taken from protein data bank (ligand ID: PSF). The grid was set up at the position where the biophore interactions are high. The GA runs of 100 and cluster tolerance of 2 per Å were used along with the torsional degrees of freedom 6. A maximum of 2500000 energy evaluations was performed for scoring and binding energy (kcal/mol) calculations.

TH-2507_156106009

2.2.12. Residue contribution analysis for PS binding: The most optimal binding pose obtained from binding energy calculations was used as the starting structure for Molecular Dynamics simulations for 20 ns. The mean structure of the largest cluster obtained through simulations were analyzed for the residues important for interaction using web server ABS-scan (Anand et al., 2014) to rank the relative prominence of individual residues in Protein-PS complex. The structural integrity of interaction fingerprint was ascertained by verifying the Φ, Ψ Ramachandran basins of receptor atoms from MD trajectory, using g_rama program in gromacs program suite.

2.2.13. Molecular dynamics studies of CD36_PS and mutants: The crystal structures of CD36 (PDB id 5LGD) or, different mutants were the starting structures for molecular dynamics simulations. Topology file of phosphatidylserine was obtained from PRODRG server. The simulations were performed with GROMACS 4.6.5 package using the GROMOS96 43a1 force field, on Dell precision T1700 workstations. The system was placed such that, any protein atom was at least 1.5Å away from the edge of the simulation box with periodic boundary conditions applied and solvated by simple point charge (spc) water. The structures were energy minimized by steepest descent algorithm successively in vacuum and water, in a simulation box with the size relatively 1.5 nm distant from the peptide in the all three axes. The 20 ns production runs for wild-type, and mutational variants of CD36 were performed with an integration step of 2 fs under NVT conditions. LINCS algorithm with geometric accuracy of 10^{-4} was used as the bond length constraint. Maxwell distribution was used for initial velocity calculations with 0.1 ps of coupling relaxation time at 300 K. The non-bonded interaction cut off was set at 1.4 nm for both van der Waal's and electrostatics (PME). The MD trajectories after production run were analyzed for root mean square deviation (RMSD), structure-based clustering, radius of gyration (Rg), root mean square fluctuation (RMSF) and generation of Ramachandran map for (Φ, Ψ) dihedral angle distribution.

2.3. Results:

2.3.1. Human CD36 Ectodomain is successfully expressed and purified in bacterial expression system

The gene fragment encoding for human CD36 ectodomain was PCR amplified (Figure 2.1A) from the mAPPLE-CD36-C-10 (Addgene plasmid # 55011) and cloned into the expression vector pET23a (Figure 2.1B). The clone containing human CD36 ectodomain

TH-2507_156106009

is labelled as hCD36_ecto throughout the thesis. hCD36_ecto was transformed into the BL21(DE3) and expression was found in inclusion bodies at 37 °C (Figure 2.1C). Expression of eukaryotic proteins in the bacterial expression system gives trouble due to large size, codon incompatibility and required machinery to correctly fold the mammalian protein in soluble form (De Marco et al., 2005). The Urea denaturation and refolding is not suitable in some cases as it does not give consistent results (Rosano and Ceccarelli, 2014). An alternate approach is to reduce the rate of protein synthesis to provide bacterial cells to fold the protein correctly (Jones et al., 1987; San-Miguel et al., 2013). Temperature programmed induction approach has slow down the protein production rate and gave us 46% protein in soluble fraction (Figure 2.1C). The inducer IPTG was also optimized (0–0.3 mM) to achieve best protein production in soluble fractions (data not shown). Further to the protein induction was confirmed by western blot using anti-His antibody (Figure 2.1D). The CD36 ectodomain was purified to homogeneity using affinity chromatography as evident by single band in SDS-PAGE (Figure 2.2A).

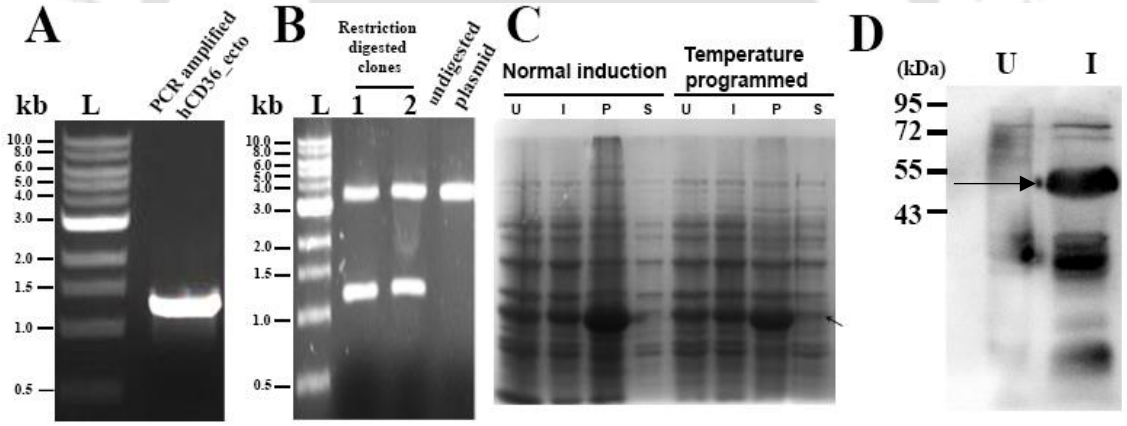

Figure 2.1. Cloning, over-expression of hCD36_ecto protein. (A) The CD36 ectodomain sequence harbouring from the mApple-CD36-C-10 PCR amplified using site specific primers and **(B)** cloned into pET23a(+) between NcoI and XhoI restriction sites. **(C)** The overexpression and soluble expression analysis in BL21(DE3) following temperature programming approach. Un-uninduced, I-Induced, P-pellet, S-supernatant. **(D)** Western blot used to verify the expressed proteins. (The lysates were probed with anti-His antibody). The black arrow indicates the position of the hCD36ecto. U-uninduced lysate and I-induced with IPTG.

The yield of CD36 ectodomain in bacterial expression system is ~2 mg per litre of bacterial culture. Human CD36 ectodomain exists as a monomer on plasma membrane in native state and forms dimer or multimers in ligand-bound state (Thorne et al., 1997). It is

TH-2507_156106009

the first report to express CD36 ectodomain in bacterial expression system in soluble form, and it is necessary to determine the oligomeric status of the protein. In gel filtration chromatography, protein elute at 12.65 ml which corresponds to native molecular weight 53 kDa, and it matches well with subunit molecular weight of CD36 ectodomain (Figure 2.2B and 2.2C). Gel filtration analysis indicate that the CD36_ecto is monomeric and present in native conformation.

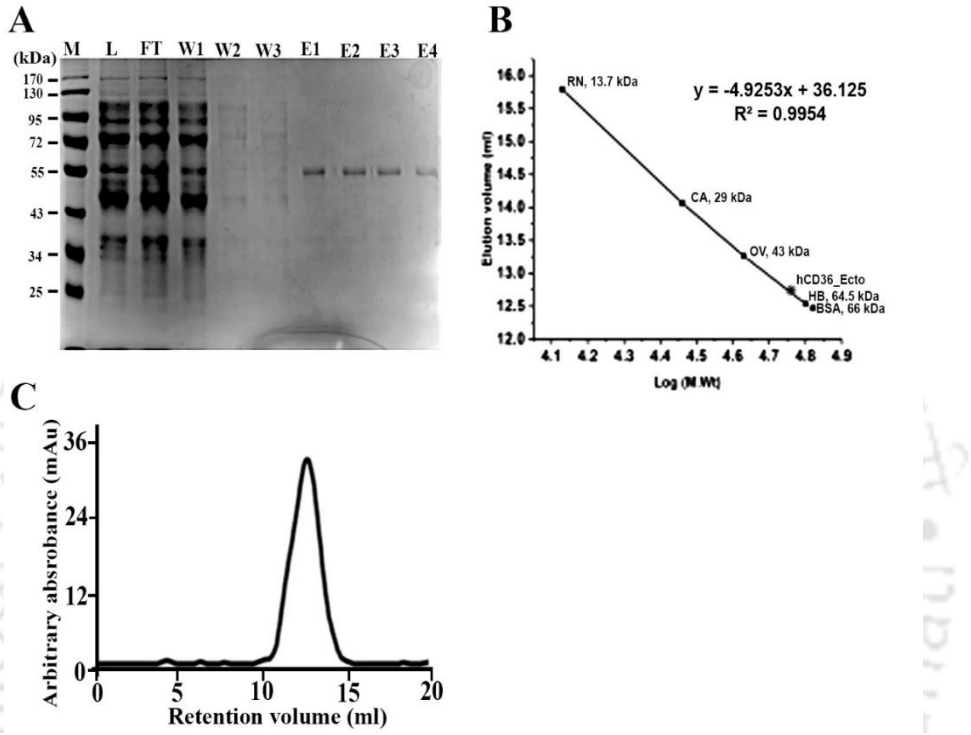

Figure 2.2. Purification and size exclusion chromatography of hCD36_ecto protein. **(A)** The purification of hCD36_ecto using Ni-NTA sepharose. L-Load, FT-flowthrough, W1, W2-wash, E1-E4-eluted fractions with 250 mM imidazole. **(B)** Low molecular weight size exclusion chromatography calibration curve. **(C)** Size exclusion chromatography of purified hCD36_ecto. Inset shows the calibration curve between K_{av} and Log molecular weight (kDa). The calculated molecular weight of CD36_ecto was found to be 53 kDa.

2.3.2. hCD36_ecto has high affinity towards phosphatidylserine

Human CD36 ectodomain have been reported binding of various endogenous and exogenous ligands (Greenberg et al., 2006; Gruarin et al., 2001; Hoebe et al., 2005; Jay et al., 2015; Leung et al., 1992; Pepino et al., 2014; Stewart et al., 2010; Yesner et al., 1996). Initially, we attempt to see that CD36_ecto can recognize PS on the membranous support (to mimic plasma membrane like support). A dot blot analysis was per-formed by blotting individually different

lipid vesicles (PA, PC, PE, PG, PS) on the nitrocellulose membrane. The membrane was incubated with purified hCD36_ecto for 1hr followed by probing CD36_ecto by anti-CD36 antibody. Dot blot analysis indicate that hCD36_ecto binds specifically to PS and gives high signal (Figure 2.3A). CD36_ecto did not bind any other phospholipid blotted on the membrane highlight the specificity of CD36 towards PS compared to other phospholipids (Figure 2.3A). To further confirm the qualitative Dot blot finding, we did direct binding experiment of PS to the CD36_ecto using Isothermal Titration Calorimetry. The binding of PS to CD36 involves releasing of heat, which is circulated into The system as evident from the exothermic re-action and negative enthalpy values (Figure 2.3B).

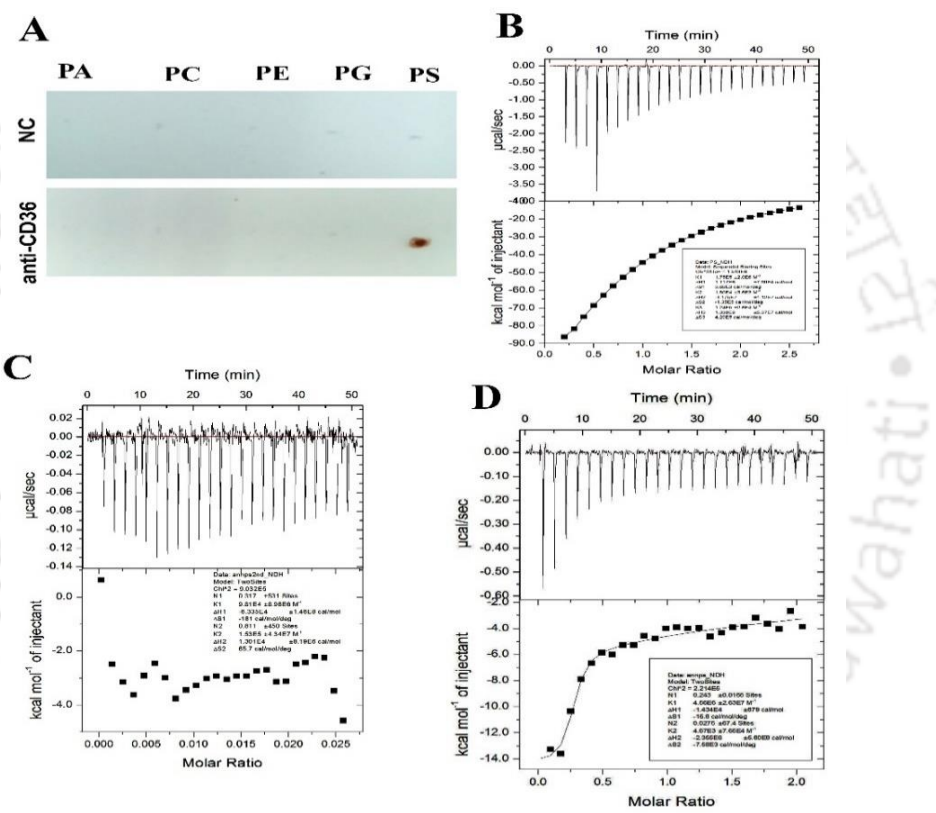

Figure 2.3. hCD36_ecto has high affinity towards phosphatidylserine. (A) Dot blot assay of PS. Various phospholipids spotted onto nitrocellulose membrane (NC) and blocked with 3% BSA. The membrane was incubated with purified hCD36_ecto for 2 h at 37 °C. The blot was washed, and binding of hCD36_ecto was detected with anti-CD36 antibody. Dot blot was developed using DAB (10 mg/ml) as chromogenic substrate. **(B)** ITC thermogram of the hCD36_ecto upon titration with PS vesicles. The saturation indicates the specific interaction of PS with ectodomain. **(C)** ITC thermogram of BSA with POPS vesicles. **(D)** ITC thermogram of the Annexin-V upon titration with PS vesicles.

The curve fitting results showed that the stoichiometry between the CD36 and PS is 1:2. The hCD36_ecto-PS thermogram revealed that the interactions between the components

were driven by the hydrophobic and salt bridge interactions. The calculated dissociation constant K_D between hCD36_ecto and PS was calculated as 53.7 ± 0.48 μM. There is possibility that PS could binds to the protein residues in a non-specific manner due to hydro-phobic interactions. To rule out such a possibility, we have performed ITC experiment to analyze PS liposomes binding to the bovine serum albumin (BSA). The thermogram of BSA-PS revealed that there is no binding of PS to BSA and heat evolved in BSA-PS titration is purely due to the buffer dilution in cell (Figure 2.3C). Annexin V binds PS present on the plasma membrane and is known to detect apoptotic cells under different treatments (Deshmukh and Trivedi, 2013; Koopman et al., 1994). The Annexin V was titrated with PS liposomes using similar parameters as that of hCD36_ecto-PS thermogram (Figure 2.3D). Similar to hCD36_ecto, annexin V-PS interaction is exothermic involving salt bridges instead of hydrophobic interaction. The stoichiometric ratio between the Annexin V and PS is 1:1 and dissociation constant K_D of 0.21 ± 0.03 μM. Comparative studies with Annexin V highlight two aspects of hCD36_ecto with PS; (1) the mode of interaction is different between two proteins, Annexin V is extensively using salt bridge interaction whereas hCD36_ecto is using hydrophobic interaction and salt bridge. (2) The stoichiometric ratio of protein to PS is different. Also, dissociation constant K_D between two proteins is very different. All these different features might be crucial for CD36 to interact with PS containing cells to modulate down-stream signalling and immunological outcomes. Secondary structure arrangement analysis indicates that CD36 ectodomain consists of α-helix, β-sheet and unordered region to Provide binding site for different types of ligands. Co-incubation of CD36 ectodomain with PS vesicles causes no significant changes of secondary structure within protein (Figure 2.4).

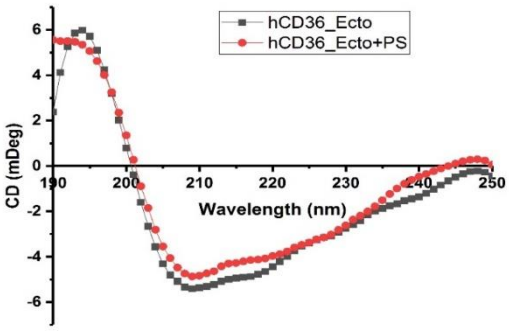

Figure 2.4. Phosphatidylserine incubation with hCD36_ecto does not affect the protein conformation. The circular dichroism spectra of hCD36_ecto recorded in presence and absence of PS vesicles. The spectra from both conditions almost identical and suggests there is no structural changes upon PS binding to hCD36_ecto.

TH-2507_156106009

2.3.3. Biophore fingerprint of PS is a well-defined microenvironment consisting of the Asp, Arg, Asn, Thr and Trp

CD36 ectodomain is a well-defined environment to bind PS. Biophore fingerprints of Protein-PS complexes were analysed for possible recurring interaction patterns. Aspartic acid (D), Asparagine (N), Arginine (R) and Tryptophan (W) were identified as the four critical residues in interaction fingerprints (Table 2.2). Ligand and Protein atoms were mapped and encoded in a distance matrix (Figure 2.5), colour coded in VIBGYOR scale. A higher resolution, atomic level examination suggested that a recurring pattern of NH2 and N atoms of guanidinium group of arginine side-chain were found to be forming hydrogen bonds with the O3 and O11 atoms of PS (Table 2.3).

Table 2.2. List of residues recurring in six Protein-PS biophore models from Protein Data Bank.

PDB/Residue	M	D	P	N	E	G	L	R	W	K	F	V	Q	T
1DSY	1	1	1	1	0	1	1	1	1	0	0	0	0	1
2HJ6	0	0	1	1	0	1	1	0	1	0	0	1	0	0
2JG8	0	1	0	1	0	0	1	1	1	1	0	0	1	1
3BIB	1	1	0	1	1	0	0	1	1	1	1	0	0	0
3KAA	1	1	0	1	1	1	0	1	1	1	1	0	1	0
4B2Z	1	1	1	1	1	0	1	1	1	1	0	1	1	1
	4	5	3	6	3	3	4	5	6	4	2	2	3	3

Similarly, N and OD1 atoms of Asn sidechain was found to interact with OT2, O4 atoms of PS through hydrogen bonding in three complexes. The third prominent interaction that was observed in 4 out of six complexes is the OD1 of Asp with N of PS. Apart from these, Tryptophan is the other residue consistently featuring in four out of six complexes analysed (Figure. 2.6A). Further to validate the biophore fingerprint, the molecular docking studies were performed using the biophore as grid centre. The predicted binding energy of the PS-CD36 complex was found to be 5.1 kcal/mol. The LigPlot+ interaction analysis of PS binding pocket in docked complex showed that the residues R63, R96, N118, D270 and E418 were forming hydrogen bonds with PS at a distance of 2.61, 2.87, 2.62, 2.78 and 2.69 Å respectively (Figure. 2.6B).

TH-2507_156106009

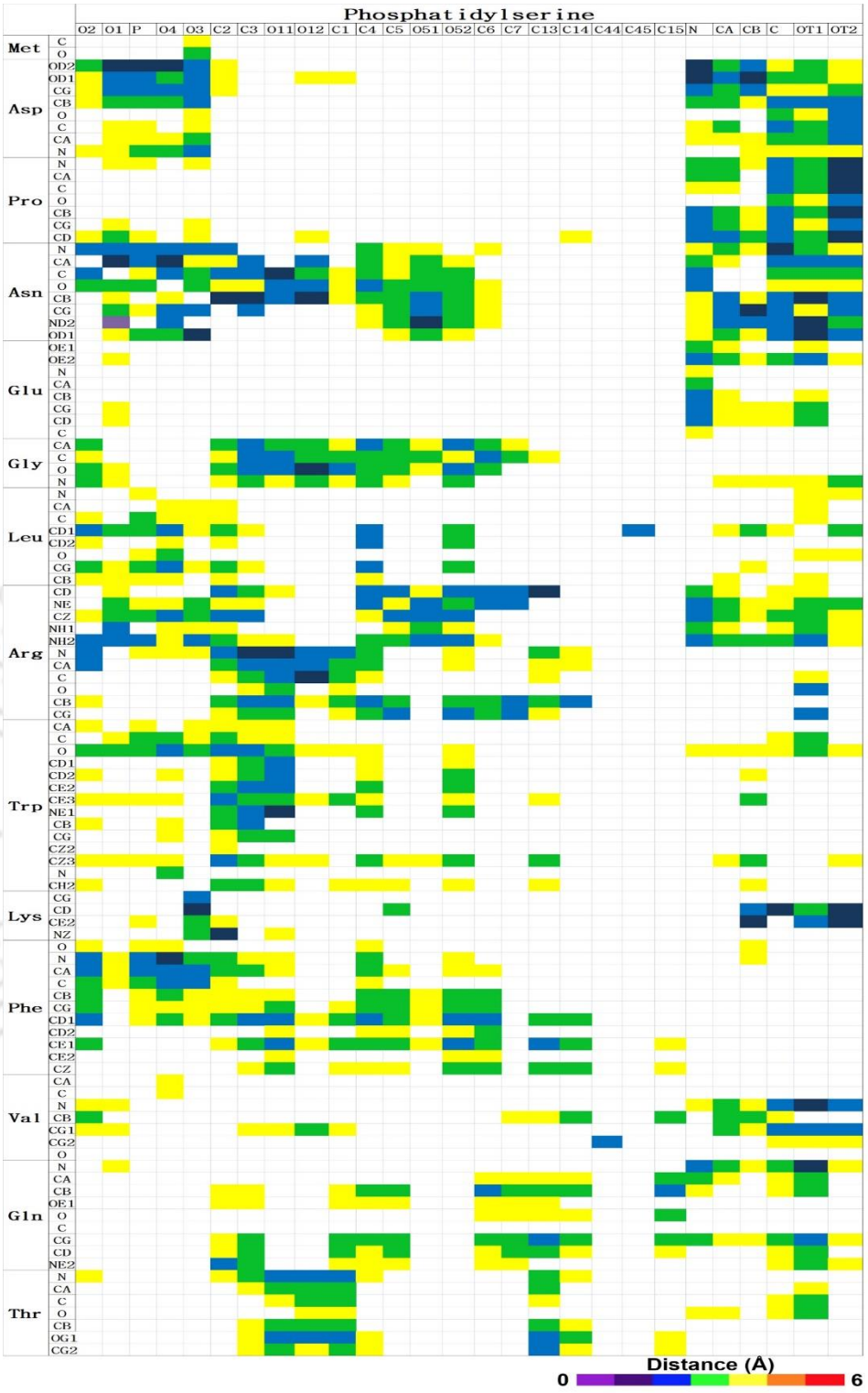

Figure 2.5. Protein-PS biophore heat map. Biophore constitution of various Protein-PS complexes are represented as heat map. The distances of the amino acid backbone and side chain atoms from various atoms of phosphatidylserine within 6 Å radius were included. Colour coding as per VIBGYOR pattern with violet indicating shortest and red indicating largest distances between biophore elements.

TH-2507_156106009

Table 2.3. Principal component analysis of Protein-PS biophore.

Feature /ID	2HJ6	3BIB	2JG8	3KAA	4B2Z	Feature details	Repeats
A	1	0	1	0	1	Trp-(CE3-C2, 3.69)	4
B	0	1	0	1	0	Arg-(NH1-C, 2.8–3)	2
C	1	1	0	1	0	Leu-(CD1-C48, 3.84)	3
D	1	0	0	0	0	Val-(CG2-C44, 3.78)	1
E	0	0	1	0	1	Lys-(C-OT1, 2.23–2.9)	3
F	0	0	1	0	0	Gln- (N-C, 3.9–4.2)	1
G	1	0	0	0	0	Trp-(O-CA, 2.34)	2
H	1	1	0	1	0	Asp-(N-O3, 2.5–2.7)	4
I	1	0	1	1	1	Arg-(N-O11, 2.52)	5
J	1	0	1	0	1	Asn-(N-OT2, 2.23)	2
K	1	1	0	1	0	Asn-(OD1-NA, 2.74)	3
L	1	0	0	0	0	Leu-(OD1-N1, 3.2–4.7)	2
M	1	1	0	0	1	Gln- (N-OT1, 2–3)	3
N	0	0	0	1	1	Arg-(NH2-O4, 3.61)	4
O	1	0	1	1	0	Arg-(O-OT1, 3.61)	4
P	0	1	0	0	0	Lys-(CD-OT2, 2–3.2)	1
Q	0	1	0	1	0	Lys-(CE2-P, 3.9–5.8)	2
R	1	0	1	0	0	Arg-(N-O11, 2–3.1)	2
S	0	1	0	0	0	Asn-(C-O11, 2.1–3.6)	2
T	1	0	1	0	0	Lys-(CD-OT1, 3–4.3)	2

The residue R63 atoms (293-NE, 296-NH2) were interacting with the atom (3944-N1) of the PS at a Donor-Acceptor distance of 3.67 and 3.86Å respectively. In addition to the hydrogen bonding, R63, R96 and K334 are forming a salt bridge with phosphate group and carboxylate groups of PS at a distance of 4.19 Å, 4.87 Å and 3.91 Å respectively. Further, all 35 biophore interacting residues were systematically mutated to Alanine using ABS-scan web server, to evaluate their relative contribution to the overall stability of the complex. Our analysis suggests that Y204, R63, R96, D270, E418, Y238 and N118 are showing significant changes in free energy estimates (Figure 2.7).

The mutation in residue K385 showed enhanced binding energy suggests the alanine mutation in this residue positively contributes the binding of PS. Besides, the free energy estimates from alanine substitution in D209, Y238, and F201 suggests these residues are also found in PS binding site and may contribute to the binding of PS to CD36.

TH-2507_156106009

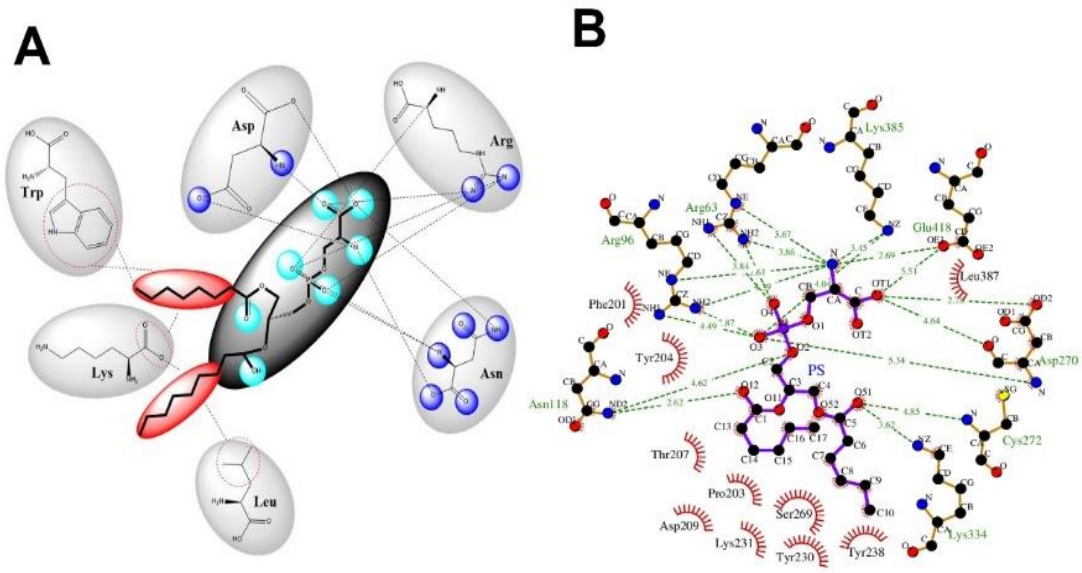

Figure 2.6. PS biophore model. (A) The PS biophore model representing most recurring residues found in PS-protein complexes. **(B)** Biophore consisting of PS and CD36. All amino acids within 6 Å of PS binding pocket presented in ligand plot.

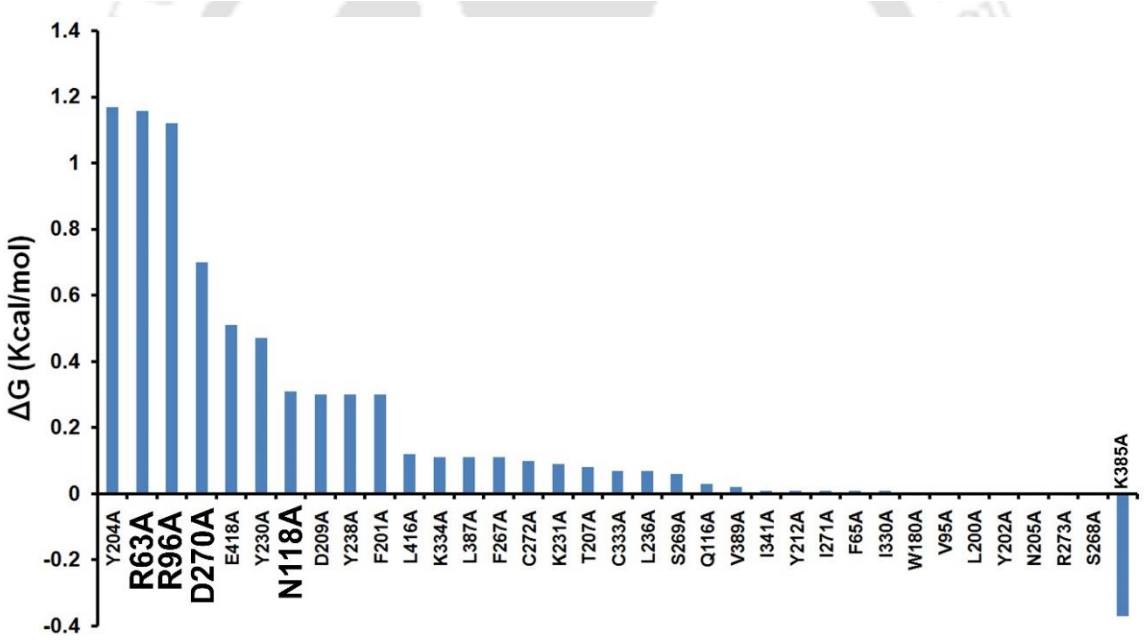

Figure 2.7. Residue contribution analysis of hemin biophoric residues. All amino acids within 6 Å of PS binding pocket were identified, and systematically mutated using ABS-Scan server. The difference in free energy estimate upon mutation is indicative of their relative contribution to the overall stability of PS-CD36 complex.

2.3.4. CD36-PS molecular dynamics studies indicate R63A, N118A and D270A mutations destabilizing the PS interactions

Molecular dynamics simulations were carried out for 20 ns time scale under NVT conditions to assess the stability of the different CD36-PS complexes (wild-type, R63A, R96A, D270A and N118A). The ensemble of structures generated were clustered with an

TH-2507_156106009

RMSD cut-off of 0.2 nm and the representative structure from the largest cluster was analysed for Hydrogen bonds, RMSD, Radius of gyration and RMSF. The hydrogen bonds formed by R63, N118 and D270 were found to be retained in the wild type complex. The R63 mutation to alanine has disrupted the integrity of biophoric constituents, directly affecting the hydrogen bonding from R96, N118 and D270. The other two systems, N118A and D270A, showed conservation of hydrogen bonds from R63, R96. However, N118A resulted in the disruption of the hydrogen bond connecting D270 and R63. The systematic analysis of hydrogen bonding in wild type and mutants suggested the residues R63, N118 and D270 are crucial for binding of PS to CD36 (Figure 2.8). Analysis of RMSD and Radius of gyration of all six systems do not suggest any unfolding of the protein upon mutations (Figure 2.9A and 2.9B).

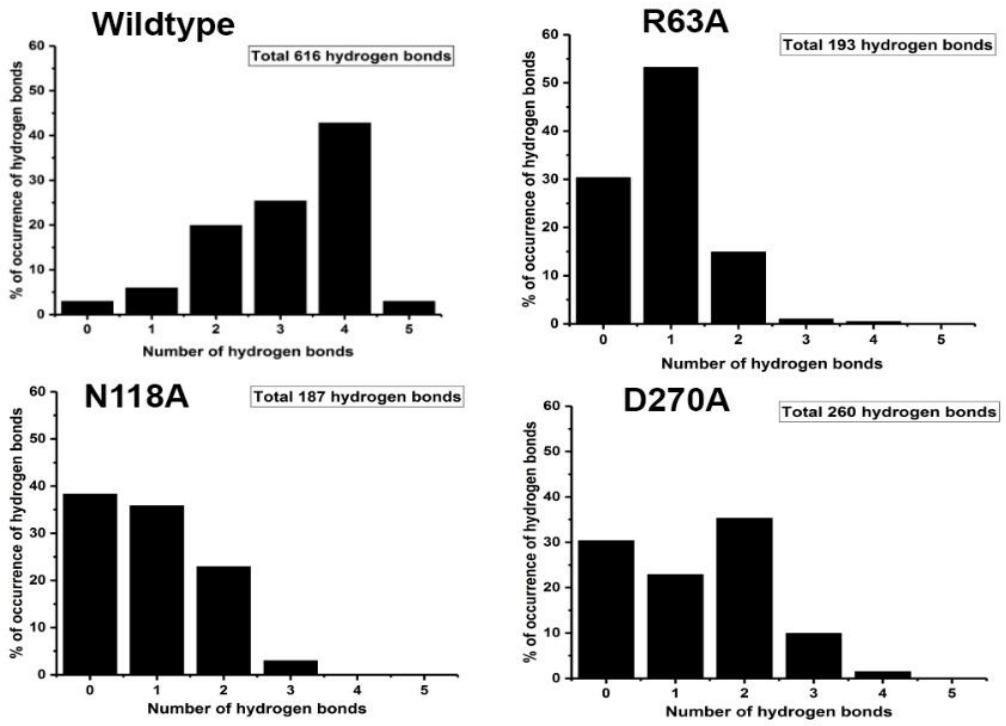

Figure 2.8. Statistics of hydrogen bonding for 20 ns simulation run using g_hbond program of Gromacs suite. Total number of hydrogen bonds summed over all structures is given in each graph. The impact of alanine mutation at R63, N118 and D270 may be directly inferred from hydrogen bond statistics.

However, we performed root mean square fluctuation (RMSF) analysis of PS atoms to quantitatively assess the binding strength and specificity upon mutation. RMSF of PS atoms in the binding site pocket of wild-type consisting of R63, R96, N118 and D270 residues were analysed. Average RMSF value of all PS atoms was found to be 0.17 nm. In case of mutants, the mean RMSF value is approximately 0.4 nm (Figure 2.9C), clearly

TH-2507_156106009

suggesting dis-orientation of the PS in binding pocket. To further verify this, we have analysed the Ramachandran (φ, Ψ) basins of binding site residues in wild-type receptor. Residues R96, Y204 were found to shift from left-handed alpha helical conformational basin to a forbidden basin in the fourth quadrant of Ramachandran Map. Other residues such as N118, D270, R63 and E418 are more or less confined in their structural space. Other binding site residues such as K334, P203 and F201 also exhibit fluxional behaviour, but in the allowed regions of Ramachandran Map (Figure 2.9D). Dihedral combinations of a key binding site residue, forming hydrogen bond with ligand adopting an unusual structure, even in higher energy regions of Ramachandran Map suggest the pivotal role this residue plays in ligand binding (Gunasekaran and Nussinov, 2007).

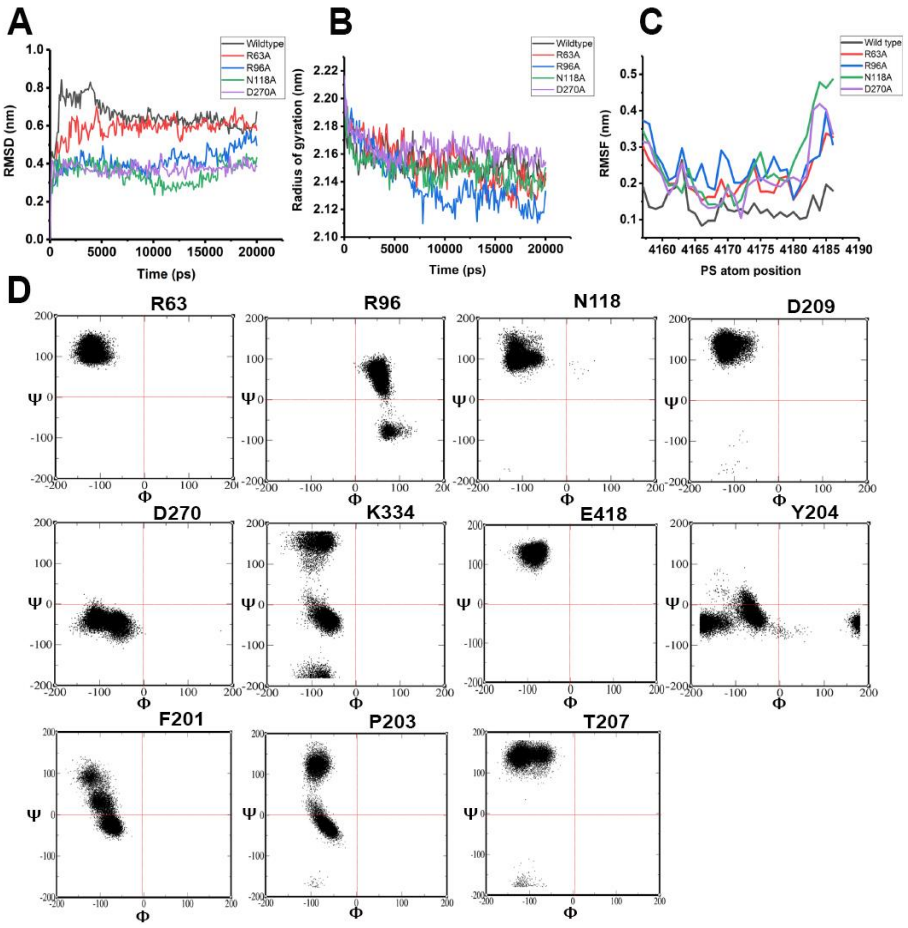

Figure 2.9. Molecular Dynamics Simulations analysis of CD36-PS binding. Effect of mutation in the stability of CD36-PS complex and their global effect in overall folded conformation were estimated using **(A)** Root Mean Square Deviation (RMSD) and **(B)** Radius of gyration. **(C)** The effect of mutation in binding specificity may be understood from the Root Mean Square Fluctuation (RMSF) value of PS atoms, interacting with CD36 residues. **(D)** Ramachandran map of PS interacting residues and their respective structural integrity were evaluated from their backbone dihedral angles (φ, Ψ) combinations. Residues with representation in more than one basin throughout MD production run at 300 K indicate their respective structural non-homogeneity.

TH-2507_156106009

2.3.5. The residues R63A and D270A are crucial for binding of PS

Molecular dynamics indicated that R63 and D270 residues are crucial for PS binding. To verify the role of R63 and D270, the residues mutated to alanine by site-directed mutagenesis. The PCR amplification of complete pET23a-hCD36_ecto with site directed primer (Table 2.1) gives amplified DNA (Figure 2.10A). Restriction digestion of D270A plasmid with Msp-I confirms the presence of mutation. The transformed colonies carrying R63A or D270A mutant plasmid were screened and trans-formed into NEB-5α competent cells for overexpression (Figure 2.10B). The mutant proteins (R63A and D270A) were purified and tested for their oligomeric status. For R63A the elusion volume was found to be 13.49 ml and 12.40 ml in case of D270A both indicates no major changes in elution volume (Figure 2.10C). Initially, the purified mutant proteins were used to test their affinity towards PS vesicles using dot blot assay as mentioned in methods section. There was no reactivity with R63A or D270A mutants but wild type binds to the PS vesicles blotted on to the nitrocellulose membrane (Figure 2.11A).

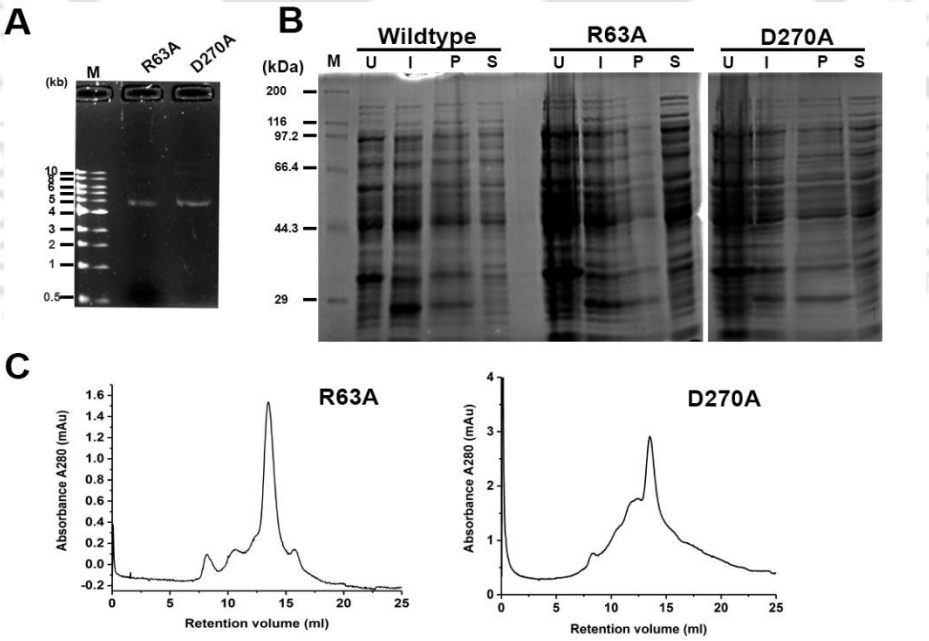

Figure 2.10. Site-directed mutagenesis, overexpression and size-exclusion chromatography of mutants. **(A)** The mutants R63A and D270A were generated using mutagenic primers (Table S1) by conventional PCR amplifications. The amplified product was analysed on 1% agarose gel-electrophoresis. **(B)** Overexpression studies of mutant proteins. After induction the bacterial cells were centrifuged and lysed as mentioned in protein purification section in materials and methods. The pellet and supernatant were separated and loaded onto 12% SDS-PAGE. M-marker, U-Uninduced, I-Induced, P-Pellet, S-supernatant. (C) size-exclusion chromatography of R63A and D270A mutants.

TH-2507_156106009

Further, we have tested the ability of the purified R63A or D270A interaction with PS by isothermal titration calorimetry. For R63A, the heat generated for each injection was negligible which clear indication of no binding is (Figure 2.11B). The heat value generated in between each injection was due to buffer dilution. For D270A, the curve fitting in sequential binding model showed that the D270A is giving K_D of 833 ± 3.8 μM, with almost sixteen folds lower affinity compared to wild type (Figure 2.11C). To support the idea that the observed effects is not because of any structural changes, we did the circular dichroism spectroscopy of R63A and D270A mutant proteins. The CD spectra showed no change in secondary structural features as compared to wild type (Figure 2.12A and 2.12B). The ITC titration curve and circular dichroism spectra suggested that the R63A lost the affinity towards PS whereas D270A is giving ~16 folds lower affinity towards PS. These results provide direct evidence that the residue R63, D270 are playing crucial role in PS interaction to the CD36.

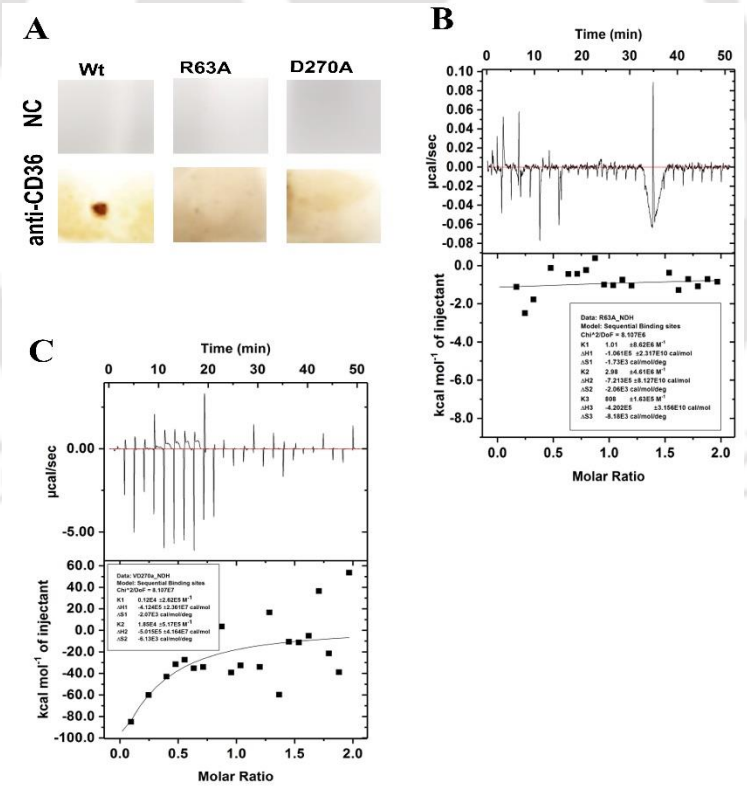

Figure 2.11. The R63 and D270 residues are crucial for PS binding. (A) Dot blot assay of mutant proteins with PS. The top panel shows the nitrocellulose membrane after applications of PS and dried. The lower panel shows blot developed with DAB as described in material and methods**. (B &C)** ITC thermogram of the mutant CD36ecto R63A **(B)** or D270A **(C)** upon titration with PS vesicles.

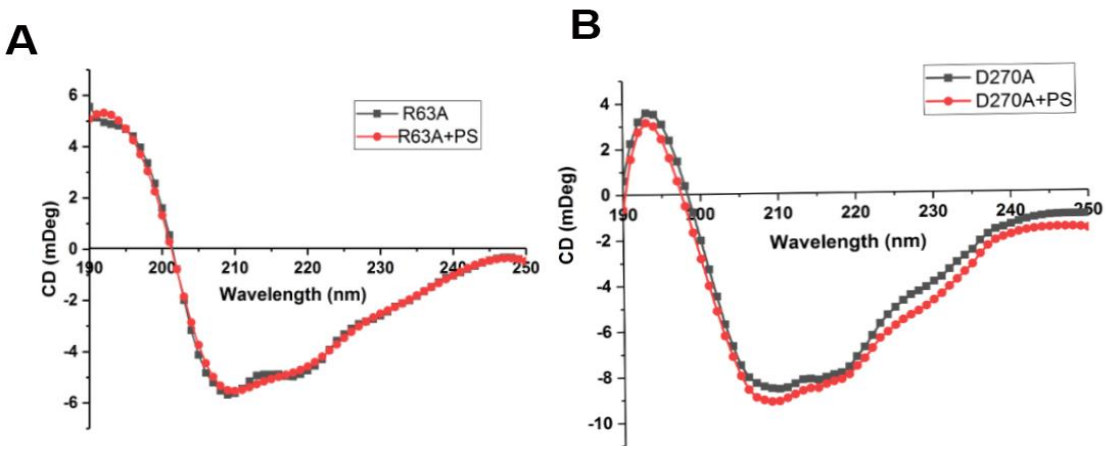

Figure 2.12. CD spectrum of purified mutant protein in absence or presence of POPS. **(A)** R63A CD spectrum in absence or presence of POPS. **(B)** D270A CD spectrum in absence or presence of POPS.

2.4. Discussion and future prospects

In current study, we have optimized human CD36 ectodomain production through temperature programmed induction approach (Jiang et al., 2013), a unique approach test first time for this class of protein. The properly folded form of protein is essential for any ligand interaction studies (Greenfield, 2006). Proteins from mammalian origin which are toxic to the bacterial cells are generally expressed in mammalian expression system as these proteins sometimes form aggregates (insoluble inclusion bodies) in bacterial system due to toxicity (Khow and Suntrarachun, 2012). Besides solubility, proper conformation of protein required for any biochemical studies. Previously attempts are made to express CD36 ectodomain in bacterial expression system which is denatured and refolded (Wang et al., 2010). Only native form of CD36 able to accept oxiPS as ligand. We have tested the ability of purified CD36 ectodomain from bacterial expression system to bind PS. Phosphatidylserine is one of the cell membrane constituents which is a key marker of apoptosis. The binding of PS to the CD36 receptor was implicated in the phagocytic uptake of the apoptotic cells. The recognition of apoptotic cells may have mediated through the PS or vitronectin receptor (Fadok et al., 1998). It was reported that PS vesicles are internalized in Long Evans (LE) and Royal College of Surgeons (RCS) rat Retinal Pigment Epithelium cells (Ryeom et al., 1996). In another study, THP1, J774A.1 cells blocked with anti-CD36 antibody reduces the uptake of the PS liposomes significantly comparing to other phospholipids (Tait and Smith, 1999). The Dot Blot analysis of different phospholipids with hCD36_ecto clearly high-lights the fact about high specificity of

TH-2507_156106009

hCD36_ecto towards PS and explain this observation (Figure 2A). The study on OxiPS binding to CD36 was highlighted the binding of oxidised phosphotidylserine, but the affinity parameters or microenvironment responsible for ligand binding is not explored (Greenberg et al., 2006). An in-depth molecular modelling allowed us to propose a suitable pharmacophore for PS and identified critical residues responsible for PS binding to CD36. It is the first such effort to under-stand CD36-PS interaction and molecular interactors playing crucial role. A follow-up study can be designed to use the information to ex-ploit soluble CD36 (wild type or mutant variant) to scavenge cellular debris or modulate immune response to control inflammation (Febbraio et al., 2001). Platelets play crucial role in thrombosis to maintain homeostasis in human (Trivedi et al., 2009). Cell-derived microparticle expresses PS on their surface, and they activate CD36 downstream signalling in platelets to contribute into thrombosis. Inhibition of CD36 expressed on platelets through anti-CD36 antibodies or blockade of exposed PS through Annexin-V abolishes the interaction between microparticle and platelets (Ghosh et al., 2008). Soluble CD36 ectodomain can also serve as blocking agents to disrupt platelet-microparticle interaction to modulate down-stream events. In the cur-rent study, we have characterized the PS pharmacophore, and this in-formation can be exploited to design better blocking agents for therapeutic outcomes. CD36_ecto produced in bacterial expression system coupled with anti-CD36 antibodies can be used to efficiently remove dead and aged cells from circulation. It may help to overcome immunological over-activation or control inflammation to protect the organ from damage. The safety concerns regarding the bacterial protein needs to be workout before testing this scenario in a particular disease condition. Since we have clear idea about minimum structure or 3-D fold needed to recognize PS expressed on vesicles, a short peptide stretch can also be tried out in down-stream therapeutic or other bio-logical applications.

In the current study, we have explored few aspects related to CD36 and its interaction with PS present on apoptotic cells. In the current study, we have successfully produced hCD36_ecto in bacterial expression system, and we found a yield of ~2 mg per litre of bacterial culture. The produced protein is monomeric with native molecular weight of 53 kDa. The protein is specifically binding PS vesicles blotted on nitrocellulose membrane, and PS binds strongly to CD36_ecto with a dissociation constant (K_D) of 53.7 ± 0.48 μM and stoichiometry be-tween CD36 and PS is 1:2. Pre-incubation of PS vesicles with CD36_ecto induces no significant re-arrangement of structural elements. The pharmacophore model for PS was generated after taking structural and physio-chemical

information from previously available crystal structures of proteins-PS complexes from protein data bank. PS was docked on predicted pharmacophoric region on CD36 ectodomain using Autodock 4.1. PS docked nicely into the predicted biophore with binding energy of 5.1 kcal/mol. The LigPlot + interaction analysis of CD36-PS molecular model showed that the residues R63, R96, N118, D270 and E418 were forming hydrogen bonds with PS. The mutation of critical residues R63, R96 and D270 to alanine is reducing the affinity of PS towards CD36. These finding may help to design suitable agents mimicking PS biophore with potentials in diagnostics of apoptotic cells and cardiovascular intervention.

References: Please refer to the Bibliography section at the end of the thesis.

TH-2507_156106009

Chapter-III

CD36 Ectodomain as a probe to detect apoptotic cells.

TH-2507_156106009

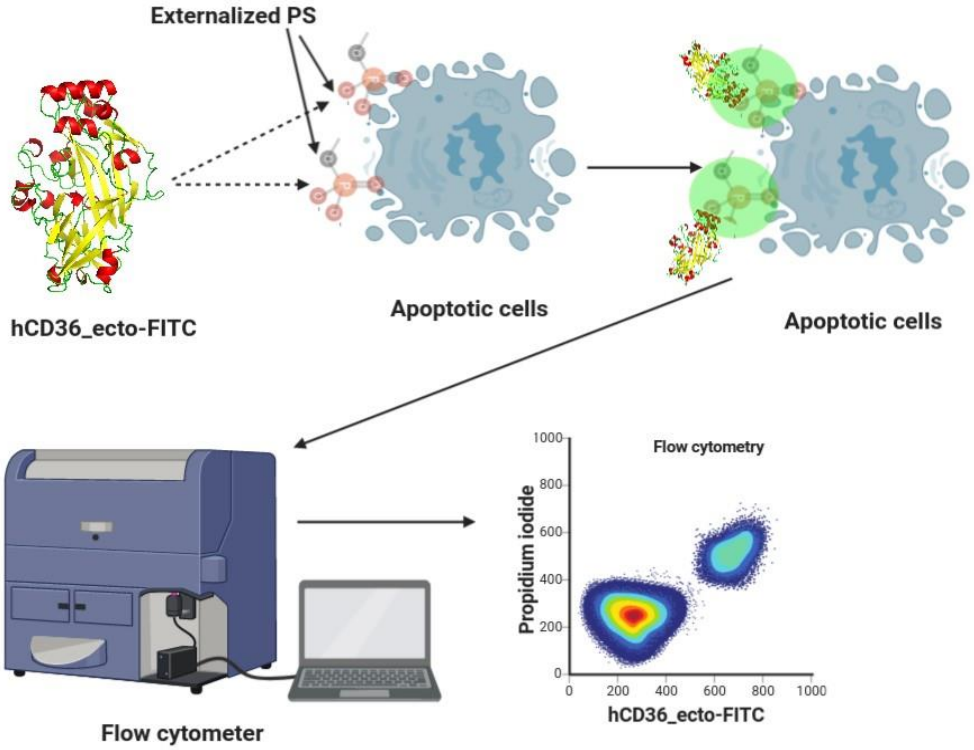

Summary

In this chapter we have explored the potentials of fluorophore labelled human CD36 ectodomain as a probe to detect apoptotic cells. The fluorescently labelled hCD36_ecto is staining and detecting apoptotic cells in a flow-based assay comparable to the gold standard Annexin-V detection. The blocking with unlabelled CD36ecto reduces the staining of annexin-V-FITC for apoptotic cells, whereas R63A does not affect the binding of Annexin V-FITC to apoptotic cells. It indicates the role of CD36-PS interaction in detecting apoptotic cells. Dual staining with hCD36_ecto-FITC/PI is universally detecting apoptosis in different nucleated cells or eryptosis in non-nucleated RBCs. Hence, our study highlights the utility of CD36 as a probe to detect apoptosis in mammalian cells. It might be a robust, economical reagent for the scientific community to facilitate their research.

Key words: Apoptosis, Annexin V, CD36 ectodomain, Cells, Flow Cytometry, phosphatidylserine.

3.1. Introduction:

The functioning and coordination between billions of cells in the body are vital for successful completion of life-cycle. Cell perform different functions, run the metabolic reactions and undergoes apoptosis to end their life without disturbing homeostasis (Elmore, 2007; Gavrilescu and Denkers, 2003). During the apoptosis, the cell membrane undergoes several changes, including loss of membrane symmetry and externalisation of phosphatidylserine (PS) from the inner leaflet (Rysavy et al., 2014). The exposure of PS from the cell-surface to activate the host machinery to clear the apoptotic cells and debris to prevent unwanted inflammatory responses (Kuhtreiber et al., 2003; Mahajan et al., 2016). The recognition of PS is carried out by the cell surface receptor expressed on different types of immune cells (Penberthy and Ravichandran, 2016). The cell surface receptor, brain angiogenesis inhibitor 1 and 3 (BAI1, BAI3) (Das et al., 2011), T-cell immunoglobulin and mucin receptor 1 (TIM-1) and TIM-4 (Flannagan et al., 2014; Ichimura et al., 2008), MerTK (Wu et al., 2005), Stabilin 1 (Tamura et al., 2003), αvβ3 (Hanayama et al., 2002), scavenger receptor type F family member 1 (Berwin et al., 2004), low-density lipoprotein receptor-related protein 1 (Su et al., 2002) has been well studied well in context to PS recognition and eliciting the anti-inflammatory activity. Few studies reported the scavenger receptor CD36 role in detecting the apoptotic cells (Fadok et al., 1998b; Greenberg et al., 2006).

The detection of apoptosis in cells is paramount importance as it will increase our understanding of the mechanism of drug action, and it helps in designing suitable therapeutic molecules. Several methods have been described in literature such as electron microscopy to observe membrane alterations, genomic and proteomic methods, spectroscopy-based methods, immunological detection to detect apoptosis in mammalian cells (Archana et al., 2013; Blankenberg, 2008; Hotchkiss et al., 1999; Martinez et al., 2010). A flow cytometry-based detection method has been developed to detect externalised PS on apoptotic cells using a combination of Annexin-V and propidium iodide (PI). The staining gives the fraction of cells in early apoptosis, late apoptosis and necrosis/death phase in a semi-quantitative manner. Oxidised Phosphatidylserine present on apoptotic cells binds to scavenger receptor CD36 expressed on immune cells. It allows the phagocytosis mediated clearance of apoptotic cells from the host (Greenberg et al., 2006; Tait and Smith, 1999). In a recent study, we have put an attempt to understand the CD36-PS interaction and tried to explore the PS biophore present on CD36 ectodomain

TH-2507_156106009

(Banesh et al., 2018). The residues R63 and D270 were found to be crucial for binding of PS as determined by isothermal titration calorimetry binding studies (Banesh et al., 2018). Based on the previous results, we have explored the possibility of using fluorescently labelled human CD36 ectodomain to detect apoptotic cells.

Interestingly, we found that hCD36_ecto-FITC is binding to the apoptotic cells exclusively with no staining of healthy cells. The staining of apoptotic cells is following CD36-PS interaction, as R63A-FITC is not giving an intense fluorescence signal. More-over, hCD36_ecto-FITC in combination with propidium iodide (PI) is universally detecting apoptotic cells developed in different nucleated cells (Hela, HCT116, HEK293, HT29) or non-nucleated RBCs. The results of flow cytometric analysis of labelled cell with hCD36_ecto-FITC/PI is comparable to the commercially available Annexin-V-FITC/PI results. Hence, our study highlights the utility of CD36-PS interaction as an axis to develop suitable probe to detect apoptosis in mammalian cells. It may provide alternate robust and economically viable reagent for the scientific community to facilitate their research.

3.2. Experimental procedures:

3.2.1. Reagents: Acridine orange (Cat.No# TC262) and Propidium iodide (Cat.No# TC252) were purchased from HiMedia (India), Staurosporine (Cat.No# S4400-0.1MG), Fluorescein isothiocyanate (Cat.No# F7250) Annexin-V-FITC based detection kit (Cat.No# APOAF-20TST) were from Sigma-Aldrich (Missouri-USA), anti-CD36 antibody (Cat.No# sc-7309) from Santacruz biotechnology (Texas-USA), Texas-red conjugated secondary antibody (Cat.No#) was from Zymed and PD-10 column was from GE Healthcare (Chicago-USA).

3.2.2. hCD36_ecto purification: The cloning, overexpression and purification of hCD36_ecto was performed as described in Chapter-II, section 2.2.4, page no. 56.

3.2.3. Fluorescent Labelling of hCD36_ecto with fluorescein: The purified hCD36_ecto was buffer exchanged against 0.1M sodium carbonate buffer, pH 9.0 and concentrated (with a final concentration of 2mg/ml). The protein solution was mixed with FITC solution (1mg/ml) with gentle stirring the solution. The mixture was incubated in the dark with gentle agitation for 8 h at 4^0C. In the next step, the NH_4Cl solution (final concentration 50mM) was added and stirred for another 2h at 4 ^{0}C. The Fluorescently labelled hCD36_ecto was separated from free dye using size exclusion column PD-10. The labelled

protein was aliquoted and stored in brown Eppendorf at -20^{0}C until further use.

3.2.4. Culturing of different mammalian cells: The different mammalian cell lines such as (HEK 293, DLD1, HCT116, HT29) were cultured in DMEM containing 10% FBS and 1% antibiotic cocktail (10,000 units/ml Penicillin and 10 mg/ml Streptomycin) as described previously (Deka et al., 2016; Deshmukh and Trivedi, 2014).

3.2.5. Preparation of RBC and WBC Suspension: Blood was collected from a healthy volunteer (either sex and age, 20–35 years) with informed consent in EDTA containing tubes. RBCs and blood plasma were separated, and hematocrit (5%) was prepared in PBS as described previously (Abed et al., 2013).

The WBC isolated as per the manufacturer's instructions. The blood is collected in an EDTA containing sterile 15 ml centrifuge tube using sterile syringe and needle. The blood is immediately mixed with the EDTA by inverting the tube. The blood is diluted using diluent buffer in 1:1 ratio. In a fresh and sterile 15 ml centrifuge tube containing 2.5 ml of HiSep LSM 1077 (lymphocyte separating medium) was overlayed with 7.5 ml of diluted blood. The separating medium containing wole blood centrifuged at 2300 RPM for 30 min in a fixed angle rotor. After centrifugation the lymphocyte layer was separated and placed in a new 15 ml centrifuge tube in sterile condition. The WBC containing layer is diluted with PBS, pH7.4 and centrifuged thrice to remove remnants of EDTA or diluent buffer. In another tube the blood is collected without any coagulant and the serum is collected. The WBC pellet obtained in final step suspended in RPMI medium with 5% serum obtained in previous step and seeded in a 35 mm cell culture plate.

3.2.6. Preparation of healthy and apoptotic cells: The mammalian cells were used to prepare healthy and apoptotic cells by two different well-established protocols. Serum deprivation is known to induce apoptosis in mammalian cells (Kim et al., 2017a). In Protocol 1, mammalian cells were grown in serum-free media for 24hrs at 37 ^{0}C. Cells were washed gently and used in the study. In another protocol, cells were treated with chemical toxicants to induce apoptosis. The 5 x 10^5 cells were seeded per well in a six-well plate and allowed to adhere for 10hr at 37 ^{o}C. The cells were treated with the Staurosporine (100 ng/ml) for 24hr in serum-free Dulbecco's modified eagles medium (DMEM). Post-treatment, apoptosis was confirmed and used in the study.

Eryptosis (apoptosis) in RBC was induced by a method described previously (Abed

et al., 2013). Briefly, the 0.4% RBC solution was incubated in Ringer solution (32 mM HEPES pH 7.4, 125 mM NaCl, 5 mM KCl, 1 mM $MgSO_4$, 5 mM Glucose, 1 mM $CaCl_2$) containing 50 µM tannic acid for 48hrs at 37^0C. For induction of apoptosis in WBC, the cells were centrifuged to remove medium and resuspended in RPMI medium without serum and kept at 37 ºC in CO_2 humidified chamber for 48 hrs. Post-treatment, apoptosis was confirmed and used in the study.

3.2.7. Detection of Apoptotic Cells with CD36_ecto-FITC: The mammalian cells were used to prepare healthy and apoptotic cells by two different well-established protocols. Serum deprivation is known to induce apoptosis in mammalian cells (Kim et al., 2017b). In Protocol 1, mammalian cells were grown in serum-free media for 24 hrs at 37 °C. Cells were washed gently and used in the study. In another protocol, cells were treated with chemical toxicants to induce apoptosis. The 5 x 10^5 cells were seeded per well in a six-well plate and allowed to adhere for 10 hr at 37 °C. The cells were treated with the Staurosporine (100 ng/ml) for 24 hr in serum-free Dulbecco's modified eagle's medium (DMEM). Post-treatment, apoptosis was confirmed and used in the study. Healthy or Apoptotic cells were prepared as described. Cells were washed gently without damaging apoptotic cells. In the next step, the cells were detached from the plate using 0.6% EDTA in phosphate-buffered saline, pH 7.4. The cell suspension (1 ml) was incubated with 200 µL of hCD36_ecto-FITC (100 µg/ml stock) and 10µl of PI (1mg/ml) for 30mins at 37 ℃ and 5% CO2 condition in a light protected condition. The cells were washed three times very gently with PBS to remove unbound hCD36_ecto-FITC. Finally, the cell was re-suspended in 500 µL PBS and analyzed in BD FACS Calibur flow cytometer in FL-1 channel (λex-488 nm, λem-530/30nm) and FL-3 (λex-488 nm, λem-695/40nm). The quadrant analysis was performed by FCS express v6.0 to calculate the percentage of healthy, low apoptotic, high apoptotic and dead cells. For Annexin-V labelling, we followed the manufacturer's instructions and analysed in flow cytometry under identical instrumental conditions.

The healthy or apoptotic Hela cells were incubated with 0, 0.1, 0.3, 1, 10, 50 and 100 µM of hCD36_ecto-FITC for 1 hr. Later the cells were gently washed and analyzed in BD FACS Calibur flow cytometer in FL-1 channel (λex-488 nm, λem-530/30nm) and FL-3 (λex-488 nm, λem-695/40nm). The percentage of apoptotic cells were analysed by quadrant analysis. The log concentration of hCD36_ecto-FITC was plotted against the early apoptotic cells. Similarly imging was done to correlate with the dose response. The

healthy or apoptotic Hela cells were incubated with hCD36_ecto-FITC in presence of serum for 1 h. Later the cells were washed and analysed on Flow cytometer.

3.2.8. Fluorescence microscopy: Healthy or Apoptotic cells were prepared as described. These cells were fixed with 4% of paraformaldehyde in PBS pH 7.4 at 4^0C. Cells were stained with CD36_ecto (0.1mg/ml) at 4^0C for 1hr. To localize CD36_ecto, cells were washed with PBS and blocked with blocking buffer (5% BSA in PBS) at 4^0C for 1hr. The blocking solution was removed and stained with anti-CD36 antibody followed by Texas-Red conjugated secondary antibody. The images of 10 random fields were captured in-phase and fluorescence channel using Cytell imaging system.

3.2.9. Statistical Analysis: All experiments were performed in duplicate or triplicate and repeated at least three times. Data are presented as the mean ±SD unless otherwise noted. Statistical analysis was performed by one-way ANOVA followed by unpaired Student t-test.

3.3. Results

3.3.1. CD36 ecto-domain stains apoptotic cells

PS externalization from the inner leaflet of the plasma membrane to the outer layer is the crucial step to signal the onset of apoptosis in the cell (Fadok et al., 1998a). In our previous work, we have studied the interaction between PS vesicles and ectodomain expressed in bacterial expression system (Banesh et al., 2018). CD36 ectodomain binds PS vesicles with a dissociation constant of 53.7 ± 0.48µM. The crucial residues important for CD36_ectomain-PS interaction are R63, R96, N118, D270 and these residues are providing suitable micro-environment to support binding of PS present on lipid vesicles (Banesh et al., 2018). CD36 ecto-domain provides a docking site for phosphatidylserine (PS) and could be used for staining apoptotic cells. To test this possibility, we have prepared apoptotic cells in two different conditions representing the natural process (starvation) or external toxic agent (anticancer drugs). Annexin V is a well-established probe used to detect apoptosis (Vermes et al., 1995; Zhang et al., 1997). Staining of healthy or apoptotic cells with Annexin V-FITC indicate staining of healthy cells with weak fluorescence, whereas bright fluorescence was observed with apoptotic cells (Figure 3.1A). It is interesting to note that background fluorescence was more with Annexin V-

FITC (Figure 3.1B) compared to CD36ecto-FITC, and it may result in a relatively higher count of apoptotic cells in the sample. Healthy or apoptotic cells were stained with hCD36 ecto-FITC as described in "material and methods". Healthy cells are not getting stained with hCD36 ecto-FITC, whereas apoptotic cells are showing very intense green fluorescence (Figure 3.1A). The cells (healthy or apoptotic) incubated with FITC indicate that the dye is accumulating inside the cells non-specifically give green fluorescence from healthy or apoptotic cells (Figure 3.1C). hCD36 ecto R63A is not binding PS blotted on nitrocellulose membrane or present on lipid vesicles (Banesh et al., 2018).

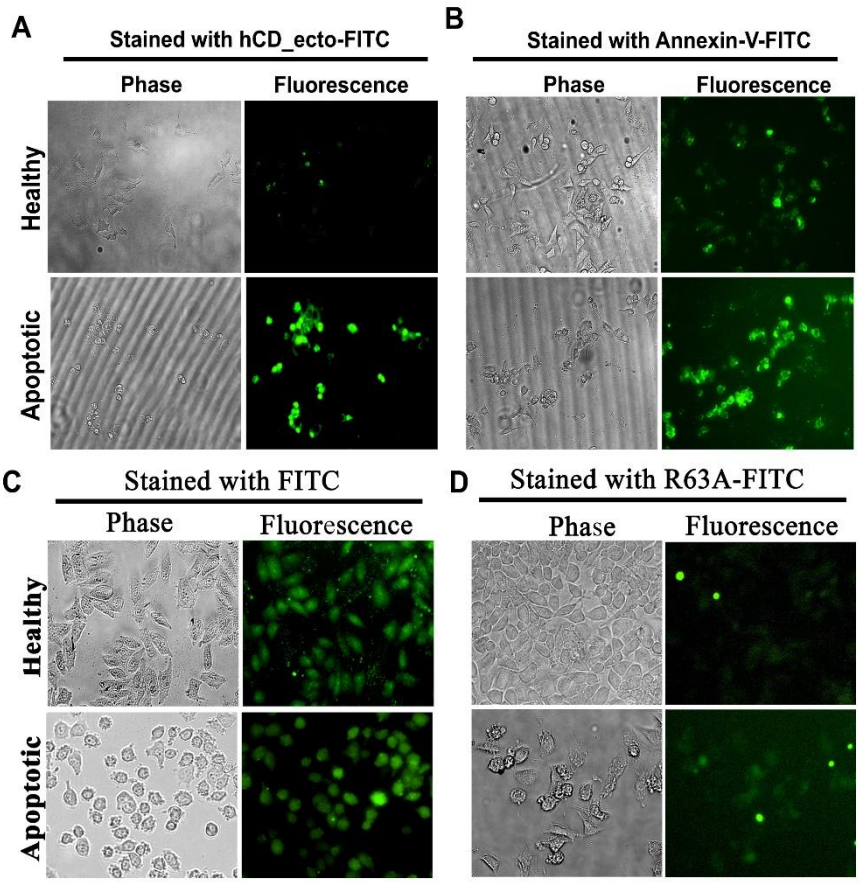

Figure 3.1. hCD36_ecto detect apoptosis in mammalian cells. (A) hCD36_ecto-FITC stain the apoptotic cells exclusively. Healthy and apoptotic cells were prepared as described in "Material and methods". Healthy and apoptotic HeLa cells were incubated with hCD36_ecto-FITC for 1 h at 4 ^{o}C. Cells were observed, and images from random fields were acquired in bright field and fluorescence green channel (λex-461 nm, λem-525 nm) using Cytell cell imaging system. **(B)** Annexin V-FITC is used as a positive control. hCD36_ecto is staining apoptotic cells with no or minimal staining for healthy cells. The healthy or apoptosis Hela cells were prepared as described in material and methods. Healthy or Apoptotic cells were stained with FITC **(C),** R63A_FITC (**D**) and imaging has done in Cytell cell imaging system. The FITC non-specifically accumulating inside the cells and giving fluorescence where as R63A-FITC stained cells giving negligible fluorescence.

TH-2507_156106009

To rule out the possibility of non-specific binding by protein part, R63A-FITC was used in staining the healthy or apoptotic cells. As expected, cells stained with R63A-FITC is giving very low binding to healthy or apoptotic cells (Figure 3.1D). The result indicates the hCD36_ecto-FITC staining the apoptotic cells while not binding to other molecules present on the cell surface of the healthy cells.

3.3.2. CD36 Ectodomain dose-dependently detect apoptotic cells:

The CD36 ectodomain conjugated to FITC successfully detected the apoptotic cells in a imaging based experiments. The CD36 ectodomain concentration was used for staining in imaging experiment is 100 µg/ml which is much lower (~166 times) than the IC50 of CD36 ectodomain with PS vesicles (Banesh et al., 2018). It has been shown that most of the proteins or probes detect analytes at dose dependently (Gupta et al., 2008). To check whether CD36 ectodomain dose dependently detects the PS, we have stained the healthy or apoptotic cells with varying concentrations of hCD36_ecto-FITC (0, 0.1, 0.3, 1, 10, 50, and 100 µM) in two sets. The first set of stained cells were used in flow cytometry and second set of cells for imaging. The first set of cells incubated with propidium iodide (PI) along with hCD36_ecto-FITC and analysed on BD FACs calibur. The cells stained with 0.1 µM probe showed 0.81% of early apoptotic cells, 11.01% of late apoptotic cells and 27.33% of dead cells whereas as 0.3 µM stained cells showed 17.62% of early apoptotic, 18.49% of late apoptotic and 0.7% of dead cells. The possible explaination for 0.1 µM probe detecting higher percentage of dead cells could be the predominant signal from propidium iodide but not from probe (Figure 3.2A).

The hCD36ecto concentration was plotted against the percentage of early apoptotic cells. The curve indicates at 0.3 µM concentration CD36ectodomain detects the early apoptotic cells (17%) whereas upon increasing concentration of CD36 ectodomain the curve is flattened (Figure 3.2B). In fluorescence imaging, the cells stained with 0.1 µM of hCD36_ecto-FITC showed very high background in apoptotic cells whereas the cell stained with 0.3 µM of probe showed bright fluorescence in apoptotic cells whereas no fluorescence was observed in healthy cells (Figure 3.3). Interestingly, the apoptotic cells stained with higher concentrations of hCD36_ecto-FITC does not show any enhancement in fluorescence of apoptotic cells. The results clearly suggests the working concentration

for hCD36_ecto-FITC to detect apoptotic cells is ~0.3 µM.

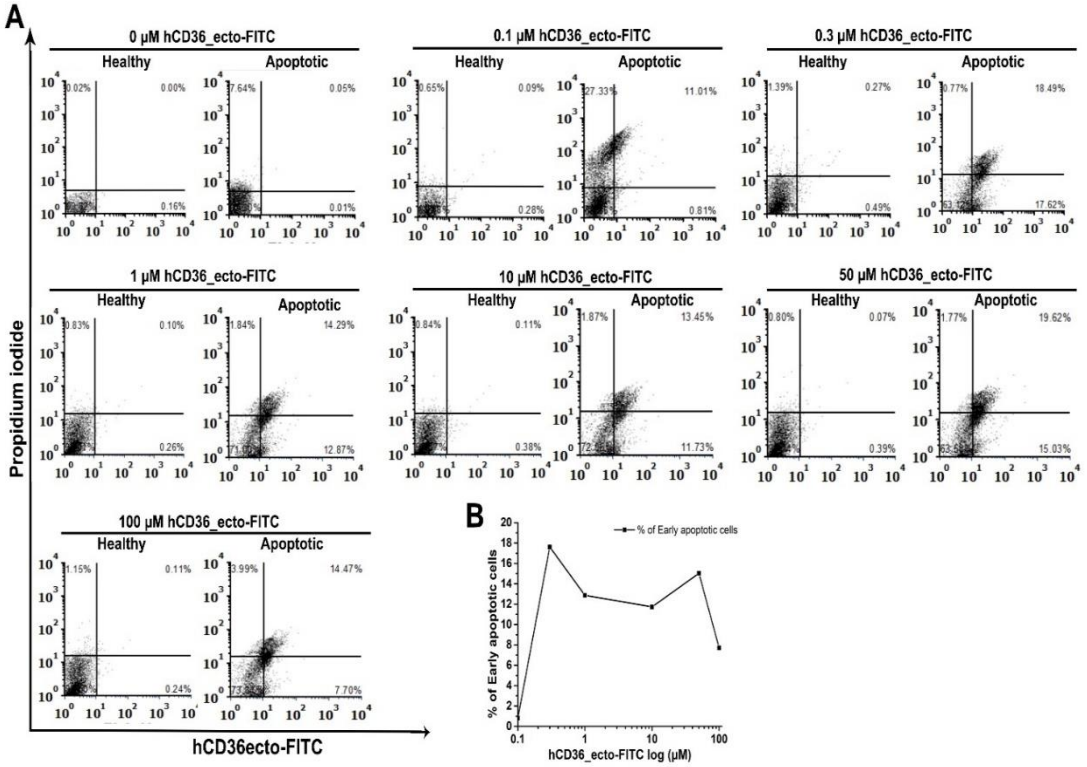

Figure 3.2. hCD36_ecto-FITC dose dependently detect apoptotic cells in flow cytometry. (A) The apoptotic or healthy Hela cells incubated with 0, 0.1, 0.3, 1, 10, 50 and 100 µM of hCD36_ecto-FITC/PI for 1 hr and analyzed on flow cytometer. The quadrant analysis was performed to estimate the early or late apoptotic cells and dead cells. **(B)** The log concentration of hCD36_ecto_FITC ploatted against percentage of early apoptotic cells. At 0.3 µM of probe the early apoptotic cell population is maximum and

3.3.3. hCD36_ecto-FITC is a versatile reagent to detect apoptotic cells in presence of serum and the apoptotic cells generated by serum starvation.

Earlier we have employed Staurosporine to induce apoptosis in mammalian cells. We want to see whether the detection ability of hCD36_ecto-FITC alters if the apoptosis induced through other methods. The Hela cells serum starved for 48 h and stained with hCD36_ecto-FITC for imaging and hCD36_ecto-FITC/PI for flow cytometry. The apoptotic cells stained with probe/PI showing 2.57% of early apoptotic cells, and 14.17% of late apoptotic wheras for healthy cells it was 0.41%, and 0.02% respectively (Figure 3.4A). The cells stained with hCD36_ecto-FITC giving bright green fluorescence in apoptotic cells whereas little or no signal was observed in healthy cells (Figure 3.4B). The results are consistent with chemically induced apoptosis. The serum contains several proteins and antibodies which might affect the detection ability of CD36_ecto towards apoptotic cells sensing. To investigate whether CD36_ecto detects apoptotic cells in

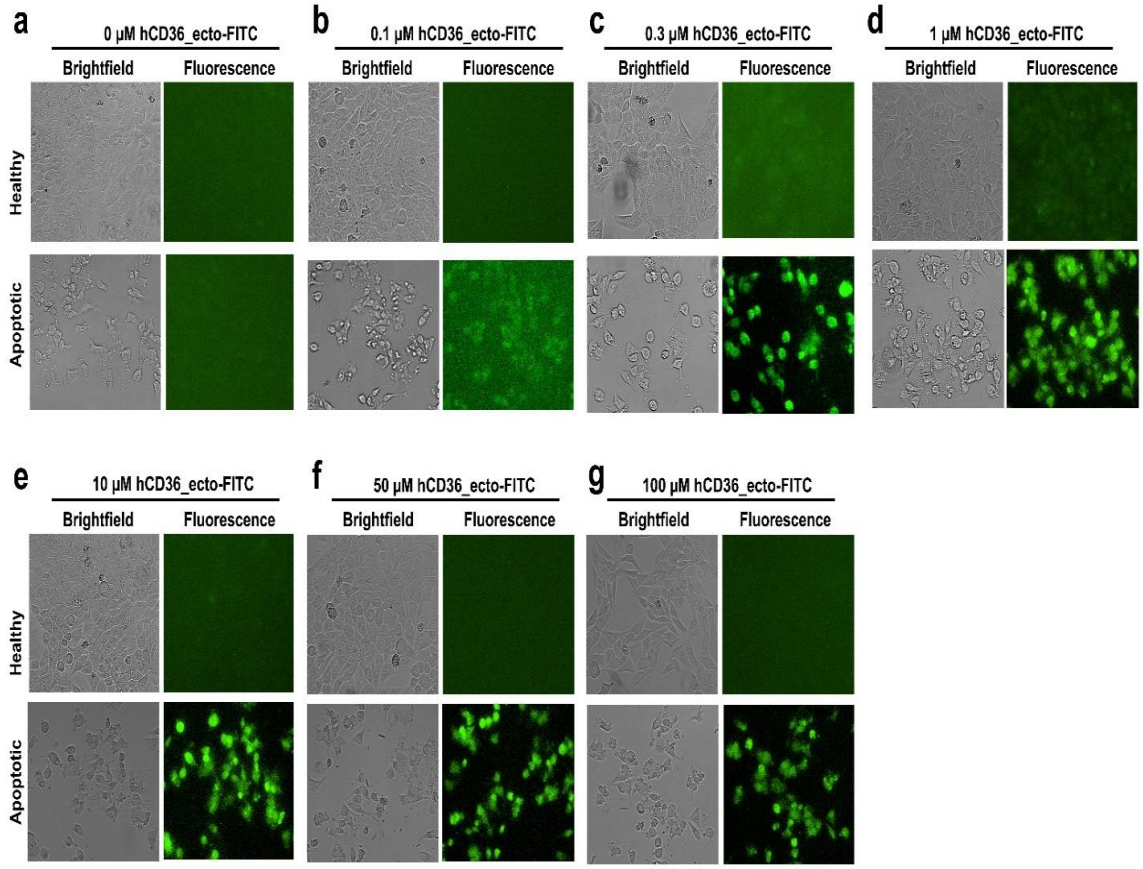

Figure 3.3. hCD36_ecto-FITC dose dependently detect apoptotic cells in fluorescence imaging. The apoptotic or healthy Hela cells incubated with 0, 0.1, 0.3, 1, 10, 50 and 100 µM of hCD36_ecto-FITC and collected fluorescence images in cytell cell imaging system. At 0.1 µM of probe very high background was observed but at 0.3 µM of probe the selective staining of apoptotic cells was observed. Further increase in hCD36_ecto-FITC concentration does not produce any better results.

presence of serum, we have induced apoptosis in HeLa cells and incubated with hCD36_ecto-FITC in presence of serum (FBS). The flow cytometry quadrant analysis indicates the the ability of hCD36_ecto-FITC to detect apoptotic cells does not altered in presence of serum (Figure 3.4C). The fluorescence imaging revealed that CD36_ecto recognizes apoptotic cells in presence of serum also without any interference or background noise (Figure 3.4D). The flow cytometry results are consistent with other results and suggest serum is not a factor that affects the CD36_ecto ability to sense PS expressing apoptotic cels. The study confirms the hCD36_ecto-FITC is not only sensitive detection reagent but also detects apoptosis in serum starvation induced apoptotic cells and

TH-2507_156106009

in presence of serum as well.

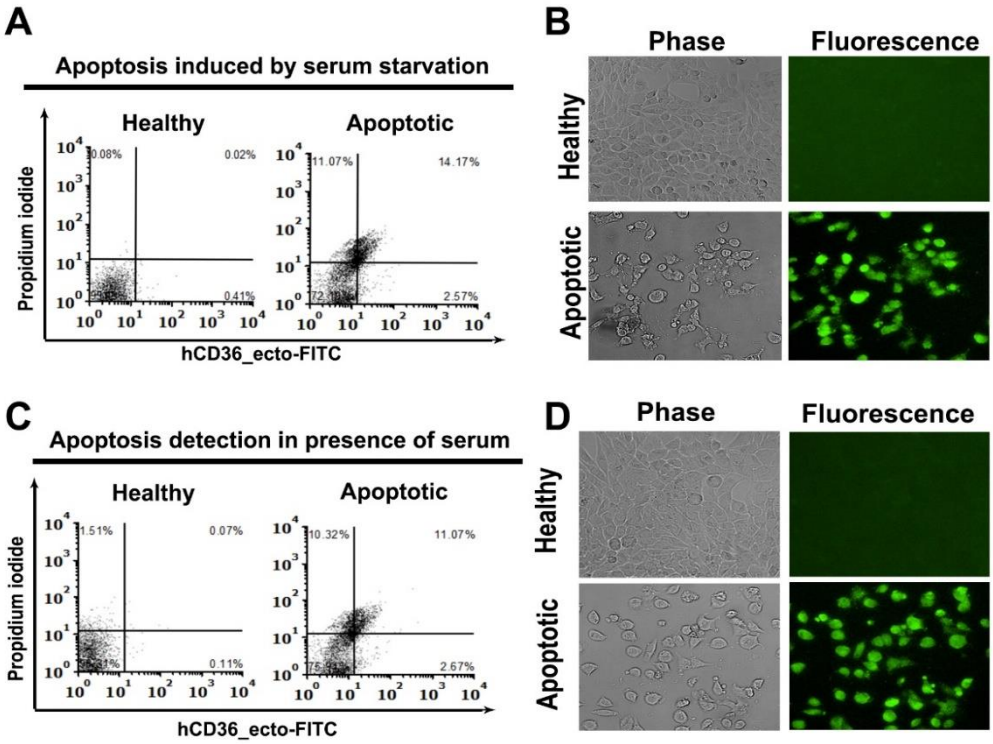

Figure 3.4. hCD36_ecto is a sensitive and selective reagent to detect apoptosis in mammalian cells. (A) The Hela cells serum starved for 48 h to induce apoptosis. The serum starved apoptotic cells or healthy cells were incubated with hCD36_ecto-FITC/PI and analyzed on Flow cytometer (upper panel). As it is evident from apoptotic cell quadrant analysis, the selectivity of probe does not affected. **(B)** The same was confirmed in a fluorescence imaging study. **(C)** The healthy or apoptotic Hela cells were incubated with hCD36_ecto-FITC/PI in presence of serum and analyzed on flow cytometer to investigate the specificity of the probe. The apoptotic cells population in different quadrant (upper panel) suggests the serum does not hinders the probe specificity and same was

3.3.4. CD36 ectodomain detects the PS present on cell surface

The hCD36_ecto-FITC specifically stains the apoptotic cells. To further confirm that the signal is coming from CD36 ecto-domain binding to the cell surface, the location of CD36-ecto was determined by immunolocalization study using anti-CD36 antibody. The cells stained with CD36ecto-FITC are used to counterstained with antiCD36 antibodies in conjugation with Texas red labelled secondary antibody. The healthy cells are not showing any green fluorescence signal, and immune-staining of these cells with anti-CD36 antibodies is giving the bright red fluorescence, but the signal is not overlapping with green signal (Figure 3.5A, top panel, Overlay).

The apoptotic cells stained with CD36ecto-FITC is giving bright green fluorescence and counterstain of these cells with anti-CD36 is giving bright red fluorescence (Figure 3.5A). Interestingly, the signal of CD36_ecto-FITC (green) and anti-CD36 (red) signal are overlapping with each other (yellow) in apoptotic cells (Figure 3.5A, lower panel, Overlay). It highlights two aspects of CD36ecto-FITC mediated staining of apoptotic cells. (1) CD36ecto-FITC is not accumulating inside the cells and giving the green signal. (2) CD36ecto-FITC is binding to a specific ligand phosphatidylserine (PS) present exclusively on the apoptotic cells cell surface, and this ligand is completely absent on healthy cells. CD36ecto can recognize several ligands present on cell surface, including phosphatidylserine, and we have explored next if CD36ecto is recognizing phosphatidylserine present on the cell surface of apoptotic cells. To explore this aspect,

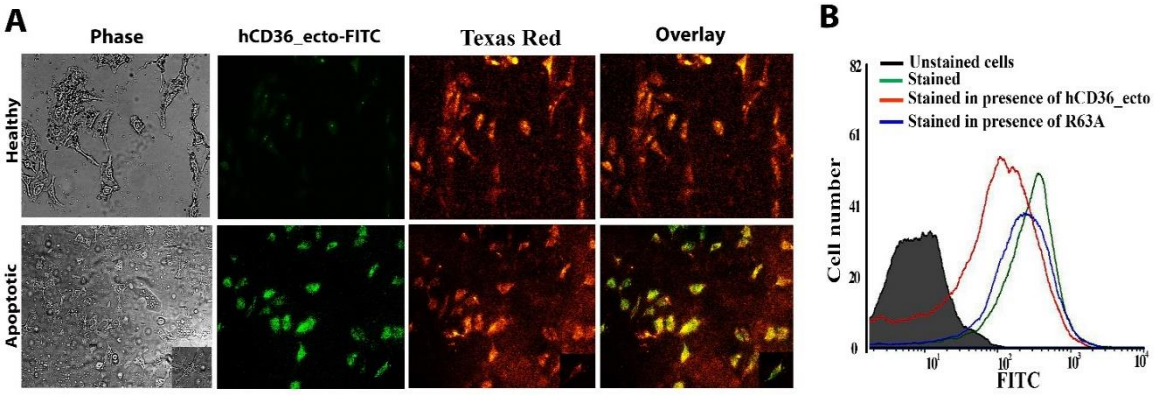

Figure 3.5. Human CD36 ectodomain stains apoptotic cells through CD36-PS interaction. (A) CD36 ectodomain binds to ligands present on the cell surface. The healthy or apoptotic HeLa cells were incubated with hCD36_ecto-FITC followed by counter immunolocalization of CD36 using anti-CD36 antibody in conjugation with Texas red labelled secondary antibody. Cells were observed, and images from random fields were acquired in bright field and fluorescence channels (Green-λex-461 nm, λem-525 nm) (Orange- λex-528 nm, λem-597 nm) using Cytell cell imaging system. The CD36_ecto-FITC signal from apoptotic cells is matching with the location of CD36 on the cell surface (Overlay, top panel) whereas no overlay of both signals was found in healthy cells. **(B)** CD36 binds apoptotic cells exploiting PS biophore. The apoptosis was induced in HeLa cells and the cells were incubated with CD36_ecto or CD36ecto R63A mutant for 1 h at 37 0C to block PS present on the cell surface. Now, these cells were stained with Annexin V-FITC to label PS present on apoptotic cells. Cells were analyzed in BD FACS Calibur flow cytometer in FL-1 channel (λex-488 nm, λem-530/30nm). Histogram analysis of all samples were done by FCS express v6.0, and it indicates that CD36ecto is utilizing PS on the cell surface for their binding as it is reducing Annexin V signal from the apoptotic cells.

we have performed labelling of PS on apoptotic cells with Annexin V-FITC in the presence of unlabelled CD36ecto. Annexin V-FITC is binding exclusively to PS present and stain

apoptotic cells with intense green fluorescence signal (Figure 3.5B). Pre-incubation of apoptotic cells with unlabelled CD36ecto is blocking PS present on cells surface and reducing the fluorescence signal of Annexin V-FITC (Figure 3.5B). Whereas pre-incubation of apoptotic cells with CD36ecto R63A does not affect reducing the binding of Annexin V-FITC and fluorescence signal from stained cells (Figure 3.5B). Hence, the data presented in Figure 3.5 fortify the idea that CD36ecto has the potential to be used as an analytical reagent to stain and detect apoptotic cells.

3.3.5. CD36 ecto-domain can be used to detect apoptotic cells in flow based assay

Annexin V/PI combination is extensively used to detect early apoptotic, late apoptotic and dead cells in a flow based assay (Wlodkowic et al., 2009). The preliminary results in figure 1 indicate that CD36ecto stains the mammalian cells, and it can discriminate apoptotic cells (strong green fluorescence) from healthy cells (low background signal). Also, it is binding PS present on the cell surface of apoptotic cells, similar to well-known apoptosis detection tool annexin V (Schutte et al., 1998). We have further explored the ability of CD36ecto-FITC/PI to be used in flow based assay to discriminate and quantitate apoptotic and healthy cells. Healthy and apoptotic cells were stained with CD36ecto-FITC/PI as described in “material and methods”. The flow cytometric analysis of stained cells in different quadrant indicate the presence of 19.14% cells in early apoptotic, 56.84% late apoptotic and 0.06% necrotic/dead cells (Figure 3.6). The PS biophore present on CD36 ectodomain and mutant CD36ecto R63A is not binding PS blotted on nitrocellulose membrane or present on lipid vesicles (Banesh et al., 2018). To rule out the possibility of non-specific binding of protein part, the R63A-FITC was used in the staining the healthy or apoptotic cells. As expected, CD36ecto R63A is not giving any pattern in quadrant analysis to represent apoptotic cells (data not shown). The detection of apoptosis with CD36_ecto/PI is in close agreement with commercially available apoptosis kit containing Annexin-V/PI in flow cytometry based assay (Table 3.1). Healthy and apoptotic cells were stained with CD36ecto-FITC/PI (Figure 3.6) or Annexin V/PI (data not shown) as described in “material and methods”. Comparing the flow cytometry results indicate that both probes are predicting cells present in the different quadrant with a marginal difference of maximum of 10% (Table 3.1). Interestingly, CD36_ecto is not predicting false positives in Un-treated sample, similar to Annexin V indicate the robustness of the probe to predict apoptotic cells.

TH-2507_156106009

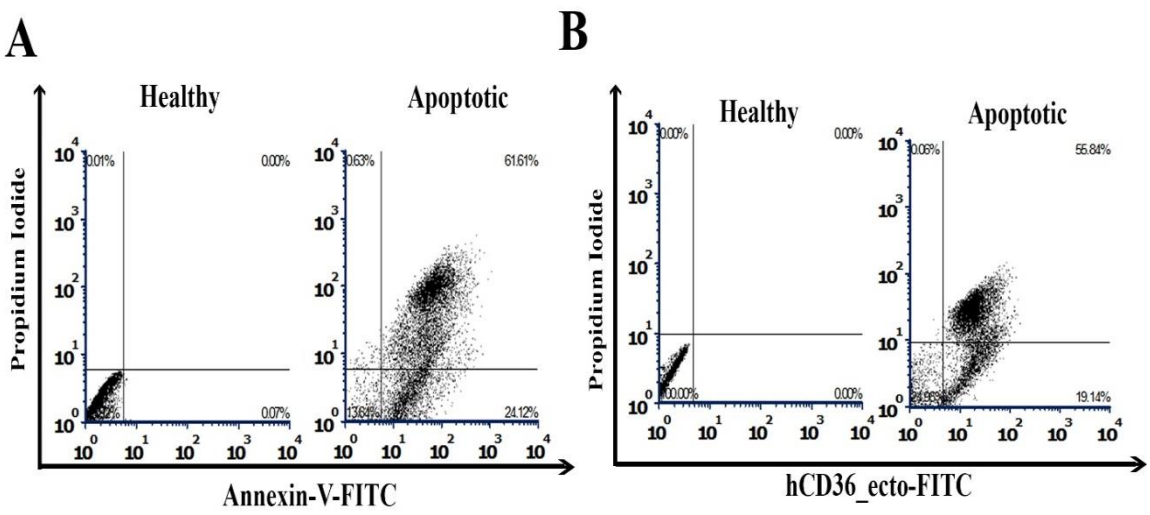

Figure 3.6. Comparison of apoptotic cell detection ability of CD36_ecto-FITC and annexin-V-FITC in a flow based assay exploiting PS biophore. The healthy or apoptosis Hela cells were prepared as described in material and methods. Healthy or Apoptotic cells were stained with Annexin-V-FITC/PI (**panel A**) or hCD36ecto_FITC/PI (**panel B**) or R63A_FITC/PI (panel C) and 10,000 events were recorded in BDFACs calibur. Results were analysed and presented in four quadrant using FCS express v6.0 software. The appearance of the cells in pre-apoptotic and late apoptotic quadrant region indicates the specificity of CD36ecto to stain apoptotic cells and performance level is comparable with annexin-V-FITC.

Table 3.1. Comparison of Annexin-V-FITC and hCD36_ecto-FITC for detection of Apoptotic cells population.

	Quadrant	Annexin-V-FITC (%)	hCD36_ecto-FITC (%)	Difference (%)
Control Cells	LL (Healthy)	99.92	100	± 0.08
	LR (Early apoptotic)	0.07	0.00	± 0.07
	UR (Late apoptotic)	0.00	0.00	± 0.00
	UL (Dead)	0.01	0.00	± 0.01
Apoptotic Cells	LL (Healthy)	13.64	24.96	± 11.32
	LR (Early apoptotic)	24.12	19.14	± 4.98
	UR (Late apoptotic)	61.61	55.84	± 5.77
	UL (Dead)	0.63	0.06	± 0.57

Hela cells either remained untreated (Control) or treated with stauroporine (Apoptotic cells) to induce apoptosis in cells. These cells were stained with hCD36_ecto-FITC or Annexin V-FITC and then stained cells were analysed in flow cytometry. The fraction of cells present in different quadrants is been calculated for both probe and compared. The difference in % cells present in different quadrant is given and these values indicate no relative difference in detection of apoptotic cells by both probes.

3.3.6. CD36_ecto is a robust reagent to detect apoptosis in mammalian cells

The molecular tools should have specificity to detect apoptosis, and on the other hand, it should be universal to perform this task in diversified mammalian cells. So far, we have focused on specificity and the presented data highlighting several aspects of CD36_ecto as apoptosis probe. We have induced apoptosis under the standard conditions described

previously in different nucleated mammalian cells (HCT116, HEK293, HT29, DLD1) (Kleinert et al., 1998; Nagata et al., 2005; Qiao et al., 1996; Sordet et al., 2004). Healthy or Apoptotic cells were labelled with CD36_ecto-FITC/PI and labelled cells were analysed in Flow cytometry. The checkerboard analysis of stained cells indicates different cell population with early/late apoptotic and necrotic cells (Figure 3.7 and Table 3.2). Eryptosis in RBC is also associated with the expression of PS on their cell surface, and interestingly we found that the CD36 ecto-FITC is robust enough to detect eryptosis in RBCs (Figure 3.7 and Table 3.2). Further, we have tested the ability of the probe to detect apoptosis in WBC. The apoptosis in WBC was induced by serum starvation. The cells incubated with CD36_ecto-FITC/PI and analyzed on flow cytometer. As expected the probe has detected apoptotic cells in WBC. The results suggest the potentials of hCD36_ecto-FITC to detect apoptosis in different types of the mammalian cell, including non-nucleated RBCs.

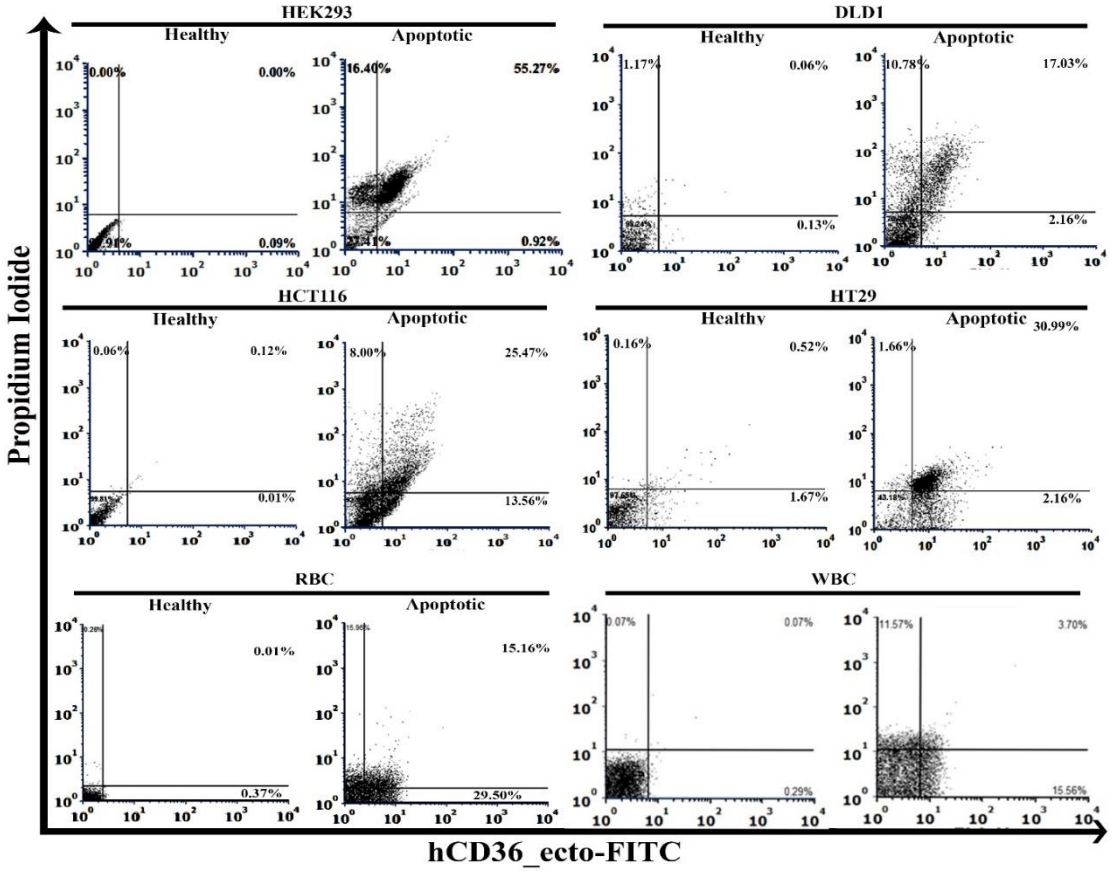

Figure 3.7. CD36_ecto-FITC/PI double staining is a robust tool for apoptosis detection. The healthy or apoptosis cells for different nucleated (HEK293, DLD1, HCT116 and HT29, WBC) or non-nucleated (RBC) cells were prepared as described in material and method. Healthy or Apoptotic cells were stained with hCD36ecto_FITC/PI and 10,000 events were recorded in BDFACs calibur. The data was analysed and presented in four quadrant using FCS express v6.0 software. The quadrant analysis suggests that hCD36_ecto-FITC/PI double staining is a robust tool to detect early/late

TH-2507_156106009

Table 3.2. Detection of apoptosis in different types of mammalian cells.

Cell lines	Untreated Cells		Apoptosis induced	
Quadrant	LR (%) (Early apoptotic)	UR (%) (Late apoptotic)	LR (%) (Early apoptotic)	UR (%) (Late apoptotic)
HEK293	0.09	0.00	0.92	55.27
DLD1	0.13	0.06	2.16	17.03
HCT116	0.01	0.12	13.56	25.47
HT29	1.67	0.52	2.16	30.99
RBC#	0.37	0.01	29.50	15.16
WBC	0.29	0.07	15.56	3.70

Different Mammalian cells either remained untreated or treated with stauroporine (100µg/ml) for 24hrs to induce apoptosis in cells as described in material and methods. (# eryptosis in RBC was induced by ringer solution). These cells were stained with hCD36_ecto-FITC as given material and methods and then stained cells (10,000 events) were analysed in flow cytometry. The fraction of cells present in different quadrants is been calculated and given.

3.4. Discussion and future prospectives

New probes for apoptotic cells that show sensitivity and specificity may be of great importance to study of cell death for basic and biomedical sciences (Martinez et al., 2010). In this study, we have discussed flow-cytometry based apoptotic cell detection assay exploiting CD36 ectodomain as an apoptosis probe through its ability to recognize PS present on the cells surface. Previous studies suggested the CD36 interaction with oxidized phosphatidylserine (oxiPS) promotes apoptotic cells clearance from the systemic circulation via macrophages (Greenberg et al., 2006). Several lines of evidence were made to understand the role of CD36 present on macrophages to engulf oxiPS expressed on dead or aged cells produced in the host body (Greenberg et al., 2006). So far, no experimental evidence exists to explore the utilization of CD36 for detecting apoptotic cells. In the current study, we have tested fluorescently labelled CD36ecto-FITC for detecting apoptotic cells. The apoptotic Hela cells labelled with CD36ecto-FITC showed a bright green fluorescence comparing to healthy cells, suggesting the ability of CD36 to discriminate healthy vs apoptotic cells (Figure 1A). It was unclear whether CD36 detects the apoptotic cells by recognizing phosphatidylserine or sugar moieties present on the apoptotic cell surface (Lorenz et al., 2000; Mahoney and Rosen, 2005). The binding of phosphatidylserine vesicles to J774A.1 or THP-1 cells is highly specific, and blocking with anti-CD36 antibody reduced the binding of PS vesicles in a flow-cytometry based assay (Tait and Smith, 1999). The competitive binding studies between CD36ecto and

TH-2507_156106009

annexin-V revealed the apoptotic cell detection by CD36ecto is based on PS recognition (Figure 1C). Whereas, mutant CD36ecto-R63A pre-incubation does not decrease the Annexin-V-FITC signal further confirms the role of CD36-PS interaction for detection of apoptotic cells. Also, CD36ecto-FITC/PI double staining procedure is robust enough to detect early/late apoptotic and dead/necrotic cell population being generated during cytotoxic treatment to nucleated or non-nucleated RBCs. This study suggests the CD36ecto utility in universal detection of apoptotic cells.

There are various methods such as TUNEL assay (Grasl-Kraupp et al., 1995), antibody-based detection of cytochrome-c release (Eleftheriadis et al., 2016), mitochondrial membrane potential (Sivandzade et al., 2019) available for detection of apoptotic cells. All these methods are either time consuming or need expensive fluorescently labelled probes or antibodies (Archana et al., 2013). Annexin-V based apoptosis detection kits (Kylarová et al., 2002) is user-friendly but it is not economical (Banfalvi, 2017). The isolation of high purity grade Annexin-V from the human placenta is tedious, and purification is cumbersome due to the presence of closely related contaminants (Poghosyan et al., 2003). However, the over-expression and purification of Annexin V in a bacterial expression system are giving low yield (Marder et al., 2014). Due to these difficulties, people have developed other flow based assays such as acridine orange/PI method double method to detect apoptosis during cytotoxic treatments to the cells (Chan et al., 2016; Chan et al., 2012). Compared to Annexin V/PI, double staining method is cost-effective, but it needs standardization as well as method gives high background and false positives. It is mainly because the AO/PI method exploits the presence of damaged DNA and membrane permeability as a phenomenon to detect apoptosis/necrosis in mammalian cells . CD36ecto-FITC/PI double staining is based on the presence of damaged DNA (to bind PI) and the presence of PS on the cell surface. It provides several advantages compared to Annexin V/PI or AO/PI methods. The production of CD36ecto in bacterial expression is efficient, cost-effective. As per calculation, production and labelling of CD36ecto to prepare apoptosis probe is ~Rs. 241 per reaction (Table 3). Compared to AO/PI, the developed method is specific for cell surface ligand, and as a result, it gives a low background signal with no false positives. Also, AO/PI cannot be used as a probe to detect eryptosis in non-nucleated RBCs whereas CD36ecto-FITC detects PS present on non-nucleated RBCs. On the other hand, CD36ecto is stable in a wide range of temperatures ranging from 4-37^{o}C compared to temperature-sensitive Annexin-V.

As PS biophore present on CD36 is known, an alternate approach could be to

design suitable biophore directed immunogenic peptides to tag PS present on apoptotic cells for their faster clearance from the host. Apart from the role of CD36 as apoptosis probe, PS expressing infected host cells can also be targeted for their faster clearance from circulation. Hence, our study highlights potentials of CD36ecto as apoptosis marker to develop a diagnostic tool and as a chelating agent to remove PS expressing pathogenic host cells.

References: Please refer to the Bibliography section at the end of the thesis.

TH-2507_156106009

Chapter-IV

CD36: Hemin interaction axis to control cytokine secretion involving Lyn kinase.

TH-2507_156106009

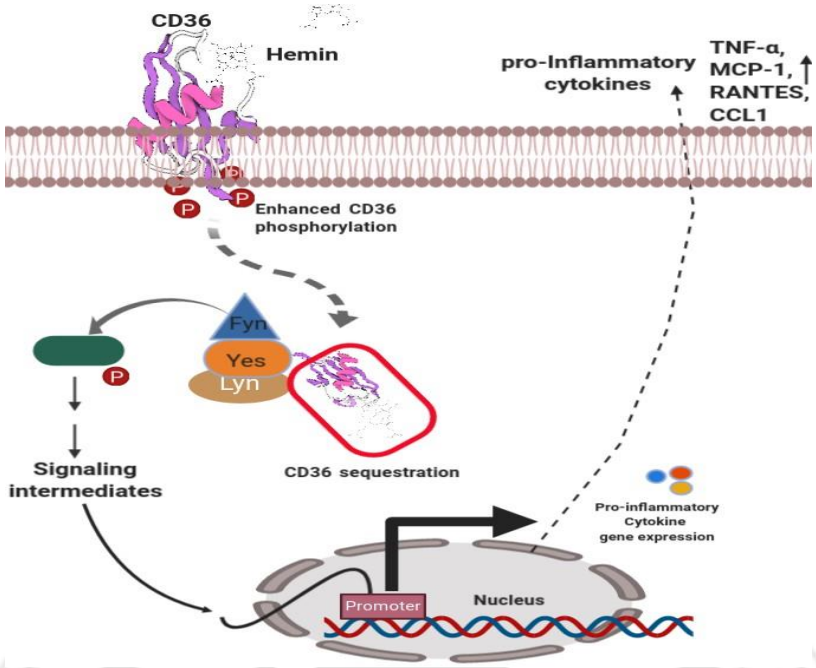

Summary

In this chapter we have investigated the role of CD36 in hemin mediated immune dysfunction in macrophages and downstream signalling. The molecular modelling and in-vitro experiments suggested the residues R292, D372 and Q382 are crucial for hemin intercation. The MG63 cell line (with very low CD36 expression) MG63 cells with wild type CD36 ectopic expression showed several folds increment in cytokines TNF-α, MCP-1, RANTES and CCL1 in response to hemin stimulation but no significant amount of cytokines released in mutants (R292A, D372A or Q382A) validates the hemin act as a ligand for CD36 and responsible for immune-dysfunction. The phosphoprotein western blot and immunoprecipitation studies revealed that hemin activating the down-stream signalling through phosphorylation of CD36 and subsequent recruitment of Src family kinase protein to cytosolic domain of CD36. The Lyn targeted siRNA restored the phagocytic activity, reduced the pro-inflammatory cytokine levels to normal suggests the Src family protein Lyn is crucial for cytokine signaling. In summary, hemin-CD36-Lyn cytokine signalling axis could be a contribution factor to severe malaria pathology and prognosis.

Key words: Hemin, CD36, pro-inflammatory cytokines, Src family kinases, downstream signalling.

TH-2507_156106009

4.1. Introduction

Plasmodium falciparum, the causative agent of malaria, is responsible for high mortality rate especially in children and pregnant women (Toure and Oduola, 2004). During the course of malaria, RBC lysis releases the large amount of pro-oxidant molecules including free hemin and its derivative. During the infection the concentration of hemozoin and hemin immediate after RBC rapture may be as high as 100 µg/ml (Balaji and Trivedi, 2013). Macrophages control parasite load through phagocytosis of IRBC in an opsonic or non-opsonic dependent mechanism (Gowda et al., 2013). Phagocytic internalization of IRBC, as well as parasite-derived products, release the large quantity of methemoglobin and hemin inside the macrophages. It is in-turn inhibits the fusion of lysosome to phagosome; disrupts the antigen processing and presentation through partially characterized mechanism.

Macrophage utilizes cell surface and cytosolic receptors to identify infected RBCs (IRBC) and parasite-derived products. Hemin, glycophosphatidylinositol (GPI) and hemozoin activate macrophages to produce cytokines which can excessively fuel inflammatory outcomes (Anstey et al., 2007). Experimental evidences suggest that hemozoin can activate macrophages through TLR9 to produce pro-inflammatory cytokines such as TNF-α. Earlier studies have established that the intensity and duration of TNF-α production are mutually correlated with the level of CD36 expression (Serghides and Kain, 2001). Moreover, it has been found that macrophage CD36 present on the cell surface binds multivalent ligands, which triggers signal transduction and receptor ligand internalization. Hence it is interesting to explore the effect of hemin on non-opsonic phagocytosis of macrophages, and whether it is related to the CD36 expression on the cell surface and down-stream cytokine secretion.

Previously our lab has explored hemin mediated immune-dysfunction in macrophages. Macrophages treated with different concentrations of hemin (0-200µM) exhibits phagocytotic activity with a unique pattern in a flow-cytometry based phagocytosis (unpublished work). Further, the hemin exposure caused global depression of phagocytotic activity of macrophages towards amine, LPS and phosphatidyl-serine containing oxidized RBCs. Interestingly, the depression in macrophage phagocytosis is more severe towards oxidized RBCs (containing PS) compared to the normal RBCs. Phagocytosis is followed by internalization of the infectious agent and its destruction within phagolysosomes through the action of lytic enzymes (Trivedi et al., 2006). Hemin treated macrophages

were showing severe reduction in bactericidal activity compared to the untreated cells. Presence of CD36 on macrophage plasma membrane is crucial for phagocytosis of RBCs to facilitate the clearance from circulation. The macrophages (treated with hemin) exhibit low level of CD36 o plasma membrane. CD36 localization inside the cells indicates the high level of CD36 on the vesicular structures and major sequestration of CD36 within the vesicular structures. Macrophages treated with different concentrations of hemin (0-200 µM) show dose-dependent secretion of TNF-α. Moreover, macrophages stimulated with bacteria were giving several folds high TNF-α secretion compared to the unstimulated cells. Whereas, cells treated with hemin and stimulated with bacteria did not show much TNF-α secretion. It indicates a functional defect in the hemin treated macrophages towards immunological stimuli to secrete TNF-α for clearing the infection from the site of action.

In this study, we have observed that hemin potentiates drastic changes in the cellular physiology of macrophages such as non-opsonic phagocytosis, ability to kill bacteria and production of pro-inflammatory cytokine TNF-α. Interestingly we have found that hemin exposure not only modulates the pattern of phagocytosis but also leads to sequestration of CD36 receptors within the intracellular storage. The hemin treatment, also induced secretion of series of pro-inflammatory cytokines such as TNF-α, MCP-1, RANTES and CCL1. The pro-inflammatory cytokine secretion upon hemin treatment could explain the pathological outcome during severe malaria. The molecular modelling and affinity studies have confirmed that hemin interacts with the human CD36 ectodomain on a well-defined region consisting of R292, Q382 and D372 residues. The mutations in biophoric residues drastically reduced the affinity and validates the predicted biophore for hemin. We have further, investigated whether TLRs has any role in hemin mediated immune response. The cell line MG63 (with low levels of TLRs and CD36) has been chosen to express CD36 ectopically. The CD36 ectopic expressing MG63 cells migrated towards hemin and confirms the membrane bound CD36 is crucial for hemin to interact and TLRs has no role in it. Besides, the CD36 (wildtype) expressing MG63 cells responded to hemin but mutants (R292A or D372A or Q382A) expressing MG63 cells failed to produce significant levels of cytokine in presence of hemin. Further the hemin treatment activated several proteins including CD36 and suggests the possible downstream signalling. It has been reported that activated CD36 enables the docking of adaptor proteins to cytosolic domain. Our study has found that Src family member adaptor protein Lyn interacts with CD36 in hemin stimulated macrophages as evident from the co-immunoprecipitation study. The Lyn knockdown in macrophages corrected the abnormal phagocytic behaviour and cytokine

TH-2507_156106009

burst and indicates the Hemin-CD36-Lyn axis is the reason behind pro-inflammatory cytokine secretion. We have also highlighted that dysfunctional CD36 receptor dynamics (from intracellular vesicles to the cell membrane) may have promising implication in correcting the coherent secretion of cytokines and immunopathology. Our study may provide fundamental understanding role of macrophage in cellular protection, cytokine secretion to contribute into inflammation and brain pathology.

4.2. Experimental procedures:

4.2.1. Reagents: Peptone Type-III bacteriological, Yeast extract powder, Sodium chloride, ampicillin, skim milk powder, tween-20, dialysis membrane-70, foetal bovine serum were procured from HiMedia labs, India. Isopropyl β- d-1-thiogalactopyranoside (IPTG), nickel sulfate hexahydrate, Dulbecco's modified eagle's medium were purchased from Sigma-Aldrich, India. Site specific primers were procured from Bioserveindia, India, and Ni-NTA affinity columns were from Qiagen, Hilden, Germany. Restriction enzymes and 1 kb DNA ladder were purchased from New England Biolabs, USA. PCR master mix (2x) was purchased from Fermantas, India. Dual color proteins standards purchased from Biorad, California, USA. T4 DNA ligase was purchased from genetix, India. Desalting column (PD-10) was purchased from GE life sciences, India. Human CD36 gene, mApple-CD36-C-10 was a gift from Michael Davidson (Addgene plasmid # 54874). The pET23a vector, BL21-(DE3), DH5α bacterial strains were from novagen. Mouse polyclonal anti-6xHis antibody, rabbit polyclonal anti-phosphotyrosine antibody purchased from Sigma-Aldrich, India. Rabbit anti-CD36 antibody, Mouse anti-CD36 antibodies rabbit HRP conjugated secondary antibody were procured from Santa Cruz Biotechnology, USA. ECL reagent was procured from Bio-Rad labs, USA. DMEM-F12, DMEM-high glucose are from Sigma-Aldrich. PEiRfect transfection reagent was procured from Biobharati lifesciences, India. The cytokine ELISA kits for TNF-α (cat#. KRBA10602-5), MCP1 (cat#.KRB10134-5) and RANTES (cat#.KB1102) were purchased from Krishgen Biosystems, Mumbai, India and CCL1 (cat#.KTL11769) from (Kreative Technolabs, Los Angeles, CA, USA)

4.2.2. Mammalian cell culture: Different cell lines J774A.1, MG63, MDAMB-231, A549, HeLa, HEK-293, SAS, Sf-9, and Sf-21 were purchased from NCCS, Pune, India. All the cell lines were maintained in DMEM high glucose medium supplemented with 10% of Foetal bovine serum containing 1% penicillin and streptomycin at 37^{o}C in a

humidified chamber with 5% CO_2.

4.2.3. Phagocytosis assay: Macrophages were either remain untreated or treated with different non-toxic concentration of hemin (0-200mM) in serum free medium for 1 hr at 37^{o}C in a humidified chamber with 5% CO_2. Post treatment, hemin was washed three times with PBS and cells were removed from the culture dish by incubating with 0.5% EDTA for 30 mins and phagocytosis was measured in flow cytometry-based assay as described (Rodríguez et al., 2001). In the assay, cell suspension was incubated with FITC-labelled *E. coli* (1:10) for 1hr at 37°C with intermittent shaking and then placed on ice. Trypan blue (1%) was mixed with the cells to quench the fluorescence from the bacteria sticking to the cells. Ten thousand cells were analysed by flow cytometry (FL1 channel) using FACS Calibur (Becton-Dickson) to calculate the proportion of cells phagocytose bacteria whereas mean fluorescence intensity (MFI) was used to calculate number of bacteria taken up per cell. Data is expressed as phagocytic index using the formula; phagocytic index= % phagocytic macrophages X MFI.

To study the phagocytosis of different objects in the microscopy based assay, normal RBC (NRBC), oxidized RBCs (oxiRBC), latex beads coated with LPS, Amine beads (+Ve charged) were incubated with untreated or hemin (75µM) treated macrophages for 1hr at 37 °C. Cells were washed with PBS to remove un-phagocytosed objects and stained with fluorescent dye filipin (5 µg/ml) to identify the phagosomes. Cells were observed under the fluorescence microscope 80i (Nikon) and random 10 different fields were selected to count number of phagosomes to calculate the phagocytic activity of macrophages.

4.2.4. Bactericidal Assay: Bactericidal assay was performed as described previously (Peck, 1985). Hemin treated macrophages (10^6) were incubated with live *E.coli* suspension (1:50) for 1hr at 37 °C. After 1hr, tubes containing the cell suspension were centrifuged (300×g) for 12mins at 4°C. Cell pellet was washed thrice with PBS to remove unbound bacteria and macrophages were lysed with chilled milli-Q water. Cell lysate was added to the 3ml LB and allowed to grow at 37°C overnight, number of bacteria were counted and used to calculate bactericidal activity.

4.2.5. Immunolocalization of CD36 in macrophages: The murine macrophages J774A.1 were grown on a cover slip (in a 24 well plate) and treated with hemin (0, 25 or 200 µM) for 1 h in serum free medium. The cells were washed with PBS to remove free hemin then

TH-2507_156106009

fixed and permeabilized. The cells were incubated with blocking solution (3% BSA in PBS) for 1 h in CO_2 incubator followed by anti-CD36 antibody (1:500 dilution) incubation at 4 °C for 4 h. The cells were washed with PBS to remove any unbound antibody and incubated with FITC conjugated secondary antibody (1:700 dilution) for 2 h at 4 °C. The secondary antibody removed and washed with PBS. The coverslip was mounted on a glass slide and observed under Nikon fluorescence microscope. The images for bright field or fluorescence were collected from ten random fields and analysed.

4.2.6. Macrophage cell fractionation and assessment of purity: The macrophages were fractionated as described (Andreyev et al., 2010). The macrophages seeded at 5 x 10^6 per well in a 6 well plate. The cells were treated with 25 or 200 µM of hemin for 1 hr at 37 ^oC. The cells were gently washed three times with PBS to remove free hemin. The cells were harvested by scraping and pelleted by centrifuging at 1500 RPM for 5 min. The cell pellet suspended in cell lysis buffer (10 mM HEPES, pH 7.4, supplemented with 1 mM PMSF) and homogenized by passing through 2 bend 25 gauge needed. The homogenates were centrifuged at 3000 RPM for 5 min. The pellet containing nuclei was discorded and the supernatant used for further fractionation. Before fractionating into membrane and cytosol, the protein concentration was estimated using Bradford assay. Equal quantity of cell lysates taken from each condition and further centrifuged at 20000 RPM for 1 h. The pellet contains membrane fraction and the supernatant is cytosol. The washed for 2 times using cell lysis buffer to minimize cytosolic contamination. At final step the membrane fraction re-suspended in cell lysis buffer and passed through 2 bend 25 gauge needle to homogenize.

The membrane and cytosolic fractions were assessed for their purity LDH assay (Deka et al., 2017). Briefly, the NADH (0.13 mM) and sodium pyruvate (0.2 mM) dissolved in 1M Tris.HCl, pH 7.3. From NADH and sodium pyruvate solution placed in a cuvette and introduced membrane or cytosol into cuvette. The absorbance was recorded at 340 nm over 4 min. The cytosol contains lactate dehydrogenase (LDH) which oxidizes the NADH and show reduced absorbance. Since the membrane fraction lacks LDH, the absorbance of NADH unaffected.

4.2.7. Cytokine profiling: Macrophages J774A.1 were either remain untreated or treated with hemin (25µM) in serum free DMEM medium for 1hr and subsequently cells were allowed to secrete cytokines overnight (~18 hrs) in cell culture supernatant at 37^0C in

humidified CO_2 incubator. The cytokines released from macrophages treated with hemin were detected by mouse cytokine proteome profiler array panel A kit (ARY006, R&D Systems, USA) as per the manufacturer's instructions. The dots corresponding to different cytokine signals were analysed using densitometry (ImageJ, National Institute of Health, USA) and normalized to control dots present in the array.

4.2.8. Measurement of cytokines in cell culture supernatants: The murine macrophages maintained in DMEM medium were seeded at 2 x 10^4 cells per well in a 96 well plate and allowed to adhere. The cells were washed and treated with hemin (prepared in a serum free medium) for 1 hr. Post-treatment, cells were washed with PBS and the serum free medium was added to the cells and allowed to secrete the cytokine overnight at 37^0C in humidified CO_2 incubator. The cell culture supernatants were collected and centrifuged to remove the debris and dead cells. TNF-α level was measured using ELISA kit (555268, BD Biosciences, Sa Jose, CA, USA). In experiments with human osteosarcoma (MG63) cells transfected with CD36_cherry, different cytokines such as TNF-α (KRBA10602-5, Krishgen Biosystems, Mumbai, India), MCP1 (KRB10134-5, Krishgen Biosystems, Mumbai, India), RANTES (KB1102, Krishgen Biosystems, Mumbai, India), and CCL1 (KTL11769, Kreative Technolabs, Los Angeles, CA, USA) level in the cell culture supernatant were quantified as per the manufacturer's instructions. All the data was corrected for substrate absorbance and plotted using Origin pro software (Origin labs, Northampton, MA, USA). The levels of cytokines were expressed in 'folds' change considering the level of cytokine present in 'untreated' cells.

4.2.9. Prediction of Hemin biophore in CD36: The hemin co-crystalized proteins (1O9X, 2BLI, 2QSP, 2R7A, 2ZDO, 3NU1, 4MF9 and 4MYP) were downloaded from protein data bank (www.rcsb.org) and analysed for binding environment of hemin within 6 Å using protein contact map webserver ContPro (Firoz et al., 2010). The interactions between protein and hemin atoms were analysed using Ligplot+ and protein-ligand interaction profiler webserver (https://projects.biotec.tu-dresden.de/plip-web/plip/). The residues found consistently featuring in majority of the analysed complexes were mapped and a matrix has been generated with hemin and protein atoms. The distance between atoms scaled and colour coded in VIBGYOR.

4.2.10. Generation of CD36-Hemin molecular model: The Autodock v4.2 with

TH-2507_156106009

autodock tools v1.5.6 application with genetic algorithm as a scoring function was used for CD36-hemin molecular docking (Morris et al., 2009). The molecular docking was performed on predicted biophore as grid centre. A total of 100 GA runs with 2500000 energy evaluations were carried out. The docking log file was analysed for binding energy, number of clusters and conformations in each cluster. The best pose with highest conformations and lowest binding energy was analysed for hemin-CD36 interactions using ligplot+ and protein-ligand interaction profiler webserver application.

4.2.11. Molecular dynamics simulations: The crystal structure of CD36 (PDB id 5LGD) was downloaded from protein data bank and mutants were generated using modeller. The topology file for hemin was generated based on the topographical inputs from the webservers PRODRG and automated topology builder (ATB) (Malde et al., 2011). The MD simulations were performed on Dell precision T1700 workstation using GROMACS 4.6.5 package. The GROMOS96 43a1 force field was used for simulations. The protein-hemin complex was placed in the simulation box such that the complex is 1.5 nm distant from the wall of the simulation box. The system was solvated with simple point charge water and energy minimized by steepest descent algorithm. The production run was performed for 10 ns for wild-type, and mutational variants (R292A, D372A and Q382A) with an integration step of 1 fs under NVT conditions. LINCS algorithm with geometric accuracy of 10^{-4} was used as the bond length constraint. Maxwell distribution was used for initial velocity calculations with 0.1 ps of coupling relaxation time at 300 K. The non-bonded interaction cut off was set at 1.4 nm for both van der Waal's and electrostatics (PME). The MD trajectories after production run were analysed for root mean square deviation (RMSD), structure-based clustering, and radius of gyration (Rg), root mean square fluctuation (RMSF).

4.2.12. Molecular dynamics simulations of membrane bound CD36-Hemin complex: For membrane bound CD36 molecular dynamics study, a 128 membered Dipalmitoylphosphatidylcholine (DPPC) lipid bilayer was constructed using the MemBuilder server (Ghahremanpour et al., 2013). GROMOS 53a6 force field parameters were used in combination with Berger lipid parameters. Water as simple point charge was used as the solvent. Parrinello-Rahman barostat was used for pressure coupling and isothermal compressibility was set at 4.5×10^{-5} bar^{-1}. The system was energy minimized by the steepest descent algorithm and equilibrated for one nano second (ns) under NVT

(conserved Number of particles, Volume and Temperature) and NPT (conserved Number of particles, Pressure and Temperature) conditions successively. A total of 100 ns production run was performed on the system containing CD36-hemin integrated into DPPC bilayer. Post-simulation, the system was analysed for the bilayer thickness, RMSD (root mean square deviation) and Rg (radius of gyration) and solvent accessible surface area (SASA).

4.2.13. Cloning, over-expression and purification of hCD36ecto wild type and mutants: The cloning, overexpression, and purification of hCD36ecto was done as reported in our previous publication (Banesh et al., 2018). Different mutants were also prepared following the similar procedure.

4.2.14. Site-directed mutagenesis: The conventional long-range PCR amplification (Kumar, 1996) performed to introduce mutations at R292 (R292A), D372 (D372A) and Q382 (Q382A) positions in pET23a-hCD36ecto (for expression in bacterial system) or pmApple-CD36-C-10 (for expression into mammalian system). The different primers used for generation of mutant CD36 is given in Table S1. The PCR reaction was performed in a total volume of 50 µL containing 20 ng of template (pET23a-hCD36ecto or pmApple-CD36-C-10), 15 pM of mutagenic primers (Table 4.1) and PCR master mix. The PCR amplification was carried out at 94 °C initial denaturation for 4 min followed by 16 cycles of denaturation (at 94 °C for 30 s), annealing (60 °C for 1 min) and extension (68 °C for 7 min). The amplified products were PCR cleaned up and eluted in nuclease-free water. Subsequently, the eluted product digested with *Dpn-I* for 2 h at 37 °C. Finally, the digested product transformed into NEB 5α competent cells (New England Biolabs, Ipswich-MA, USA). The mutation was confirmed by sequencing and restriction digestion.

Table 4.1: Mutagenic primers used in this study.

S.No.	Primer ID	Sequence
1	**R292A_FP**	5′-ctgaaaggaatccctgtgtatgcatttgttcttccatccaaggc-3′
2	**R292A_RP**	5′-gccttggatggaagaacaaatgcatacacagggattcctttcag-3′
3	**D372A_FP**	5′-gaatccagttataggttcaatagccaagtatgtcctatgttcttc-3′
4	**D372A_RP**	5′-gaagaacataggacatacttggctattgaacctataactggattc-3′
5	**Q382A_FP**	5′-gcagccgttttgcaaatgctaaagtgaatccagttataggttcaatatc-3′
6	**Q382A_RP**	5′-gatattgaacctataactggattcactttagcatttgcaaaacggctgc-3′

TH-2507_156106009

4.2.15. Dot blot assay: The dot-blot assay was performed as described (Banesh et al., 2018). Briefly, the hemin solution (50 micromolar) was applied to a nitrocellulose membrane blot as a dot and air-dried. The membrane was incubated with the blocking buffer containing 3% BSA in TBST buffer (50 mM Tris-HCl, 150 mM NaCl, 0.05% Tween-20, pH 7.5) for 2 hr at room temperature. The membrane was incubated with purified hCD36ecto for 2 hr at room temperature with mild shaking on a shaker. Subsequently, the NC membrane was washed with TBST buffer to remove any unbound proteins and incubated with anti-CD36 antibodies for 2 h at room temperature. After washing, the blot was incubated with HRP-conjugated secondary antibody to detect the presence of CD36 on the membrane. Dot blot was developed using Clarity western ECL substrate (1705061, Biorad labs, California, USA) and images were acquired in the ChemiDoc MP imaging system (Biorad labs, USA). Similarly, the assay was performed on mutants (R292A, D372A, and Q382A) as well to test the affinity of hemin to the mutant proteins. The signal intensity was normalized or calculated by considering wild type as 100 %.

4.2.16. Isothermal titration calorimetry: The affinity measurements of hemin towards wild type (hCD36ecto) or mutants (R292A, D372A and Q382A) were performed in MicroCal iTC200 isothermal titration calorimeter (GE Healthcare, Chicago, USA). Unless specified, all the titrations were carried out at 37°C. The wild type or mutant proteins (0.01 mM) were loaded into ITC titration cell in a total volume of 200 µL. The syringe is filled with hemin solution (0.1 mM) and placed in ITC titration cell. A total of 25 injections were carried out consisting of 0.4 µL of first injection and 1.6 µL in subsequent injections. To correct background heat generated due to buffer or hemin dilution, another blank titration was carried out with hemin against buffer only. The data were analysed using ITC200 analysis software v7.2 application integrated in ORIGIN7 graphing software (Origin Lab, USA) and fitted with sequential binding mode to calculate the dissociation constant.

4.2.17. Transfection studies: All the transfections were performed according to the manufacturer's instructions. The MG63 cells with low passage number were seeded at 3 x 10^5 cells per well in a 6 well plate one day prior to the transfection. The wild type (pmApple-CD36-C-10) or mutant (pmApple-R292A, pmApple-D372A and pmApple-Q382A) plasmids were diluted in 50 µL of serum free DMEM medium and vortexed briefly for 5 sec. The PEI transfection reagent was added to diluted plasmid DNA at 1:2

TH-2507_156106009

ratio (2 µg of PEI for 1 µg of plasmid). The DNA+PEI mixture vortexed for 5 sec and incubated at 25^0C for 15 min to form the DNA-PEI complexes. The transfection mixture was added drop-wise to the cells and after 6 hr, medium was replaced with DMEM complete medium and incubated for another 48 hr for expression. The expression was analysed by fluorescence imaging, flow cytometry [using (FL-2 channel, λ ex488/λ em575)] and western blotting.

4.2.18. Chemotaxis assay: The chemotaxis assay was performed as described (Trivedi et al., 2009). The transfected MG63 cells seeded at 2 x 10^4 cells in serum free DMEM in upper chamber of inserts (with 12 µm pore size) in a 24 well dish. The bottom chamber is filled with either serum free medium or hemin (prepared in serum free medium). The cells were kept in a CO_2 incubator at 37 ^{o}C for 6 h to allow the migration. After 6 h incubation, the inserts were washed with PBS to remove dead cells and floating debris and fixed in 95% ice-cold ethanol for 8 min. The inserts were stained with hematoxylin and eosin successively. The inserts were washed with the PBS to remove the excess dye and the cells in upper chamber side were removed by gently scraping with cotton swab. The cells in lower chamber side were observed and photographed in ten random fields. The chemotactic index (CI) was calculated as given in Equation 4.1.

$$CI = \frac{Cells\ migrated\ (sample) - Cells\ migrated\ (control)}{Total\ number\ of\ cells} x100 \quad \text{.....Equation 4.1}$$

4.2.19. Immuno-precipitation: The J774A.1 cells were seeded at 5 x 10^7 in a 100 mm cell culture dish one day before the experiment. The cells were treated with hemin (25 µM) for 1 h in serum free medium and washed three times with PBS. The cells were detached using cell scraper and the cell pellets was re-suspended in IP lysis buffer (10 mM HEPES pH 7.4, 250 mM NaCl, 1 mM EDTA, 0.5% NP-40 and 0.2% Tween-20) supplemented with freshly prepared protease (1 mM PMSF) or phosphatase inhibitors (10 mM NaF and 0.1 mM Na_3VO_4). The cell suspension passed through 2-bend 25-gauge needle ten times to homogenize the lysate and incubated on ice for 20 min. Subsequently, the lysates were clarified by centrifuging at 14,000 rpm for 2 min at 4^{o}C. The protein concentration was estimated using Bradford assay (Kruger, 2009). The clarified lysates was pre-cleared by incubating with 20 µL of protein AG plus agarose beads slurry (BB-PAG001PA, Biobharati lifesciences, Kolkata, India) at 4 ^{o}C for 1 hr under rotating condition. The pre-cleared lysates were incubated with mouse anti-CD36 antibody (2 µg) or anti-Lyn antibody (1:50 dilution) at 4 ^{o}C overnight under rotating condition. The pre-washed 20 µL

of protein AG agarose beads were added to the lysate-antibody mixture and incubated overnight at 4^{o}C on a rotator. The protein AG agarose beads were washed with IP lysis buffer four times and eluted in SDS-PAGE sample buffer containing 150 mM of DTT.

4.2.20. Analysis of the phospho signal in hemin treated macrophage cell lysates

The J774A.1 cells maintained in DMEM high glucose with serum supplementation were seeded in a 100 mm cell culture dish one day before the experiment. The cells were incubated with indicator free DMEM and kept for 4 h in incubator to eliminate the phenol red induced phosphorylation in cells. After 4 hr, the cells were treated with hemin (25µM or 200 µM) in indicator free DMEM for 10 min. The cells were lysed in 10 mM HEPES, pH 7.4 buffer and the protein concentration was estimated using Bradford assay. The 50 µg lysate was resolved in 10% SDS-PAGE and transferred onto PVDF membrane using wet transfer method. The blots were incubated with blocking solution (5% BSA in TBST buffer, pH 7.4). Post-blocking, the membranes were incubated with anti-phosphotyrosine followed by HRP conjugated secondary antibody. After washing with TBST buffer, the blots were developed using chemiluminscence substrate. The blots were analysed for molecular weight and number of phosphor-reactive protein bands using Biorad's Imagelab software V.6.0.1. The molecular weight of the bands was compared with the phosphosite-plus server (https://www.phosphosite.org/homeAction.action) for probable proteins involved in signalling event.

4.2.21. Statistical analysis: All experiments unless otherwise stated were performed in triplicate and repeated at least three times. All the data are presented as the mean ±SD unless otherwise noted. Differences between groups were analysed using the Sigmaplot (Systat software inc, San jose, CA, USA) and Originpro (Originlabs, Northampton, MA, USA) data analysis and graphing software. Statistical analysis was performed by one-way ANOVA followed by unpaired Student t-test and the $p < 0.05$ were considered as statistically significant.

4.3. Results

4.3.1. CD36 has a well-defined microenvironment to accommodate hemin

The scavenger receptor CD36 interactions with its ligands often induce the internalization of CD36 (Heit et al., 2013). It has been shown that the binding of α-Tocopherol to CD36 induces CD36 internalization. Further, the use of selective inhibitor of lipid transport by

CD36 prevented the α-Tocopherol mediated CD36 internalization (Zingg et al., 2017). The sequestration of CD36 into vesicles and defect in phagocytosis upon hemin treatment lead us to hypothesize that the hemin could be a ligand for CD36. It has shown that the receptor internalization is often associated with ligand-receptor interaction (Heit et al., 2013). To understand how hemin modulates the surface CD36 levels, we need to examine the binding environment that facilitates the hemin interaction. To investigate the favourable microenvironment for hemin binding, we have analysed the hemin binding pocket from various hemin/heme co-crystallized proteins and extracted the recurring amino acids and their interaction patterns. The residues aspartic acid (D), phenylalanine (F), methionine (M), arginine (R), serine (S), valine (V) and glutamine (Q) were found to be repeating consistently in seven complexes out of hemin-protein complexes analysed (Table 4.2). A distance map was generated using hemin and protein atoms, and the distance between atoms was color-coded with the VIBGYOR where violet for the lowest distance to the red for highest distance (Figure 4.1). The high resolution atomic-level examination of hemin and its surrounding residues in biophore has revealed that the arginine, aspartic acid and glutamine residue atoms were in close distance with the hemin carboxylate group and provides hydrophilic environment which facilitates the hemin binding (Figure 4.1). The relative contribution of each residue in the hemin binding pocket was analysed using webserver ABS-Scan (Anand et al., 2014) (http://proline.biochem.iisc.ernet.in/abscan/), and their relative binding energies were estimated (Figure 4.2A).

Table 4.2. Recurring amino acids in hemin biophore

Amino Acid /PDB ID	A	C	D	E	G	H	I	K	L	M	N	P	Q	R	S	T	V	W	Y
1o9x	1	0	1	0	1	1	1	1	1	1	0	1	0	1	1	0	1	0	1
2bli	1	0	1	0	0	1	1	1	1	0	0	1	0	1	1	1	1	1	1
2qsp	1	0	1	0	0	1	0	1	1	1	1	0	0	0	1	1	1	0	1
2r7a	1	0	1	1	1	0	1	0	1	1	1	0	1	1	1	1	1	1	1
2zdo	1	0	0	1	1	1	1	1	1	1	1	0	0	1	0	1	1	1	0
3nu1	1	0	1	0	1	1	0	0	1	1	1	0	0	1	1	1	0	0	1
4mf9	0	0	1	0	1	1	1	1	1	1	0	1	1	1	1	1	1	0	0
4myp	1	0	1	0	0	0	0	1	0	1	1	1	1	1	1	1	1	0	1
	7	**0**	**7**	**2**	**5**	**6**	**5**	**6**	**7**	**7**	**5**	**4**	**3**	**7**	**7**	**7**	**7**	**3**	**6**

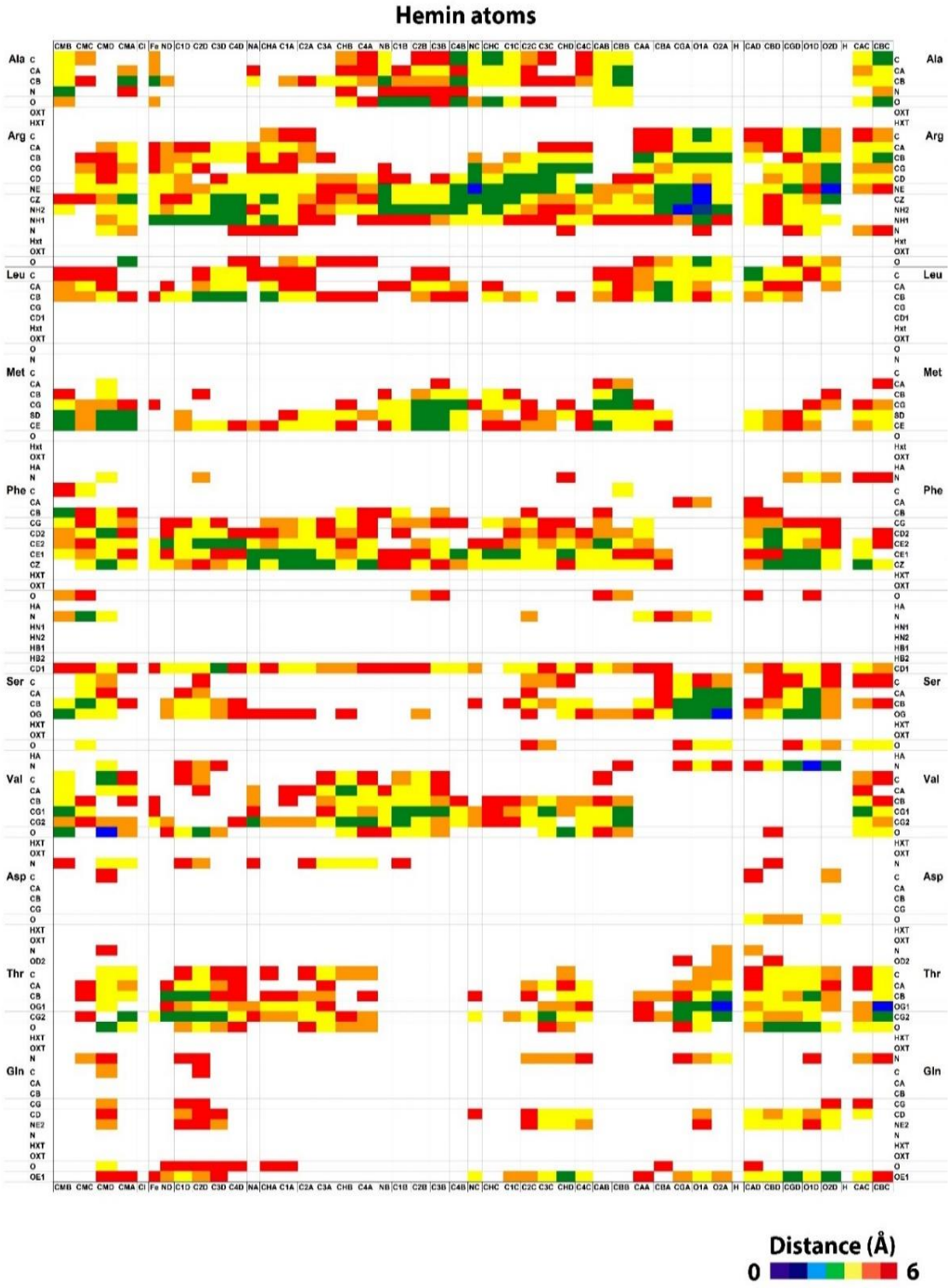

Figure 4.1. Distance matrix representing hemin biophore. The hemin bound protein complexes were identified and extracted the hemin binding region to ascertain biophoric features. The distance between the hemin atoms to amino acid atoms were analysed and generated a 105x46 matrix and colour coded with VIBGYOR (violet for lowest distance to red for highest). The matrix represents distance data from a total of eight hemin bound complexes. The carboxylate group of the hemin and the polar side chains of amino acids were found to be enriched in heat map.

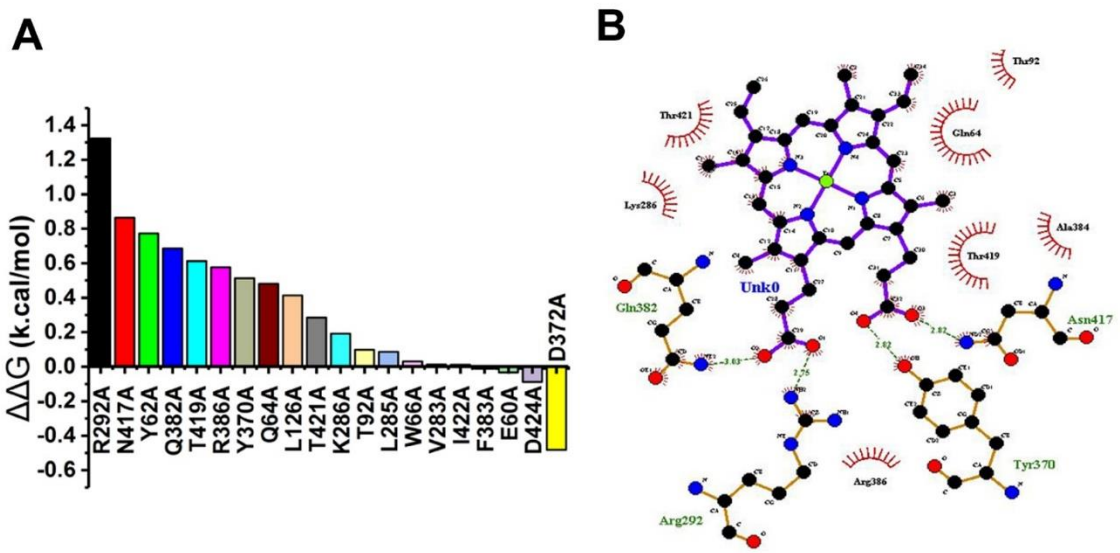

Figure 4.2. Free energy estimates of hemin biophoric residues. (A) The relative contribution of biophoric residues to CD36-hemin affinity. The residues in hemin binding domain on CD36 were analyzed for their contribution towards CD36-hemin interaction using alanine scanning mutagenesis. The complex was uploaded into ABS-scan webserver for predictions. The results were plotted as difference in binding energy difference to wildtype and mutant. The residues R292, N417, Y62, and Q382 were showing significant change in the binding energy indicates they could be strongly influence the CD36-hemin interaction. **(B)** The interaction analysis of CD36-hemin complex using ligplot+ software. The residues R292, Q382, Y370 and N417 can be found in interaction through hydrogen bonding (green dotted lines). The other residues K286, T421, T92, Q64, T419 and A384 were found to be associated with hemin through hydrophobic interaction.

The molecular docking of hemin within CD36 has revealed that the residues R292, Q382 interacting with hemin through hydrogen bonding and D372 residue through salt bridges with the hemin carboxylate group (Figure 4.2B). The mutation of R292, Q382 to alanine found to be destabilizing the CD36-hemin complex, whereas the mutation in D372 to alanine was found to be enhancing the affinity between CD36 and hemin. Further, the stability of the wild type CD36 or different mutants (R292A, D372A, and Q382A) complexed with hemin, was studied by molecular dynamics simulation using RMSD, radius of gyration and RMSF as evaluating criteria. The average RMSD value of CD36 (wildtype), R292A, D372A and Q382A complexed with hemin were found to be 0.58, 0.82, 1.13 and 0.44 nm respectively. Notably, the D372A mutant showed higher deviation compared to the R292A and Q382A (Figure 4.3A). The aspartic acid residues contributes to the ionic character of proteins and replacement of it with non-polar alanine residue may imparts hydrophobicity hence higher fluctuation in RMSD (Aier et al., 2016). The other

explanation could be the mutants were constructed on the wild type structure and it may introduced structural perturbations which is reflected by the increased in RMSD (Piao et al., 2019). The RMSD value of wild type and mutants throughout the simulation suggests the complexes were converged which is an indicator of stability, although the minor

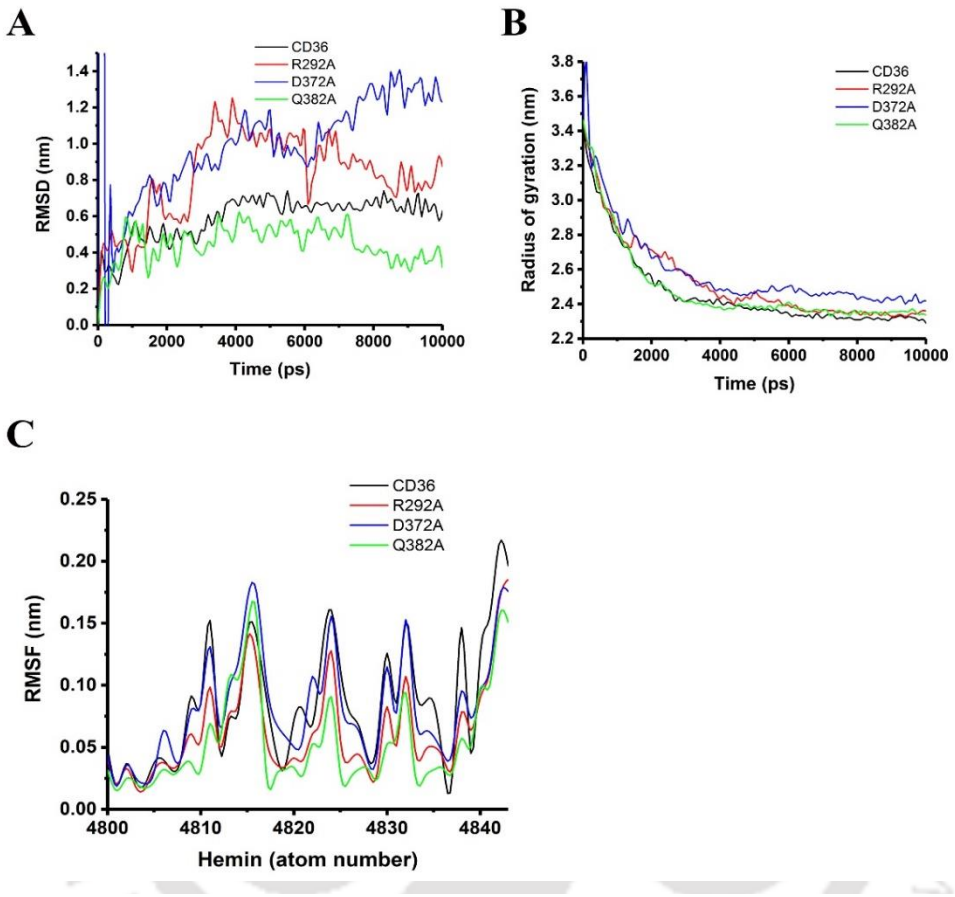

Figure 4.3. Stability analysis of wild-type and mutant proteins complexed with hemin using molecular dynamics simulations. The wildtype or mutant complexes were subjected to molecular dynamics simulations and the trajectories were analysed for the Root mean square deviation (RSMD), radius of gyration (Rg) and root mean square fluctuation (RMSF). **(A)** The root mean square deviation (RMSD) throughout the 10 ns stimulation suggests the complexes are stable and there is no major fluctuations. **(B)** The radius of gyration (Rg) of the CD36 and mutants indicates the compactness of the structures. The simulation trajectory analysis suggests the proteins are tightly packed and remain in that condition throughout the simulation. **(C)** The RMSF of hemin atoms during simulation run was analyzed using g_RMSF module of the Gromacs. For CD36, the average RMSF value of 0.15 nm was observed but the mutants there is a deviation from this value can be seen. The deviation in RSMF value of mutants suggests the instability in hemin binding pocket.

perturbations were observed (Figure 4.3A). The radius of gyration can be used to investigate the compactness of protein-ligand complexes. The average radius of gyration for CD36 (wildtype) was found to be 2.46 nm whereas for R292A, D372A and Q382A it

was 2.53, 2.58 and 2.48 nm respectively (Figure 4.3B). There is no major change in radius of gyration of wild type and mutant complexes indicate the compactness of protein-ligand complexes. Further, the fluctuation of hemin during the simulation was assessed using root mean square fluctuation (RMSF). As it is evident from the (Figure 4.3C) the fluctuation is minimal among the wildtype and mutants. The overall molecular dynamics studies indicates the stability of CD36 and mutants complexed with hemin.

4.3.2. Hemin serves as a ligand for CD36

Molecular modelling, molecular dynamics and in-silico mutation studies indicate a suitable hemin biophore and perfect microenvironment to allow the binding of hemin into CD36 ectodomain. To verify these findings, purified CD36ecto wild type and different mutants (R292A, D372A and Q382A) were used in dot blot assay to test their binding towards hemin blotted on the nitrocellulose membrane. The dot blot analysis indicate strong reactivity of CD36ecto wild type with an appearance of intense spot whereas ~48% signal reduction with R292A and almost 70% reduction in signal for D372A or Q382A (Figure 4.4A). The affinity of the hemin to the CD36ecto wild type or mutants was investigated using Isothermal Titration calorimetry (ITC). The ITC thermogram of hCD36ecto against hemin indicates the strong binding between the components. The high negative ΔH value suggests the two molecules interacting through hydrogen bonding and van der Waals interactions (Figure 4.4B). The DP (differential power) change/injection suggests the hemin occupied the binding sites completely to saturate DP values (Figure 4.4B, upper portion of thermogram). The K_D value calculated by fitting the raw data into the two-site binding model and found to be 1.26±0.24 μM and the stoichiometry of hCD36ecto to hemin was found to be 1:2. Similarly, under the identical experimental conditions, the CD36ecto mutants (R292A, D372A and Q382A) were titrated with hemin and the ITC thermogram was recorded. The ITC titration curve for R292A indicated reduction in enthalpy values and increase in entropy values which highlight weak interaction between hemin with CD36ecto R292A. It is probably be mediated by weak non-covalent hydrogen bonding (Figure 4.4C). The K_D value calculated from data fitting was found to be 115±2.14 μM. It is 100 folds lower compared to the wild type CD36ecto. The R292A thermogram clearly indicates that the hemin is unable to fit within binding pocket and as a result it is exhibiting reduced affinity towards hemin (Figure 4.4C). The thermodynamic parameters of R292A is purely due to the disruption of hemin favourable biophore microenvironment. The ITC thermogram of other two mutants (D372A or

Q382A) revealed that the mutation has drastically reduced the affinity of hemin towards CD36 ectodomain (Figure 4.4D and Figure 4.4E). The K_D value calculated for D372A or Q382A mutants were found to be 295±5.26 μM and 420.16±22.5 respectively. The significantly higher K_D values for D372A and Q382A suggests the prominence of these residues in hemin binding pocket.

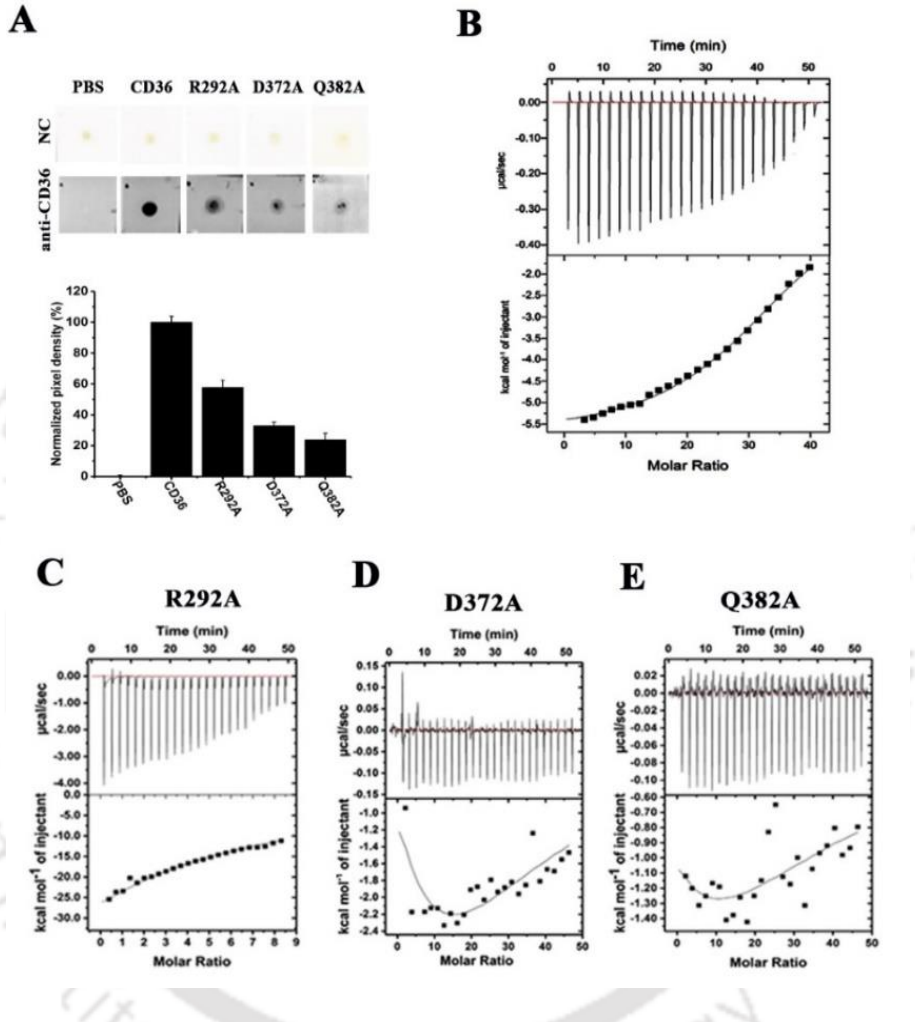

Figure 4.4. The residues R292, D372 and Q382 are crucial for the active engagement of hemin within CD36. (A) Dot blot assay of CD36 or mutants (R292A, D372A and Q382A) with hemin. After blocking, the hemin spotted individual nitrocellulose membrane strips were incubated with CD36 or mutants for 2 h, washed and probed with anti-CD36 antibodies. The developed blot (upper portion) represents the strong affinity for CD36 and the relative signal intensity quantified is showed in bottom graph. **(B)** ITC thermogram of CD36 against hemin. The affinity of hemin towards CD36 was studied using ITC as described in materials and methods. The saturation of the binding indicates all the binding sites were occupied by hemin and the molar ratio between CD36 to hemin is 1:2. The K_D value for CD36 caluclated after fitting the data in a two site binding model was found to be 1.26±0.24 μM. **(C)** ITC themogram of R292A titrated with hemin. **(D)** The D372A mutant titrated with hemin. **(E)** Q382A titrated with hemin. Except R292A, all other mutants showed no binding to hemin.

To rule out the observed effects are not due to the structural changes or aggregation of mutant proteins, the circular dichroism spectrum and size exclusion chromatography was performed on purified mutant proteins. The size exclusion elution profile and CD spectrum analysis indicates there is no change in oligomer status and no significant secondary structural changes taken place upon mutation and it is identical to the hCD36ecto (Figure 4.5A and 4.5B). The cumulative results represented in Figure 5, suggest that the residues R292, D372 and Q382 are crucial for hemin binding and there are sufficient evidences to claim that hemin act as a ligand for CD36.

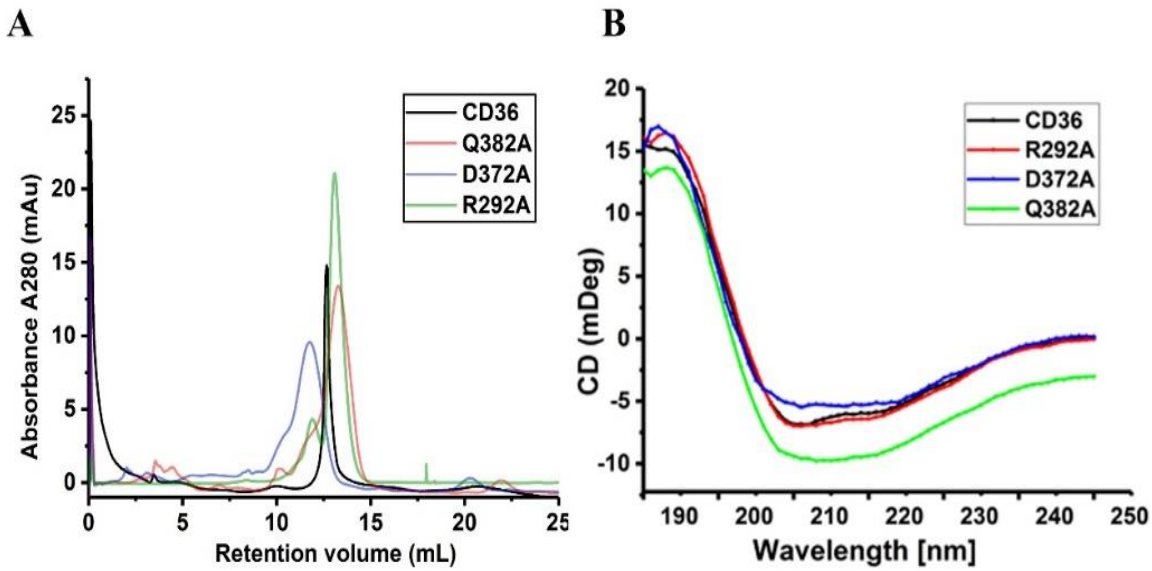

Figure 4.5. Hemin biophoric mutants are structurally similar to wild-type (CD36). (A) The hemin biophoric mutants (R292A, D372A and Q382A) were investigated for oligomeric status using size exclusion chromatography. The overlay shows there is no change in oligomeric status of mutants. **(B)** The mutants further verified for structural changes upon mutation using Circular Dichroism spectroscopy. The result indicates there is no structural deformations in mutants.

4.3.3. Hemin is non-toxic towards macrophage:

Hemin is a toxic pro-oxidant molecule but at higher concentration and longer exposure time periods (Deshmukh and Trivedi, 2014). Hemin exposure to macrophages at different concentrations (0-300µM) in serum free or complete medium for 1hr at 37 ^{0}C in humidified CO_2 incubator is not causing reduction in cellular viability (Figure 4.6). Almost more than 90% viability was observed for macrophages treated with hemin concentration up-to 200 µM and this range is been used for experiments throughout current work.

TH-2507_156106009

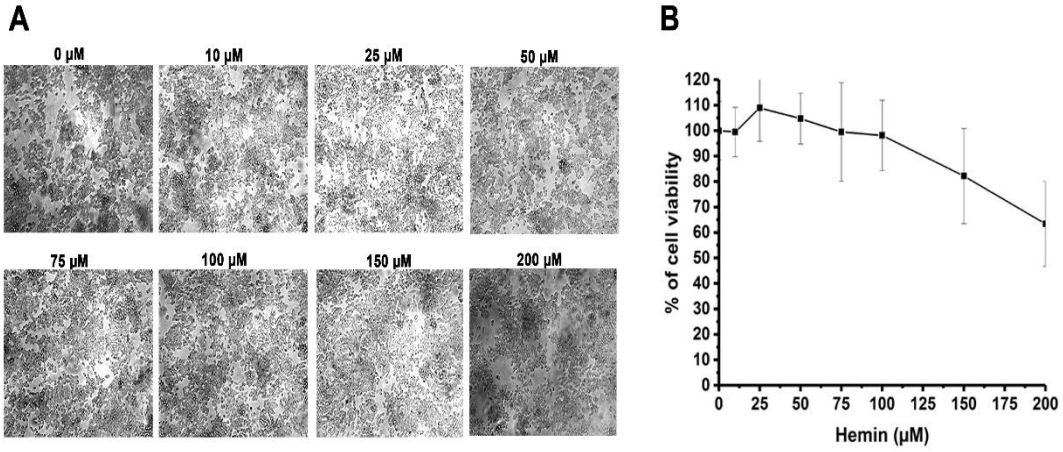

Figure 4.6. Hemin is non-toxic to macrophages under experimental conditions. The macrophages were treated with hemin (0-200 µM for 1 hr at 37 ^{o}C. Post treatment the cells were gently washed and (**A)** acquired images in bright field in cytell cell imaging system**. (B)** MTT assay performed on macrophages treated with varying concentrations of hemin. The cell viability is not reduced even at 200 µM hemin treatment.

4.3.4. CD36-Hemin interactions likely to be a contribution factor for pathological outcome during severe malaria

Receptor recycling from intracellular vesicles to the plasma membrane is vital for proper stimulation and regulation of down-stream events such as cytokine secretion (Walker and Burgess, 1987). The CD36-hemin complex sequestration into intracellular vesicles may contribute to the pathological outcome. Besides, during severe malaria, the free heme levels are correlating with the severity of malaria, organ damage, and the cytokine levels (Dalko et al., 2015). To assess the impact of CD36 sequestration on the secretion of different types of pro-inflammatory or anti-inflammatory cytokines, we have treated macrophages with hemin (25 µM) or 200µM and the secreted cytokines were detected using mouse cytokine array profiler kit as described in experimental procedure. In untreated macrophage cell culture supernatants, the cytokines such as IP-10, KC, CCL3, CCL4, CXCL2 found to be constitutively expressing whereas very low reactivity was observed for cytokine/chemokines such as G-CSF, GM-CSF, CCL-1, IL-7, IL-16, CXCL-1, MCP-1, TIMP-1 and TNF-α (Figure 4.7A, top panel). The presence of pro-inflammatory cytokines in untreated could be due to the cell debris in cultures which could activate the macrophages to produce cytokines (Kono and Rock, 2008). Further, the cytokines/chemokines such as CS/C5a, sICAM-1, IFN-γ, IL-1α, IL-1β, IL-1ra, IL-2, IL-3, IL-4, IL-13, IL-17, IL-23, IL-27, M-CSF, CXCL9 and TREM-1 were found exclusively in hemin treated macrophage cell culture supernatants but not in untreated (Figure 4.7A,

25 µM panel). In 25 µM hemin treated macrophage cell culture supernatants the upregulation of pro-inflammatory cytokines such as TNF-α (32 folds), RANTES (7 folds), MCP-1 (2.4 folds), IL-16 (7.5 folds), IP-10 (3.4 folds), GM-CSF (10.6 folds), CCL-1 (3 folds), IFN-γ (1 fold) CS/C5a (1 fold) was significant (Figure 4.7B).

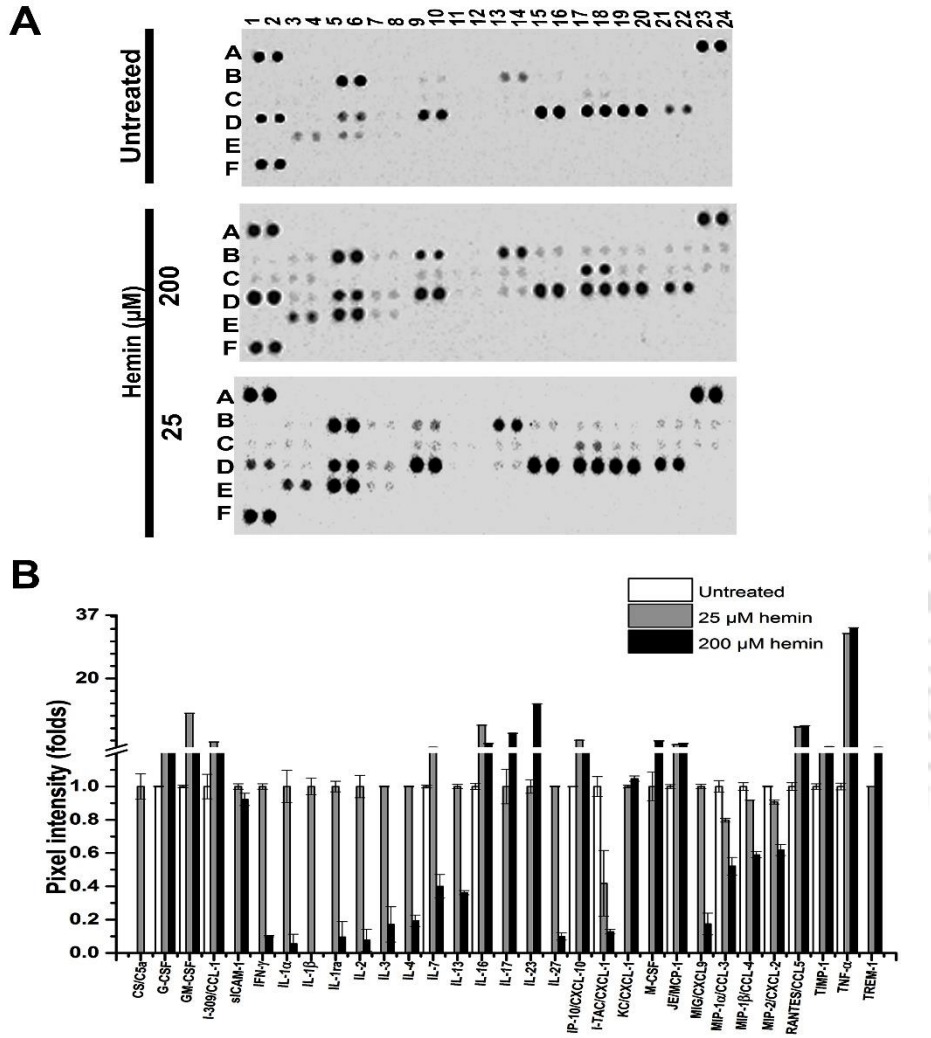

Figure 4.7. Hemin treatment upregulates various pro-inflammatory cytokines in macrophages. Macrophages were stimulated with various concentrations of hemin (25 or 200 µM) and analysed for various cytokines. **(A)** The macrophages were treated with hemin (25 µM) and the cell culture supernatant was collected. The culture supernatant was assessed for the presence of cytokines using cytokine array kit. The upper blot shows the presence of various constitutively expressing cytokines along with control spots (A (1,2); A(23,24); F(1,2)) and a negative control spot (F(23,24). The hemin treated culture supernatant blot (lower array) showing upregulating cytokines such as CCL1, IL-16, CXCL1, RANTES, MCP-1 and TNF-α. **(B)** The cytokine dot intensity was semi quantified and normalized by control spots provided in the array. The cytokine levels plotted as normalized pixel density calculated using ImageJ application (NIH, USA). The cytokine such as TNF-α, RANTES and MCP1 showing upregulated cytokine levels whereas other cytokines such as G-CSF, CCL1, and sICAM1 were also showed lower upregulation levels.

The CS/C5a is a complement protein involved in recruitment and activation of polymorph nuclear cells to site of infection and inflammation. In experimental cerebral malaria model, the knockdown of CS/C5a showed improved survival of mice. The knockdown is associated with reduced levels of MCP-1, IFN-γ, and TNF-α levels (Kim et al., 2014). Interestingly, the CS/C5a is present in hemin treated macrophage cell culture supernatants but not in untreated. It has been shown that the cytokines IFN-γ, TNF-α, and IL-12 are crucial for development of CM (Angulo and Fresno, 2002). The knock down of IFN-γ in mice showed no signs of cerebral malaria compared to wildtype suggests IFN-γ plays crucial role in development of cerebral malaria pathology (Amani et al., 2000). The absence of IFN-γ in untreated macrophage cell culture supernatants but in hemin treated macrophages imparts hemin could be a potential pro-oxidant molecule in development of cerebral malaria pathology. Surprisingly, few cytokines IL-17 (5.3 folds), IL-23 (13.2) and M-CSF (3.2 folds) were upregulated in 200 µM hemin treated macrophages but not in 25 µM (Figure 4.7B). The cerebral malaria patients with multiple organ damage especially acute renal failure (ARF) distinctly showed elevated levels of cytokines IL-17, IL-10 and IP-10 (Herbert et al., 2015). The study underlined that IL-17 is crucial for development of ARF pathology associated with malaria but the mechanistic details yet to ascertained (Herbert et al., 2015). The cytokine array results clearly indicate that the multiple organ damage and the pathology associated with cerebral malaria could be due to hemin interaction with various receptors present on macrophages or endothelial cells on brain.

4.3.5. Hemin directs the sequestration of membrane bound CD36 into intracellular vesicles

The scavenger receptor CD36 is a transmembrane protein required for fatty acid transport, non-opsonic phagocytosis and regulation of inflammation. Earlier observation in hemin treated macrophages suggested the CD36 sequestered in large amounts to cytosol (unpublished work). The membrane bound CD36 is crucial for control the secretion of pro-inflammatory cytokines such as TNF-α. The global cytokine profiling of hemin treated macrophages indicate the unbalanced secretion of pro-and anti-inflammatory cytokines. This could be due to CD36 translocation into cytosol which might involve in controlling cytokine secretion. To support our argument we have separated membrane and cytosol fractions from hemin treated or untreated cell lysates and probed with anti-CD36 antibodies. The fractions verified for purity using Lactate dehydrogenase assay (data not shown).

The untreated macrophage cells cytosol fraction showed no cytosolic CD36 whereas 44.6% of CD36 found in cytosol fraction of hemin treated macrophages (Figure 4.8). The hemin treatment significantly inducing translocation of CD36 to cytosolic side. The cytosolic CD36 along with ligand may trigger the pro-inflammatory cytokine secretion and could be the reason behind the cytokine burst.

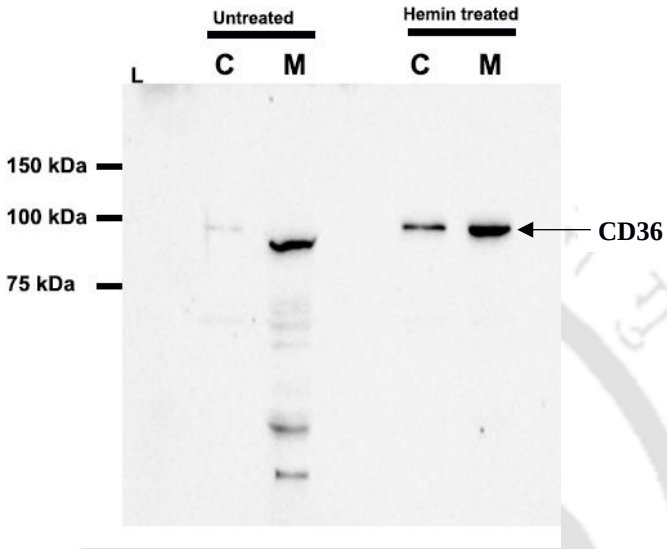

Figure 4.8. Hemin treatment induces CD36 translocation into cytosol. Macrophages either remain untreated or treated with hemin (25 μM) for 1 hr were fractionated into membrane (M) and cytosol (C). The fractions were resolved on SDS-PAGE gel and transferred onto nitrocellulose membrane. The blot is probed with anti-CD36 antibody. There is a significant fraction of CD36 was observed in cytosolic fraction of hemin treated macrophages.

4.3.6. Hemin binding induces CD36 passage through DPPC bilayer

It has been shown that CD36 ligands induce internalization of receptor. The hemin treated macrophages cell lysates western blot showed CD36 sequestration into cytosol. To study the hemin mediated CD36 translocation, we performed molecular dynamics simulations on membrane bound CD36-hemin complex. The simulations were performed in GROMACS package and GROMOS96 with 53a6 forcefield parameters. The CD36-hemin molecular model was generated using molecular docking and placed in 256 DPPC lipid bilayer. After successfully integrating the complex into membrane, the system was successively equilibrated in NVT and NPT conditions. A production run for 100 ns was carried out. The structural distortions in CD36-hemin complex during the simulation run was analysed using root mean square deviation (RMSD) and radius of gyration (Rg). The RMSD of membrane bound CD36-Hemin complex showed minor perturbations at 60 ns however the system is converged later stage and indicates the overall stability of complex

TH-2507_156106009

(Figure 4.9A). The radius of gyration of the membrane bound CD36 indicates there is no major conformation changes occurred upon ligand binding (Figure 4.9B). The density DPPC, CD36, Hemin and water was assessed using gmx density function of Gromacs suite. The DPPC and water densities were found less affected through the simulation run whereas CD36 bound to hemin showed penetration into the DPPC bilayer (Figure 4.9C). To assess further, the time lapse frames of simulation run were captured at 0, 20, 50, 70 and 100 ns. The time lapse images suggests the lower region of ectodomain was found to be penetrated in upper leaflet of DPPC (Figure 4.9D). Further the solvent accessible surface area (SASA) was calculated on bilayer without protein-ligand complex.

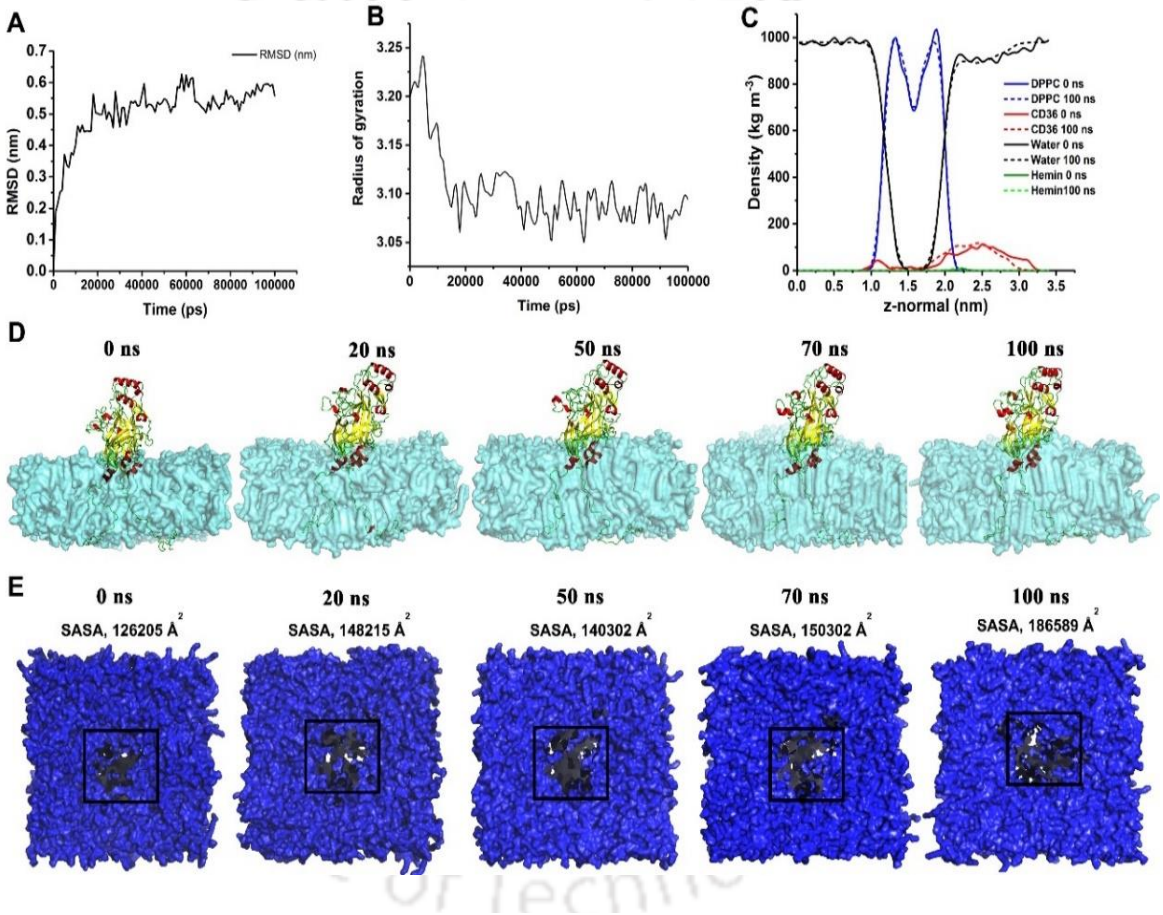

Figure 4.9. Hemin binding facilitates the CD36 passage through DPPC bilayer. The MD run trajectories were analysed for **(A)** RMSD, **(B)** Radius of gyration to confirm there is no structural perturbation in membrane bound state. **(C)** The density of DPPC, CD36, Hemin and water molecules were estimated for 0 ns and 100 ns. The CD36 was found to be penetrated into DPPC bilayer. **(D)** The time lapse membrane bound CD36-hemin complex. **(E)** The top view of DPPC in a time lapse scale. The solvent accessible surface area (SASA) was measured for 0 ns, 20 ns, 50 ns, 70 ns and 100 ns. The thinning of membrane was observed over time frame as evident from SASA. The overall study indicates the hemin binding may facilitate the CD36 passage through DPPC bilayer and supports the CD36 translocation in hemin treated macrophages.

TH-2507_156106009

A significant area (186589 $Å^2$) was found to be accessible by solvent at 100 ns compared to initial structure (126205 $Å^2$) (Figure 4.9E). The results indicates the thinning of the bilayer over the simulation. The thinning of bilayer means CD36 penetrated into the membrane in hemin bound form. The MD simulation data supports the hemin induces the CD36 translocation.

4.3.7. CD36-hemin interaction on cell surface is crucial for immune-dysfunction in macrophages

The scavenger receptor CD36 acts as a receptor for various ligands from diversified sources at cellular level (Ramasamy et al., 2012). It has been shown that CD36 also acts as a co-receptor for TLRs which are also involved in innate-immune response (Erdman et al., 2009). As professional macrophages J774A.1 harbours functional CD36 and TLRs on their cell surface to contribute into hemin mediated innate immune response. To understand the role of CD36 in hemin mediated immune response, we have screened several cell line with a requisite phenotype of $CD36^{-/-}$ (Figure 4.10A). The flow cytometry based screening suggested that the MG63 cells have no or very low levels of CD36 level (Figure 4.10A and 4.10B) and TLR expression on their cell surface (Bachtiar and Bachtiar, 2017; Jing et al., 2015). Further, the wildtype (CD36) or mutant's transfection was assessed using flow cytometry before employing them into experiments (Figure 4.11A). The cells transfected with wild type CD36 showed enhanced migration towards the hemin placed in lower chamber whereas very few number of cells were migrated in absence of hemin (Figure 4.11B, wildtype panel).

The R292A transfected MG63 cells showed migration in presence of hemin but in case of D372A or Q382A transfected cells, the migration is very less (Figure 4.11B). The chemotaxis index for CD36 transfected cells in presence of hemin was found to be 31 folds compared to the non-specific migration (chemophoresis) in absence of hemin (Figure 4.11C). Disruption of hemin biophore in CD36 through mutation in ectodomain abolishes the chemotaxis towards hemin but didn't affect the non-specific migration of cells (Figure 4.11C). The MG63 transfected with empty vector (mock transfected) didn't allow chemotaxis towards hemin further strengthen the observation that functionally active CD36 on the cell surface is crucial for chemotactic migration of cells towards hemin. These experimentation results provide direct evidences that hemin is being recognized by CD36 presented on cell surface with high affinity and specificity.

TH-2507_156106009

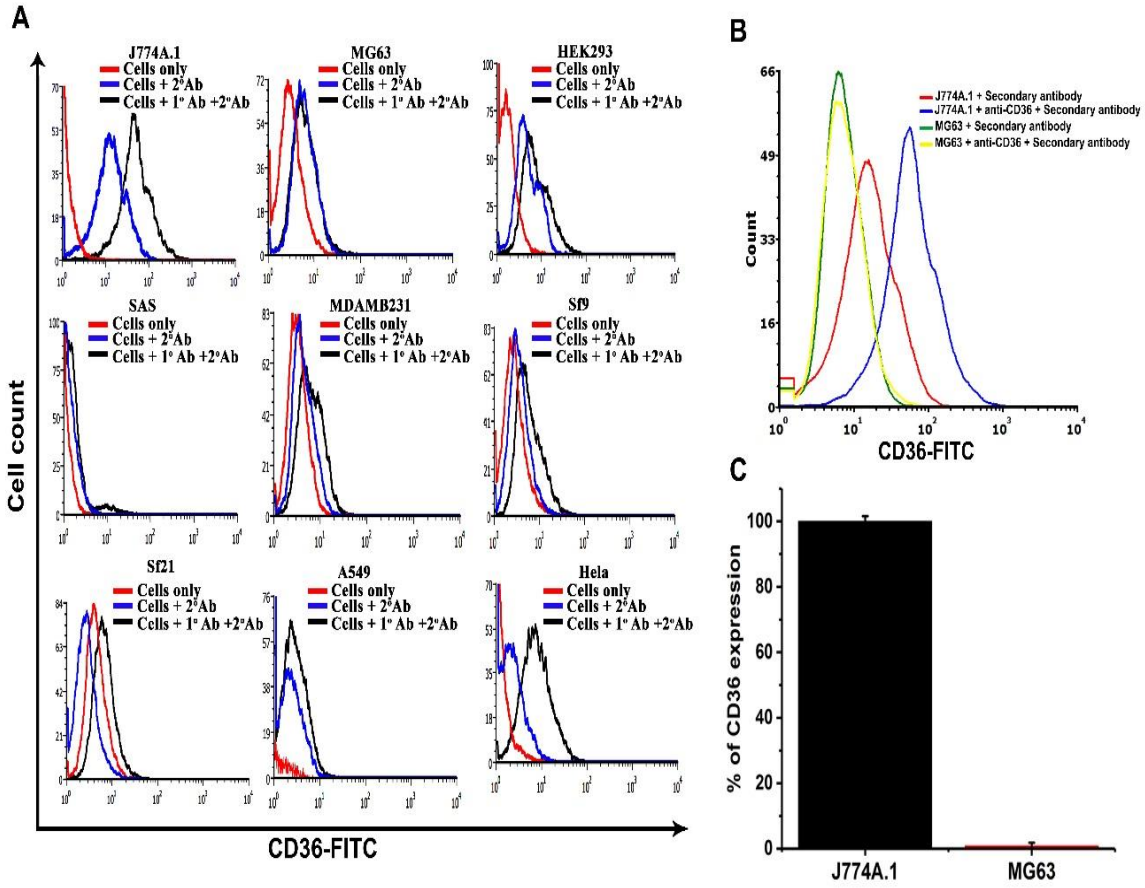

Figure 4.10. The osteosarcoma cell line MG63 has minimal levels of CD36 compared to the J774A.1 cells. (A) The cell lines J774A.1, MG63, HEK293, SAS, MDAMB231, Sf9, Sf21, A549 and Hela were fixed and incubated with blocking buffer containing 3% BSA in PBS. After 1 h the blocking buffer removed and incubated with anti-CD36 antibody for 2 h following washing twice with PBS. Further the cells incubated with FITC conjugated secondary antibody for 1 h. After incubation cells were washed gently with PBS and analysed on flow cytometer. The flow cytometry histogram representing the anti-CD36 antibody and FITC conjugated secondary antibody labelled J774A.1 and MG63 cells. The J774A.1 cells labelled with anti-CD36 antibody followed FITC conjugated secondary antibody showing fluorescence intensity mean of 60 whereas for MG63 it was 4. **(B)** Overlay histogram of J774A.1 with MG63. **(C)** The % of CD36 expression was semi quantified based on the flow cytometry data and plotted by considering the J774A.1 as 100%. The minimal expression was observed in MG63 cells. The data represents the three independent experiments data (* $p<0.05$).

Now we explored whether the CD36-hemin interaction is responsible for immunological responses in macrophages under malaria like environment. The MG63 cells with wild type CD36 is exhibiting enhanced phagocytosis in response to hemin (25 µM) treatment (Figure 4.12A).

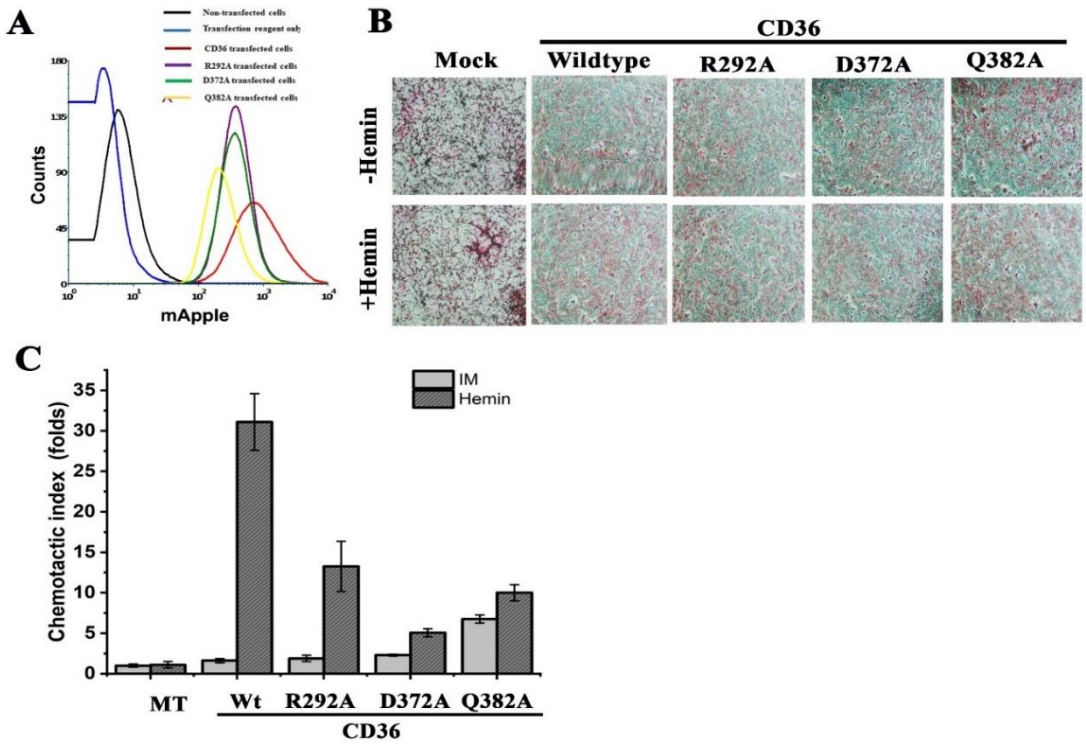

Figure 4.11. MG63 cells with CD36 ectopic expression shows chemotaxis towards hemin. (A) The MG63 cells were transfected with wildtype (CD36) or mutants (R292A, D372A, and Q382A). Post transfection the cells were analysed on flow cytometer in FL-2 channel (λ_{ex}-488 nm, λ_{em}-575). The overlay histogram suggests the expression of CD36-mApple is efficient. **(B)** The MG63 cells transfected with either CD36 or mutants (R292A, D372A and Q382A) and carried out migration assay in presence or absence of hemin. The images captured after cell migration in CD36 or mutant's transfected cells in presence or absence of hemin. The upper panel shows absence of hemin and the lower panel for cells migrated in presence of hemin. There is no clear distinction was observed in mutants or mock transfected cells either in presence or absence of hemin. **(C)** The number of cells migrated in CD36 transfected MG63 in presence of hemin is significant and indicates the hemin interacts with the scavenger receptor CD36. Further the mutants transfected cells show reduced chemotaxis suggests intact biophore is crucial for hemin interaction with CD36 (n=3). (* $p<0.05$).

In comparison to wild type, phagocytosis index of the MG63 transfected with mutant R292A, D372A or Q382A were not showing enhanced phagocytosis with hemin at 25µM (Figure 4.12A). The phagocytic pattern of mutants R292A, D372A and Q382A clearly highlights role of CD36-hemin interaction in dysregulation of phagocytic activity of macrophages. Similar to phagocytosis, MG63 transfected with wild type CD36 was exhibiting reduction in bactericidal activity in presence of hemin (0, 25 or 200µM) whereas MG63 cells transfected with different mutants (R292A, D372A and Q382A) were showing no significant effect of hemin exposure (Figure 4.12B). Presence of functional CD36 on cell surface to interact with hemin is crucial for observed functional defects in

macrophages.

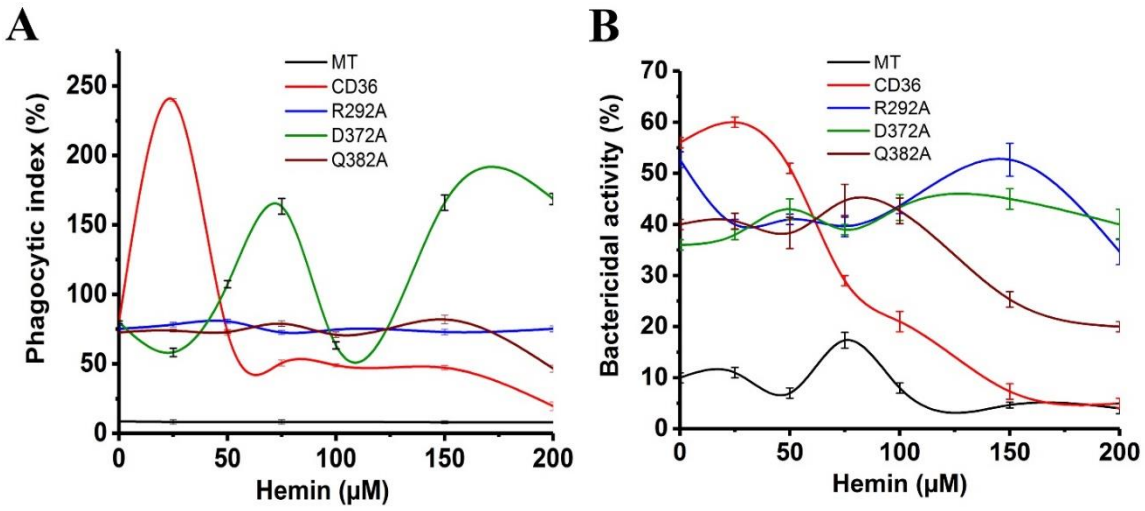

Figure 4.12. The CD36 is the key receptor for the hemin at cellular level and responsible for the immune-dysfunction. (A) The MG63 cells were transfected with either CD36 or its mutants. The successfully transfected cells either remain untreated or treated with 0-200 μM of hemin for 1 hr were incubated with FITC conjugated bacteria for 1h. The cells were washed with PBS and the fluorescence counts were acquired in BD FACS calibur flow cytometer in FL-1 channel (λ_{ex}-488 nm, λ_{em}-530/30 nm). The phagocytotic index was calculated as described in materials and methods section. The CD36 transfected cells showing initial spike in phagocytosis index to 30% when compared to untreated and gradual decrease upon increasing concentration of hemin whereas R292A or Q382A transfected cells were showing no response to hemin stimulation. The D372A mutant showed abnormal phagocytosis activity upon hemin treatment. **(B)** The bactericidal activity of transfected MG63 cells assessed as described in materials and methods section. The bactericidal activity of the CD36 transfected MG63 cells decreasing with increasing hemin concentration but the decrease in activity is not prominent in mutants (R292A, D372A and Q382A) transfected MG63 cells.

4.3.8. Scavenger receptor CD36 is crucial for hemin mediated inflammatory response

It has been reported that the scavenger receptor CD36 interaction with its ligands (endogenous or exogenous) primes the cytokine signalling and could be responsible for host pathology (Kennedy et al., 2011). The cytokine array revealed that several pro-inflammatory cytokines up-regulating upon hemin stimulus (Figure 4.7A, B). We have further explored the CD36-hemin interaction as an axis to regulate the cytokine secretion. MG63 cells transfected with wild type CD36 or different mutants (R292A, D372A and Q382A) were either remain untreated or treated with hemin (25 or 200μM) for 1 hr and secreted cytokines were measured as described in material and methods. The pro-inflammatory cytokines TNF-α (Perera et al., 2013), MCP-1 (Royo et al., 2019), RANTES

TH-2507_156106009

(Bujarbaruah et al., 2017), and CCL1 (Bobade et al., 2019) were directly linked to the pathology associated with severe malaria. The cytokine TNF-α produced by the macrophages during various infectious or non-infectious diseases, and responsible for regulating the pathophysiology of the host. The TNF-α levels in MG63 cells transfected with wild type CD36 was found to be 4.5 folds higher with hemin treatment compared to untreated cells (Figure 4.14A). In mock or R292A transfected MG63 cells, TNF-α levels were reduced significantly and it is in agreement with our chemotaxis results. The MG63 cells transfected with D372A showing significantly higher levels of TNF-α (8.7 folds) at 200 µM hemin compared to MG63 cells transfected with wild type (CD36) (3.2 folds) (Figure 4.13A). Contrary to other mutants, Q382A is giving very high TNF-α with an identical pattern to the wild type CD36 (Figure 4.14A). The monocyte chemo-attractant protein 1 (MCP1) plays crucial role in migration of monocytes/macrophages (Jiang et al., 1992). The wild type CD36 transfected (untreated) cells showed basal levels of MCP-1 but secretion went up 2 fold after treatment with hemin (Figure 4.13B). In R292A mutant transfected cells, MCP-1 secretion was much reduced and secretion pattern is different from wild type CD36 transfected cells. It is exhibiting complete suppression of secretion at high hemin (200µM) treatment. D372A transfected MG63 cells were exhibiting similar secretion pattern as observed for wild type CD36 transfected cells. MCP-1 secretion from Q382A transfected MG63 cells was much low but it follows similar secretion pattern as observed for wild type CD36 transfected cells (Figure 4.13B). The cytokines RANTES and CCL1 were found to play crucial role in cerebral malaria pathology (Miu et al., 2006). The RANTES levels in CD36 transfected MG63 cells were found to be increased to 4.6 folds at low hemin (25µM) but it was reduced significantly at 200 µM hemin (Figure 4.13C). MG63 cells transfected with mutants (R292A, D372A and Q382A) was exhibiting basal level of cytokine secretion and cells were not showing any up-regulation in cytokine secretion in response to hemin stimulation (Figure 4.13C). The CCL1 levels in wild type CD36 transfected MG63 cells were found to be upregulated two folds at low hemin (25µM) but it was reduced back to basal level at 200 µM hemin (Figure 4.13D). MG63 cells transfected with mutants (R292A, D372A and Q382A) was exhibiting basal level of cytokine secretion and cells were not showing any up-regulation in cytokine secretion in response to hemin stimulation (Figure 4.13D). The data presented in figure 6 further confirm the role of CD36-hemin interaction and its crucial role in functional defects and immune responses in macrophages. More-importantly, these effects are independent to TLR and purely mediated by CD36 and its ability to bind hemin in macrophages.

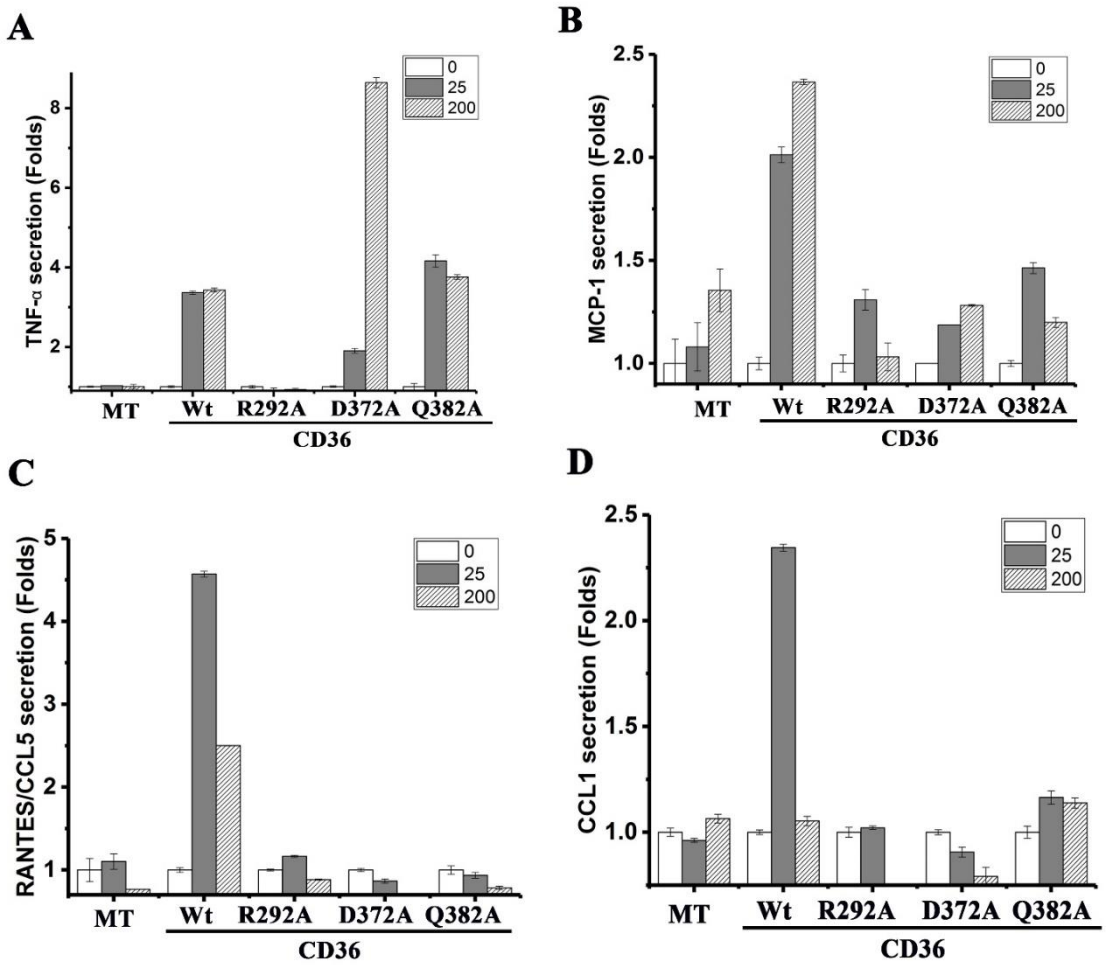

Figure 4.13. The undisturbed hemin biophore on CD36 is crucial to prime pro-inflammatory cytokine secretion. The MG63 cells transfected with wildtype (CD36) or mutants (R292A, D372A and Q382A) and treated with hemin (25 or 200 μM). The cytokines released were estimates using ELISA. **(A)** The TNF-α levels in wildtype transfected cells were found to be >3 folds in 25 as well as 200 μM hemin treated cells whereas significant reduction was observed in R292A transfected cells. The D372A transfected cells treated with 200 μM showing 8 fold increment in cytokine levels compared to 25 μM hemin treated cells. The Q382A transfected cells showing 4 fold increment. **(B)** The MCP-1 cytokine levels in wildtype transfected cells showing >2 fold secretion whereas in mutant transfected cells significantly reduced. **(C)** The RANTES levels significantly reduced upon mutation in biophoric residues compared wildtype. **(D)**The disruption in hemin biophore significantly reduced the CCL-1 cytokine levels. The cytokine levels in MG63 cells transfected with wildtype and mutants indicates the intact biophore is crucial for hemin mediated cytokine secretion.

4.3.9. Hemin induces the phosphorylation of membrane bound CD36

The phosphorylation of proteins during intracellular signalling is crucial as it controls various cellular events (Ardito et al., 2017). Since the hemin modulating the immune-response through scavenger receptor CD36 we are interested to know the signal transduction process associated with CD36-hemin interaction. To determine whether

hemin binding CD36 is causing phosphorylation of membrane bound receptor. We have treated the cells with different concentration of hemin (0, 25µM, 200µM) for 1 hr and immune-precipitated the CD36 from untreated or hemin treated lysates. The IP elute was resolved on SDS-PAGE and probed with anti-phosphotyrosine antibody. Hemin treatment leads to the phosphorylation of membrane bound as well as soluble CD36 present in cytosol (Figure 4.14A). The CD36 phosphorylation follows biphasic pattern with different concentration of hemin (low/high). The cells treated with low concentration of hemin (25µM) is exhibiting 40% more phosphorylation of CD36 present on plasma membrane whereas 10% soluble CD36 was phosphorylated in cytosol (Figure 4.14B). Cells treated with high hemin (200µM) is showing inhibition of CD36 phosphorylation with appearance of very low level of phosphorylated CD36 on membrane and soluble form in cytosol (Figure 4.14B). CD36 phosphorylation in macrophages in response to different concentration of hemin (low/high) might explain the immunological responses from macrophages.

4.3.10. CD36-Hemin interaction is relaying down-stream signalling

The enhanced phosphorylation of CD36 in hemin treated macrophages indicates the possible signalling event associated with CD36-hemin interaction. We have treated the cells with different concentration of hemin (0, 25µM, 200µM) for 1hr and cell lysate was probed with anti-phospho tyrosine. Further, the analysis of molecular weight of phosphor-reactive bands suggested that various proteins with molecular weight between 50-100 kDa were found to be phosphorylating (Table 4.3). The prediction of different phosphor-protein using phosphoprotein database (https://www.phosphosite.org/) gives list of potential candidate present in different treatment groups. Macrophage treated with hemin (low/high) is causing appearance of Nitric oxide synthase (Nos1), Receptor-type tyrosine kinase FLT 3(FLT3), E3 Ubiquitin ligase (CBL), serine threonine protein kinase D1 (PRKD1) compared to the untreated cells. Whereas, macrophage treated with low hemin (20µM) is causing appearance of RB1-inducible coiled-coil protein 1 (RB1cc1), STAT1, STAT3, proto-oncogene Src, Yes, Fyn and Heat shock protein β-1 (HSP27). It is also showing phosphorylation of CD36 as well (Figure 4.14C). Interestingly, few exclusive phosphorylated protein bands appeared in macrophage treated with high hemin (200µM). Ribosome binding protein 1 (RBP1), Mitogen-activated protein kinase kinase kinase kinase 4 (MAP4K4), Adenylate cyclase type 8 (Adcy8) and protein C-ets-2 (ETS-2) was phosphoprotein appeared in macrophage treated high hemin (200µM) compared to untreated cells (Figure 4.14C) (Table 4.3). CD36 phosphorylation recruit several adaptor

proteins to relay intracellular signalling for different immune responses (Chu and Silverstein, 2012). To explore these adaptor proteins down-stream to CD36-hemin signalling, we have used C-terminal end of CD36 as a bait protein to identify the interacting partner using Cluspro web server (https://cluspro.bu.edu/). The server is predicting the binding efficiency of different adaptors with the bait protein and provide binding energy for the resulting complexes. The results suggest the top hits could be from NF-κB/STAT signalling, Ras kinase signalling, AKT1, MAPK1/ERK2, STAT signalling pathway. The predicted adaptor protein interactome of CD36 is presented in (Figure 4.15).

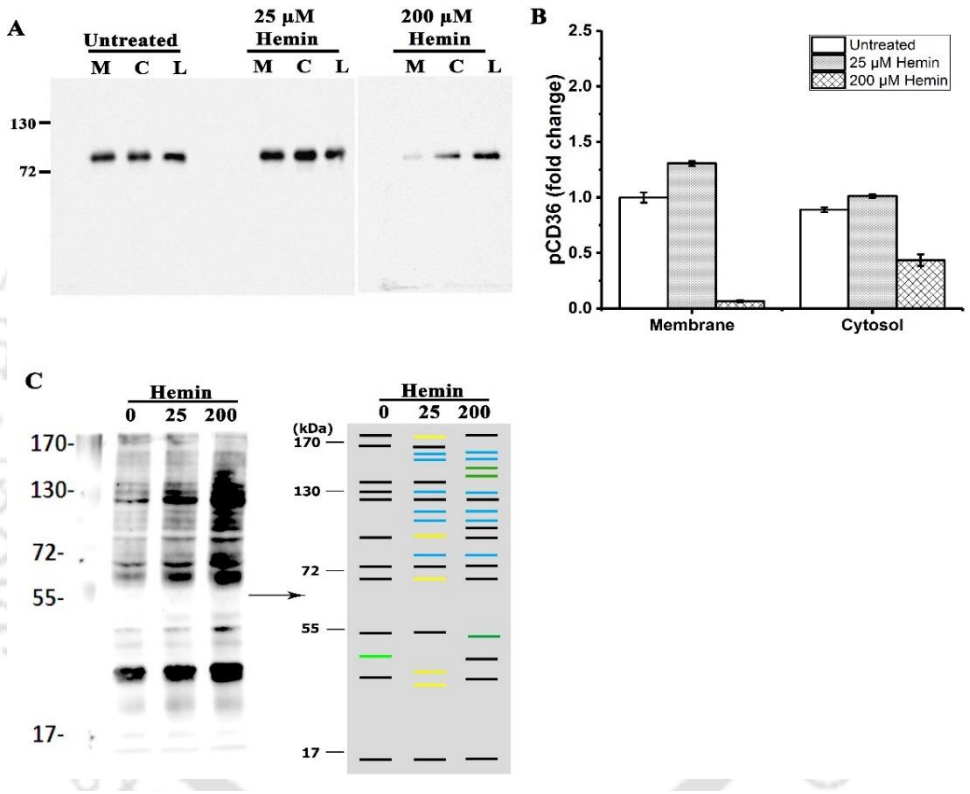

Figure 4.14. Hemin treatment induces the phosphorylation of CD36. (A) The cells either hemin (25 or 200 µM) treated for 1 h or remain untreated were lysed and fractionated into membrane and cytosol. The lysated immunoprecipitated with anti-CD36 antibody as described in materials and methods section. The resolved proteins transferred onto membrane and probed with anti-phosphotyrosine antibodies. The enhanced phosphorylation of CD36 (cytsolic or membrane fractions) in 25 µM hemin treated cell lysates can be observed whereas in 200 µM hemin terated cells the reduction of phosphorylation was observed. The blots were analyzed for signal intensity and the fold change in the CD36 phosphorylation was plotted in **(B). (C)** The cell lysates prepared from hemin treated or untreated macrophages, resolved on SDS-PAGE and transferred onto membrane. The membrane was probed with anti-phosphotyrosine antibody indicates the activation of several proteins in hemin treated condition. A mock blot was developed to clearly represent the differential phosphrylation of proteins from untreated to treated condition. The proteins exclusively phosphorylating in 25 µM hemin treated lysates coloured in Yellow and the phosphoproteins exclusive to 200 µM color coded in dark green. The phosphoreactive bands common in 25 and 200 µM lanes color coded in Blue.

TH-2507_156106009

Table 4.3. List of proteins phosphorylating in hemin treated macrophages

S.No.	Untreated		25 µM Hemin		200 µM Hemin	
	M.Wt.	Predicted proteins[#]	M.Wt.	Predicted proteins	M.Wt.	Predicted proteins
1	183	Thrombospondin type-1 domain-containing protein 7A (Thsd7a), DNA (cytosine-5)-methyltransferase 1 (Dnmt1),	180	RB1-inducible coiled-coil protein 1 (RB1cc1)	185	Myomesin-1 (Myom1)
2	170	Bifunctional glutamate/proline-tRNA ligase (EPRS)	170	Bifunctional glutamate/proline--tRNA ligase (EPRS)		
3			167	Mediator of RNA polymerase II transcription subunit 1 (Med1)	167	Mediator of RNA polymerase II transcription subunit 1 (Med1)
4			160	Nitric oxide synthase (Nos1)	160	Nitric oxide synthase (Nos1)
5					152	Ribosome binding protein 1 (RBP1)
6					140	Mitogen-activated protein kinase kinase kinase kinase 4 (MAP4K4), Adenylate cyclase type 8 (Adcy8)
7	130	Tyrosine-protein kinase JAK2	130	Tyrosine-protein kinase JAK2		
8	125	MHC class II transactivator (CIITA)	125	MHC class II transactivator (CIITA)	125	MHC class II transactivator (CIITA)
9	120	Focal adhesion kinase 1 (FAK)	120	Focal adhesion kinase 1 (FAK)	120	Focal adhesion kinase 1 (FAK)
10			111	Receptor-type tyrosine-protein kinase FLT3 (FLT3)	111	Receptor-type tyrosine-protein kinase FLT3 (FLT3)
11			99	E3 ubiquitin-protein ligase CBL (CBL), Serine/threonine-protein kinase D1 (PRKD1)	99	E3 ubiquitin-protein ligase CBL (CBL), Serine/threonine-protein kinase D1 (PRKD1)
12			88	Signal transducer and activator of transcription 1-alpha/beta (STAT1), Signal transducer and activator of transcription 2-alpha/beta (STAT3), Scavenger receptor (CD36)		
13	85	Catenin beta-1 (CTNNB1), Phosphatidylinositol 3-kinase regulatory subunit alpha (PIK3R1)	80	Dolichyl-diphosphooligosaccharide--protein glycosyltransferase subunit STT3A (STT3),	80	Dolichyl-diphosphooligosaccharide--protein glycosyltransferase subunit STT3A (STT3),
14	64	5'-AMP-activated protein kinase catalytic subunit alpha-1 (AMPKA1), Paxillin (PXN)	64	5'-AMP-activated protein kinase catalytic subunit alpha-1 (AMPKA1), Paxillin (PXN)	64	5'-AMP-activated protein kinase catalytic subunit alpha-1 (AMPKA1), Paxillin (PXN)
15	56	Cytochrome P450 26A1 (P450ra), Zinc transporter ZIP5 (ZIP5)	60	Proto-oncogene tyrosine-protein kinase Src (Src), Tyrosine-protein kinase Yes (YES), Tyrosine-protein kinase Fyn (Fyn)	56	Cytochrome P450 26A1 (P450ra), Zinc transporter ZIP5 (ZIP5)
16			23	Heat shock protein beta-1 (HSP27)	52	Protein C-ets-2 (ETS2)
17	35	CMRF35-like molecule 1 (IREM1), Low affinity immunoglobulin gamma Fc region receptor II-a (FCGR2A),Transcription factor AP-1 (JUN), Nuclear factor of kappa light polypeptide gene enhancer in B-cells inhibitor, alpha (IκBα)				
18	25	Eukaryotic translation initiation factor 4E (EIF4E)	20	Myosin regulatory light polypeptide 9 (MRLC1)	25	Eukaryotic translation initiation factor 4E (EIF4E)
	8	Protein transport protein Sec61 subunit gamma (SEC61G), EDRK-rich factor 1 (SERF1),Copper transport protein ATOX1 (ATOX1), BBSome-interacting protein 1 (BBIP1)	8	Protein transport protein Sec61 subunit gamma (SEC61G), EDRK-rich factor 1 (SERF1),Copper transport protein ATOX1 (ATOX1), BBSome-interacting protein 1 (BBIP1)	8	Protein transport protein Sec61 subunit gamma (SEC61G), EDRK-rich factor 1 SERF1),Copper transport protein ATOX1 (ATOX1), BBSome-interacting protein 1 (BBIP1)

The molecular weight of phosphoreactive proteins corresponding to figure 7C were determined using Biorad's Image lab software v4.1. The protein bands were epresented as a mock blot.

Approximate molecular weight used for hit search.

TH-2507_156106009

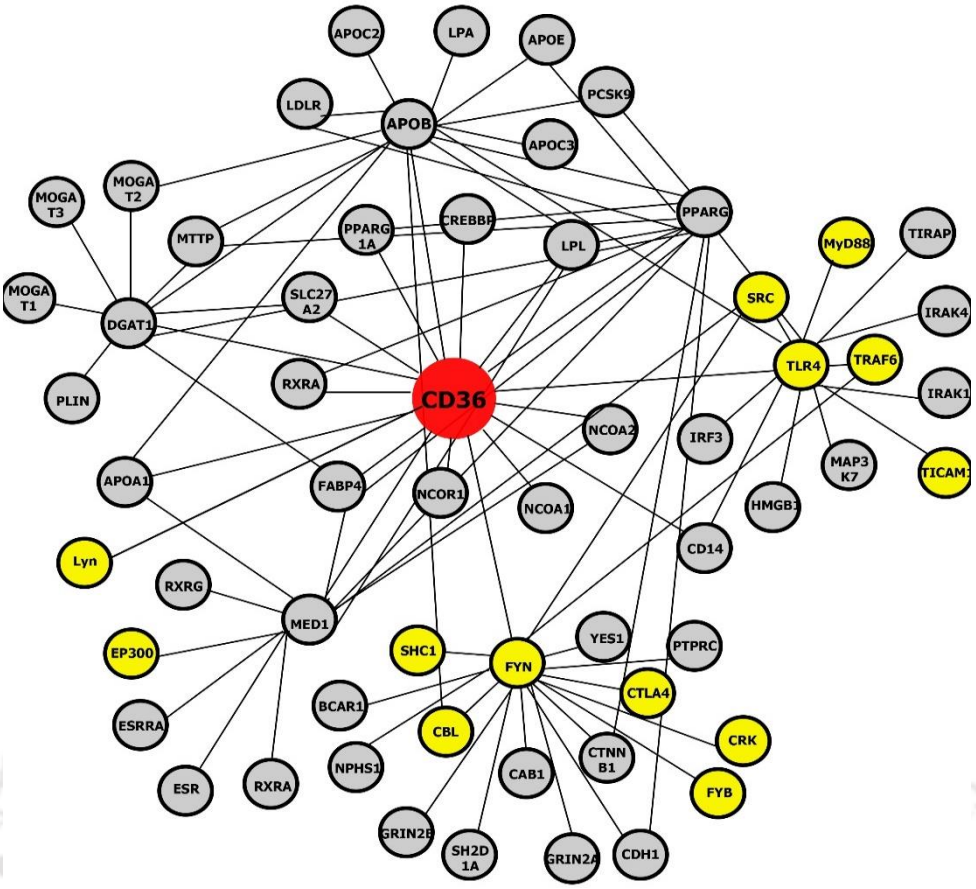

Figure 4.15. Predicted CD36 downstream adaptor protein interactome. Webserver Cluspro predicted adaptor proteins downstream to CD36. To predict possible adaptor protein downstream to CD36 a protein-protein docking was carried out using the C-terminal domain of CD36 as a bait. The interactome indicates the association of Src family kinases to CD36. The grey color filled adaptor molecules are extracted from string server and the yellow filled adaptor molecules were predicted downstream to CD36. The top hits could be from NF-κB/STAT signalling, Ras kinase signalling, AKT1, MAPK1/ERK2, STAT signalling pathway.

4.3.11. Tyrosine kinase Lyn is down-stream to the CD36-hemin signalling axis

Src family tyrosine kinases were reported to down-stream to the receptor mediated down-stream signalling in response to extracellular ligands (Parsons and Parsons, 2004). Several potential adaptor proteins from src family was predicted by Cluspro web server (https://cluspro.bu.edu/). We have treated J774A.1 with hemin or remain untreated, CD36 was immunoprecipitated and re-probed with respective src family kinases antibodies (Lyn, Fyn, Src, Lck, Csk) as described in material and methods. The immunoblot analysis with anti-Yes indicate that the Yes is associated with CD36 and hemin treatment is not changing the level of protein associated with CD36 (Figure 4.16A). It indicates that the Yes has strong affinity to the membrane bound CD36 and confirm our earlier prediction of the

Cluspro web server. C-terminal src kinase and src kinase have very low affinity to CD36 and the protein levels remained unchanged (Figure 4.16A). Probing the blot with anti-Fyn is not giving any band with untreated but give cryptic band in hemin treated cells but there is no change in protein level associated with CD36 (Figure 4.16A). Testing the presence of Lyn in the IP eluent, we have found change in the level of protein associated with CD36. A very little protein was associated with CD36 in untreated cells compared to high amount in hemin treated J774A.1 cells (Figure 4.16A). To confirm the interaction of Lyn with CD36, we have immune-precipitated Lyn from untreated or hemin treated cells and probed the IP eluent with anti-CD36 antibodies. As expected, there was a change of level of CD36 between untreated and hemin treated cells. A very little CD36 was present in the untreated cells compared to high amount in hemin treated J774A.1 cells (Figure 4.16B).

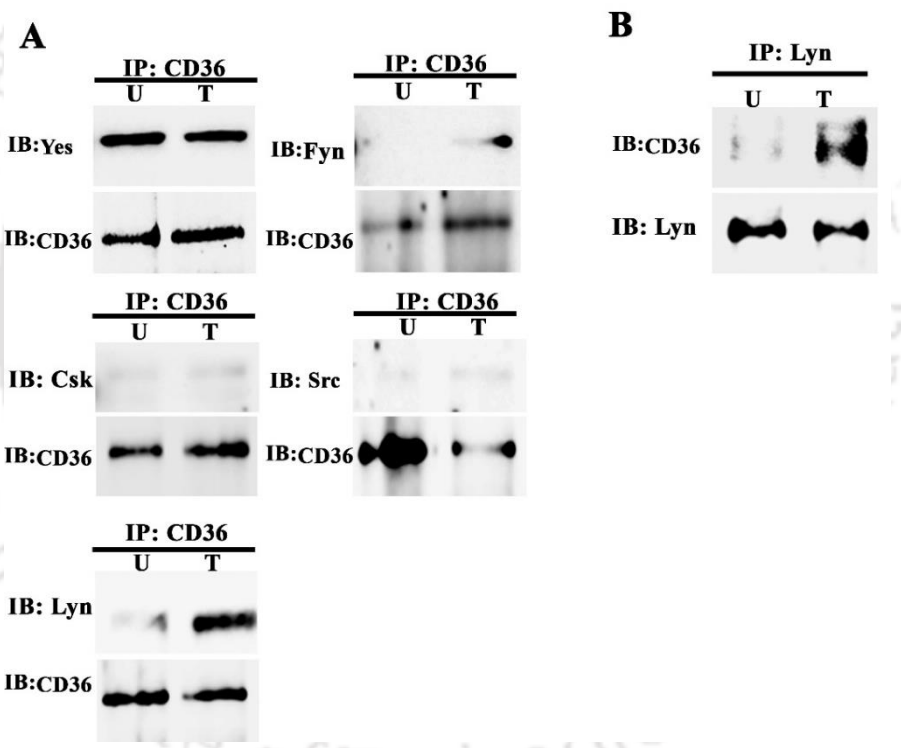

Figure 4.16. CD36 associates with Src family kinases in hemin treated macrophages. **(A)** The macrophages either treated with hemin for 1 h or remain untreated were lysed in IP lysis buffer supplemented with protease inhibitors. The cell lysates immuno-precipitated with anti-CD36 antibody as described in methodology and probed with anti-Yes, anti-Fyn, anti-Csk, anti-Src and anti-Lyn antibodies or anti-CD36 antibody. A significant co-precipitation of Lyn with CD36 was observed in hemin treated macrophage cell lysates. Besides a minor levels of Fyn kinase found to be associated with CD36 in hemin treated cells. More-over, the Yes, Csk and Src kinases were found to be constitutively associated with CD36. **(B)** The macrophages cell lysates from treated with hemin or left untreated condition, immuno-precipitated with anti-Lyn antibody and probed with anti-CD36 or anti-Lyn. The (A) and (B) confirms the recruitment of Src family kinase Lyn to downstream to CD36 in hemin treated condition.

It has been shown by various research groups that CD36 downstream association is often found with src family adaptor proteins (Yipp et al., 2003). The recruitment and activation of Lyn to the docking site leads to the activation of Lyn and recruitment of Vav and FAK proteins which initiates the macrophage foam cell formation (Rahaman et al., 2011).

4.3.12. Tyrosine kinase Lyn is controlling immune responses down-stream to the CD36-hemin signalling

The main complication with hemin treated macrophages is the secretion of pro-inflammatory cytokine especially TNF-α. Lyn was present as an adaptor protein down-stream to the CD36-hemin signalling. Now, we have explored whether Lyn has a role in cytokine secretion and immune responses from macrophages treated with hemin. Lyn was knockdown in J774A.1 using siRNA and level of lyn was confirmed by western blotting using anti-Lyn antibodies (Figure 4.17A). Lyn knockdown in J774A.1 is reducing the secretion of TNF-α compared to the scrambled siRNA treated control cells. There is almost more than 50% reduction in the level of cytokine in Lyn knockdown J774A.1 cells (Figure 4.17B). J774A.1 contains toll-like receptors and other hemin responsive receptors, there is a possibility that remaining cytokine secretion could be due to the hemin interaction with these receptors. The global cytokine profiling in absence of Lyn in hemin treated macrophages were studied using cytokine array. The lyn knockdown macrophages treated with hemin showed reduced levels of TNF-α, G-CSF, sICAM1, MCP-1, and CXCL2 reduced compared to controls (Figure 4.17C, cytokine array). To investigate whether adaptor molecules Lyn has any role in hemin mediated pro-inflammatory cytokine signalling, the macrophages with Lyn knockdown treated with 25 or 200 µM of hemin. The nonspecific siRNA transfected macrophages used as a control to compare the Lyn knockdown macrophages. A cytokine array was performed on Lyn knockdown macrophages treated with hemin. The control siRNA (si RNA) transfected macrophages treated with 25 µM hemin showing the reactivity towards CXCL-13, IL-4, M-CSF, MCP-5 and CXCL-9 but they are completely absent in Lyn transfected macrophages either treated with 25 or 200 µM hemin (Figure 4.17C and D). Interestingly the pro-inflammatory cytokine IL-16 was found to be upregulated to 26 folds in untreated macrophages with control siRNA and Lyn knockdown macrophages treated with 25 or 200 µM of hemin whereas control siRNA transfected macrophages treated with hemin showed significantly low (1.7 folds) levels of IL-16 (Figure 4.17C and D). The IL-16 act as a chemoattractant for CD4+ T cells and protects in HIV-1 infection by protecting against

activation induced cell death (Mathy et al., 2000) (Idziorek et al., 1998).

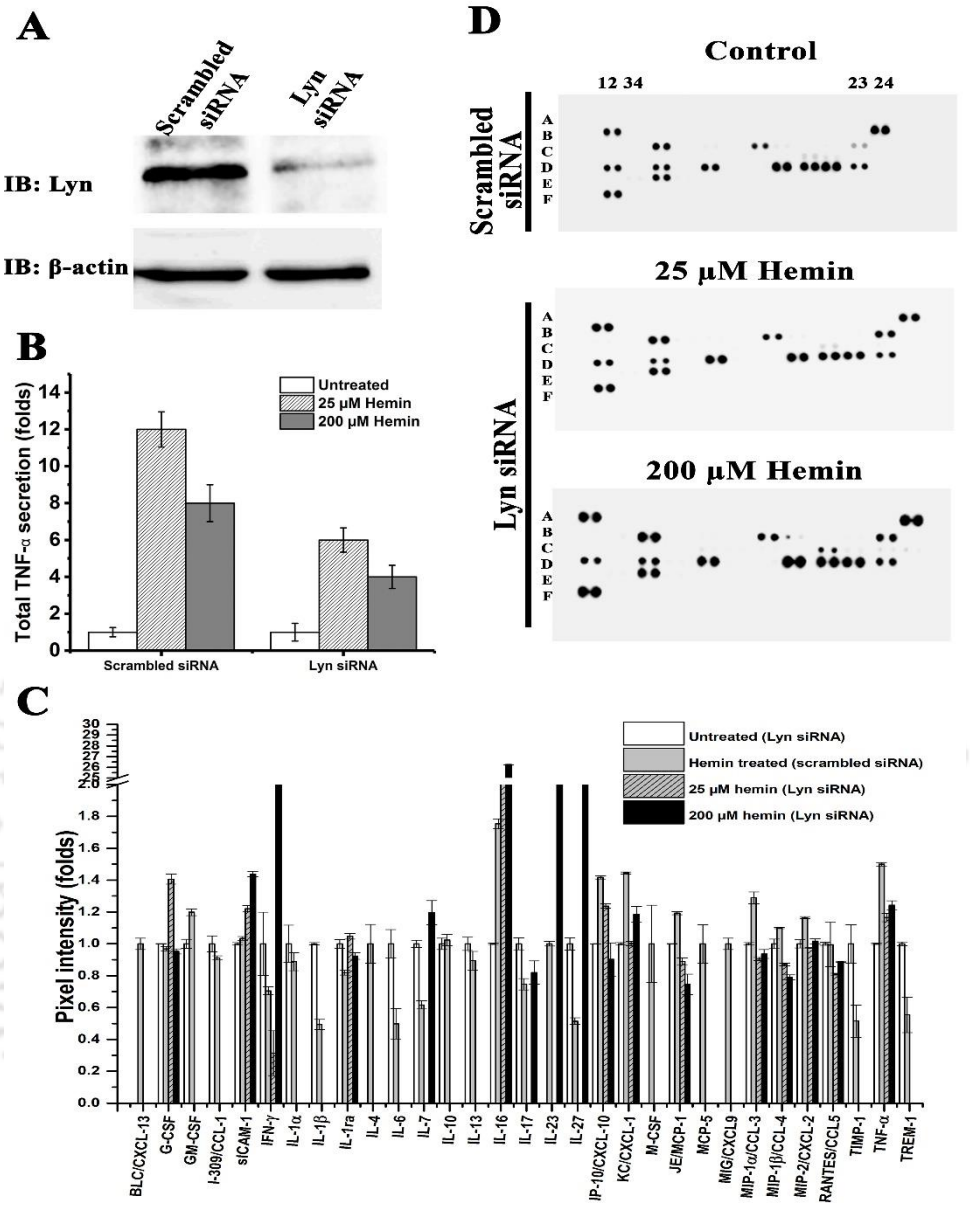

Figure 4.17. Recruitment and docking of Src family kinase Lyn to downstream of CD36 is crucial for hemin mediated immune-dysfunction. (A) The validation of Lyn knockdown in macrophages. The macrophages either transfected with scrambled siRNA (sc siRNA) or Lyn siRNA and 48 h post transfection, lysates were probed with anti-Lyn antibody or anti-β actin antibody. The blot shows the 70-80% knockdown of Lyn protein. **(B)** Estimation of TNF-α levels from Lyn knockdown macrophage cell culture supernatants. The lyn knockdown macrophages treated with hemin showed reduced levels of TNF-α comparing to scrambled siRNA transfected macrophages indicates the hemin activates the cytokine signalling through CD36 and recriitment of lyn to the cytosolic domain of CD36. **(C)** Global cytokine profiling of Lyn knockdown macrophages. The macrophages were transfected with scrambled siRNA or Lyn target siRNA and either untreated or treated with hemin. The cytokine array was carried out on cell culture supernatants using mouse cytokine profiler array kit panel A. **(D)** The cytokines were normalized and plotted as fold change. Several cytokines such as CXCL-10, CXCL-1, MCP-1, CCL-3, CCL-4, CCL-2, and TNF-α levels were reduced (expressed in fold change) upon lyn knockdown.

In normal condition the elevated IL-16 might impart protection against activation induced cell death but in hemin treated condition the levels are down regulated. In Lyn knockdown macrophages treated with hemin, the levels of IL-16 restored and indicates the hemin-CD36 mediated downstream signalling depends on Lyn recruitment to downstream to CD36. However the reduced levels of IL-16 in untreated Lyn knockdown macrophages need further investigation. Further, the cytokines IL-23, IL-27 were found upregulated to 3, 2 folds respectively in Lyn knockdown macrophages treated with 200 µM of hemin but absent in 25 µM of hemin treated macrophages (Figure 4.17C and D). The pro-inflammatory cytokine IP-10 mediated homing of T-cells promotes the cerebral inflammation in malaria condition (Nie et al., 2009). The elevated levels of IP-10 is associated with cerebral malaria development in mouse models (Wilson et al., 2011). The macrophages with control siRNA transfection and treated with 25 µM hemin showed 1.41 folds enhancement in IP-10 levels whereas with Lyn knockdown macrophages treated with 25 or 200 µM hemin levels were reduced to 1 fold and 1.21 folds respectively (Figure 4.17C and D). This might explain the elevated IP-10 levels during cerebral malaria since hemin levels were high (Hunt and Stocker, 2007) and hemin-CD36 signalling via Lyn recruitment to CD36 downstream regulates the pro-inflammatory cytokine secretion.

Further we have evaluated the phagocytic activity and bactericidal activity of Lyn knockdown macrophages. The lyn knockdown macrophages failed to correct the phagocytic depression (Figure 4.18A) or bactericidal activity (Figure 4.18B). Further the phagocytic activity of Lyn knockdown macrophages was evaluated using normal and oxidized RBC as phagocytic objects (Figure 4.18C). The control cells treated with 25 µM hemin showed phagocytosis of normal as well as oxidized RBC. Conversely the higher hemin concentration (200 µM) abolished the erythrophagocytosis. Interestingly, the lyn knockdown macrophages treated with 25 µM or 200 µM showed phagocytosis of oxidized RBC but not normal RBC (Figure 4.18C and D). The results strongly suggest that hemin binding to CD36 causes the CD36 phosphorylation at tyrosine residue and recruitment of signalling protein Lyn kinase to cytosolic domain. Further, the hemin-CD36-Lyn involved in the pro-inflammatory cytokine secretion.

TH-2507_156106009

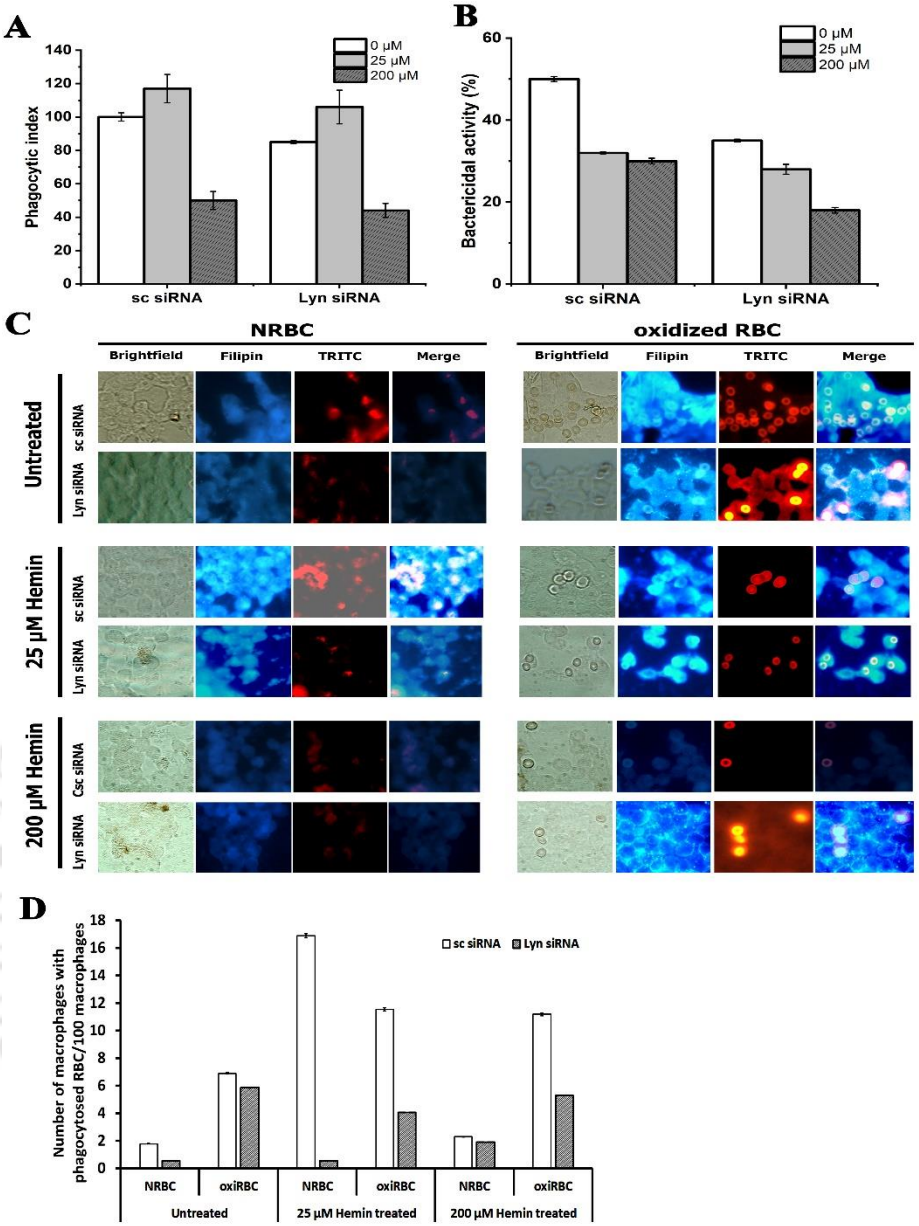

Figure 4.18. Recruitment and docking of Src family kinase Lyn to downstream of CD36 is crucial for hemin mediated immune-dysfunction. The macrophages were transfected with either sc siRNC (control siRNA) or Lyn siRNA as described in experimental procedures. 48 h post transfection the experiments performed on macrophages. **(A)** The phagocytic activity of Lyn knockdown macrophages treated with hemin. **(B)** The bactericidal activity of Lyn knockdown macrophages treated with hemin. **(C)** The phagocytic activity of macrophages (with lyn knockdown) towards RBC. The macrophages either transfected with scrambled siRNA (sc siRNA) or or Lyn siRNA were either treated with hemin or remain untreated were incubated with normal RBC or oxidized RBC. Macrophages were stained with filipin to identify phagosomes containing engulfed material and observed under Nikon 80i fluorescence microscope in DAPI and TRITC filters to acquire filipin (Blue) and RBC (Red) fluorescence respectively. **(D)** The number of phagocytic macrophages were counted and plotted as number of phagocytic macrophages per 100 counted macrophages. The lyn knockdown in macrophages significantly reduced the non-opsonic phagocytosis of NRBC or oxiRBC in hemin treated condition.

4.4. Discussion

The balance between pro-inflammatory and anti-inflammatory cytokines is the deciding factor in resolution of infection (Cicchese et al., 2018). Macrophages in host body serves as the first line of defence against pathogens by capturing and engulfing pathogenic or non-pathogenic, living or dead entities. The macrophages activated by the stimulus from PAMPS or endogenous ligands secrete pro-inflammatory or anti-inflammatory cytokines such as TNF-α, IL-1*β,* IL-10, IL-4 (Varin and Gordon, 2009). During the malaria, macrophages are activated by sensing of IRBC and the parasite proteins expressing on RBC such as PfEMP-1 (McGilvray et al., 2000). The opsonisation of IRBCs brings the macrophages to engulf and induce innate immune response by secreting IL-10, IL-12, IL-18, and TNF-α, and IFN-γ cytokines (Gowda et al., 2013). The cytokines IFN -γ and IL-18 are crucial for the early clearance of parasite burden (Torre et al., 2001). The most prominent pro-inflammatory cytokines associated with malaria infection are IFN-γ, TNF-α, MCP-1, IL-6, IL-8, RANTES, IP-10, and IL-18 (Lyke et al., 2004). In placental malaria, the macrophages cause local inflammation and low birth weight by releasing the cytokines after activation signal from sequestered iRBCs from placenta (Beeson et al., 2000). Besides the opsonisation based phagocytosis, the macrophages are also involved in the non-opsonic phagocytosis of the iRBCs. The expression of PS on cell surface is essential for the phagocytosis by macrophages. During vascular injury, oxidative stress or pathogenic infections, the phosphatidylserine exposed on RBC surface (Holovati et al., 2008). The macrophages use various cell surface receptor to sense the senescence or IRBCs (Shiono et al., 2003). The scavenger receptor CD36 on macrophage recognizes the apoptotic/senescence RBCs (Nakamura et al., 1992). The macrophage scavenger receptor CD36 not only recognizes PS (Banesh et al., 2018) but also serves as a receptor for parasite PfEMP-1 (Hsieh et al., 2016). Several line of evidence highlighted the CD36 mediated non-opsonic phagocytosis is crucial to check the unbalanced pro-inflammatory cytokine secretion. The hemin (free heme) released during vascular injury, or malaria implicated in pathological outcomes of host (Porto et al., 2007). The hemin is highly cytotoxic and removed by host machinery through hemopexin and albumin binding and further catabolized by heme oxygenase-1 (Gozzelino et al., 2010). During hematoma a large amounts of hemin (10 mM) released in brain and could lead to stroke and permanent damage to brain (Robinson et al., 2009). Further, the toxicity of hemin has been demonstrated on cultured astrocytes (Dang et al., 2011). The cytotoxicity of heme is attributed to the hydrophobic porphyrin ring which can easily intercalates into plasma

membranes and damage the cell integrity and production of free radicals (Schmitt et al., 1993). The exposure of RBC to hemin causes PS exposure on RBC surface. The PS expressing RBC removed from circulation by non-opsonic phagocytosis by macrophages. Intravascular haemolysis during malaria releases large amounts of free heme which can be deposited in liver. The free heme activates NF-κB which induces the VCAM-1, KC and MIP-1 cell adhesion molecules and cytokines expression (Dey et al., 2012). The heme treatment induced TNF-α secretion by macrophages through TLR-4, CD18 and MyD88 dependent manner (Figueiredo et al., 2007). The expression of cytokines attract the neutrophils and their attachment to liver tissue. The levels of free heme in liver is correlating with the neutrophil extravasation and liver damage (Dey et al., 2012).

The scavenger receptor CD36 play crucial role in controlling the pathophysiology of the host during infectious and non-infectious diseases (Banesh and Trivedi, 2020). The macrophages expressing CD36 recognizes various ligands from pathogens or host cells, get activated and secret pro-inflammatory cytokines (Ren, 2012). The binding of oxiLDL with CD36 triggers the association of CD36 with Toll like receptors (TLR-4 and 6) and responsible for sterile inflammation in macrophages (Stewart et al., 2010). The macrophage CD36 mediated oxiLDL internalization activates pro-inflammatory cytokines, generation of ROS which is involved in macrophage foam cell formation in atherosclerosis (Kumar et al., 2012). The binding of TSP-1 to endothelial CD36 leads to apoptosis of endothelial cells through Src family kinase Fyn and phosphorylation of p38MAPK (Zhao et al., 2018). The scavenger receptor CD36 mediated pro-inflammatory cytokine secretion is also attributed to ischemic brain injury. In ovarian cancers and gastric cancers the widespread metastasis is linked to the enhanced fatty acids uptake (Ladanyi et al., 2018). It was found that the fatty acid uptake in visceral adipocytes and gastric cells is facilitated by CD36 upregulation. Further the CD36 inhibition in mouse ovarian cancer xenografts, reduced the tumour burden, and intracellular oxidative stress (Ladanyi et al., 2018). The CD36 knockdown reduced the pro-inflammatory cytokine secretion, macrophage migration, ROS generation and plaque formation (Geng et al., 2018). The CD36 is crucial for non-opsonic phagocytosis of dead or aged cells or pathogenic molecules; the macrophages with CD36 knockdown are not efficient to perform these functions so there will be a systemic immune response which might affect the functioning of the organs. Further, the fatty acid uptake in adipocytes is mediated largely by CD36 and its reduction on adipocytes leads to impaired fatty acid metabolism.

The scavenger receptor CD36 and the pro-oxidant molecule hemin play crucial roles

during malaria pathology. Cell surface CD36 level is crucial for non-opsonic phagocytosis of IRBC and proper TNF-α secretion (Serghides et al., 2003). The macrophages treated with hemin showed defective in phagocytosis, bactericidal activity and phagocytic depression is more severe towards oxiRBC. In addition, the CD36 translocated into cytosol in hemin treated macrophages. The senescence RBC or parasitized RBC express PS on their surface and can be recognized by scavenger receptor CD36 (Tait and Smith, 1999). The hemin treatment might be causing CD36 to sequester into cytosol and could explain the phagocytic depression towards oxiRBC.

The macrophages exposed to hemin showed marked increase in levels of pro-inflammatory cytokines CS/C5a, sICAM-1, IL-1α, IL-1β, IL-1ra, IL-13, IL-17, IL-23, IL-27, M-CSF, CXCL9, CCL1, IFN-γ, IL-16, CXCL-10, CXCL-1, MCP-1, RANTES, and TNF-α. The observed cytokine secretion is consistent with previous reports that hemin upregulates several pro-inflammatory cytokines such as TNF-α, MCP-1, IL-16, and CCL1 but the target receptor or the hemin biophore details are not known (Ma et al., 2007). We have employed various biochemical and computational tools to study hemin biophore on CD36. The hemin biophore environment consist of R292, Q382 and D372 residues. The affinity studies suggested the wildtype CD36 showing very high affinity towards hemin (1.26±0.24 μM) whereas for mutant versions of CD36 (R292A, D372A and Q382A) it reduced significantly. The ligand binding to CD36 often involved internalization of ligand-CD36 complex (Heit et al., 2013). It has been shown that t*he* CD36 mediated cytokine secretion requires TLR2 (Hoebe et al., 2005). Contrary to the previous observation, we have found that CD36 solely interact with hemin as evident from chemotaxis assay in cell line with (low CD36 and low TLR expression). It has been shown that the IRBC uptake by macrophages does not require TLRs but for enhanced internalization of IRBC, the CD36 functionally cooperate with TLRs (Erdman et al., 2009). The evaluation of phagocytosis, bactericidal activity and cytokine secretion of wildtype (CD36) or mutants (R292A, D372A and Q382A) further confirmed that the hemin interactions with CD36 is highly specific and need intact biophore. The study also establishes CD36 as an independent receptor for hemin. However, the TLRs shown to be a primary receptor for heme and derived products which needed a further investigation whether in presence of TLRs, still CD36 accept hemin as a ligand. The engagement of ligand to membrane bound receptors has been shown to activate intracellular signalling. The hemin treated macrophages showed there is an enhancement in phosphorylated CD36 compared to untreated. It could be possible that the phospho CD36 internalization could be preventing

CD36 to recycle back and might explain the reduced CD36 levels on membrane (Innamorati et al., 1998) however a mechanistic study need to be warranted to explore the CD36 trafficking in cytosol and unable to recycle back. Further the adaptor protein screening revealed most of hit proteins could be from NF-κB/STAT signalling, Ras kinase signalling, AKT1, MAPK1/ERK2, STAT signalling pathway. The pull-down assay using anti-CD36 antibodies suggested the recruitment of Src family kinase proteins Lyn and Fyn to the cytosolic domain of CD36 in hemin treated macrophage cell lysates whereas the Yes, Csk and Src found constitutively associated with CD36. The CD36-dependent signaling cascade requires the recruitment of src kinases Fyn and Lyn, and the MAP kinase kinase and the JNK2 (Chen et al., 2008). The heme bind TLR activates the downstream signalling involving recruitment of TIRAP and MyD88 to the cytosolic side of TLRs. The intermediate signalling molecules TRAF6 and TAK1 activates the NF-κB transcription which induce pro-inflammatory cytokine secretion (Diamond et al., 2015). There is a possibility that heme mediated downstream signaling is receptor specific rather than prototype. Further, the Lyn knockdown macrophages treated with hemin showed improved phagocytosis of oxiRBC but not the bacteria suggests the CD36 is specifically phagocytose oxiRBC through non-opsonic phagocytic mechanism. The scavenger receptor CD36 is seen to be forming a multimolecular signaling complex consisting β1/β2 integrins, CD9/CD81, and FcRγ. This molecular association enables the CD36 to engage the Src family kinases (Heit et al., 2013). Besides, the docking of other Src family proteins, Vav1 and Rac1 to the Lyn and phosphorylation and activation of MEKK activate the cytokine proteins transcription and likely to be responsible for the observed pro-inflammatory cytokine secretion in hemin stimulated macrophages. Although we have predicted adaptor molecules to downstream to CD36-hemin complex, the intermediate adaptor molecules and transcription regulators have not been explored in this study. The identification of complete signalosome molecules may provide more precise information regarding the pro-inflammatory cytokine signalling. Our study provides direct evidence that hemin act as a ligand for CD36. During cerebral malaria, the hemin levels are very high and correlating with pro-inflammatory cytokine secretion. The endothelial receptor CD36 interact with IRBC or hemin released during the RBC lysis and responsible for the pathological outcome. This study has not explored TLR role in hemin dysfunction but focussed on CD36 mediated response.

References: Please refer to the Bibliography section at the end of the thesis.

TH-2507_156106009

Chapter-V

CD36 blockers from natural sources have potentials in controlling Immune responses down-stream to CD36

TH-2507_156106009

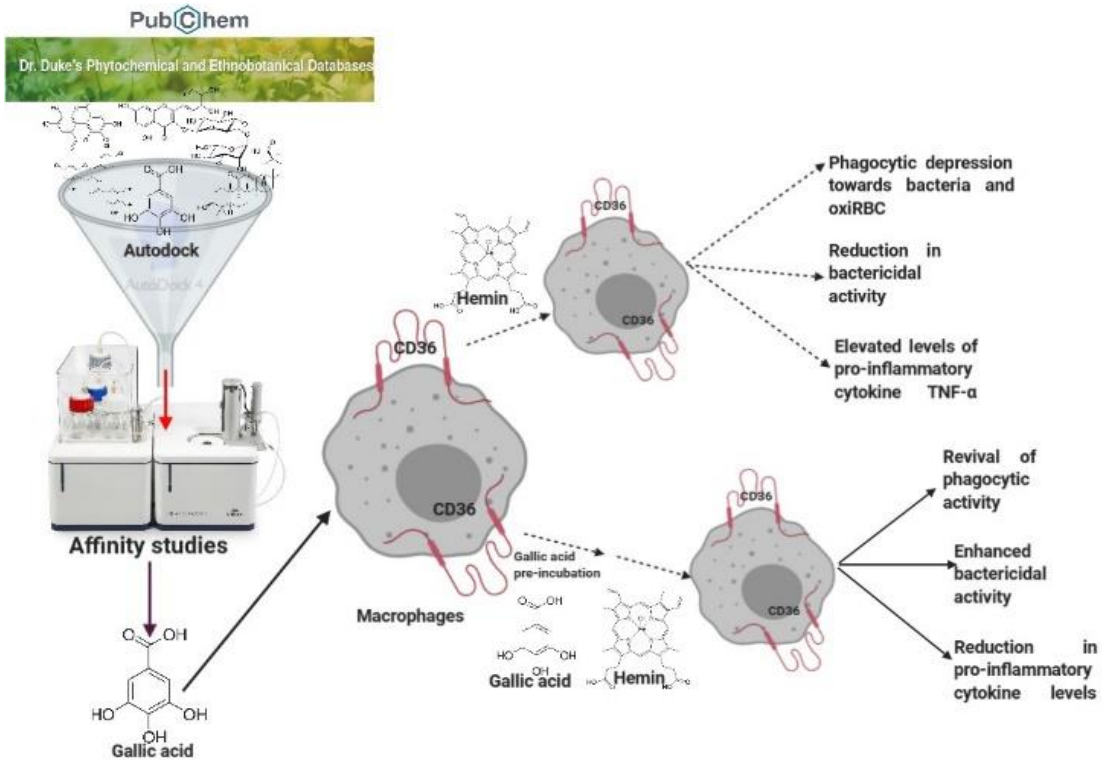

Summary

In this chapter we have explored the potentials of CD36 blockers in rescuing the macrophages from hemin mediated immune-dysfunction. The virtual screening of phytochemicals against CD36 gave several hits which are interacting in-silico with CD36. The top hits from phytochemical screening were belongs to phenolic, alkaloids, flavonoids and glycosides. ITC based affinity studies of purified human CD36 ectodomain with top phytochemicals suggested the phytochemical Gallic acid show strong binding with CD36 with K_D value of 0.32±0.02 µM. In addition, two of the hemin biophoric (R292A and D372A) mutants showed reduced binding towards Gallic acid whereas Q382A not binding as evident from ITC and dot blot assay. The binding studies suggests the Gallic acid is a ligand for CD36. The Gallic acid pre-incubation effectively restored phagocytic activity, bactericidal activity and reduced higher cytokine levels in macrophages treated with hemin. In summary the Gallic acid could be promising candidate to be employed in adjuvant therapy during cerebral malaria.

Key words: Natural resources, phytochemicals, inflammation, immune dysfunction, drug discovery.

5.1. Introduction

Indian ancient medicine involves use of plant or plant derived materials to treat wide range of infectious as well as metabolic disorders (Mukherjee et al., 2017). The use of plant products in the form of tincture, decoction, powder, and herbal tea is been practiced and it is very popular in common people (Dhama et al., 2018). Plants secrete or produce a variety of secondary metabolites such as alkaloids, phenolic, glycosides, terpenoids, and defensins. The plants produce these secondary metabolites for their defense and maintenance (Zaynab et al., 2018). The phytochemicals have been established as source of diverse chemical compounds. The high throughput screening expedited the process of drug discovery from natural sources (Zang et al., 2012). Over 100 molecules extracted from natural sources were under clinical trial stages (Katiyar et al., 2012). There are various phytochemicals successfully used in treatment of broad range of ailments (Dillard and German, 2000). The reason behind investigating phytochemicals and their curative actions during a disease condition lies in its vast number of compounds. One study states there are thousands of phytochemicals which are unexplored and no structural similarity with FDA approved drugs (Mohanraj et al., 2018). Further, their wide availability, cost involved is less and have literature support from ancient medicine systems such as Indian Ayurveda and Chinese herbal medicine.

The phenolic group phytochemicals such as catechin, curcumin, and reservatol have been reported to reduce pro-inflammatory cytokine secretion in various chronic inflammatory conditions. Several phytochemicals from glycosides, alkaloids, and terpenoids were found to be immune-stimulatory nature. Using phytochemicals to treat the inflammation is still in infancy stage but identifying phytochemical blockers to target a particular receptor could be useful and gives momentum to carry forward the results to clinical trial stage.

The scavenger receptor CD36 is pivotal in development of pathology or protection during various infectious and non-infectious diseases (Banesh and Trivedi, 2020). The CD36 mediated pathology or protection is dependent on ligand binding to CD36 (Xu et al., 2018). The most prominent ligands involved in pathology or protection are oxiLDL, TSP-1, oxidized phospholipids, IRBC, β amyloid fibrils, and hexarelin (Park, 2014). The oxiLDL binding to CD36 is involved in atherosclerosis plaque formation, generation of oxidative stress and pro-inflammatory cytokine secretion (Zhao et al., 2018). The TSP-1 binding to CD36 is implicated in anti-angiogenesis and apoptosis in endothelial cells (Wang and Li, 2019). Further, the CD36 interaction with β amyloid plaques induce pro-inflammatory cytokine secretion and contribute to cerebrovascular pathology (El Khoury et al., 2003).

TH-2507_156106009

The senescence or dead cells present the PS on their surface. The CD36 recognizes the apoptotic cells through PS sensing and facilitate non-opsonic phagocytosis by macrophages (Banesh et al., 2018). The detection of the parasite proteins or externalized PS is crucial for clearance of parasite infected RBC from circulation in order to prevent immune response (Hannemann et al., 2018). The CD36 mediated uptake of IRBC by macrophages has its own complications such as enhanced erythro-phagocytosis induces apoptosis of macrophages (Cambos and Scorza, 2011). The enhanced erythrophagocytosis by macrophages leads to accumulation of hemin in macrophages and involved in generation of oxidative stress (Cambos and Scorza, 2011). In chapter-IV we showed that hemin mediates the macrophage dysfunction and pro-inflammatory cytokine secretion through scavenger receptor CD36. The current understanding is that by blocking the interactions of CD36 and pathological ligand with blockers could be beneficial and proven in many instances (Yamanaka et al., 2012). The ligands binds at a well-defined regions on CD36. The reasons behind searching compounds from phytochemical database, is they are easily available, low toxicity and economical.

The phytochemicals were screened against CD36 using Autodock tools. The virtual screening suggested the phenolic compounds from phytochemicals more particularly Gallic acid showing nice binding within CD36 ectodomain. The affinity of Gallic acid affinity reduced with CD36 mutants (R292A, D372A and Q382A). The Gallic acid pre-incubated macrophages treated with hemin showed normal phagocytic behaviour towards bacteria and oxiRBC. Moreover the Gallic acid pre-treatment rescued macrophages from uncontrolled cytokine (TNF-α) secretion. The study can be taken up to test the possibility of adjuvant therapy during cerebral malaria.

5.2. Experimental procedures

5.2.1. Collection and curation of Phytochemicals: The phytochemical list was obtained from Dr. Duke's phytochemical and ethnobotanical database (https://phytochem.nal.usda.gov/phytochem). A total of 565 chemicals with biological activity category were downloaded. The 2D structure files for phytochemicals were retrieved from the PubChem (https://pubchem.ncbi.nlm.nih.gov/) and zinc database (https://zinc.docking.org/). The 2D structures were converted into 3D using the openbabel software, followed by geometry cleaning of the structure. The energy minimization was performed on 3D structures using ChemBioDraw 3D with maximum iterations for the minimization were set to 1000 steps.

5.2.2. Molecular docking and interaction analysis of collected compounds against CD36: The molecular docking was performed as described in Chapter-II, Experimental procedures 2.2.11 section, page no.58.

5.2.3. Molecular dynamics simulations: The MD simulations were performed as described in Chapter-II, Experimental procedures 2.2.13 section, page no.59.

5.2.4. Protein purification: The protein expressed and purified as described in Chapter-II, Experimental procedures 2.2.4 section, page no.56.

5.2.5. Dot-blot assay: The dot blot assay was performed as described in Chapter-II, Experimental procedures 2.2.7 section, page no.57.

5.2.6. Affinity studies of phytochemicals with CD36 ectodomain: The affinity studies were performed as described in Chapter-II, Experimental procedures 2.2.8 section, page no.57.

5.2.7. Cell culture: The cell culture and maintenance was done as described in Chapter-III, Experimental procedures 3.2.4 section, page no.79.

5.2.8. Phagocytosis assay: The phagocytosis assay was performed as described in Chapter-IV, Experimental procedures 4.2.3 section, page no.99.

5.2.9. Bactericidal assay: The bactericidal assay was performed as described in Chapter-IV, Experimental procedures 4.2.4 section, page no.99.

5.2.10. Estimation of TNF-α secretion: The secreted TNF-α was estimated as described in Chapter-IV, Experimental procedures 4.2.8 section, page no.101.

5.3. Results

5.3.1. Identification of suitable CD36-hemin interaction blockers from phytochemical library

Several endogenous and exogenous molecules interact with CD36 and the binding of these ligands implicated in immune response during infectious and non-infectious diseases (Banesh and Trivedi, 2020). It has been shown that the blocking the interaction of CD36 with ligands involved in pathological response could be useful and can be exploited as an adjuvant therapy (Yu et al., 2016). The objective of this virtual screening is to identify the

TH-2507_156106009

potential phytochemical molecules to block the CD36. The scheme for identification of molecules is depicted in Figure 5.1. Phytochemicals use in adjuvant therapy offers low toxicity, very effective, economical and easily available (Shirsath and Goswami, 2020). A total of 565 phytochemicals (from Dr. Duke's phytochemical and ethnobotanical database) were used in virtual screening against CD36 as a target receptor. The docking log files were analysed for binding energy, clusters and conformations. The compounds were sorted based on the binding energy and clusters. The phytochemicals with binding energy less than -3.0 kcal/mol and cluster number less than 10 were shortlisted for further analysis. A total of 40 phytochemicals were found to be coming under above selected criteria and enoxolone (binding energy -6.04 kcal/mol) showing lowest binding energy. The binding energies for top phytochemicals summarized in (Table 5.1). The top hits belongs to diverse group of chemicals such as flavonoids, phenolic compounds and glycosides.

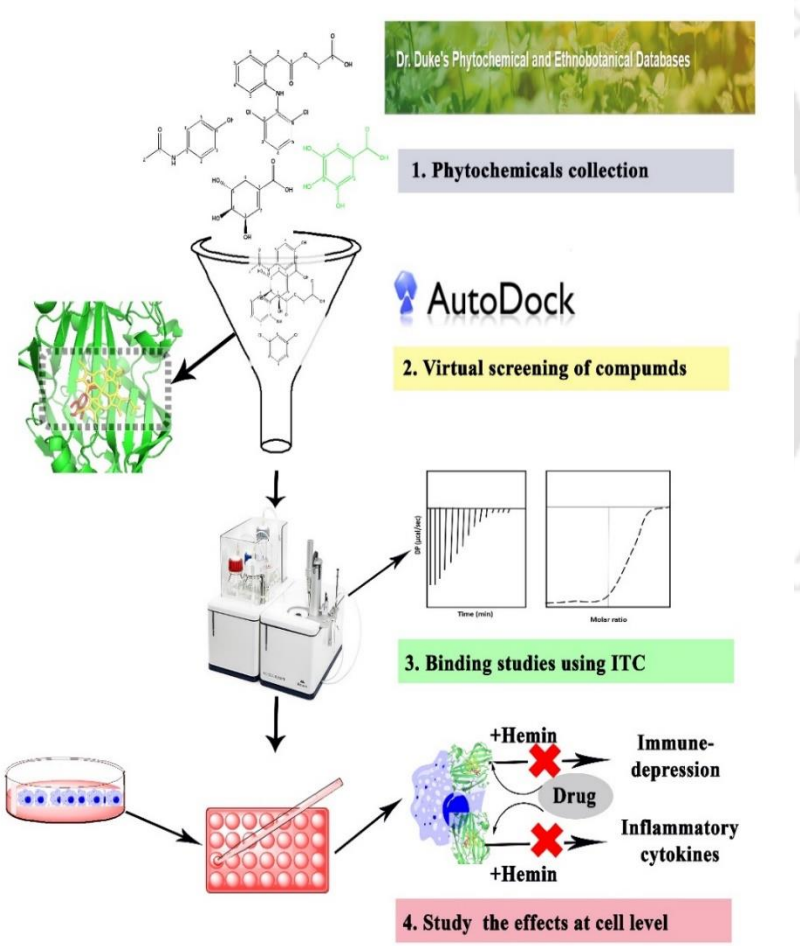

Figure 5.1. Scheme for screening and identification of suitable phytochemicals to block CD36. The process involves retrieval and curing of phytochemicals and molecular docking with CD36. The best hits were taken further for affinity studies with purified CD36 ectodomain. The compounds with high affinity towards CD36 were evaluated for controlling immune response to downstream to CD36.

Table 5.1. Binding energies of top phytochemicals.

S.No.	Name of phytochemical	Binding energy (Kcal/mol)	Clusters
1	Helenalin	-6.26	3
2	Enoxolone	-6.04	9
3	Cepharanthine	-5.84	10
4	Chelerythrine chloride	-5.73	4
5	Aristolochic acid	-5.51	10
6	Berberine chloride	-5.44	7
7	Plumbagin	-5.25	5
8	gossypol	-5.15	5
9	Lapachol	-5.09	7
10	Diospyrin	-5.03	3
11	Catechin	-4.97	8
12	Oxymatrine	-4.96	9
13	Rosmarinic acid	-4.92	1
14	Daphnetin	-4.86	10
15	Isorhynchophylline	-4.81	3
16	Luteolin	-4.69	6
17	Mitraphylline	-4.63	10
18	Emetine	-4.62	2
19	Berbamine	-4.52	10
20	Genistein	-4.5	4
21	Coumarin	-4.45	9
22	Isomitraphylline	-4.44	5
23	Matrine	-4.41	7
24	Anethole	-4.38	4
25	Emodin	-4.32	10
26	Emodin	-4.32	10
27	Caffeic acid	-4.21	9
28	Vit E	-4.15	1
29	Protocatechuic acid	-4.04	9
30	Pilocarpine nitrate	-4.02	8
31	Curcumin	-4.02	5
32	Chlorogenic acid	-4.01	3
33	Gallic acid	-3.84	6
34	Phorbol	-3.73	5
35	(-)-Epicatechin gallate	-3.69	4

5.3.2. Interaction analysis of phytochemicals bound with CD36

Among the top hits phenolic compounds such as gallic acid, ellagic acid and catechin were showing good in-silico fitting into CD36. It was expected to see these molecules interact with CD36 owing to their hydrophilic nature. Further, the overlay of binding poses in a 3D surface model of CD36 suggested the phytochemicals fitting perfectly into CD36

TH-2507_156106009

binding cavity (Figure 5.2A, zoom-in inset). The CD36-phytochemical complex from best binding pose was analysed for protein-ligand interactions using ligplot v4.5. The interaction plot analysis suggests the phytochemicals interacting with one or more of the CD36 residues T59, E60, Q64, K286, Y370, R386, T419 and T421. A total of four contacts were observed in Gallic acid bound complex whereas for chlorogenic acid seven such hydrogen bonds were observed (Figure 5.2B). The curcumin is interacting with CD36 through hydrophobic interactions but not the hydrogen bonding. Berberine chloride, catechin and ellagic acid were found to be interacting with CD36 through hydrogen bonding. The Gallic acid interacting with CD36 through hydrogen bonding and hydrophobic interactions. The residues T59, T421 forming hydrogen bonds with hydroxyl groups of Gallic acid within a distance of 2.78 and 2.62 Å respectively.

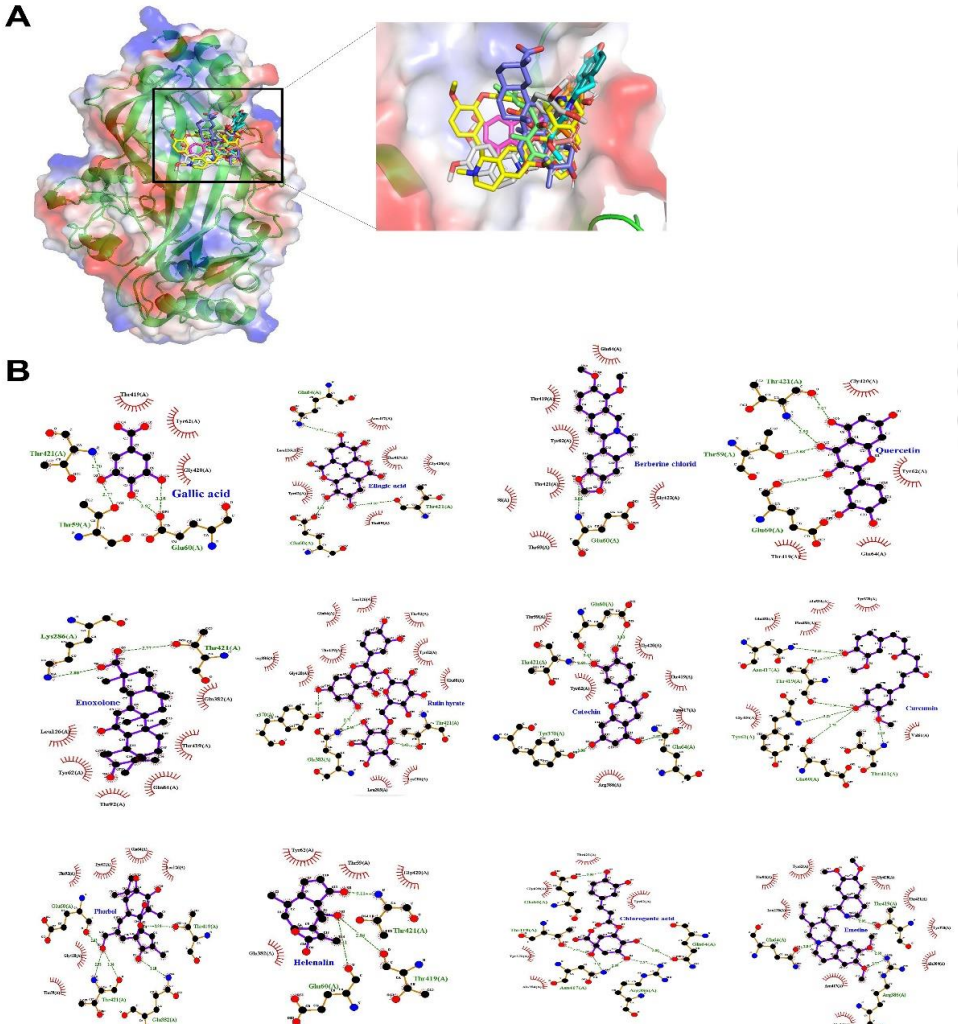

Figure 5.2. Interaction analysis of phytochemical bound CD36. (A) The phytochemical bound complexes were aligned in single model and represented in surface pocket model. Most of the phytochemicals were interacting at similar position (inset). **(B)** The Ligplot+ was used to analyze interactions. All of the phytochemicals were interacting through hydrogen bonding.

5.3.3. Affinity studies of top hit phytochemicals indicates Gallic acid binds with high affinity into CD36 ectodomain

Scavenger receptor CD36 accepts ligands from endogenous as well as exogenous sources (Ramasamy et al., 2012). It has been shown that the endothelial CD36 interacts with the CiDR domain of the PfEMP-1 and mediate tethering which prevents the parasite splenic clearance (Hsieh et al., 2016). Not only the parasite but parasite derived products interact with macrophage and endothelial CD36 and induce pro-inflammatory cytokine secretion which could complicate the host survival (Gowda et al., 2013). Identifying the compounds that could block the parasite derived products interaction with CD36 could be beneficial to host and helps to alleviate the inflammation. The virtual screening of phytochemicals against CD36 suggested that the phenolic category phytochemicals found to be interacting with CD36. Earlier reports have highlighted that phenolic group compounds can be effective against inflammation during malaria (Thrisnadia, 2019). In order to identify the potent CD36 blockers, we have evaluated the affinity of few selected phytochemicals using isothermal titration calorimetry. Based on the binding energy, clusters and conformations a total of 10 molecules were taken further to study their affinity towards CD36 ectodomain using isothermal titration calorimetry. The thermograms of phytochemicals titrated against CD36 suggested the molecule such as Gallic acid strongly interacting with CD36 (Figure 5.3). The Gallic acid interacting with CD36 with high affinity (K_D value 0.32±0.02 µM). The reaction between CD36 and Gallic acid is an exothermic reaction. The thermogram suggests that the Gallic acid interacting with CD36 through hydrogen bonding, hydrophobic interactions and salt bridges. The thermal saturation was observed at fourteenth injection but in subsequent injection showed endothermic peaks. The possible explaination could be either due to protein or ligand dilution or the conformation change in protein induced by the Gallic acid binding to the CD36. Either of the way the ITC data conclusively suggests the Gallic acid interacting with purified CD36 ectodomain. The alkaloid Berberine chloride or (-)-Catechin or (-)-Epicatechin gallate are not binding to CD36. The list of phytochemicals screened and their K_D values are enlisted in (Figure 5.3) and (Table.5.2).

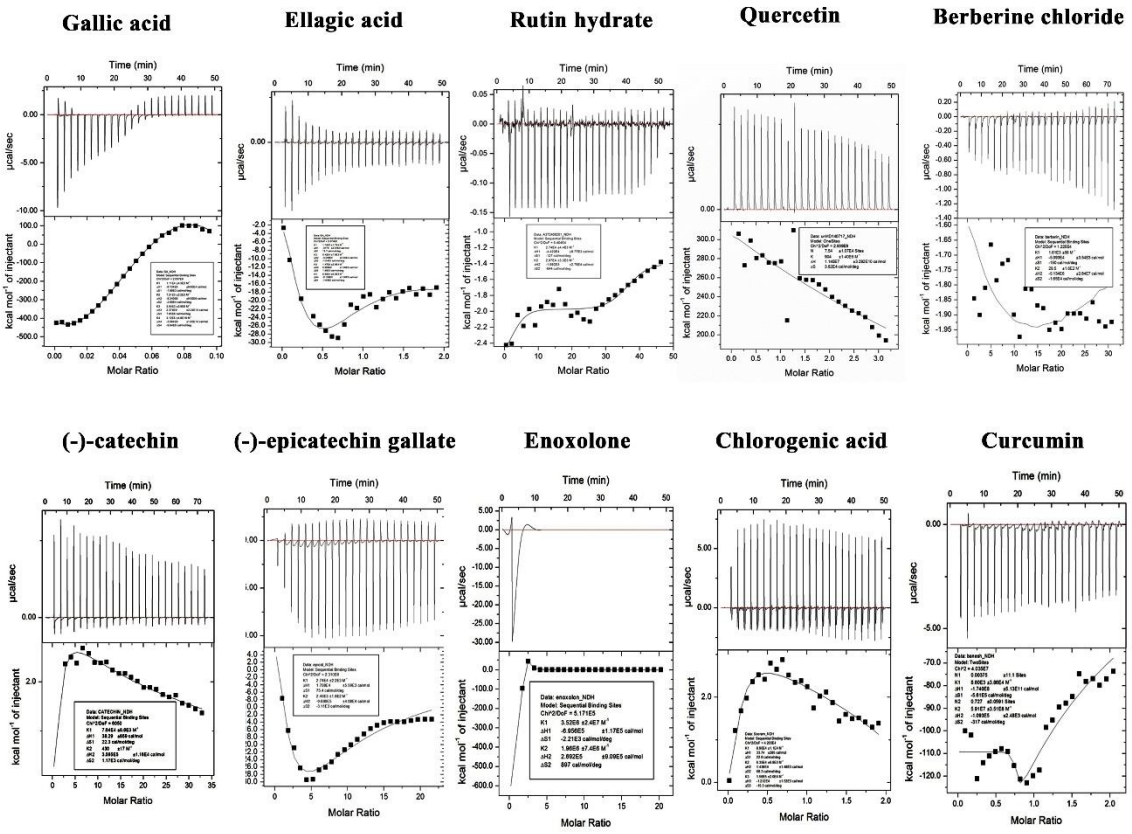

Figure 5.3. Phytochemicals binding studies with purified CD36 ectodomain. All of the titration performed at 37 ^{o}C in a MicroCal ITC200 calorimeter. Typically 20 injections were recorded and plotted in Origin 7 software. Gallic acid interacting with CD36 with high affinity whereas other phytochemicals such as ellagic acid, rutin hydrate, quercetin, berberine chloride, (-)-catechin, (-)-epicatechin gallate, enoxolone, chlorogenic acid and curcumin were shown no binding with CD36.

Table 5.2. Affinity constants of phytochemicals titrated aginst CD36 ectodomain

S.No.	Phytochemical	Affinity constant, K_D (µM)	Inferencce
1	Gallic acid	0.32±0.02	Strong binding
2	Ellagic acid	5.7±0.158	Moderate binding
3	Quercetin	106.3±0.7	Low binding
4	Rutin hydrate	336.4932±2.72	Low binding
5	Enoxolone	500±0.041	Low binding
6	Chlorogenic acid	5000±6.41	No binding
7	Berberine chloride	>10000	No binding
8	(-)-catechin	>10000	No binding
9	(-)-epicatechin gallate	>10000	No binding
10	Curcumin	16005±0.0002	No binding

5.3.4. The phytochemical Gallic acid interacts with CD36 ectodomain and blocks hemin binding

The CD36-Gallic acid molecular model indicated the Gallic acid binds in hemin binding pocket but we do not know whether this binding effectively blocks the hemin binding region. To ascertain, the purified human CD36 ectodomain pre-incubated with Gallic acid and titrated with hemin to see still hemin be able to interact with CD36. Surprisingly, the Gallic acid prevented binding of hemin to CD36 as the K_D value calculated was found 116±2.68 µM (Figure 5.4A) whereas the affinity of CD36 towards hemin is (1.26±0.24 µM). Further, hemin alone was titrated against Gallic acid alone to confirm the changes observed are coming from the specific interaction between Gallic acid and CD36 ectodomain. Further, to check whether hemin biophoric mutants effect the Gallic acid affinity towards CD36, the ITC studies were performed on purified hemin biophoric mutants (R292A, D372A or Q382A). We hypothesized that, Gallic acid occupying hemin binding site and blocking the hemin biophoric residues to interact with hemin. The purified mutants titrated with Gallic acid and resulting thermograms analysed for binding sites saturation. The heat profiling of R292A titrated with Gallic acid indicates complete saturation of binding sites. The molar ratio indicates that the Gallic acid binding to R292A at 1:1 ratio (Figure 5.4B). The data fitted into binding site model and the affinity constant was calculated. The K_D value for R292A was found to be 0.86±0.05 µM. The R292A mutation does not changed the affinity of Gallic acid towards CD36 significantly. The mutants D372A and Q382A titrated with Gallic acid did not show any significant binding as evident from the thermograms (Figure 5.4C and 5.4D). A dot blot assay was performed using CD36 wildtype or mutants. A strong signal was observed in Wildtype incubated blot but the signal intensity was reduced in R292A or D372A. The complete loss of signal was observed in Q382A mutant. The dot blot results further confirms the ITC observations (Figure 5.4E). In an ideal condition the residue R292 does not affect the binding of gallic acid but mutation in Q382 residue may alter the binding. The complete loss of binding upon Q382A mutation possibly the change in native environment of gallic acid binding pocket.

5.3.6. Gallic acid forms stable complex with CD36:

It was evident from ITC that the Gallic acid interact with CD36 ectodomain. We want to investigate the dynamics of Gallic acid interaction with CD36. A standard 10 ns molecular dynamics simulations was performed on CD36-Gallic acid complex in aqueous solvent to

TH-2507_156106009

evaluate stability. The RMSD, RMSF and Rg were used as stability markers. The RMSD of the Gallic acid bound CD36 showed fluctuation at 2 ns simulation trajectory but eventually stabilized. The initial fluctuation in RMSD could be the conformation change in the protein in bound state. The average RMSD value throughout the simulation was found to be 0.62 nm and suggests the stable bonding between CD36 and Gallic acid (Figure 5.5A). Besides, the CD36-Gallic acid complex analysed for structural fluctuation and packing of the protein during the simulation using radius of gyration.

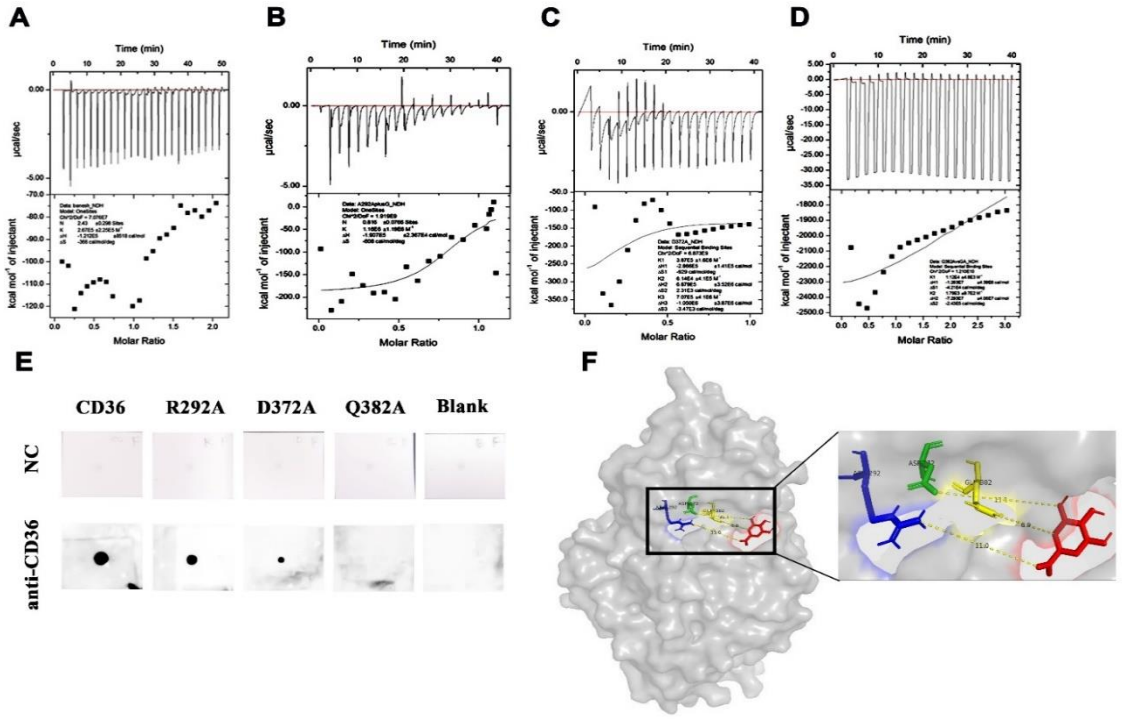

Figure 5.4. Gallic acid interacts with hemin biophoric residues on CD36. (A) The hCD36ecto pre-incubated with Gallic acid titrated with Hemin. The hemin failed to show significant binding with CD36. **(B)** R292A mutant titrated with Gallic acid. **(C)** D372A mutant titrated with Gallic acid. **(D)** Q382A mutant titrated with Gallic acid. **(E)** The dot blot assay of CD36 and mutants. The sever reduction in D372A affinity towards Gallic acid was observed whereas Q382A completely unable to interact. **(F)** The distance of Gallic acid to hemin biophoric residues.

The average Rg value of CD36 found to be 2.177 nm and indicates the overall shape and compactness of protein unchanged upon ligand binding (Figure 5.5B). Further, the Gallic acid atomic fluctuation during simulation was enumerated using RMSF value. The average RMSF value for Gallic acid was found to be 0.03 nm during simulation. The average RMSF value reveals the stability of Gallic acid bound to CD36 (Figure 5.5C). The molecular interaction analysis of Gallic acid bound CD36 suggested that the Gallic acid interact with the hydrophilic residues through hydrogen bonding and hydrophobic

TH-2507_156106009

interactions. The trajectories were analysed for hydrogen bonds through the simulation and their relative occurrence during simulation was plotted. Throughout the simulation Gallic acid interacted with CD36 through one hydrogen bond only with 65.65% of occurrence. The % of occurrence of 2, 3 or 4 hydrogen bonds are 5%, 4% and 1% respectively (Figure 5.5D). The MD simulation data indicates the relative stability of Gallic acid bound to CD36.

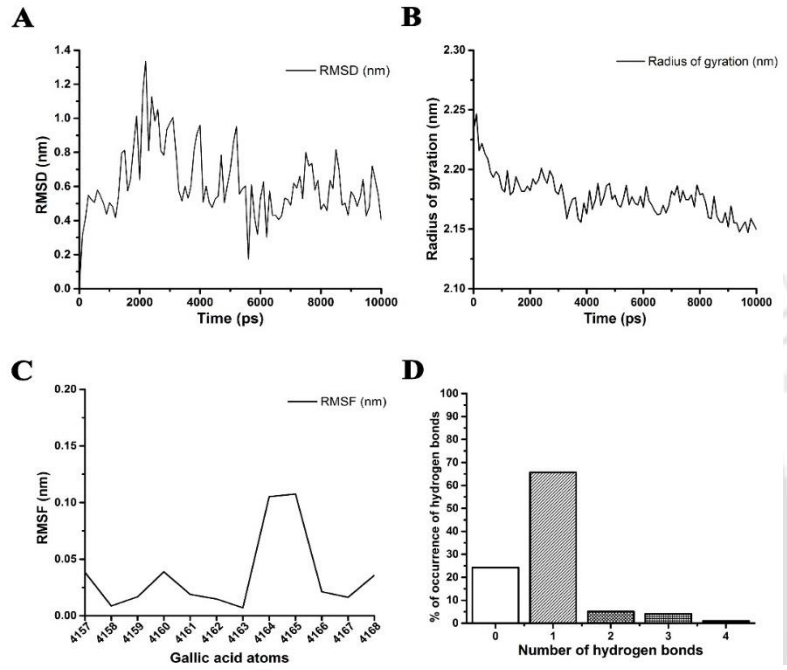

Figure 5.5. Gallic acid forms stable complex with CD36. A 10 ns molecular dynamics simulation was performed on Gallic acid-CD36 complex and the resulted trajectories were analyzed for **(A)** Root mean square deviation, **(B)** Radius of gyration, **(C)** Root mean square fluctuation of Gallic acid atoms, and **(D)** Hydrogen bonds statistics. The result indicates the Gallic acid bound to CD36 is stable.

5.3.7. Gallic acid pre-incubation corrects the phagocytic depression of macrophages by acting through non-opsonic phagocytic receptor CD36

The macrophages stimulated with heme show treated with hemin shows abnormal phagocytic behaviour. Further, the 25 µM hemin enhancing phagocytosis by 20% compared to control and subsequent hemin concentrations abolishing the activity to near zero levels. Our studies confirmed that the hemin interacts with non-opsonic phagocytic receptor CD36 and modulates the phagocytosis. The non-availability of CD36 on membrane renders the reduced phagocytic activity of macrophages. Since, the Gallic acid pre-incubation preventing the hemin interaction with CD36 and reducing CD36 sequestration there is possibility that Gallic acid can bring the phagocytic activity to

normal levels. The macrophages pre-incubated with 1, 5 or 10 µg/mL of Gallic acid and treated with 25, 75 and 200 µM concentrations of hemin. The phagocytic activity is evaluated using FITC labelled bacteria in a flow based assay. The phagocytic activity of 25 µM hemin treated macrophages increased several folds (phagocytic index (PI), 265%) when compared to untreated cells (PI, 81%) whereas in 10 µg/mL Gallic acid pre-incubated reduced to normal (PI, 75%) (Figure 5.6A). Further hemin treatment with 75 µM or 200 µM hemin significantly lowered the phagocytic activity but in Gallic acid pre-treated macrophages showed normal levels of phagocytic activity (Figure 5.6A). CD36 detects the infected RBCs and responsible for non-opsonic phagocytosis of iRBCs. The macrophages treated with hemin showed differential response toward oxidized or normal RBCs. Here oxidized RBCs were used to mimic infected RBCs. In 25 µM hemin treated condition, the phagocytosis of NRBC was also observed along with oxidized RBC (Figure 5.6B). The macrophages treated with gallic acid showed phagocytosis of oxiRBC but not NRBC (Figure 5.6B). The gallic acid pre-incubated macrophages treated with hemin phagocytic activity towards NRBC reduced significantly whereas the oxiRBC phagocytosis is unaffected and similar to untreated cells oxiRBC uptake (Figure 5.6A).

5.3.8. Gallic acid protects the macrophages from hemin mediated inflammatory responses

Gallic acid is a phenolic compound available in fruits and tea leaves. Gallic acid has antioxidant and anticancer properties along with various industrial applications. The affinity studies suggested that Gallic acid blocks the hemin binding region on CD36 and reduces the hemin mediated CD36 sequestration into intracellular vesicles. The CD36 sequestration into cytosol and inability to recycle back onto membrane is responsible for the uncontrolled TNF-α secretion in macrophages. Here we particularly interested in whether Gallic acid pre-treatment reduces the TNF-α levels in hemin treated macrophages. The macrophages pre-incubated with 10 µg/mL Gallic acid and treated with hemin (200 µM) showed 80 pg/mL TNF-α levels whereas only hemin (200 µM) treated macrophages showing 700 pg/mL (Figure 5.7). Although the lower Gallic acid concentrations (1 or 5 µg/mL) pre-incubated-macrophages showed reduced levels of TNF-α (300 pg/mL or 100 pg/mL respectively) still the levels are slightly higher side (at 200 µM hemin) (Figure 5.7). The results highlights the Gallic acid as a protecting agent from hemin induced pro-inflammatory cytokine secretion. Conversely, the cells treated with Gallic acid only showed slightly higher levels of cytokine compared to untreated macrophages. This study

shows Gallic acid can be used in to correct CD36 mediated immune dysfunction in macrophages.

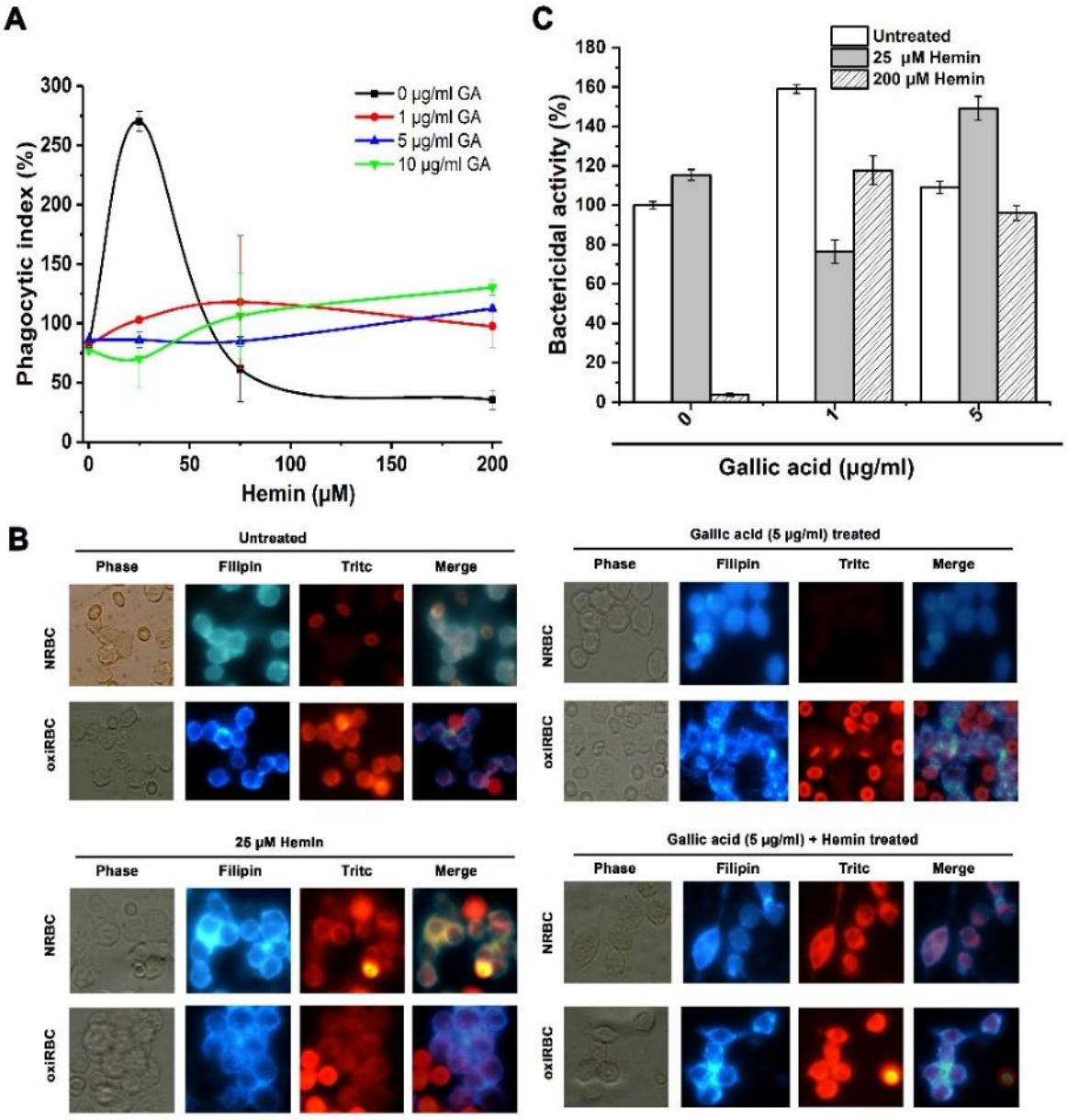

Figure 5.6. Gallic acid rescues macrophages from immune dysfunction. **(A)** The macrophages pre-treated Gallic acid for 1 h and treated with Hemin. The phagocytic activity of macrophages was treated with hemin showed depression in activity at 200 μM Hemin wheras 10 μg/ml Gallic acid pre-incubated macrophages showing normal phagocytic behavior. **(B)** The macrophages after treatment was incubated with normal RBC or oxiRBC. The Gallic acid pre-incubation restored the oxiRBC phagocytosis. **(C)** The bactericidal activity of macrophages was evaluated. The Gallic acid treatment restored the bactericidal activity of macrophages.

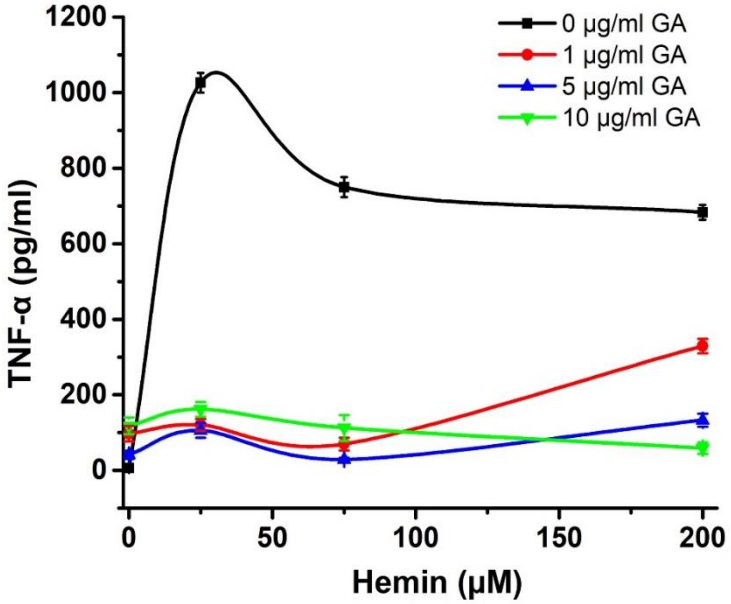

Figure 5.7. Gallic acid pre-incubation reduces TNF-α pro-inflammatory cytokine levels in macrophages treated with hemin. The macrophages pre-incubated with Gallic acid (1, 5, 10 µg/ml) for 1 hr and washed gently. Following incubation with Hemin for 1 hr the cells were washed and allowed to secrete cytokines overnight. The Hemin only treated macrophages showed very high levels of TNF-α whereas macrophages with Gallic acid pre-incubation levels were reduced significantly.

5.4. Discussion and future prospective

The nature is source of millions of molecules and provide rich repertoire for drug discovery process. The advantage of natural compounds are their wide availability and cost is low. Several of currently FDA approved drugs such as quinine, artemisinin, taxol, apomorphine and arteether came from the natural resources (Choudhari et al., 2020). The key objective of this study is to identify suitable CD36 interaction blockers from natural resources and study their utility in mitigating the immune dysfunction caused due to CD36 pathological ligands (Yamashita et al., 2007). We have identified hemin as a potential ligand from scavenger receptor CD36 (Chapter-IV). The CD36 is also involved in recognition of malaria parasite through CiDRα domain of PfEMP1. The CD36 and hemin interaction contributes to the phagocytic depression and pro-inflammatory cytokine secretion. Along with other factors, CD36-hemin interaction is also contributes pathology associated with malaria.

The modified low density lipoproteins uptake by macrophages through CD36 is implicated in vascular inflammatory diseases (Bieghs et al., 2012). The salvianolic acid b a phytochemical from Salvi miltirrhiza roots has been found to be effective in blocking the mLDL uptake by macrophages (Bao et al., 2012). The salvianolic acid B directly binds to

the CD36 and reduces oxiLDL induced CD36 gene expression. The phytochemical has been tested as anti-atherosclerotic agent (Bao et al., 2012). The ursolic acid a triterpenoid compound distributed pervasive in plant species (Cargnin and Gnoatto, 2017). The interactions of amyloid beta with CD36 promotes disease progression and severe pathological outcome during alzheimers. The ursolic acid blocks the amylod beta and CD36 interactions and prevents the pro-inflammatory cytokine secretion (Wilkinson et al., 2011). In pursuit of identifying CD36-hemin interaction blockers, we have screened compounds from phytochemical database against hemin biophore. The screening exercise provided thirty five top hit phytochemicals. Based on the availability and cost factors, we have chosen ten molecules to perform binding studies with purified CD36. The ITC based binding study has identified the phytochemical Gallic acid interacting with CD36 with high affinity.

Further ITC based binding experiments suggested the Gallic acid could be a potential CD36-hemin interaction blocker. This could be the first such report where Gallic acid reported to bind to the macrophage CD receptors. The gallic acid previously tested for antimicrobial, anticancer, anti-inflammatory, and antioxidant properties (Kahkeshani et al., 2019). Earlier studies shown that gallic acid targets G-protein coupled receptor 35 (Deng and Fang, 2012). Our study conclusively suggests the gallic acid can also binds to CD36 and modulate the inflammatory response in pathological condition. Concurrent with previous reports the gallic acid was found to be modulating the immunological response of macrophages. The hemin treated macrophages showed phagocytic depression toward bacteria and oxiRBC. The macrophages pre-incubated with gallic acid treated with hemin showed normal phagocytic behaviour. On macrophages CD36 is crucial for phagocytosis of pathogens or endogenous debris (Baranova et al., 2008). The gallic acid mediated improvement of phagocytic activity further supports the gallic acid binds to CD36. The observed results are in agreement with gallic acid conjugate enhances phagocytic activity of macrophages. The molecule further taken up for animal studies to verify the findings.

References: Please refer to the Bibliography section at the end of the thesis.

Chapter-VI

Meropenem reduces CD36 down-stream Immune responses in malaria like conditions.

TH-2507_156106009

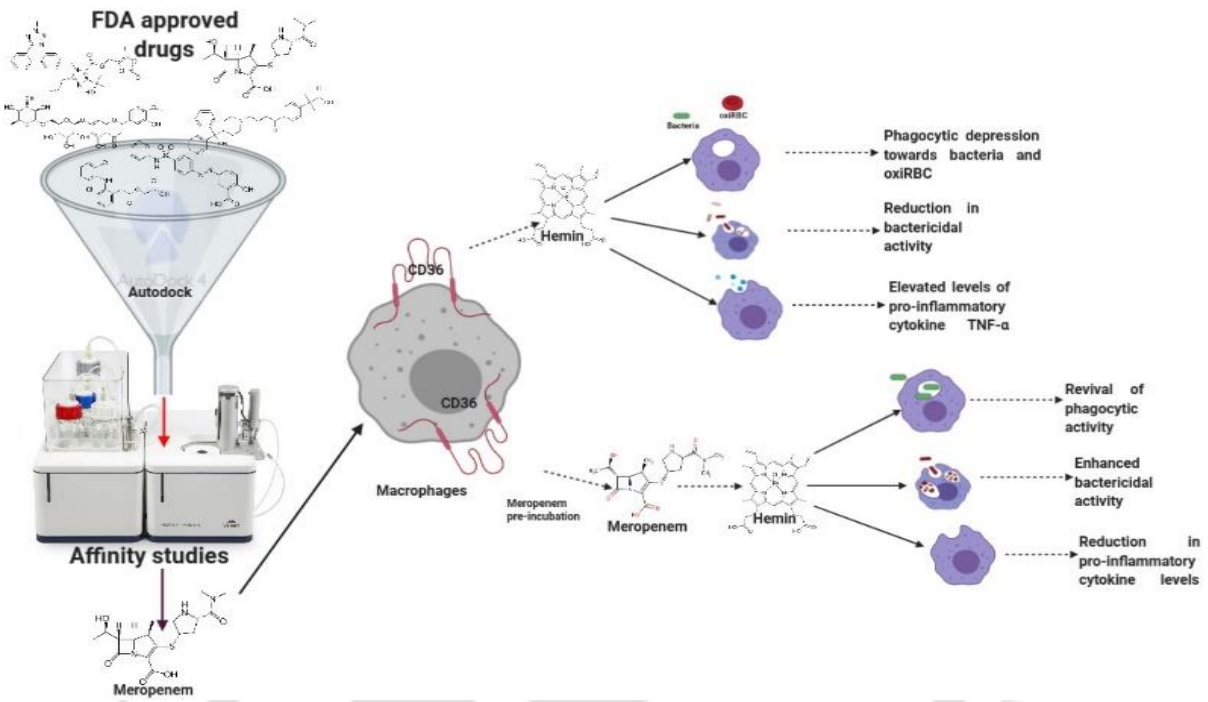

Summary

In this chapter we have screened compounds from FDA approved drug database against CD36. The virtual screening suggested several hits belongs to the NSAIDS, antibiotics, anti-diabetic drugs, anti-histamines and steroidal drugs. The selected top nine molecules were studied for their affinity towards CD36 ectodomain using isothermal titration calorimetry. The FDA approved drug meropenem, a broad spectrum antibiotic interacting with CD36 with high affinity. Further, the dot blot assay suggested meropenem interact with hemin biophoric mutants as well. The meropenem pre-incubation restored phagocytic activity of macrophages, improved bactericidal activity and reduced pro-inflammatory cytokine TNF-alpha levels. The re-purposing of this drug during malaria could be beneficial and reduce pathological burden in human.

Key words: Approved drugs, database, inflammation, immune dysfunction, malaria like condition.

6.1. Introduction:

The FDA drug database has over ~2000 compounds approved including heterocyclic (Chen et al., 2011). The cost of developing one drug from identification to marketing takes over 20 years and costs millions of dollars. The drug re-purposing is beneficial and could save time and money (Morgan et al., 2011). The advantage of the FDA approved drugs re-purposing is the availability of in-vitro and in-vivo assessment, toxicity analysis and pharmacokinetic information (Pushpakom et al., 2019). It is very challenging to find a new drug to treat a disease because of the right efficacy, safety and toxicity of the new compound may not be consistent with the needs (Mahajan and Gupta, 2010). Further, the lack of funding in academia to invent new therapeutics mostly contributes the drug-repositioning (Tralau-Stewart et al., 2009). In last few decades researchers are trying to test the FDA approved drugs for alternative diseases and even re-positioned for new disease treatment also. The drug Sildenafil, a phosphodiesterase 5 inhibitor initially approved for the treatment of angina but later it was re-purposed for the treatment of erectile dysfunction (Pushpakom et al., 2019). The anti-fungal drug Itraconazole and its utility in anticancer therapy has shown promising and could be employed in treatment (Boogaerts et al., 2001). Recent approval of anti-Ebola drug Remedsivir to use in humans to treat Covid-19 is an example for drug repurposing (Beigel et al., 2020).

The scavenger receptor CD36 involved in protection and pathology during infectious and non-infectious diseases (Banesh and Trivedi, 2020). The receptor facilitates the removal of apoptotic cells, cell debris and pathogens from systemic circulation (Albert et al., 1998). The scavenger receptor detects the gram positive and gram negative bacterial cell wall components, PfEMP-1 expressing IRBC and oxidized RBC and induce pro-inflammatory cytokine secretion (Stewart et al., 2010). During malaria like condition very high amount of heme released and the levels of heme correlating with severity of inflammatory cytokine levels (Ferreira et al., 2008). In chapter-IV we have showed that hemin acts as a ligand for scavenger receptor CD36. The macrophages treated with hemin showed abnormal phagocytic behavior, reduced bactericidal activity and secretion of very high levels of pro-inflammatory cytokine TNF-α.

In this chapter we have explored FDA approved drugs as a potential CD36 blockers and their utility in mitigating macrophage dysfunction mediated by CD36. The refined, and curated

TH-2507_156106009

FDA approved drugs screened against CD36 using Autodock tools1.5.6. The docking log file analyzed for clusters, conformations and binding energy and saved the best pose. The best pose was analyzed for molecular interactions using ligplot+. The top hits were taken further to study affinity towards purified CD36 ectodomain. The isothermal titration calorimetry binding studies suggested the meropenem a broad spectrum antibiotic binding to CD36 comparing to other FDA approved drugs. Initially, we have tested whether meropenem is competiting with hemin. In ITC based assay the purified CD36 ectodomain pre-incubated with meropenem and titrated with hemin. In addition the meropenem also titrated against the hemin biophoric mutants. The affinity studies indicates meropenem pre-incubation reduced the affinity of hemin towards CD36 though it was not significant. All of the mutants showing binding towards meropenem as it is evident from dot blot assay. The conclusion from the binding studies is the meropenem not interact in hemin biophoric region rather it is different from it. Further, to investigate meropenem for its immuno protective roles, the macrophages pre-incubated with meropenem and treated with hemin. The meropenem treatment significantly restored the phagocytic and bactericidal activity of macrophages. The main concern of CD36 mediated immune dysfunction in macrophages is the secretion of pro-inflammatory cytokines such as TNF-α. The meropenem pre-incubation effectively reduced the TNF-α secretion from macrophages. The study highlights the meropenem as a ligand for CD36 and its utility in mitigating immune dysfunction in macrophages.

6.2. Experimental procedures

6.2.1. Collection and curation of compounds from FDA approved drug database: The FDA approved drugs were obtained from the drug bank (https://www.drugbank.ca/) in a single SDF file format and an excel format. The peptide or protein approved therapeutic molecules and the salts or ions were removed from the list. The molecules from the single SDF file was converted and extracted to individual 3D structure (.mol2) files using openbabel software (http://openbabel.org). The 3D structures with fragmentation were refined and used for molecular docking study. A total of 2143 drugs were taken up for the virtual screening study.

6.2.2. Virtual screening of the FDA approved drugs against CD36: The molecular docking was performed as described in Chapter-II, Experimental procedures 2.2.11 section, page no.58.

6.2.3. Binding studies of top hits with CD36 ectodomain: The affinity studies were performed as described in Chapter-II, Experimental procedures 2.2.8 section, page no.57.

6.2.4. Phagocytosis assay: The phagocytosis assay was performed as described in Chapter-IV, Experimental procedures 4.2.3 section, page no.99.

6.2.5. Bactericidal assay: The bactericidal assay was performed as described in Chapter-IV, Experimental procedures 4.2.4 section, page no.99.

6.2.6. Estimation of TNF-α secretion: The secreted TNF-α was estimated as described in Chapter-IV, Experimental procedures 4.2.8 section, page no.101.

6.3. Results

6.3.1. The NSAIDS, antibiotics and steroidal heterocyclic compounds from FDA approved drug bank fits well into hemin binding pocket on CD36

The new drug development and institute it into healthcare system as a treatment regimen is time consuming and required huge financial input (Adams and Brantner, 2006). By searching better therapeutic molecules from FDA drug database for a different disease or disorder proven to save money and time. Decades of research on scavenger receptor CD36 suggested its role in immune dysfunction and pathology. Various research group's targeted CD36 using heterocyclic molecules and proven to be beneficial in treating inflammation during atherosclerosis. In chapter IV we have identified hemin as a ligand for CD36 and modulates the macrophage response during malaria like condition. By targeting hemin binding region on CD36 may useful to reduce inflammation and immune dysfunction in macrophages. In pursuit of identifying suitable CD36 blockers, we have screened compounds from FDA approved drug bank against CD36. The compounds were sorted based on binding energy, clusters and conformations. The virtual screening indicated that most of the hit compounds were belongs NSAIDS, antibiotics, anti-diabetics, anti-cancer and drugs used in metabolic disorders (Table 6.1). The binding of such a diverse structural compounds could be due to CD36 has a large ligand repertoire with structural diversity.

TH-2507_156106009

Table 6.1. Top FDA approved drugs and their in-silico binding energies towards CD36			
S.No.	**Name of the drug**	**Binding energy (Kcal/mol)**	**Clusters**
1	Methyltestosterone	-8.8	4
2	Natamycin	-8.57	4
3	Rimexolone	-8.34	2
4	Aceclofenac	-8.31	3
5	Tixocortol	-8.17	8
6	Eplerenone	-8.15	4
7	Medroxyprogesterone acetate	-7.99	8
8	Cefonicid	-7.94	65
9	Ibrutinib	-7.86	9
10	Megestrol acetate	-7.8	7
11	Dolasetron	-7.78	2
12	Medrogestone	-7.7	4
13	Etonogestrel	-7.69	4
14	Sulfasalazine	-7.64	25
15	Diphenidol	-7.62	15
16	Artemether	-7.62	5
17	Rolitetracycline	-7.59	3
18	Ulobetasol	-7.55	11
19	Mometasone	-7.54	8
20	Atovaquone	-7.5	4
21	Dabrafenib	-7.47	30
22	Dutasteride	-7.47	8
23	Cocaine	-7.43	11
24	Dihydrotachysterol	-7.42	9
25	Cyproterone acetate	-7.41	3
26	Calcitriol	-7.41	15
27	Norelgestromin	-7.4	8
28	Olmesartan	-7.31	13
29	Nandrolone phenpropionate	-7.31	7
30	Flurandrenolide	-7.31	7
31	Ergoloid mesylate	-7.23	6
32	Gestodene	-7.22	2
33	Diosmin	-7.18	51
34	Ergonovine	-7.18	11
35	Fluprednidene	-7.17	10
36	Meropenem	-7.17	13
39	Norethisterone	-7.15	3
40	Empagliflozin	-7.14	32
41	Tibolone	-7.14	3
42	Fexofenadine	-5.64	25
43	Mesalazine	-4.21	15

6.3.2. Meropenem, Mesalamine and Sulfasalazine interacts with CD36 through hydrogen bonding and hydrophobic interactions

The drug-CD36 complexes from best pose were analyzed for molecular interactions using ligandplot+. The binding site of the drugs overlaid and presented in (Figure 6.1A). Most of the top hits binding at same region on CD36. The mesalamine used in treatment of inflammatory bowel disease is showing very strong hydrogen bond network with the CD36. The OG1 atom of residue T59 forming hydrogen bond with O2 of mesalamine and the distance of hydrogen bonding is 2.74 Å (Figure 6.1B). The T421 residue forming three hydrogen bonds with O2 and O1 atoms of mesalamine and the average hydrogen bond distance was found to be 2.69 Å. Similarly E60 is also involved in hydrogen bonding with mesalamine. A total of seven such hydrogen bonds were found in Mesalamine-CD36 complex. The other top hits such as sulfasalazine, diosmin and meropenem were interacting through hydrogen bonding and hydrophobic network. The residues T419, T421 and E60 were interacting with meropenem through hydrogen bonding with an average donor-acceptor distance of 2.91Å (Figure 6.1B). It was established that the protein-ligand binding affinity is largely regulated by the hydrogen bonding network (Chen et al., 2016). So it was expected to see binding between the molecules with high hydrogen bonding network. The NSAID aceclofenac is not participating in any hydrogen bonding rather involved in hydrophobic interactions with E60, Y62, T419, G420, and T421 residues. Similarly the other top compounds empagliflozin, fexofenadine and olmesartan were also involved in hydrophobic interactions but not hydrogen bonds (Figure 6.1B).

6.3.3. The broad spectrum antibiotic Meropenem has high affinity towards CD36

The criteria for selecting the FDA approved drugs for binding studies is the binding energy, clusters, conformations, availability of drug and cost factor. The drugs that are steroidal in nature were excluded from the binding studies although they are showing prominent binding energy. The drugs aceclofenac, diosmin, empagliflozin, fexofenadine, mesalamine, meropenem, natamycin, olmesartan and sulfasalazine were studied using isothermal titration calorimetry (Figure 6.2). The ITC study was performed as described in experimental procedures. Out of the nine drugs studied, only meropenem was found to be binding to CD36 ectodomain very strongly. The K_D value calculated for meropenem-CD36 complex was found to be, 0.402 ±0.0002 μM) (Figure 6.2A).

TH-2507_156106009

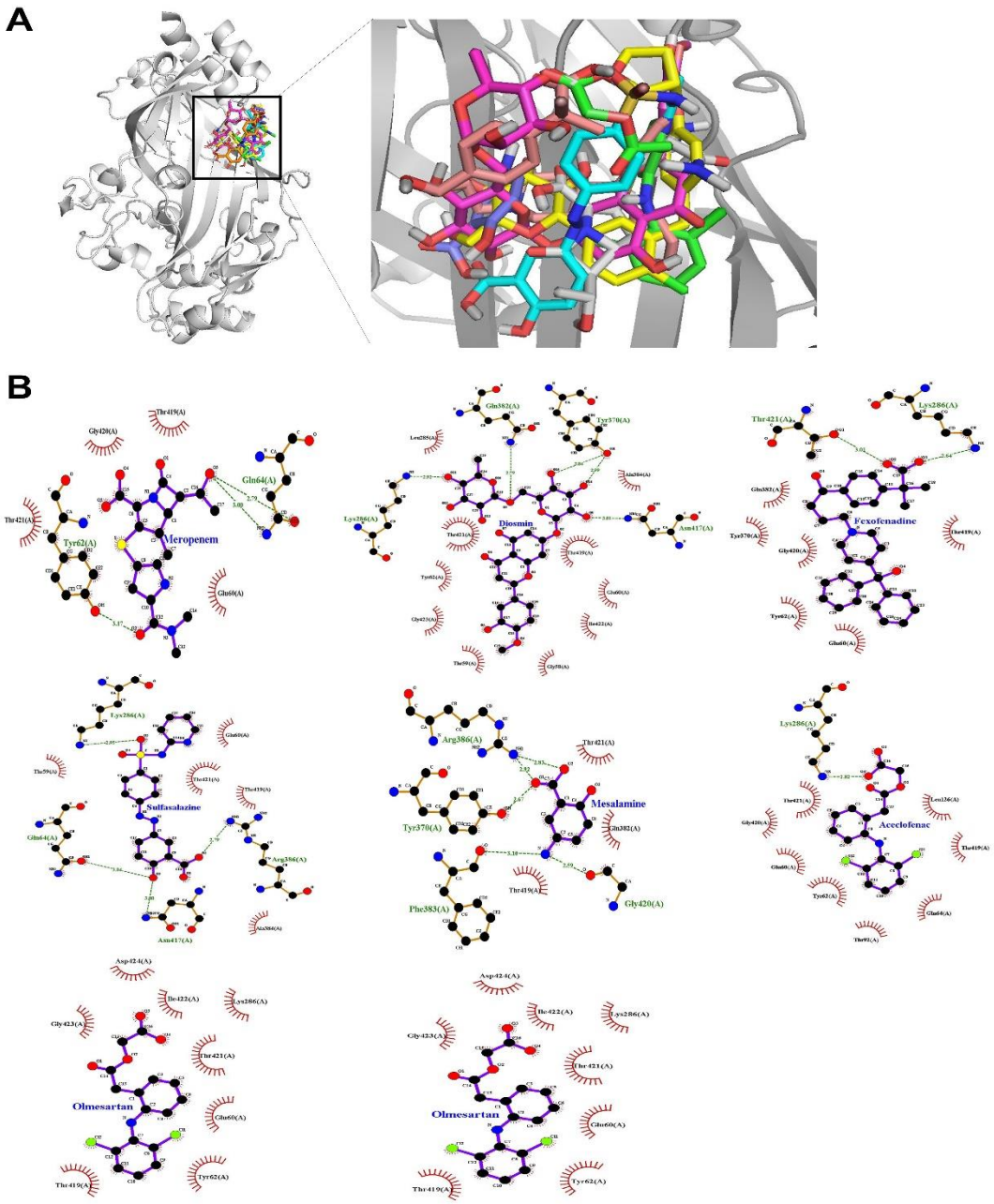

Figure 6.1. FDA approved drugs interaction with CD36. **(A)** The overlay of drugs binding position on CD36. **(B)** The drug bound CD36 complexes analysed for interactions using ligplot+. Mesalamine, meropenem, sulfasalazine were showing hydrogen bonding with CD36 whereas aceclofenac, olmesartan and empagliflozin showing only hydrophobic interactions.

The binding of meropenem with CD36 is an exothermic reaction as evident from the thermogram. An in-depth evaluation of heat profile values suggests the reaction between

CD36 and meropenem is largely mediated through hydrogen bonding and hydrophobic interactions. The findings are in agreement with the CD36-meropenem interaction presented in previous section. The meropenem is a hydrophilic molecule with carboxylic group, hydroxyl and keto groups. The CD36 ectodomain has two tunnel like domains to accommodate hydrophobic ligands and the apex domain is more hydrophilic regions. When we see in this perspective it is not surprising the meropenem interacts with CD36. The interaction analysis suggested mesalamine has a very good hydrogen bond network with the CD36. Contrary to in-silico findings the mesalamine failed to show the binding with CD36 (K_D, 1197.37±11 μM) (Figure 6.2B). The other drug diosmin also failed to bind the CD36 as the calculated K_D value is very high (K_D , 156±5 μM). The other tested compounds are also did not show efficient binding to CD36 (Table 6.2).

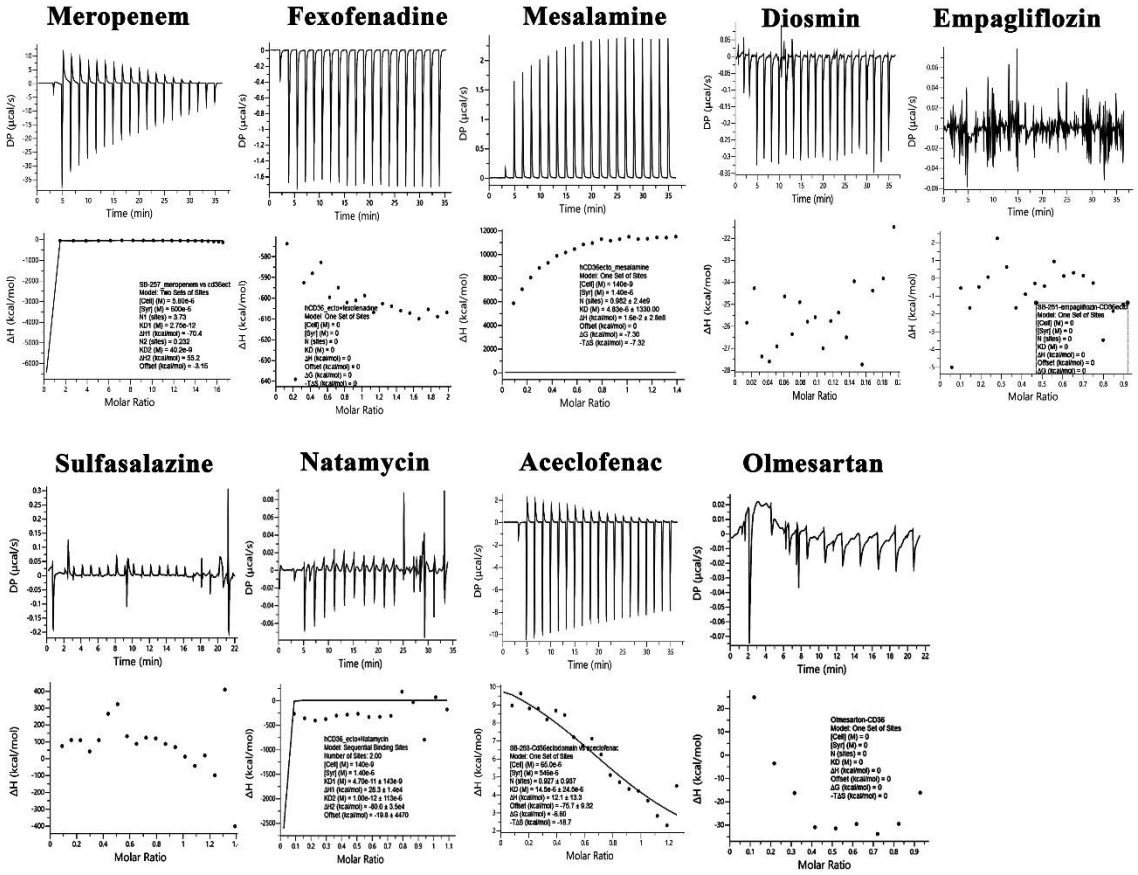

Figure 6.2. Affinity studies of selected FDA approved drugs with CD36 . (A) Meropenem interact with CD36 with high affinity. **(B)** The ITC thermograms of fexofenadine, mesalamine, diosmin, empagliflozin, sulfasalazine, natamycin, aceclofenac and olmesartan.

Table 6.2. Affinity of selected FDA approved drugs towards CD36			
S.No.	**Name of the drug**	**Affinity constant, K_D (µM)**	**Inference**
1	Meropenem	0.402 ±0.0002	Strong binding
2	Natamycin	143±0.047	Weak binding
3	Aceclofenac	145±2.18	Weak binding
4	Diosmin	156±5	Weak binding
5	Mesalamine	1197.37±11	Very weak binding
6	Sulfasalazine	>10000	No binding
7	Olmesartan	>10000	No binding
8	Fexofenadine	>10000	No binding
9	Empagliflozin	>10000	No binding

6.3.4. The meropenem binding region on CD36 is different from the hemin binding site.

The affinity studies of FDA approved drugs with purified CD36 ectodomain indicated the meropenem interact with CD36 with high affinity. The hemin modulates the macrophage immune response by interacting with CD36. To ascertain whether meropenem competes for hemin binding region on CD36, the purified CD36 pre-incubated with meropenem and titrated with hemin. In ideal condition the hemin binding to CD36 should be reduced. The ITC thermogram indicates the meropenem pre-incubation reduced the binding of hemin (0.589 ±0.01 µM) although failed to prevent it from binding (Figure 6.3A). The hemin interacts with CD36 in a well-defined region consisting of R292, D372 and Q382 residues. To investigate the mutant's affinity towards meropenem, the purified mutants were titrated with meropenem. The R292A mutant titrated with meropenem showed similar kind of thermogram as that of wildtype (CD36)-meropenem (Figure 6.3B). The affability value of meropenem towards R292A was found to be 11.48 ±1.2 µM which is 28 folds more than the wildtype. The D372A mutant titrated with meropenem showing K_D value 48.5 ±1.3 µM (Figure 6.3C). Similarly, the Q382A titrated with meropenem showed K_D value of 27 ±0.057 µM (Figure 6.3D). The probable reason behind the reduction in affinity towards mutants could be due to their role in positioning meropenem in binding site. Further, to verify these finding we have performed dot blot assay as described in experimental procedures. The relative intensity of each dot was calculated by considering wildtype (CD36) as 100%. For mutants R292A and D372A there is

no significant change in intensity was observed (R292A-93% and D372A-91%). But for mutant Q382A a 20% reduction was observed (Figure 6.3B). The dot blot results are consistent with the ITC analysis.

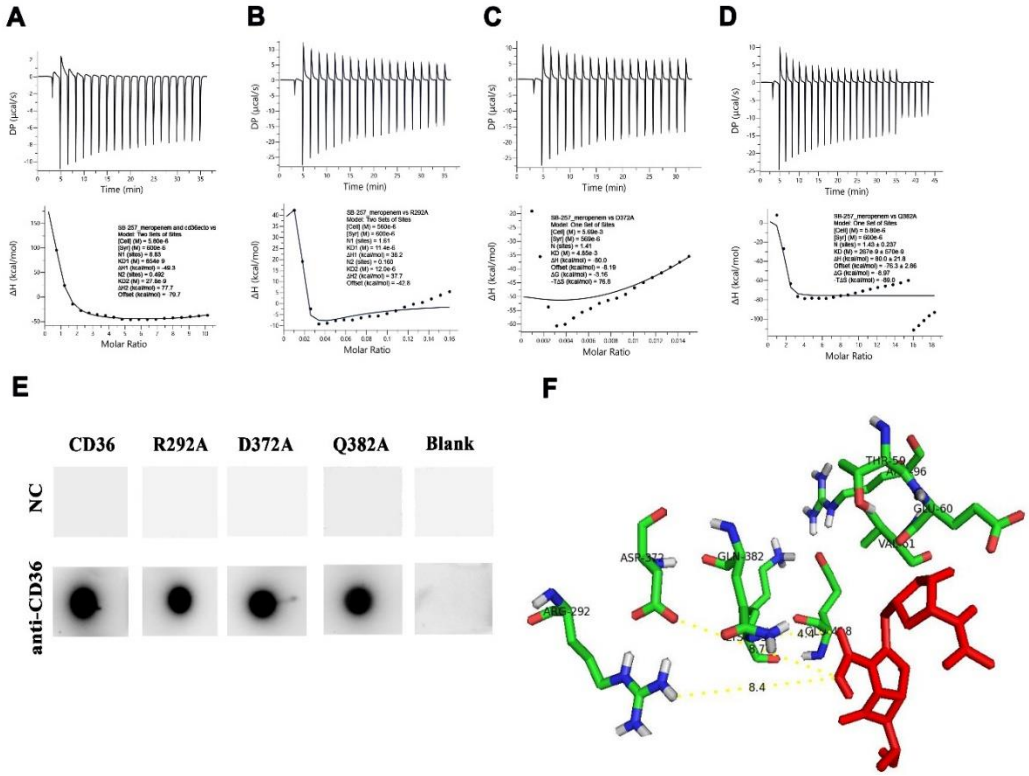

Figure 6.3. Meropenem binding site is different from hemin. (A) Meropenem pre-incubated CD36 titrated with hemin and the ITC thermogram recorded. **(B)** ITC thermogram of meropenem titrated against R292A mutant. **(C)** ITC thermogram of meropenem titrated against D372A. **(D)** The thermogram of Q382A titrated with meropenem. **(E)** The dot blot study of meropenem with wildtype (CD36) and mutants. The dot blot suggests the mutants has no significant role in meropenem binding. (F) The distance of mutants from meropenem binding site. The R292 is 10.5 Å distance from meropenem whereas Q382A is 7.5 Å.

6.3.5. Meropenem enhanced phagocytic activity and bactericidal activity of macrophages

The scavenger receptor CD36 is involved in non-opsonic phagocytosis of dead or aged cells, oxiRBC, and pathogens. The CD36 detects LTA or LPS of bacterial cell wall and mark them for phagocytosis by macrophages. The hemin treated macrophages showed abnormal reduction in phagocytic activity at 200 µM of hemin (Figure 6.4A, subsets b, and Figure 6.4B). We have established that hemin interactions mediated through CD36. Since, the meropenem

TH-2507_156106009

has very high affinity towards CD36, we want to explore whether the, meropenem treated macrophages show any improvement in phagocytic activity. The macrophages treated with 100 µg/ml meropenem showed normal phagocytic activity (PI, 68.14%) (Figure 6.4A, d and Figure 6.4B). The macrophages pre-incubated with 100 µg/ml meropenem and treated with 200 µM hemin showed comparatively higher phagocytic index than macrophages treated with 200 µM hemin alone (Figure 6.4B).

Interestingly, the phagocytic activity is significantly improved in meropenem pre-incubated macrophages treated with 200 µM hemin (Figure 6.4B). It has been shown that meropenem treated human macrophages showed enhanced phagocytosis, however how it modulates the phagocytic activity of macrophages yet to be investigated (Cuffini et al., 1993). Apart from activating CD36 mediated phagocytosis, meropenem also modulates the phagocytic activity of macrophages through unknown mechanism and likely to be reason behind observed enhancement in phagocytic activity.

The hemin treatment severely reduced the bactericidal activity of macrophages. So further we tested the bactericidal activity of macrophages. The macrophages pre-incubated with meropenem and treated with 200 µM of hemin. The bactericidal activity of 200 µM of hemin only treated macrophages showed 50% compared to untreated (100%) (Figure 6.4C) but the meropenem pre-incubated macrophages treated with hemin showed significant improvement. The human macrophages uptake the meropenem and accumulates inside the macrophages. It was shown that the concentration of meropenem is very high inside the cells comparing to external side (Cuffini et al., 1993). The meropenem treated cells showed increased bactericidal activity against Staphylococcus aureus (Cuffini et al., 1993). Owing to the bactericidal properties of meropenem a very high levels of bactericidal activity is expected in the study. The scavenger receptor recognizes PS externalized RBC and facilitate their non-opsonic phagocytosis. The hemin treatment reduced the phagocytic activity of macrophages towards oxiRBC (Chapter-IV). The oxiRBC or IRBC in circulation may trigger the immune response which involves the secretion of pro-inflammatory cytokines. The meropenem pre-incubated macrophages treated with hemin and incubated with NRBC or oxiRBC for 1 h and analysed on flow cytometer. The untreated macrophages showed 6.13% of oxiRBC

TH-2507_156106009

phagocytosis whereas the hemin (25 µM) treated macrophages showed 5.74% and for 200 µM hemin treated macrophages it was 5.76% (Figure 6.5) (Table 6.3).

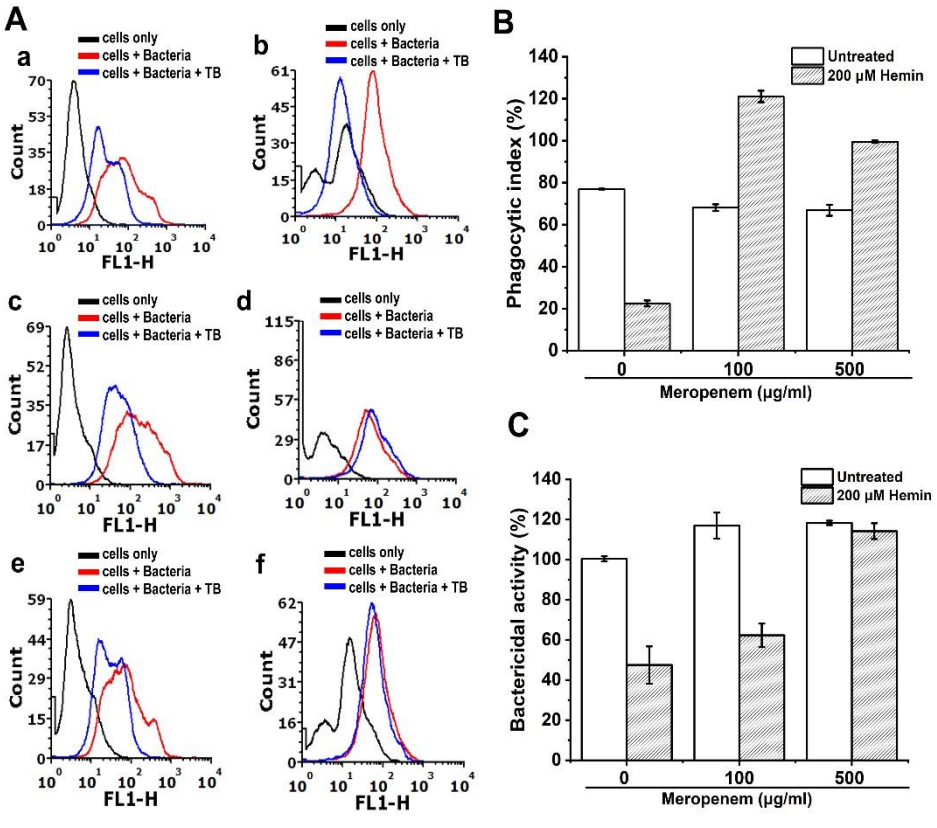

Figure 6.4. Meropenem pre-treatment enhances phagocytic and bactericidal activity of macrophages. (A) Meropenem pre-incubated macrophages treated with hemin and assessed their phagocytic activity as described in experimental procedures. The fluorescence histograms represented. The upper panels shows a) untreated, b) 200 µM hemin treated. The middle panel, c) 100 µg/ml meropenem only, and d) 100 µg/ml meropenem + 200 µM hemin treated. The lower panel, e) 500 µg/ml meropenem only, and f) 500 µg/ml meropenem + 200 µM hemin treated. **(B)** The phagocytic index of hemin treated and meropenem pre-incubated and hemin treated macrophages. The meropenem treatment significantly enhanced phagocytic activity of macrophages. **(C)** Bactericidal activity of macrophages also enhanced in 500 µg/ml meropenem pre-treated macrophages.

The meropenem (100 µg/ml) pre-incubated macrophages treated with hemin (25 or 200 µM) showed reduction in oxiRBC phagocytosis 4.97 and 4.32% respectively (Figure 6.5A, 6.5B). We were expecting the enhanced oxiRBC phagocytosis but conversely we could only see further reduction. The possible explanation could be meropenem binding to CD36 is not dependent on hemin binding region.

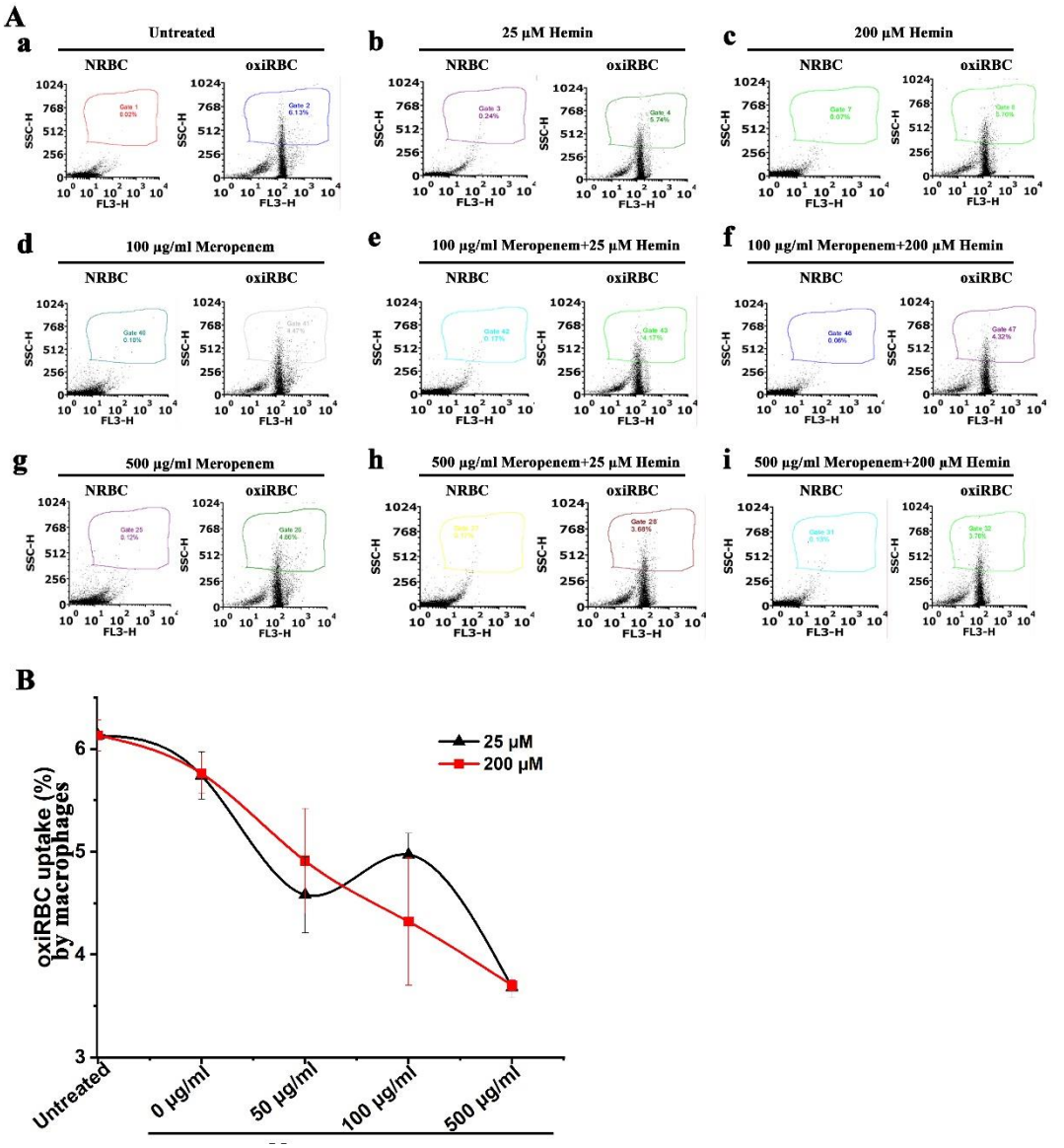

Figure 6.5. Meropenem pre-treatment reduces oxiRBC uptake by macrophages. (A) The macrophages pre-incubated with meropenem (100 or 500 µg/ml) and treated with hemin (25 or 200 µM). After treatment the cells were incubated with NRBC or oxiRBC for 1 h. The cells were washed and analysed on BDFACS flow cytometer. The untreated NRBC istaken for gating and applied to remaining plots. The untreated **(a)**, 25 µM hemin treated **(b)** and 200 µM hemin treated **(c)** panels were shown in top and meropenem 100 µg/ml alone treated **(d)** or pre-incubated and treated with hemin showed in **(e)** and **(f)**. The lower panels **(g-i)** treated with 500 µg/ml meropenem. **(B)** A decrease in oxiRBC uptake by macrophages was observed in meropenem pre-incubated and hemin treated macrophages.

6.3.6. Meropenem can be employed to treat inflammation during malaria like condition.

Most of the infectious or non-infectious disease pathology involved pro-inflammatory cytokine secretion. The pro-inflammatory cytokines act on the cells and induce apoptosis in cells. During malaria like condition the scavenger receptor CD36 mediates the inflammation by non-opsonic phagocytosis of IRBC, and detecting heme or hemin. The hemin treatment induced secretion of uncontrolled levels of pro-inflammatory cytokine TNF-α. During malaria the pro-inflammatory cytokine levels are very high especially TNF-α. The macrophages treated with 25 or 200 μM hemin secreted 1091 or 950 pg of TNF-α respectively comparing to untreated macrophages showed (32.5 pg) (Figure 6.6). The macrophages pre-incubated with 100 μg/ml meropenem showed 44 pg (25 μM hemin) and 43 pg (200 μM hemin). Similar kind of results were observed in 500 μg/ml meropenem pre-incubated macrophages. It has shown that the meropenem mediated killing of E.coli in human umbilical card endothelial cells prevented the secretion of pro-inflammatory mediators IL-6, MCP-1 and IL-8 (Nau and Eiffert, 2002). This results fortifies meropenem as ligand of CD36 and can be exploited in to mitigate hemin-CD36 mediated inflammation.

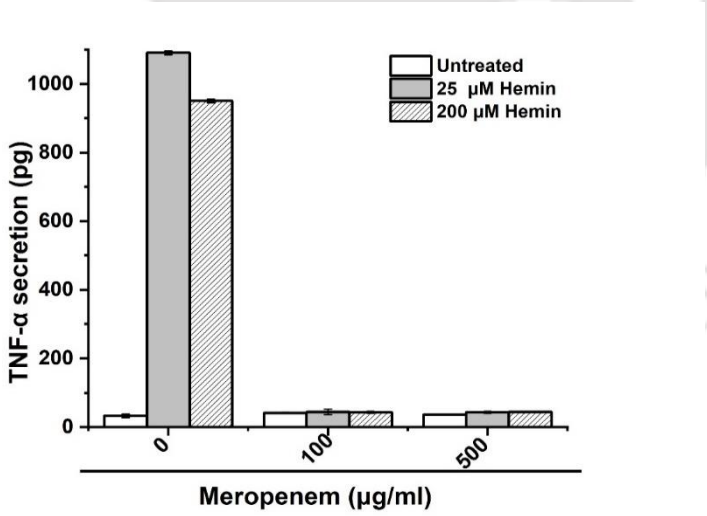

Figure 6.6. Meropenem pre-treatment abolishes TNF-α secretion from macrophages. The macrophages pre-incubated with 100 or 500 μg/ml of meropenem and treated with hemin 25 or 200 μM. Very high TNF-α levels were found in 25 and 200 μM hemin treated cells. The macrophages with meropenem pre-incubation showed significant reduction in cytokine.

TH-2507_156106009

6.4. Discussion

The FDA approved drug bank serves as a repertoire of new drugs. The advantage of using FDA approved drugs is that they are clinically tested and all the information that required for new drug application is readily available (Conrado et al., 2013). In last few years the screening of FDA approved drugs against various disease targets has acquired much interest in scientific community who are closely working in drug discovery field. This kind of drug discovery process is less time consuming and need small financial input. One estimate showed that the re-purposing of drugs has a success rate of 30% of newly approved drugs by FDA (Pillaiyar et al., 2020). The drug bank contains several of approved drugs targets receptors, enzymes, transporter proteins, and clusters of differentiation (CD) proteins (Reichert, 2003). In this study we have explored FDA approved drugs that target and block the scavenger receptor CD36. The scavenger receptor involved in angiogenesis, metabolism and immune response (Febbraio et al., 2001). The key functions of this receptor is fatty acid uptake and non-opsonic phagocytosis. The CD36 facilitates the uptake of pathogens, dead cells or infected RBCs by macrophages. The receptor may contribute to escape of pathogens such as Mycobacterium and from immune response (Hawkes et al., 2010). In endothelial cells in aorta express CD36 and the levels are increased upon stimulation from oxiLDL. The oxiLDL binding to CD36 attracts the infiltrating immune cells to the site and responsible for macrophage foam cells formation (SILVERSTEIN, 2009). Further, the oxiLDL-CD36 interactions induce the pro-inflammatory cytokine secretion, ROS generation and at the end macrophage dysfunction (Kennedy et al., 2011). By targeting CD36 with suitable blockers could be useful in treated CD36 mediated immune-dysfunction or diseases. Earlier the FDA approved anti-diabetic drugs statins were tested for their CD36 inhibitory actions. The statins treated macrophages showed reduced CD36 expression in adipocytes and showed improved immune response (Han et al., 2004).

We have screened FDA approved drugs against hemin binding region on CD36. Although there are several hits produced from molecular docking we have selectively taken compounds based on binding energy, clusters and conformations, type of drug (eg. steroidal or non-steroidal), cost of the drug and availability. Based on the above criteria we have chosen to study binding of nine compounds with purified CD36 ectodomain. The compounds predicted high affinity towards CD36 in in-silico study has failed to perform well in the in-vitro binding

TH-2507_156106009

study. The false positives in molecular docking is more common since the scoring function does not consider receptor plasticity and binding energy landscape (Awuni and Mu, 2015). Only one compound that is meropenem binding to CD36 with high affinity with K_D value of 0.402 ±0.0002 μM. There is previous reports on CD36 binding to any antibiotics. The meropenem pre-incubated macrophages showed no phagocytic depression upon hemin treatment. Further, the meropenem also corrected the phagocytic depression towards oxiRBC. Previous reports suggests the meropenem pre-incubated human macrophages showed enhancement in phagocytosis but the mechanism behind this is unclear. Our study in consistent with their observation suggests the meropenem modulates the phagocytic activity of macrophages through binding to CD36. Further, the meropenem treatment prevented the elevated secretion of pro-inflammatory cytokine TNF-α. Initially when we started this study our aim is to screen the blockers and test whether the drug can rescue macrophages from CD36 mediated immune dysfunction. Here after studying the meropenem at cell level we confident that meropenem can be used to treat CD36 mediated immune-dysfunction during malaria like condition or any other disease which is a victim of CD36.

References: Please refer to the Bibliography section at the end of the thesis.

TH-2507_156106009

Bibliography:

- Abed, M., Herrmann, T., Alzoubi, K., Pakladok, T., and Lang, F. (2013). Tannic acid induced suicidal erythrocyte death. Cellular Physiology and Biochemistry *32*, 1106-1116.
- Abumrad, N., Perkins, R., Park, J., and Park, C.R. (1981). Mechanism of long chain fatty acid permeation in the isolated adipocyte. Journal of Biological Chemistry *256*, 9183-9191.
- Ackers, I., Szymanski, C., Duckett, K.J., Consitt, L.A., Silver, M.J., and Malgor, R. (2018). Blocking Wnt5a signaling decreases CD36 expression and foam cell formation in atherosclerosis. Cardiovascular Pathology *34*, 1-8.
- Acton, S.L., Scherer, P.E., Lodish, H.F., and Krieger, M. (1994). Expression cloning of SR-BI, a CD36-related class B scavenger receptor. Journal of Biological Chemistry *269*, 21003-21009.
- Adams, C.P., and Brantner, V.V. (2006). Estimating the cost of new drug development: is it really $802 million? Health affairs *25*, 420-428.
- Ahmed, M.U., Frye, E.B., Degenhardt, T.P., Thorpe, S.R., and Baynes, J.W. (1997). N-epsilon-(carboxyethyl) lysine, a product of the chemical modification of proteins by methylglyoxal, increases with age in human lens proteins. Biochemical Journal *324*, 565.
- Aier, I., Varadwaj, P.K., and Raj, U. (2016). Structural insights into conformational stability of both wild-type and mutant EZH2 receptor. Scientific reports *6*, 1-10.
- Akira, S., and Takeda, K. (2004). Toll-like receptor signalling. Nature reviews immunology *4*, 499-511.
- Akira, S., Uematsu, S., and Takeuchi, O. (2006). Pathogen recognition and innate immunity. Cell *124*, 783-801.
- Albert, M.L., Pearce, S.F.A., Francisco, L.M., Sauter, B., Roy, P., Silverstein, R.L., and Bhardwaj, N. (1998). Immature dendritic cells phagocytose apoptotic cells via αvβ5 and CD36, and cross-present antigens to cytotoxic T lymphocytes. The Journal of experimental medicine *188*, 1359-1368.
- Alessio, M., De Monte, L., Scirea, A., Gruarin, P., Tandon, N.N., and Sitia, R. (1996). Synthesis, processing, and intracellular transport of CD36 during monocytic differentiation. Journal of Biological Chemistry *271*, 1770-1775.
- Altenbach, D., and Robatzek, S. (2007). Pattern recognition receptors: from the cell surface to intracellular dynamics. Molecular Plant-Microbe Interactions *20*, 1031-1039.
- Amani, V., Vigário, A.M., Belnoue, E., Marussig, M., Fonseca, L., Mazier, D., and Rénia, L. (2000). Involvement of IFN-γ receptor-mediated signaling in pathology and anti-malarial immunity induced by Plasmodium berghei infection. European journal of immunology *30*, 1646-1655.
- Amar, M.J., D'Souza, W., Turner, S., Demosky, S., Sviridov, D., Stonik, J., Luchoomun, J., Voogt, J., Hellerstein, M., and Sviridov, D. (2010). 5A apolipoprotein mimetic peptide promotes cholesterol efflux and reduces atherosclerosis in mice. Journal of Pharmacology and Experimental Therapeutics *334*, 634-641.
- Anand, P., Nagarajan, D., Mukherjee, S., and Chandra, N. (2014). ABS–Scan: In silico alanine scanning mutagenesis for binding site residues in protein–ligand complex. F1000Research *3*.
- Andreyev, A.Y., Fahy, E., Guan, Z., Kelly, S., Li, X., McDonald, J.G., Milne, S., Myers, D., Park, H., and Ryan, A. (2010). Subcellular organelle lipidomics in TLR-4-activated macrophages. Journal of lipid research *51*, 2785-2797.
- Angulo, I., and Fresno, M. (2002). Cytokines in the pathogenesis of and protection against malaria. Clinical and diagnostic laboratory immunology *9*, 1145-1152.
- Anstey, N.M., Handojo, T., Pain, M.C., Kenangalem, E., Tjitra, E., Price, R.N., and Maguire, G.P. (2007). Lung injury in vivax malaria: pathophysiological evidence for pulmonary vascular sequestration and posttreatment alveolar-capillary inflammation. The Journal of infectious diseases *195*, 589-596.
- Archana, M., Yogesh, T., and Kumaraswamy, K. (2013). Various methods available for detection of apoptotic cells-A review. Indian journal of cancer *50*, 274.

- Ardito, F., Giuliani, M., Perrone, D., Troiano, G., and Lo Muzio, L. (2017). The crucial role of protein phosphorylation in cell signaling and its use as targeted therapy. International journal of molecular medicine *40*, 271-280.
- Armah, H., Dodoo, A., Wiredu, E., Stiles, J., Adjei, A., Gyasi, R., and Tettey, Y. (2005). High-level cerebellar expression of cytokines and adhesion molecules in fatal, paediatric, cerebral malaria. Annals of Tropical Medicine & Parasitology *99*, 629-647.
- Armesilla, A.L., and Vega, M.A. (1994). Structural organization of the gene for human CD36 glycoprotein. Journal of Biological Chemistry *269*, 18985-18991.
- Ashong, J., Blench, I., and Warhurst, D. (1989). The composition of haemozoin from Plasmodium falciparum. Transactions of the Royal Society of Tropical Medicine and Hygiene *83*, 167-172.
- Awuni, Y., and Mu, Y. (2015). Reduction of false positives in structure-based virtual screening when receptor plasticity is considered. Molecules *20*, 5152-5164.
- Bachtiar, B.M., and Bachtiar, E.W. (2017). Proinflammatory MG-63 cells response infection with Enterococcus faecalis cps2 evaluated by the expression of TLR-2, IL-1β, and iNOS mRNA. BMC research notes *10*, 401.
- Balaji, S., and Trivedi, V. (2013). Extracellular methemoglobin primes red blood cell aggregation in malaria: an in vitro mechanistic study. FEBS letters *587*, 350-357.
- Bali, J., Halima, S.B., Felmy, B., Goodger, Z., Zurbriggen, S., and Rajendran, L. (2010). Cellular basis of Alzheimer's disease. Annals of Indian Academy of Neurology *13*, S89.
- Banesh, S., Ramakrishnan, V., and Trivedi, V. (2018). Mapping of phosphatidylserine recognition region on CD36 ectodomain. Archives of biochemistry and biophysics *660*, 1-10.
- Banesh, S., and Trivedi, V. (2020). Therapeutic Potentials of Scavenger Receptor CD36 Mediated Innate Immune Responses Against Infectious and Non-Infectious Diseases. Current drug discovery technologies *17*, 299-317.
- Banfalvi, G. (2017). Methods to detect apoptotic cell death. Apoptosis *22*, 306-323.
- Bao, Y., Wang, L., Xu, Y., Yang, Y., Wang, L., Si, S., Cho, S., and Hong, B. (2012). Salvianolic acid B inhibits macrophage uptake of modified low density lipoprotein (mLDL) in a scavenger receptor CD36-dependent manner. Atherosclerosis *223*, 152-159.
- Baranova, I.N., Bocharov, A.V., Vishnyakova, T.G., Kurlander, R., Chen, Z., Fu, D., Arias, I.M., Csako, G., Patterson, A.P., and Eggerman, T.L. (2010). CD36 is a novel serum amyloid A (SAA) receptor mediating SAA binding and SAA-induced signaling in human and rodent cells. Journal of Biological Chemistry *285*, 8492-8506.
- Baranova, I.N., Kurlander, R., Bocharov, A.V., Vishnyakova, T.G., Chen, Z., Remaley, A.T., Csako, G., Patterson, A.P., and Eggerman, T.L. (2008). Role of human CD36 in bacterial recognition, phagocytosis, and pathogen-induced JNK-mediated signaling. The Journal of Immunology *181*, 7147-7156.
- Baranowski, E., Ruiz-Jarabo, C.M., and Domingo, E. (2001). Evolution of cell recognition by viruses. Science *292*, 1102-1105.
- Barsoum, R.S. (2000). Malarial acute renal failure. Journal of the American Society of Nephrology *11*, 2147-2154.
- Baruch, D.I., Ma, X.C., Pasloske, B., Howard, R.J., and Miller, L.H. (1999). CD36 peptides that block cytoadherence define the CD36 binding region for Plasmodium falciparum-infected erythrocytes. Blood *94*, 2121-2127.
- Bastie, C.C., Nahlé, Z., McLoughlin, T., Esser, K., Zhang, W., Unterman, T., and Abumrad, N.A. (2005). FoxO1 stimulates fatty acid uptake and oxidation in muscle cells through CD36-dependent and-independent mechanisms. Journal of Biological Chemistry *280*, 14222-14229.
- Bechmann, L.P., Gieseler, R.K., Sowa, J.P., Kahraman, A., Erhard, J., Wedemeyer, I., Emons, B., Jochum, C., Feldkamp, T., and Gerken, G. (2010). Apoptosis is associated with CD36/fatty acid translocase upregulation in non-alcoholic steatohepatitis. Liver International *30*, 850-859.

- Beeson, J.G., Rogerson, S.J., Cooke, B.M., Reeder, J.C., Chai, W., Lawson, A.M., Molyneux, M.E., and Brown, G.V. (2000). Adhesion of Plasmodium falciparum-infected erythrocytes to hyaluronic acid in placental malaria. Nature medicine *6*, 86-90.
- Beigel, J.H., Tomashek, K.M., Dodd, L.E., Mehta, A.K., Zingman, B.S., Kalil, A.C., Hohmann, E., Chu, H.Y., Luetkemeyer, A., and Kline, S. (2020). Remdesivir for the treatment of Covid-19—preliminary report. The New England journal of medicine.
- Berre, S., Gaudin, R., de Alencar, B.C., Desdouits, M., Chabaud, M., Naffakh, N., Rabaza-Gairi, M., Gobert, F.-X., Jouve, M., and Benaroch, P. (2013). CD36-specific antibodies block release of HIV-1 from infected primary macrophages and its transmission to T cells. Journal of Experimental Medicine, jem. 20130566.
- Berwin, B., Delneste, Y., Lovingood, R.V., Post, S.R., and Pizzo, S.V. (2004). SREC-I, a type F scavenger receptor, is an endocytic receptor for calreticulin. Journal of Biological Chemistry *279*, 51250-51257.
- Bieghs, V., Verheyen, F., van Gorp, P.J., Hendrikx, T., Wouters, K., Lütjohann, D., Gijbels, M.J., Febbraio, M., Binder, C.J., and Hofker, M.H. (2012). Internalization of modified lipids by CD36 and SR-A leads to hepatic inflammation and lysosomal cholesterol storage in Kupffer cells. PloS one *7*, e34378.
- Blander, J.M., and Sander, L.E. (2012). Beyond pattern recognition: five immune checkpoints for scaling the microbial threat. Nature Reviews Immunology *12*, 215-225.
- Blankenberg, F.G. (2008). In vivo detection of apoptosis. The Journal of Nuclear Medicine *49*, 81S.
- Bobade, D., Khandare, A.V., Deval, M., Shastry, P., and Deshpande, P. (2019). Hemozoin-induced activation of human monocytes toward M2-like phenotype is partially reversed by antimalarial drugs—chloroquine and artemisinin. MicrobiologyOpen *8*, e00651.
- Bocharov, A.V., Baranova, I.N., Vishnyakova, T.G., Remaley, A.T., Csako, G., Thomas, F., Patterson, A.P., and Eggerman, T.L. (2004). Targeting of scavenger receptor class B type I by synthetic amphipathic α-helical-containing peptides blocks lipopolysaccharide (LPS) uptake and LPS-induced pro-inflammatory cytokine responses in THP-1 monocyte cells. Journal of Biological Chemistry *279*, 36072-36082.
- Bocharov, A.V., Wu, T., Baranova, I.N., Birukova, A.A., Sviridov, D., Vishnyakova, T.G., Remaley, A.T., Eggerman, T.L., Patterson, A.P., and Birukov, K.G. (2016). Synthetic amphipathic helical peptides targeting cd36 attenuate lipopolysaccharide-induced inflammation and acute lung injury. The Journal of Immunology *197*, 611-619.
- Bodart, V., Febbraio, M., Demers, A., McNicoll, N., Pohankova, P., Perreault, A., Sejlitz, T., Escher, E., Silverstein, R., and Lamontagne, D. (2002). CD36 mediates the cardiovascular action of growth hormone-releasing peptides in the heart. Circulation research *90*, 844-849.
- Bonen, A., Chabowski, A., Luiken, J.J.P., and Glatz, J.F. (2007). Mechanisms and regulation of protein-mediated cellular fatty acid uptake: molecular, biochemical, and physiological evidence. Physiology.
- Bonen, A., Han, X.-X., Tandon, N.N., Glatz, J.F., Lally, J., Snook, L.A., and Luiken, J.J. (2009). FAT/CD36 expression is not ablated in spontaneously hypertensive rats. Journal of lipid research *50*, 740-748.
- Bonen, A., Tandon, N., Glatz, J., Luiken, J., and Heigenhauser, G. (2006). The fatty acid transporter FAT/CD36 is upregulated in subcutaneous and visceral adipose tissues in human obesity and type 2 diabetes. International journal of obesity *30*, 877.
- Boogaerts, M., Winston, D.J., Bow, E.J., Garber, G., Reboli, A.C., Schwarer, A.P., Novitzky, N., Boehme, A., Chwetzoff, E., and De Beule, K. (2001). Intravenous and oral itraconazole versus intravenous amphotericin B deoxycholate as empirical antifungal therapy for persistent fever in neutropenic patients with cancer who are receiving broad-spectrum antibacterial therapy: a randomized, controlled trial. Annals of internal medicine *135*, 412-422.
- Borisenko, G.G., Matsura, T., Liu, S.-X., Tyurin, V.A., Jianfei, J., Serinkan, F.B., and Kagan, V.E. (2003). Macrophage recognition of externalized phosphatidylserine and phagocytosis of apoptotic Jurkat cells—existence of a threshold. Archives of biochemistry and biophysics *413*, 41-52.

- Bruni, F., Pasqui, A.L., Pastorelli, M., Bova, G., Cercignani, M., Palazzuoli, A., Sawamura, T., Auteri, A., and Puccetti, L. (2005). Different Effect of Statins on Platelet Oxidized-LDLReceptor (CD36 and LOX-1) Expressionin Hypercholesterolemic Subjects. Clinical and applied thrombosis/hemostasis *11*, 417-428.
- Bujarbaruah, D., Kalita, M., Baruah, V., Basumatary, T., Hazarika, S., Begum, R., Medhi, S., and Bose, S. (2017). RANTES levels as a determinant of falciparum malaria severity or recovery. Parasite Immunology *39*, e12452.
- Bulgarelli, I., Tamiazzo, L., Bresciani, E., Rapetti, D., Caporali, S., Lattuada, D., Locatelli, V., and Torsello, A. (2009). Desacyl-ghrelin and synthetic GH-secretagogues modulate the production of inflammatory cytokines in mouse microglia cells stimulated by β-amyloid fibrils. Journal of neuroscience research *87*, 2718-2727.
- Cai, L., Wang, Z., Ji, A., Meyer, J.M., and van der Westhuyzen, D.R. (2012). Scavenger receptor CD36 expression contributes to adipose tissue inflammation and cell death in diet-induced obesity. PloS one *7*, e36785.
- Cambos, M., and Scorza, T. (2011). Robust erythrophagocytosis leads to macrophage apoptosis via a hemin-mediated redox imbalance: role in hemolytic disorders. Journal of leukocyte biology *89*, 159-171.
- Cargnin, S.T., and Gnoatto, S.B. (2017). Ursolic acid from apple pomace and traditional plants: A valuable triterpenoid with functional properties. Food Chemistry *220*, 477-489.
- Carlquist, J.F., Muhlestein, J.B., Horne, B.D., Hart, N.I., Lim, T., Habashi, J., Anderson, J.G., and Anderson, J.L. (2004). Cytomegalovirus stimulated mRNA accumulation and cell surface expression of the oxidized LDL scavenger receptor, CD36. Atherosclerosis *177*, 53-59.
- Carmona-Fonseca, J., Álvarez, G., and Maestre, A. (2009). Methemoglobinemia and adverse events in Plasmodium vivax malaria patients associated with high doses of primaquine treatment. The American journal of tropical medicine and hygiene *80*, 188-193.
- Casciano, J.C., Duchemin, N.J., Lamontagne, R.J., Steel, L.F., and Bouchard, M.J. (2017). Hepatitis B virus modulates store-operated calcium entry to enhance viral replication in primary hepatocytes. PloS one *12*, e0168328.
- Chan, L.L.-Y., Smith, T., Kumph, K.A., Kuksin, D., Kessel, S., Déry, O., Cribbes, S., Lai, N., and Qiu, J. (2016). A high-throughput AO/PI-based cell concentration and viability detection method using the Celigo image cytometry. Cytotechnology *68*, 2015-2025.
- Chan, L.L., Wilkinson, A.R., Paradis, B.D., and Lai, N. (2012). Rapid image-based cytometry for comparison of fluorescent viability staining methods. Journal of fluorescence *22*, 1301-1311.
- Chang, T.M., Powanda, D., and Yu, W. (2003). Analysis of polyethylene-glycol-polylactide nano-dimension artificial red blood cells in maintaining systemic hemoglobin levels and prevention of methemoglobin formation. Artificial cells, blood substitutes, and biotechnology *31*, 231-247.
- Chen, D., Oezguen, N., Urvil, P., Ferguson, C., Dann, S.M., and Savidge, T.C. (2016). Regulation of protein-ligand binding affinity by hydrogen bond pairing. Science advances *2*, e1501240.
- Chen, K., Febbraio, M., Li, W., and Silverstein, R.L. (2008). A specific CD36-dependent signaling pathway is required for platelet activation by oxidized low-density lipoprotein. Circulation research *102*, 1512-1519.
- Chen, M., Vijay, V., Shi, Q., Liu, Z., Fang, H., and Tong, W. (2011). FDA-approved drug labeling for the study of drug-induced liver injury. Drug discovery today *16*, 697-703.
- Cheng, J.-J., Li, J.-R., Huang, M.-H., Ma, L.-L., Wu, Z.-Y., Jiang, C.-C., Li, W.-J., Li, Y.-H., Han, Y.-X., and Li, H. (2016). CD36 is a co-receptor for hepatitis C virus E1 protein attachment. Scientific reports *6*, 21808.
- Cheng, Z., Ning, Y., and Wang, R. (2018). Effects of electroacupuncture on expression of CD36 in peritoneal macrophages of rabbits with atherosclerosis. Zhongguo zhen jiu= Chinese acupuncture & moxibustion *38*, 179-184.
- Cherry, S., and Perrimon, N. (2004). Entry is a rate-limiting step for viral infection in a Drosophila melanogaster model of pathogenesis. Nature immunology *5*, 81.

- Cho, S. (2012). CD36 as a therapeutic target for endothelial dysfunction in stroke. Current pharmaceutical design *18*, 3721-3730.
- Cho, S., Bao, Y., and Kim, E. (2016). CD36 inhibition to control obesity and insulin sensitivity (Google Patents).
- Cho, S., and Kim, E. (2009). CD36: A multi-modal target for acute stroke therapy. Journal of neurochemistry *109*, 126-132.
- Cho, S., Park, E.-M., Febbraio, M., Anrather, J., Park, L., Racchumi, G., Silverstein, R.L., and Iadecola, C. (2005). The class B scavenger receptor CD36 mediates free radical production and tissue injury in cerebral ischemia. Journal of Neuroscience *25*, 2504-2512.
- Cho, S., Szeto, H.H., Kim, E., Kim, H., Tolhurst, A.T., and Pinto, J.T. (2007). A novel cell-permeable antioxidant peptide, SS31, attenuates ischemic brain injury by down-regulating CD36. Journal of Biological Chemistry *282*, 4634-4642.
- Choromańska, B., Myśliwiec, P., Choromańska, K., Dadan, J., and Chabowski, A. (2017). The role of CD36 receptor in the pathogenesis of atherosclerosis. Advances in clinical and experimental medicine: official organ Wroclaw Medical University *26*, 717-722.
- Choudhari, A.S., Mandave, P.C., Deshpande, M., Ranjekar, P., and Prakash, O. (2020). Phytochemicals in cancer treatment: From preclinical studies to clinical practice. Frontiers in pharmacology *10*, 1614.
- Chu, L.-Y., Ramakrishnan, D.P., and Silverstein, R.L. (2013). Thrombospondin-1 modulates VEGF signaling via CD36 by recruiting SHP-1 to VEGFR2 complex in microvascular endothelial cells. Blood *122*, 1822-1832.
- Chu, L.-Y., and Silverstein, R.L. (2012). CD36 ectodomain phosphorylation blocks thrombospondin-1 binding: structure-function relationships and regulation by protein kinase C. Arteriosclerosis, thrombosis, and vascular biology *32*, 760-767.
- Cicchese, J.M., Evans, S., Hult, C., Joslyn, L.R., Wessler, T., Millar, J.A., Marino, S., Cilfone, N.A., Mattila, J.T., and Linderman, J.J. (2018). Dynamic balance of pro-and anti-inflammatory signals controls disease and limits pathology. Immunological reviews *285*, 147-167.
- Clem, A. (2010). A current perspective on leishmaniasis. Journal of global infectious diseases *2*, 124.
- Cliver, D.O. (2009). Capsid and infectivity in virus detection. Food and environmental virology *1*, 123.
- Coburn, C.T., Knapp, F., Febbraio, M., Beets, A.L., Silverstein, R.L., and Abumrad, N.A. (2000). Defective uptake and utilization of long chain fatty acids in muscle and adipose tissues of CD36 knockout mice. Journal of Biological Chemistry *275*, 32523-32529.
- Cohen, F.S. (2016). How viruses invade cells. Biophysical journal *110*, 1028.
- Conrado, D.J., Rogers, H.L., Zineh, I., and Pacanowski, M.A. (2013). Consistency of drug–drug and gene–drug interaction information in US FDA-approved drug labels. Pharmacogenomics *14*, 215-223.
- Cooke, B.M., Buckingham, D.W., Glenister, F.K., Fernandez, K.M., Bannister, L.H., Marti, M., Mohandas, N., and Coppel, R.L. (2006). A Maurer's cleft–associated protein is essential for expression of the major malaria virulence antigen on the surface of infected red blood cells. J Cell Biol *172*, 899-908.
- Cooke, B.M., Mohandas, N., and Coppel, R.L. (2001). The malaria-infected red blood cell: structural and functional changes.
- Cooper, G.E., Pounce, Z.C., Wallington, J.C., Bastidas-Legarda, L.Y., Nicholas, B., Chidomere, C., Robinson, E.C., Martin, K., Tocheva, A.S., and Christodoulides, M. (2016). Viral inhibition of bacterial phagocytosis by human macrophages: redundant role of CD36. PLoS One *11*, e0163889.
- Coort, S.L., Willems, J., Coumans, W.A., Van Der Vusse, G.J., Bonen, A., Glatz, J.F., and Luiken, J.J. (2002). Sulfo-N-succinimidyl esters of long chain fatty acids specifically inhibit fatty acid translocase (FAT/CD36)-mediated cellular fatty acid uptake. Molecular and cellular biochemistry *239*, 213-219.
- Coraci, I.S., Husemann, J., Berman, J.W., Hulette, C., Dufour, J.H., Campanella, G.K., Luster, A.D., Silverstein, S.C., and El Khoury, J.B. (2002). CD36, a class B scavenger receptor, is expressed on

microglia in Alzheimer's disease brains and can mediate production of reactive oxygen species in response to β-amyloid fibrils. The American journal of pathology *160*, 101-112.

- Cuffini, A.M., Tullio, V., Allocco, A., Giachino, F., Fazari, S., and Carlone, N.A. (1993). The entry of meropenem into human macrophages and its immunomodulating activity. Journal of Antimicrobial Chemotherapy *32*, 695-703.
- Dalko, E., Das, B., Herbert, F., Fesel, C., Pathak, S., Tripathy, R., Cazenave, P.-A., Ravindran, B., Sharma, S., and Pied, S. (2015). Multifaceted role of heme during severe Plasmodium falciparum infections in India. Infection and immunity *83*, 3793-3799.
- Dang, T.N., Robinson, S.R., Dringen, R., and Bishop, G.M. (2011). Uptake, metabolism and toxicity of hemin in cultured neurons. Neurochemistry international *58*, 804-811.
- Das, S., Owen, K.A., Ly, K.T., Park, D., Black, S.G., Wilson, J.M., Sifri, C.D., Ravichandran, K.S., Ernst, P.B., and Casanova, J.E. (2011). Brain angiogenesis inhibitor 1 (BAI1) is a pattern recognition receptor that mediates macrophage binding and engulfment of Gram-negative bacteria. Proceedings of the National Academy of Sciences *108*, 2136-2141.
- Davis, S.P., Amrein, M., Gillrie, M.R., Lee, K., Muruve, D.A., and Ho, M. (2012). Plasmodium falciparum-induced CD36 clustering rapidly strengthens cytoadherence via p130CAS-mediated actin cytoskeletal rearrangement. The FASEB Journal *26*, 1119-1130.
- De Marco, A., Vigh, L., Diamant, S., and Goloubinoff, P. (2005). Native folding of aggregation-prone recombinant proteins in Escherichia coli by osmolytes, plasmid-or benzyl alcohol–overexpressed molecular chaperones. Cell stress & chaperones *10*, 329-339.
- Deka, S.J., Mamdi, N., Manna, D., and Trivedi, V. (2016). Alkyl cinnamates induce protein kinase C translocation and anticancer activity against breast cancer cells through induction of the mitochondrial pathway of apoptosis. Journal of breast cancer *19*, 358-371.
- Deka, S.J., Roy, A., Ramakrishnan, V., Manna, D., and Trivedi, V. (2017). Danazol has potential to cause PKC translocation, cell cycle dysregulation, and apoptosis in breast cancer cells. Chemical biology & drug design *89*, 953-963.
- Demers, A., McNICOLL, N., Febbraio, M., Servant, M., Marleau, S., Silverstein, R., and Huy, O. (2004). Identification of the growth hormone-releasing peptide binding site in CD36: a photoaffinity cross-linking study. Biochemical Journal *382*, 417-424.
- Deng, H., and Fang, Y. (2012). Anti-inflammatory gallic acid and wedelolactone are G protein-coupled receptor-35 agonists. Pharmacology *89*, 211-219.
- Deshmukh, R., and Trivedi, V. (2013). Methemoglobin exposure produces toxicological effects in macrophages due to multiple ROS spike induced apoptosis. Toxicology in Vitro *27*, 16-23.
- Deshmukh, R., and Trivedi, V. (2014). Phagocytic uptake of oxidized heme polymer is highly cytotoxic to macrophages. PloS one *9*, e103706.
- Devaraj, S., Hugou, I., and Jialal, I. (2001). α-Tocopherol decreases CD36 expression in human monocyte-derived macrophages. Journal of lipid research *42*, 521-527.
- Dey, S., Bindu, S., Goyal, M., Pal, C., Alam, A., Iqbal, M.S., Kumar, R., Sarkar, S., and Bandyopadhyay, U. (2012). Impact of intravascular hemolysis in Malaria on liver dysfunction involvement of hepatic free heme overload, NF-κB activation, and neutrophil infiltration. Journal of Biological Chemistry *287*, 26630-26646.
- Dhama, K., Karthik, K., Khandia, R., Munjal, A., Tiwari, R., Rana, R., Khurana, S.K., Ullah, S., Khan, R.U., and Alagawany, M. (2018). Medicinal and therapeutic potential of herbs and plant metabolites/extracts countering viral pathogens-current knowledge and future prospects. Current drug metabolism *19*, 236-263.
- Diamond, C.E., Khameneh, H.J., Brough, D., and Mortellaro, A. (2015). Novel perspectives on non-canonical inflammasome activation. ImmunoTargets and therapy *4*, 131.
- Dillard, C.J., and German, J.B. (2000). Phytochemicals: nutraceuticals and human health. Journal of the Science of Food and Agriculture *80*, 1744-1756.

- Dodd, C.E., Pyle, C.J., Glowinski, R., Rajaram, M.V., and Schlesinger, L.S. (2016). CD36-mediated uptake of surfactant lipids by human macrophages promotes intracellular growth of Mycobacterium tuberculosis. The Journal of Immunology *197*, 4727-4735.
- Doens, D., Valiente, P.A., Mfuh, A.M., XT Vo, A., Tristan, A., Carreño, L., Quijada, M., Nguyen, V.T., Perry, G., and Larionov, O.V. (2017). Identification of inhibitors of CD36-Amyloid beta binding as potential agents for Alzheimer's disease. ACS chemical neuroscience *8*, 1232-1241.
- Dong, L., Yuan, Y., Opansky, C., Chen, Y., Aguilera-Barrantes, I., Wu, S., Yuan, R., Cao, Q., Cheng, Y.C., and Sahoo, D. (2017). Diet-induced obesity links to ER positive breast cancer progression via LPA/PKD-1-CD36 signaling-mediated microvascular remodeling. Oncotarget *8*, 22550.
- Du, X., Poltorak, A., Wei, Y., and Beutler, B. (2000). Three novel mammalian toll-like receptors: gene structure, expression, and evolution. European cytokine network *11*, 362-371.
- Duronio, V., Scheid, M.P., and Ettinger, S. (1998). Downstream signalling events regulated by phosphatidylinositol 3-kinase activity. Cellular signalling *10*, 233-239.
- Ekvall, H. (2003). Malaria and anemia. Current opinion in hematology *10*, 108-114.
- El Khoury, J.B., Moore, K.J., Means, T.K., Leung, J., Terada, K., Toft, M., Freeman, M.W., and Luster, A.D. (2003a). CD36 mediates the innate host response to β-amyloid. The Journal of experimental medicine *197*, 1657-1666.
- El Khoury, J.B., Moore, K.J., Means, T.K., Leung, J., Terada, K., Toft, M., Freeman, M.W., and Luster, A.D. (2003b). CD36 mediates the innate host response to β-amyloid. Journal of Experimental Medicine *197*, 1657-1666.
- Eleftheriadis, T., Pissas, G., Liakopoulos, V., and Stefanidis, I. (2016). Cytochrome c as a potentially clinical useful marker of mitochondrial and cellular damage. Frontiers in immunology *7*, 279.
- Elmore, S. (2007). Apoptosis: a review of programmed cell death. Toxicologic pathology *35*, 495-516.
- Engwerda, C.R., Beattie, L., and Amante, F.H. (2005). The importance of the spleen in malaria. Trends in parasitology *21*, 75-80.
- Erdman, L.K., Cosio, G., Helmers, A.J., Gowda, D.C., Grinstein, S., and Kain, K.C. (2009). CD36 and TLR interactions in inflammation and phagocytosis: implications for malaria. The Journal of Immunology *183*, 6452-6459.
- Eyre, N.S., Cleland, L.G., Tandon, N.N., and Mayrhofer, G. (2007). Importance of the carboxyl terminus of FAT/CD36 for plasma membrane localization and function in long-chain fatty acid uptake. Journal of lipid research *48*, 528-542.
- Fadok, V.A., Bratton, D.L., Frasch, S.C., Warner, M.L., and Henson, P.M. (1998a). The role of phosphatidylserine in recognition of apoptotic cells by phagocytes. Cell death and differentiation *5*, 551.
- Fadok, V.A., Bratton, D.L., and Henson, P.M. (2001). Phagocyte receptors for apoptotic cells: recognition, uptake, and consequences. The Journal of clinical investigation *108*, 957-962.
- Fadok, V.A., Warner, M.L., Bratton, D.L., and Henson, P.M. (1998b). CD36 is required for phagocytosis of apoptotic cells by human macrophages that use either a phosphatidylserine receptor or the vitronectin receptor (αvβ3). The Journal of Immunology *161*, 6250-6257.
- Falkinham III, J.O. (2003). Mycobacterial aerosols and respiratory disease. Emerging infectious diseases *9*, 763.
- Febbraio, M., Hajjar, D.P., and Silverstein, R.L. (2001). CD36: a class B scavenger receptor involved in angiogenesis, atherosclerosis, inflammation, and lipid metabolism. The Journal of clinical investigation *108*, 785-791.
- Ferreira, A., Balla, J., Jeney, V., Balla, G., and Soares, M.P. (2008). A central role for free heme in the pathogenesis of severe malaria: the missing link? Journal of molecular medicine *86*, 1097-1111.
- Figueiredo, R.T., Fernandez, P.L., Mourao-Sa, D.S., Porto, B.N., Dutra, F.F., Alves, L.S., Oliveira, M.F., Oliveira, P.L., Graça-Souza, A.V., and Bozza, M.T. (2007). Characterization of heme as activator of Toll-like receptor 4. Journal of Biological Chemistry *282*, 20221-20229.

- Firoz, A., Malik, A., Afzal, O., and Jha, V. (2010). ContPro: A web tool for calculating amino acid contact distances in protein from 3D-structures at different distance threshold. Bioinformation *5*, 55.
- Flannagan, R.S., Canton, J., Furuya, W., Glogauer, M., and Grinstein, S. (2014). The phosphatidylserine receptor TIM4 utilizes integrins as coreceptors to effect phagocytosis. Molecular biology of the cell *25*, 1511-1522.
- Fonager, J., Pasini, E.M., Braks, J.A., Klop, O., Ramesar, J., Remarque, E.J., Vroegrijk, I.O., van Duinen, S.G., Thomas, A.W., and Khan, S.M. (2012). Reduced CD36-dependent tissue sequestration of Plasmodium-infected erythrocytes is detrimental to malaria parasite growth in vivo. Journal of Experimental Medicine *209*, 93-107.
- Frevert, U., Sinnis, P., Cerami, C., Shreffler, W., Takacs, B., and Nussenzweig, V. (1993). Malaria circumsporozoite protein binds to heparan sulfate proteoglycans associated with the surface membrane of hepatocytes. The Journal of experimental medicine *177*, 1287-1298.
- Fridman, W.H. (1991). Fc receptors and immunoglobulin binding factors 1. The FASEB journal *5*, 2684-2690.
- Gallo, J., Raska, M., Konttinen, Y.T., Nich, C., and Goodman, S.B. (2014). Innate immunity sensors participating in pathophysiology of joint diseases: a brief overview. Journal of long-term effects of medical implants *24*.
- Garbacz, W.G., Lu, P., Miller, T.M., Poloyac, S.M., Eyre, N.S., Mayrhofer, G., Xu, M., Ren, S., and Xie, W. (2016). Hepatic overexpression of CD36 improves glycogen homeostasis and attenuates high-fat diet-induced hepatic steatosis and insulin resistance. Molecular and cellular biology *36*, 2715-2727.
- Garcia-Bonilla, L., Racchumi, G., Murphy, M., Anrather, J., and Iadecola, C. (2015). Endothelial CD36 contributes to postischemic brain injury by promoting neutrophil activation via CSF3. Journal of Neuroscience *35*, 14783-14793.
- Gautam, S., Agrawal, C., Bid, H.K., and Banerjee, M. (2011). Preliminary studies on CD36 gene in type 2 diabetic patients from north India. The Indian journal of medical research *134*, 107.
- Gavrilescu, L.C., and Denkers, E.Y. (2003). Apoptosis and the balance of homeostatic and pathologic responses to protozoan infection. Infection and immunity *71*, 6109-6115.
- Gay, N.J., and Keith, F.J. (1991). Drosophila Toll and IL-1 receptor. Nature *351*, 355-356.
- Gazzinelli, R.T., Kalantari, P., Fitzgerald, K.A., and Golenbock, D.T. (2014). Innate sensing of malaria parasites. Nature Reviews Immunology *14*, 744-757.
- Gearhart, T.L., and Bouchard, M.J. (2010). Replication of the hepatitis B virus requires a calcium-dependent HBx-induced G1 phase arrest of hepatocytes. Virology *407*, 14-25.
- Geloen, A., Helin, L., Geeraert, B., Malaud, E., Holvoet, P., and Marguerie, G. (2012). CD36 inhibitors reduce postprandial hypertriglyceridemia and protect against diabetic dyslipidemia and atherosclerosis. PLoS One *7*, e37633.
- Geng, J., Yang, C., Wang, B., Zhang, X., Hu, T., Gu, Y., and Li, J. (2018). Trimethylamine N-oxide promotes atherosclerosis via CD36-dependent MAPK/JNK pathway. Biomedicine & Pharmacotherapy *97*, 941-947.
- Ghahremanpour, M.M., Arab, S.S., Aghazadeh, S.B., Zhang, J., and van der Spoel, D. (2013). MemBuilder: a web-based graphical interface to build heterogeneously mixed membrane bilayers for the GROMACS biomolecular simulation program. Bioinformatics *30*, 439-441.
- Ghosh, A., Li, W., Febbraio, M., Espinola, R.G., McCrae, K.R., Cockrell, E., and Silverstein, R.L. (2008). Platelet CD36 mediates interactions with endothelial cell–derived microparticles and contributes to thrombosis in mice. The Journal of clinical investigation *118*, 1934-1943.
- Giunta, M., Rigamonti, A., Scarpini, E., Galimberti, D., Bonomo, S., Venturelli, E., Müller, E., and Cella, S. (2007). The leukocyte expression of CD36 is low in patients with Alzheimer's disease and mild cognitive impairment. Neurobiology of aging *28*, 515-518.
- Gkaliagkousi, E., Passacquale, G., Douma, S., Zamboulis, C., and Ferro, A. (2010). Platelet activation in essential hypertension: implications for antiplatelet treatment. American journal of hypertension *23*, 229-236.

- Gomez-Diaz, C., Bargeton, B., Abuin, L., Bukar, N., Reina, J.H., Bartoi, T., Graf, M., Ong, H., Ulbrich, M.H., and Masson, J.-F. (2016). A CD36 ectodomain mediates insect pheromone detection via a putative tunnelling mechanism. Nature communications *7*, 1-17.
- Goodpaster, B.H., and Wolf, D. (2004). Skeletal muscle lipid accumulation in obesity, insulin resistance, and type 2 diabetes. Pediatric diabetes *5*, 219-226.
- Gowda, N.M., Wu, X., Kumar, S., Febbraio, M., and Gowda, D.C. (2013). CD36 contributes to malaria parasite-induced pro-inflammatory cytokine production and NK and T cell activation by dendritic cells. PloS one *8*, e77604.
- Gozzelino, R., Jeney, V., and Soares, M.P. (2010). Mechanisms of cell protection by heme oxygenase-1. Annual review of pharmacology and toxicology *50*, 323-354.
- Grasl-Kraupp, B., Ruttkay-Nedecky, B., Koudelka, H., Bukowska, K., Bursch, W., and Schulte-Hermann, R. (1995). In situ detection of fragmented DNA (TUNEL assay) fails to discriminate among apoptosis, necrosis, and autolytic cell death: a cautionary note. Hepatology *21*, 1465-1468.
- Greco, D., Kotronen, A., Westerbacka, J., Puig, O., Arkkila, P., Kiviluoto, T., Laitinen, S., Kolak, M., Fisher, R.M., and Hamsten, A. (2008). Gene expression in human NAFLD. American Journal of Physiology-Gastrointestinal and Liver Physiology *294*, G1281-G1287.
- Greenberg, M.E., Sun, M., Zhang, R., Febbraio, M., Silverstein, R., and Hazen, S.L. (2006). Oxidized phosphatidylserine–CD36 interactions play an essential role in macrophage-dependent phagocytosis of apoptotic cells. Journal of Experimental Medicine *203*, 2613-2625.
- Greenfield, N.J. (2006). Determination of the folding of proteins as a function of denaturants, osmolytes or ligands using circular dichroism. Nature protocols *1*, 2733.
- Gruarin, P., Primo, L., Ferrandi, C., Bussolino, F., Tandon, N.N., Arese, P., Ulliers, D., and Alessio, M. (2001). Cytoadherence of Plasmodium falciparum-infected erythrocytes is mediated by a redox-dependent conformational fraction of CD36. The Journal of Immunology *167*, 6510-6517.
- Gunasekaran, K., and Nussinov, R. (2007). How different are structurally flexible and rigid binding sites? Sequence and structural features discriminating proteins that do and do not undergo conformational change upon ligand binding. Journal of molecular biology *365*, 257-273.
- Gupta, G., Oghumu, S., and Satoskar, A.R. (2013). Mechanisms of immune evasion in leishmaniasis. In Advances in applied microbiology (Elsevier), pp. 155-184.
- Gupta, S., Elias, M., Wen, X., Shapiro, J., Brillson, L., Lu, W., and Lee, S.C. (2008). Detection of clinically relevant levels of protein analyte under physiologic buffer using planar field effect transistors. Biosensors and Bioelectronics *24*, 505-511.
- Guthrie, R.A., and Guthrie, D.W. (2004). Pathophysiology of diabetes mellitus. Critical care nursing quarterly *27*, 113-125.
- Haanen, C., and Vermes, I. (1995). Apoptosis and inflammation. Mediators of inflammation *4*, 5-15.
- Han, J., Zhou, X., Yokoyama, T., Hajjar, D.P., Gotto Jr, A.M., and Nicholson, A.C. (2004). Pitavastatin downregulates expression of the macrophage type B scavenger receptor, CD36. Circulation *109*, 790-796.
- Han, S.H., Kim, J.H., Martin, M., Michalek, S.M., and Nahm, M.H. (2003). Pneumococcal lipoteichoic acid (LTA) is not as potent as staphylococcal LTA in stimulating Toll-like receptor 2. Infection and immunity *71*, 5541-5548.
- Hanayama, R., Tanaka, M., Miwa, K., Shinohara, A., Iwamatsu, A., and Nagata, S. (2002). Identification of a factor that links apoptotic cells to phagocytes. Nature *417*, 182.
- Handberg, A., Lopez-Bermejo, A., Bassols, J., Vendrell, J., Ricart, W., and Fernandez-Real, J.M. (2009). Circulating soluble CD36 is associated with glucose metabolism and interleukin-6 in glucose-intolerant men. Diabetes and Vascular Disease Research *6*, 15-20.
- Hannemann, A., Rees, D.C., Brewin, J.N., Noe, A., Low, B., and Gibson, J.S. (2018). Oxidative stress and phosphatidylserine exposure in red cells from patients with sickle cell anaemia. British journal of haematology *182*, 567-578.

- Hara, T., Kimura, I., Inoue, D., Ichimura, A., and Hirasawa, A. (2013). Free fatty acid receptors and their role in regulation of energy metabolism. In Reviews of Physiology, Biochemistry and Pharmacology, Vol 164 (Springer), pp. 77-116.
- Harb, D., Bujold, K., Febbraio, M., Sirois, M.G., Ong, H., and Marleau, S. (2009). The role of the scavenger receptor CD36 in regulating mononuclear phagocyte trafficking to atherosclerotic lesions and vascular inflammation. Cardiovascular research *83*, 42-51.
- Hashimoto, C., Hudson, K.L., and Anderson, K.V. (1988). The Toll gene of Drosophila, required for dorsal-ventral embryonic polarity, appears to encode a transmembrane protein. Cell *52*, 269-279.
- Hawkes, M., Li, X., Crockett, M., Diassiti, A., Finney, C., Min-Oo, G., Liles, W.C., Liu, J., and Kain, K.C. (2010a). CD36 deficiency attenuates experimental mycobacterial infection. BMC infectious diseases *10*, 299.
- Hawkes, M., Li, X., Crockett, M., Diassiti, A., Finney, C., Min-Oo, G., Liles, W.C., Liu, J., and Kain, K.C. (2010b). CD36 deficiency attenuates experimental mycobacterial infection. BMC infectious diseases *10*, 1-17.
- He, C., Zhang, G., Ouyang, H., Zhang, P., Chen, Y., Wang, R., and Zhou, H. (2019). Effects of β2/aβ2 on oxLDL-induced CD36 activation in THP-1 macrophages. Life sciences *239*, 117000.
- Heit, B., Kim, H., Cosío, G., Castaño, D., Collins, R., Lowell, C.A., Kain, K.C., Trimble, W.S., and Grinstein, S. (2013). Multimolecular signaling complexes enable Syk-mediated signaling of CD36 internalization. Developmental cell *24*, 372-383.
- Helming, L., Winter, J., and Gordon, S. (2009). The scavenger receptor CD36 plays a role in cytokine-induced macrophage fusion. Journal of cell science *122*, 453-459.
- Herbert, F., Tchitchek, N., Bansal, D., Jacques, J., Pathak, S., Bécavin, C., Fesel, C., Dalko, E., Cazenave, P.-A., and Preda, C. (2015). Evidence of IL-17, IP-10, and IL-10 involvement in multiple-organ dysfunction and IL-17 pathway in acute renal failure associated to Plasmodium falciparum malaria. Journal of translational medicine *13*, 1-11.
- Hernandez-Gea, V., and Friedman, S.L. (2011). Pathogenesis of liver fibrosis. Annual review of pathology: mechanisms of disease *6*, 425-456.
- Hiller, N.L., Bhattacharjee, S., van Ooij, C., Liolios, K., Harrison, T., Lopez-Estrano, C., and Haldar, K. (2004). A host-targeting signal in virulence proteins reveals a secretome in malarial infection. Science *306*, 1934-1937.
- Ho, G.J., Drego, R., Hakimian, E., and Masliah, E. (2005). Mechanisms of cell signaling and inflammation in Alzheimer's disease. Current Drug Targets-Inflammation & Allergy *4*, 247-256.
- Hoebe, K., Georgel, P., Rutschmann, S., Du, X., Mudd, S., Crozat, K., Sovath, S., Shamel, L., Hartung, T., and Zähringer, U. (2005). CD36 is a sensor of diacylglycerides. Nature *433*, 523-527.
- Holovati, J.L., Wong, K.A., Webster, J.M., and Acker, J.P. (2008). The effects of cryopreservation on red blood cell microvesiculation, phosphatidylserine externalization, and CD47 expression. Transfusion *48*, 1658-1668.
- Hosui, A., Tatsumi, T., Hikita, H., Saito, Y., Hiramatsu, N., Tsujii, M., Hennighausen, L., and Takehara, T. (2017). Signal transducer and activator of transcription 5 plays a crucial role in hepatic lipid metabolism through regulation of CD36 expression. Hepatology Research *47*, 813-825.
- Hotchkiss, R.S., Swanson, P.E., Freeman, B.D., Tinsley, K.W., Cobb, J.P., Matuschak, G.M., Buchman, T.G., and Karl, I.E. (1999). Apoptotic cell death in patients with sepsis, shock, and multiple organ dysfunction. Critical care medicine *27*, 1230-1251.
- Hsieh, F.-L., Turner, L., Bolla, J.R., Robinson, C.V., Lavstsen, T., and Higgins, M.K. (2016a). The structural basis for CD36 binding by the malaria parasite. Nature communications *7*, 1-11.
- Hsieh, F.-L., Turner, L., Bolla, J.R., Robinson, C.V., Lavstsen, T., and Higgins, M.K. (2016b). The structural basis for CD36 binding by the malaria parasite. Nature communications *7*, 12837.
- Huang, J., Zhao, L., Yang, P., Chen, Z., Ruan, X.Z., Huang, A., Tang, N., and Chen, Y. (2017). Fatty acid translocase promoted hepatitis B virus replication by upregulating the levels of hepatic cytosolic calcium. Experimental cell research *358*, 360-368.

- Huang, W., Febbraio, M., and Silverstein, R.L. (2011). CD9 tetraspanin interacts with CD36 on the surface of macrophages: a possible regulatory influence on uptake of oxidized low density lipoprotein. PLoS One *6*, e29092.
- Hunt, N.H., and Stocker, R. (2007). Heme moves to center stage in cerebral malaria. Nature medicine *13*, 667-669.
- Ibrahimi, A., and Abumrad, N.A. (2002). Role of CD36 in membrane transport of long-chain fatty acids. Current Opinion in Clinical Nutrition & Metabolic Care *5*, 139-145.
- Ichimura, T., Asseldonk, E.J., Humphreys, B.D., Gunaratnam, L., Duffield, J.S., and Bonventre, J.V. (2008). Kidney injury molecule–1 is a phosphatidylserine receptor that confers a phagocytic phenotype on epithelial cells. The Journal of clinical investigation *118*, 1657-1668.
- Idziorek, T., Khalife, J., Billaut-Mulot, O., Hermann, E., Aumercier, M., Mouton, Y., Capron, A., and Bahr, G. (1998). Recombinant human IL-16 inhibits HIV-1 replication and protects against activation-induced cell death (AICD). Clinical and experimental immunology *112*, 84.
- Ikeda, Y., Murakami, A., Fujimura, Y., Tachibana, H., Yamada, K., Masuda, D., Hirano, K.-i., Yamashita, S., and Ohigashi, H. (2007). Aggregated ursolic acid, a natural triterpenoid, induces IL-1β release from murine peritoneal macrophages: role of CD36. The Journal of Immunology *178*, 4854-4864.
- Ikeda, Y., Murakami, A., and Ohigashi, H. (2008). Ursolic acid: An anti-and pro-inflammatory triterpenoid. Molecular nutrition & food research *52*, 26-42.
- Ikenoya, M., Doi, T., Miura, T., Sawanobori, K., Nishio, M., and Hidaka, H. (2007). Investigation of binding proteins for anti-platelet agent K-134 by Drug-Western method. Biochemical and biophysical research communications *353*, 1111-1114.
- Innamorati, G., Sadeghi, H.M., Tran, N.T., and Birnbaumer, M. (1998). A serine cluster prevents recycling of the V2 vasopressin receptor. Proceedings of the National Academy of Sciences *95*, 2222-2226.
- Insull Jr, W. (2009). The pathology of atherosclerosis: plaque development and plaque responses to medical treatment. The American journal of medicine *122*, S3-S14.
- Isenberg, J.S., Yu, C., and Roberts, D.D. (2008). Differential effects of ABT-510 and a CD36-binding peptide derived from the type 1 repeats of thrombospondin-1 on fatty acid uptake, nitric oxide signaling, and caspase activation in vascular cells. Biochemical pharmacology *75*, 875-882.
- Ishii, T., Itoh, K., Ruiz, E., Leake, D.S., Unoki, H., Yamamoto, M., and Mann, G.E. (2004). Role of Nrf2 in the regulation of CD36 and stress protein expression in murine macrophages: activation by oxidatively modified LDL and 4-hydroxynonenal. Circulation research *94*, 609-616.
- Janssens, S., and Beyaert, R. (2003). Role of Toll-like receptors in pathogen recognition. Clinical microbiology reviews *16*, 637-646.
- Jaramillo, M., Godbout, M., and Olivier, M. (2005). Hemozoin induces macrophage chemokine expression through oxidative stress-dependent and-independent mechanisms. The Journal of Immunology *174*, 475-484.
- Jay, A.G., Chen, A.N., Paz, M.A., Hung, J.P., and Hamilton, J.A. (2015). CD36 binds oxidized low density lipoprotein (LDL) in a mechanism dependent upon fatty acid binding. Journal of Biological Chemistry *290*, 4590-4603.
- Jenkins, N., Wu, Y., Chakravorty, S., Kai, O., Marsh, K., and Craig, A. (2007). Plasmodium falciparum Intercellular Adhesion Molecule–1–Based Cytoadherence-Related Signaling in Human Endothelial Cells. The Journal of infectious diseases *196*, 321-327.
- Jia, S., Zhou, L., Shen, T., Zhou, S., Ding, G., and Cao, L. (2018). Down-expression of CD36 in pancreatic adenocarcinoma and its correlation with clinicopathological features and prognosis. Journal of Cancer *9*, 578.
- Jia, Y.-L., Sun, S.-J., Chen, J.-H., Jia, Q., Huo, T.-T., Chu, L.-F., Bai, J.-T., Yu, Y.-J., Yan, X.-X., and Wang, J.-H. (2016). SS31, a Small Molecule Antioxidant Peptide, Attenuates β-Amyloid Elevation, Mitochondrial/Synaptic Deterioration and Cognitive Deficit in SAMP8 Mice. Current Alzheimer Research *13*, 297-306.

- Jiang, X., Zhang, H., Yang, J., Liu, M., Feng, H., Liu, X., Cao, Y., Feng, D., and Xian, M. (2013). Induction of gene expression in bacteria at optimal growth temperatures. Applied microbiology and biotechnology *97*, 5423-5431.
- Jiang, Y., Beller, D., Frendl, G., and Graves, D. (1992). Monocyte chemoattractant protein-1 regulates adhesion molecule expression and cytokine production in human monocytes. The Journal of Immunology *148*, 2423-2428.
- Jimenez-Dalmaroni, M.J., Xiao, N., Corper, A.L., Verdino, P., Ainge, G.D., Larsen, D.S., Painter, G.F., Rudd, P.M., Dwek, R.A., and Hoebe, K. (2009). Soluble CD36 ectodomain binds negatively charged diacylglycerol ligands and acts as a co-receptor for TLR2. PloS one *4*, e7411.
- Jing, Y., Liang, H., Zhang, Y., Cleveland, J., Yan, J., and Zhang, D. (2015). Up-regulation of Toll-like receptor 9 in osteosarcoma. Anticancer research *35*, 5839-5843.
- Jones, P.G., VanBogelen, R.A., and Neidhardt, F.C. (1987). Induction of proteins in response to low temperature in Escherichia coli. Journal of bacteriology *169*, 2092-2095.
- Józefowski, S., Sobota, A., Hamasur, B., Pawłowski, A., and Kwiatkowska, K. (2011). Mycobacterium tuberculosis lipoarabinomannan enhances LPS-induced TNF-α production and inhibits NO secretion by engaging scavenger receptors. Microbial pathogenesis *50*, 350-359.
- Kahkeshani, N., Farzaei, F., Fotouhi, M., Alavi, S.S., Bahramsoltani, R., Naseri, R., Momtaz, S., Abbasabadi, Z., Rahimi, R., and Farzaei, M.H. (2019). Pharmacological effects of gallic acid in health and diseases: A mechanistic review. Iranian journal of basic medical sciences *22*, 225.
- Kar, N.S., Ashraf, M.Z., Valiyaveettil, M., and Podrez, E.A. (2008). Mapping and characterization of the binding site for specific oxidized phospholipids and oxidized low density lipoprotein of scavenger receptor CD36. Journal of Biological Chemistry *283*, 8765-8771.
- Karunakaran, U., Elumalai, S., Moon, J.S., and Won, K.C. (2019). CD36 dependent redoxosomes promotes ceramide-mediated pancreatic β-cell failure via p66Shc activation. Free Radical Biology and Medicine *134*, 505-515.
- Katiyar, C., Gupta, A., Kanjilal, S., and Katiyar, S. (2012). Drug discovery from plant sources: An integrated approach. Ayu *33*, 10.
- Kaul, D., Roth, E.J., Nagel, R., Howard, R., and Handunnetti, S. (1991). Rosetting of Plasmodium falciparum-infected red blood cells with uninfected red blood cells enhances microvascular obstruction under flow conditions.
- Kay, J.G., Koivusalo, M., Ma, X., Wohland, T., and Grinstein, S. (2012). Phosphatidylserine dynamics in cellular membranes. Molecular biology of the cell *23*, 2198-2212.
- Kehrel, B., Wierwille, S., Clemetson, K.J., Anders, O., Steiner, M., Knight, C.G., Farndale, R.W., Okuma, M., and Barnes, M.J. (1998). Glycoprotein VI is a major collagen receptor for platelet activation: it recognizes the platelet-activating quaternary structure of collagen, whereas CD36, glycoprotein IIb/IIIa, and von Willebrand factor do not. Blood *91*, 491-499.
- Kennedy, D.J., Kuchibhotla, S., Westfall, K.M., Silverstein, R.L., Morton, R.E., and Febbraio, M. (2011). A CD36-dependent pathway enhances macrophage and adipose tissue inflammation and impairs insulin signalling. Cardiovascular research *89*, 604-613.
- Khow, O., and Suntrarachun, S. (2012). Strategies for production of active eukaryotic proteins in bacterial expression system. Asian Pacific journal of tropical biomedicine *2*, 159-162.
- Kiefer, C., Sumser, E., Wernet, M.F., and von Lintig, J. (2002). A class B scavenger receptor mediates the cellular uptake of carotenoids in Drosophila. Proceedings of the National Academy of Sciences *99*, 10581-10586.
- Kiessling, L.L., Gestwicki, J.E., and Strong, L.E. (2006). Synthetic multivalent ligands as probes of signal transduction. Angewandte Chemie International Edition *45*, 2348-2368.
- Kim, E., Febbraio, M., Bao, Y., Tolhurst, A.T., Epstein, J.M., and Cho, S. (2012). CD36 in the periphery and brain synergizes in stroke injury in hyperlipidemia. Annals of neurology *71*, 753-764.

- Kim, H., Erdman, L.K., Lu, Z., Serghides, L., Zhong, K., Dhabangi, A., Musoke, C., Gerard, C., Cserti-Gazdewich, C., and Liles, W.C. (2014). Functional roles for C5a and C5aR but not C5L2 in the pathogenesis of human and experimental cerebral malaria. Infection and immunity *82*, 371-379.
- Kim, J.-H., Lee, D.-K., Kim, J., Choi, S., Park, W., Ha, K.-S., Kim, T.-H., Choe, J., Won, M.-H., and Kwon, Y.-G. (2017a). A miRNA-101-3p/Bim axis as a determinant of serum deprivation-induced endothelial cell apoptosis. Cell death & disease *8*, e2808.
- Kim, J.-H., Lee, D.-K., Kim, J., Choi, S., Park, W., Ha, K.-S., Kim, T.-H., Choe, J., Won, M.-H., and Kwon, Y.-G. (2017b). A miRNA-101-3p/Bim axis as a determinant of serum deprivation-induced endothelial cell apoptosis. Cell death & disease *8*, e2808-e2808.
- Kleinert, H., Euchenhofer, C., Fritz, G., Ihrig-Biedert, I., and Förstermann, U. (1998). Involvement of protein kinases in the induction of NO synthase II in human DLD-1 cells. British journal of pharmacology *123*, 1716-1722.
- Klonis, N., Crespo-Ortiz, M.P., Bottova, I., Abu-Bakar, N., Kenny, S., Rosenthal, P.J., and Tilley, L. (2011). Artemisinin activity against Plasmodium falciparum requires hemoglobin uptake and digestion. Proceedings of the National Academy of Sciences *108*, 11405-11410.
- Kono, H., and Rock, K.L. (2008). How dying cells alert the immune system to danger. Nature Reviews Immunology *8*, 279-289.
- Koonen, D.P., Jacobs, R.L., Febbraio, M., Young, M.E., Soltys, C.-L.M., Ong, H., Vance, D.E., and Dyck, J.R. (2007). Increased hepatic CD36 expression contributes to dyslipidemia associated with diet-induced obesity. diabetes *56*, 2863-2871.
- Koopman, G., Reutelingsperger, C., Kuijten, G., Keehnen, R., Pals, S., and Van Oers, M. (1994). Annexin V for flow cytometric detection of phosphatidylserine expression on B cells undergoing apoptosis. Blood *84*, 1415-1420.
- Krieger, M. (1997). The other side of scavenger receptors: pattern recognition for host defense. Current opinion in lipidology *8*, 275-280.
- Kruger, N.J. (2009). The Bradford method for protein quantitation. In The protein protocols handbook (Springer), pp. 17-24.
- Kubo, R., Born, W., Kappler, J., Marrack, P., and Pigeon, M. (1989). Characterization of a monoclonal antibody which detects all murine alpha beta T cell receptors. The Journal of Immunology *142*, 2736-2742.
- Kuda, O., Pietka, T.A., Demianova, Z., Kudova, E., Cvacka, J., Kopecky, J., and Abumrad, N.A. (2013). Sulfo-N-succinimidyl Oleate (SSO) Inhibits Fatty Acid Uptake and Signaling for Intracellular Calcium via Binding CD36 Lysine 164 SSO ALSO INHIBITS OXIDIZED LOW DENSITY LIPOPROTEIN UPTAKE BY MACROPHAGES. Journal of Biological Chemistry *288*, 15547-15555.
- Kuhtreiber, W., Hayashi, T., Dale, E., and Faustman, D. (2003). Central role of defective apoptosis in autoimmunity. Journal of molecular endocrinology *31*, 373-399.
- Kumar, R. (1996). Method for site-directed mutagenesis (Google Patents).
- Kumar, S., Gowda, N.M., Wu, X., Gowda, R.N., and Gowda, D.C. (2012). CD36 modulates proinflammatory cytokine responses to Plasmodium falciparum glycosylphosphatidylinositols and merozoites by dendritic cells. Parasite immunology *34*, 372-382.
- Kurt-Jones, E.A., Popova, L., Kwinn, L., Haynes, L.M., Jones, L.P., Tripp, R.A., Walsh, E.E., Freeman, M.W., Golenbock, D.T., and Anderson, L.J. (2000). Pattern recognition receptors TLR4 and CD14 mediate response to respiratory syncytial virus. Nature immunology *1*, 398-401.
- Kylarová, D., Procházková, J., Mad'arová, J., Bartoš, J., and Lichnovský, V. (2002). Comparison of the TUNEL, lamin B and annexin V methods for the detection of apoptosis by flow cytometry. Acta histochemica *104*, 367-370.
- Ladanyi, A., Mukherjee, A., Kenny, H.A., Johnson, A., Mitra, A.K., Sundaresan, S., Nieman, K.M., Pascual, G., Benitah, S.A., and Montag, A. (2018a). Adipocyte-induced CD36 expression drives ovarian cancer progression and metastasis. Oncogene, 1.

- Ladanyi, A., Mukherjee, A., Kenny, H.A., Johnson, A., Mitra, A.K., Sundaresan, S., Nieman, K.M., Pascual, G., Benitah, S.A., and Montag, A. (2018b). Adipocyte-induced CD36 expression drives ovarian cancer progression and metastasis. Oncogene *37*, 2285-2301.
- Lagassé, H.D., Anidi, I.U., Craig, J.M., Limjunyawong, N., Poupore, A.K., Mitzner, W., and Scott, A.L. (2016). Recruited monocytes modulate malaria-induced lung injury through CD36-mediated clearance of sequestered infected erythrocytes. Journal of leukocyte biology *99*, 659-671.
- Landberg, N., von Palffy, S., Askmyr, M., Lilljebjörn, H., Sandén, C., Rissler, M., Mustjoki, S., Hjorth-Hansen, H., Richter, J., and Ågerstam, H. (2017). CD36 defines primitive chronic myeloid leukemia cells less responsive to imatinib but vulnerable to antibody based therapeutic targeting. Haematologica, haematol. 2017.169946.
- Lao, W., Kang, H., Jin, G., Chen, L., Chu, Y., Sun, J., and Sun, B. (2017). Evaluation of the relationship between MARCO and CD36 single-nucleotide polymorphisms and susceptibility to pulmonary tuberculosis in a Chinese Han population. BMC infectious diseases *17*, 488.
- Lee, S., Eguchi, A., Sakamoto, K., Matsumura, S., Tsuzuki, S., Inoue, K., Masuda, D., Yamashita, S., and Fushiki, T. (2015). A role of CD36 in the perception of an oxidised phospholipid species in mice. Biomedical Research *36*, 303-311.
- Leung, L., Li, W., McGregor, J., Albrecht, G., and Howard, R. (1992). CD36 peptides enhance or inhibit CD36-thrombospondin binding. A two-step process of ligand-receptor interaction. Journal of Biological Chemistry *267*, 18244-18250.
- Li, D., Lei, H., Li, Z., Li, H., Wang, Y., and Lai, Y. (2013). A novel lipopeptide from skin commensal activates TLR2/CD36-p38 MAPK signaling to increase antibacterial defense against bacterial infection. PLoS One *8*, e58288.
- Li, S., Meng, F., Liao, X., Wang, Y., Sun, Z., Guo, F., Li, X., Meng, M., Li, Y., and Sun, C. (2014). Therapeutic role of ursolic acid on ameliorating hepatic steatosis and improving metabolic disorders in high-fat diet-induced non-alcoholic fatty liver disease rats. PLoS One *9*, e86724.
- Li, W., Febbraio, M., Reddy, S.P., Yu, D.-Y., Yamamoto, M., and Silverstein, R.L. (2010). CD36 participates in a signaling pathway that regulates ROS formation in murine VSMCs. The Journal of clinical investigation *120*, 3996-4006.
- Liu, H., and Naismith, J.H. (2008). An efficient one-step site-directed deletion, insertion, single and multiple-site plasmid mutagenesis protocol. BMC biotechnology *8*, 91.
- Liu, J., Yang, P., Zuo, G., He, S., Tan, W., Zhang, X., Su, C., Zhao, L., Wei, L., and Chen, Y. (2018). Long-chain fatty acid activates hepatocytes through CD36 mediated oxidative stress. Lipids in health and disease *17*, 153.
- Liu, Y., Cheng, F., Luo, Y., Zhan, Z., Hu, P., Ren, H., Tang, H., and Peng, M. (2017). PEGylated Curcumin Derivative Attenuates Hepatic Steatosis via CREB/PPAR-γ/CD36 Pathway. BioMed research international *2017*.
- Lorenz, H., Herrmann, M., Winkler, T., Gaipl, U., and Kalden, J. (2000). Role of apoptosis in autoimmunity. Apoptosis *5*, 443-449.
- Lyke, K., Burges, R., Cissoko, Y., Sangare, L., Dao, M., Diarra, I., Kone, A., Harley, R., Plowe, C., and Doumbo, O. (2004). Serum levels of the proinflammatory cytokines interleukin-1 beta (IL-1β), IL-6, IL-8, IL-10, tumor necrosis factor alpha, and IL-12 (p70) in Malian children with severe Plasmodium falciparum malaria and matched uncomplicated malaria or healthy controls. Infection and immunity *72*, 5630-5637.
- Ma, J.-L., Yang, P.-Y., Rui, Y.-C., Lu, L., Kang, H., and Zhang, J. (2007). Hemin modulates cytokine expressions in macrophage-derived foam cells via heme oxygenase-1 induction. Journal of pharmacological sciences *103*, 261-266.
- Mackintosh, C.L., Beeson, J.G., and Marsh, K. (2004). Clinical features and pathogenesis of severe malaria. Trends in parasitology *20*, 597-603.

- MacPherson, G., Warrell, M., White, N., Looareesuwan, S., and Warrell, D. (1985). Human cerebral malaria. A quantitative ultrastructural analysis of parasitized erythrocyte sequestration. The American journal of pathology *119*, 385.
- Magwenzi, S., Woodward, C., Wraith, K.S., Aburima, A., Raslan, Z., Jones, H., McNeil, C., Wheatcroft, S., Yuldasheva, N., and Febbriao, M. (2015). Oxidized LDL activates blood platelets through CD36/NOX2–mediated inhibition of the cGMP/protein kinase G signaling cascade. Blood, The Journal of the American Society of Hematology *125*, 2693-2703.
- Mahajan, A., Herrmann, M., and Muñoz, L.E. (2016). Clearance deficiency and cell death pathways: a model for the pathogenesis of SLE. Frontiers in immunology *7*, 35.
- Mahajan, R., and Gupta, K. (2010). Food and drug administration's critical path initiative and innovations in drug development paradigm: challenges, progress, and controversies. Journal of Pharmacy And Bioallied Sciences *2*, 307.
- Mahoney, J.A., and Rosen, A. (2005). Apoptosis and autoimmunity. Current opinion in immunology *17*, 583-588.
- Malde, A.K., Zuo, L., Breeze, M., Stroet, M., Poger, D., Nair, P.C., Oostenbrink, C., and Mark, A.E. (2011). An automated force field topology builder (ATB) and repository: version 1.0. Journal of chemical theory and computation *7*, 4026-4037.
- Maneerat, Y., Pongponratn, E., Viriyavejakul, P., Punpoowong, B., Looareesuwan, S., and Udomsangpetch, R. (1999). Cytokines associated with pathology in brain tissue of fatal malaria. Southeast Asian journal of tropical medicine and public health *30*, 643-649.
- Mansor, L.S., Sousa Fialho, M.d.L., Yea, G., Coumans, W.A., West, J.A., Kerr, M., Carr, C.A., Luiken, J.J., Glatz, J.F., and Evans, R.D. (2017). Inhibition of sarcolemmal FAT/CD36 by sulfo-N-succinimidyl oleate rapidly corrects metabolism and restores function in the diabetic heart following hypoxia/reoxygenation. Cardiovascular research *113*, 737-748.
- Mao, Y., Tokudome, T., Kishimoto, I., Otani, K., Miyazato, M., and Kangawa, K. (2014). One dose of oral hexarelin protects chronic cardiac function after myocardial infarction. Peptides *56*, 156-162.
- Marder, L.S., Lunardi, J., Renard, G., Rostirolla, D.C., Petersen, G.O., Nunes, J.E., de Souza, A.P.D., de O Dias, A.C., Chies, J.M., and Basso, L.A. (2014). Production of recombinant human annexin V by fed-batch cultivation. BMC biotechnology *14*, 33.
- Marleau, S., Harb, D., Bujold, K., Avallone, R., Iken, K., Wang, Y., Demers, A., Sirois, M.G., Febbraio, M., and Silverstein, R.L. (2005). EP 80317, a ligand of the CD36 scavenger receptor, protects apolipoprotein E-deficient mice from developing atherosclerotic lesions. The FASEB journal *19*, 1869-1871.
- Martin, C.A., Longman, E., Wooding, C., Hoosdally, S.J., Ali, S., Aitman, T.J., Gutmann, D.A., Freemont, P.S., Byrne, B., and Linton, K.J. (2007). Cd36, a class B scavenger receptor, functions as a monomer to bind acetylated and oxidized low-density lipoproteins. Protein Science *16*, 2531-2541.
- Martinez, M.M., Reif, R.D., and Pappas, D. (2010). Detection of apoptosis: A review of conventional and novel techniques. Analytical methods *2*, 996-1004.
- Mathy, N., Scheuer, W., Lanzendörfer, M., Honold, K., Ambrosius, D., Norley, S., and Kurth, R. (2000). Interleukin-16 stimulates the expression and production of pro-inflammatory cytokines by human monocytes. Immunology *100*, 63-69.
- McGilvray, I.D., Serghides, L., Kapus, A., Rotstein, O.D., and Kain, K.C. (2000). Nonopsonic monocyte/macrophage phagocytosis of Plasmodium falciparum–parasitized erythrocytes: a role for CD36 in malarial clearance. Blood, The Journal of the American Society of Hematology *96*, 3231-3240.
- Medzhitov, R. (2008). Origin and physiological roles of inflammation. Nature *454*, 428-435.
- Medzhitov, R., Preston-Hurlburt, P., and Janeway, C.A. (1997). A human homologue of the Drosophila Toll protein signals activation of adaptive immunity. Nature *388*, 394-397.
- Mehra, A., Jerath, G., Ramakrishnan, V., and Trivedi, V. (2015). Characterization of ICAM-1 biophore to design cytoadherence blocking peptides. Journal of Molecular Graphics and Modelling *57*, 27-35.

- Meroni, L., Riva, A., Morelli, P., Galazzi, M., Mologni, D., Adorni, F., and Galli, M. (2005). Increased CD36 expression on circulating monocytes during HIV infection. JAIDS Journal of Acquired Immune Deficiency Syndromes *38*, 310-313.
- Meylan, E., Tschopp, J., and Karin, M. (2006). Intracellular pattern recognition receptors in the host response. Nature *442*, 39-44.
- Miller, Y.I., Choi, S.-H., Wiesner, P., Fang, L., Harkewicz, R., Hartvigsen, K., Boullier, A., Gonen, A., Diehl, C.J., and Que, X. (2011). Oxidation-specific epitopes are danger-associated molecular patterns recognized by pattern recognition receptors of innate immunity. Circulation research *108*, 235-248.
- Milner Jr, D., Factor, R., Whitten, R., Carr, R.A., Kamiza, S., Pinkus, G., Molyneux, M., and Taylor, T. (2013). Pulmonary pathology in pediatric cerebral malaria. Human pathology *44*, 2719-2726.
- Miquilena-Colina, M.E., Lima-Cabello, E., Sánchez-Campos, S., García-Mediavilla, M.V., Fernández-Bermejo, M., Lozano-Rodríguez, T., Vargas-Castrillón, J., Buqué, X., Ochoa, B., and Aspichueta, P. (2011). Hepatic fatty acid translocase CD36 upregulation is associated with insulin resistance, hyperinsulinaemia and increased steatosis in non-alcoholic steatohepatitis and chronic hepatitis C. Gut *60*, 1394-1402.
- Miu, J., Mitchell, A.J., Ball, H.J., and Hunt, N.H. (2006). Chemokines and malaria infection. Current Immunology Reviews *2*, 331-344.
- Mogensen, T.H. (2009). Pathogen recognition and inflammatory signaling in innate immune defenses. Clinical microbiology reviews *22*, 240-273.
- Mohanraj, K., Karthikeyan, B.S., Vivek-Ananth, R., Chand, R.B., Aparna, S., Mangalapandi, P., and Samal, A. (2018). IMPPAT: A curated database of I ndian M edicinal P lants, P hytochemistry A nd T herapeutics. Scientific reports *8*, 1-17.
- Moon, J.S., Karunakaran, U., Suma, E., Chung, S.M., and Won, K.C. (2020). The Role of CD36 in Type 2 Diabetes Mellitus: β-Cell Dysfunction and Beyond. Diabetes & Metabolism Journal *44*, 222.
- Moore, K.J., El Khoury, J., Medeiros, L.A., Terada, K., Geula, C., Luster, A.D., and Freeman, M.W. (2002). A CD36-initiated signaling cascade mediates inflammatory effects of β-amyloid. Journal of Biological Chemistry *277*, 47373-47379.
- Morgan, S., Grootendorst, P., Lexchin, J., Cunningham, C., and Greyson, D. (2011). The cost of drug development: a systematic review. Health policy *100*, 4-17.
- Morris, G.M., Huey, R., Lindstrom, W., Sanner, M.F., Belew, R.K., Goodsell, D.S., and Olson, A.J. (2009). AutoDock4 and AutoDockTools4: Automated docking with selective receptor flexibility. Journal of computational chemistry *30*, 2785-2791.
- Mukherjee, P.K., Harwansh, R.K., Bahadur, S., Banerjee, S., Kar, A., Chanda, J., Biswas, S., Ahmmed, S.M., and Katiyar, C. (2017). Development of Ayurveda–tradition to trend. Journal of ethnopharmacology *197*, 10-24.
- Muller-Hill, B., and Beyreuther, K. (1989). Molecular biology of Alzheimer's disease. Annual review of biochemistry *58*, 287-307.
- Müller, B., Borrell, S., Rose, G., and Gagneux, S. (2013). The heterogeneous evolution of multidrug-resistant Mycobacterium tuberculosis. Trends in Genetics *29*, 160-169.
- Munteanu, A., Taddei, M., Tamburini, I., Bergamini, E., Azzi, A., and Zingg, J.-M. (2006). Antagonistic Effects of Oxidized Low Density Lipoprotein and α-Tocopherol on CD36 Scavenger Receptor Expression in Monocytes INVOLVEMENT OF PROTEIN KINASE B AND PEROXISOME PROLIFERATOR-ACTIVATED RECEPTOR-γ. Journal of biological chemistry *281*, 6489-6497.
- Murphy, S.C., and Breman, J.G. (2001). Gaps in the childhood malaria burden in Africa: cerebral malaria, neurological sequelae, anemia, respiratory distress, hypoglycemia, and complications of pregnancy. The American journal of tropical medicine and hygiene *64*, 57-67.
- Nagao, M., Esguerra, J.L., Asai, A., Ofori, J.K., Edlund, A., Wendt, A., Sugihara, H., Wollheim, C.B., Oikawa, S., and Eliasson, L. (2020). Potential protection against type 2 diabetes in obesity through lower CD36 expression and improved exocytosis in β-cells. Diabetes *69*, 1193-1205.

- Nagata, E., Luo, H.R., Saiardi, A., Bae, B.-I., Suzuki, N., and Snyder, S.H. (2005). Inositol hexakisphosphate kinase-2, a physiologic mediator of cell death. Journal of Biological Chemistry *280*, 1634-1640.
- Nakamura, K., Hasler, T., Morehead, K., Howard, R.J., and Aikawa, M. (1992). Plasmodium falciparum-infected erythrocyte receptor (s) for CD36 and thrombospondin are restricted to knobs on the erythrocyte surface. Journal of Histochemistry & Cytochemistry *40*, 1419-1422.
- Nash, G., O'Brien, E., Gordon-Smith, E., and Dormandy, J. (1989). Abnormalities in the mechanical properties of red blood cells caused by Plasmodium falciparum. Blood *74*, 855-861.
- Nath, A., Li, I., Roberts, L.R., and Chan, C. (2015). Elevated free fatty acid uptake via CD36 promotes epithelial-mesenchymal transition in hepatocellular carcinoma. Scientific reports *5*, 14752.
- Nau, R., and Eiffert, H. (2002). Modulation of release of proinflammatory bacterial compounds by antibacterials: potential impact on course of inflammation and outcome in sepsis and meningitis. Clinical microbiology reviews *15*, 95-110.
- Navab, M., Anantharamaiah, G., Reddy, S.T., and Fogelman, A.M. (2006). Apolipoprotein AI mimetic peptides and their role in atherosclerosis prevention. Nature Reviews Cardiology *3*, 540.
- Ndlovu, H., and Marakalala, M.J. (2016). Granulomas and inflammation: host-directed therapies for tuberculosis. Frontiers in immunology *7*, 434.
- Newbold, C., Warn, P., Black, G., Berendt, A., Craig, A., Snow, B., Msobo, M., Peshu, N., and Marsh, K. (1997). Receptor-specific adhesion and clinical disease in Plasmodium falciparum. The American journal of tropical medicine and hygiene *57*, 389-398.
- Newton, J.G., Horan, J.T., Newman, S., Rossi, M.R., Ketterling, R.P., and Park, S.I. (2017). CD36-positive B-lymphoblasts Predict Poor Outcome in Children With B-lymphoblastic Leukemia. Pediatric and Developmental Pathology *20*, 224-231.
- Nguyen, P., Leray, V., Diez, M., Serisier, S., Bloc'h, J.L., Siliart, B., and Dumon, H. (2008). Liver lipid metabolism. Journal of animal physiology and animal nutrition *92*, 272-283.
- Niculite, C.-M., Enciu, A.-M., and Hinescu, M.E. (2019). CD 36: focus on epigenetic and post-transcriptional regulation. Frontiers in genetics *10*.
- Nie, C.Q., Bernard, N.J., Norman, M.U., Amante, F.H., Lundie, R.J., Crabb, B.S., Heath, W.R., Engwerda, C.R., Hickey, M.J., and Schofield, L. (2009). IP-10-mediated T cell homing promotes cerebral inflammation over splenic immunity to malaria infection. PLoS Pathog *5*, e1000369.
- Niu, B., He, K., Li, P., Gong, J., Zhu, X., Ye, S., Ou, Z., and Ren, G. (2018). SIRT1 upregulation protects against liver injury induced by a HFD through inhibiting CD36 and the NF-κB pathway in mouse kupffer cells. Molecular medicine reports *18*, 1609-1615.
- Nowacki, T.M., Remaley, A.T., Bettenworth, D., Eisenblätter, M., Vowinkel, T., Becker, F., Vogl, T., Roth, J., Tietge, U.J., and Lügering, A. (2016). The 5A apolipoprotein A-I (apoA-I) mimetic peptide ameliorates experimental colitis by regulating monocyte infiltration. British journal of pharmacology *173*, 2780-2792.
- Ockenhouse, C.F., Klotz, F.W., Tandon, N.N., and Jamieson, G. (1991). Sequestrin, a CD36 recognition protein on Plasmodium falciparum malaria-infected erythrocytes identified by anti-idiotype antibodies. Proceedings of the National Academy of Sciences *88*, 3175-3179.
- Ohgami, N., Nagai, R., Ikemoto, M., Arai, H., Miyazaki, A., Hakamata, H., Horiuchi, S., and Nakayama, H. (2002). CD36, serves as a receptor for advanced glycation endproducts (AGE). Journal of Diabetes and its Complications *16*, 56-59.
- Okuda, K., Tong, M., Dempsey, B., Moore, K.J., Gazzinelli, R.T., and Silverman, N. (2016). Leishmania amazonensis engages CD36 to drive parasitophorous vacuole maturation. PLoS pathogens *12*, e1005669.
- Olivetta, E., Tirelli, V., Chiozzini, C., Scazzocchio, B., Romano, I., Arenaccio, C., and Sanchez, M. (2014). HIV-1 Nef impairs key functional activities in human macrophages through CD36 downregulation. PLoS One *9*, e93699.
- Op den Kamp, J.A. (1979). Lipid asymmetry in membranes. Annual review of biochemistry *48*, 47-71.

- Özer, N.K., Negis, Y., Aytan, N., Villacorta, L., Ricciarelli, R., Zingg, J.-M., and Azzi, A. (2006). Vitamin E inhibits CD36 scavenger receptor expression in hypercholesterolemic rabbits. Atherosclerosis *184*, 15-20.
- Palanisamy, G.S., Kirk, N.M., Ackart, D.F., Obregón-Henao, A., Shanley, C.A., Orme, I.M., and Basaraba, R.J. (2012). Uptake and accumulation of oxidized low-density lipoprotein during Mycobacterium tuberculosis infection in guinea pigs. PLoS One *7*, e34148.
- Palm, N.W., and Medzhitov, R. (2009). Pattern recognition receptors and control of adaptive immunity. Immunological reviews *227*, 221-233.
- Park, L., Wang, G., Zhou, P., Zhou, J., Pitstick, R., Previti, M.L., Younkin, L., Younkin, S.G., Van Nostrand, W.E., and Cho, S. (2011). Scavenger receptor CD36 is essential for the cerebrovascular oxidative stress and neurovascular dysfunction induced by amyloid-β. Proceedings of the National Academy of Sciences *108*, 5063-5068.
- Park, Y.M. (2014a). CD36, a scavenger receptor implicated in atherosclerosis. Experimental & molecular medicine *46*, e99-e99.
- Park, Y.M. (2014b). CD36, a scavenger receptor implicated in atherosclerosis. Experimental & molecular medicine *46*, e99.
- Parsons, S.J., and Parsons, J.T. (2004). Src family kinases, key regulators of signal transduction. Oncogene *23*, 7906-7909.
- Pascual, G., Avgustinova, A., Mejetta, S., Martín, M., Castellanos, A., Attolini, C.S.-O., Berenguer, A., Prats, N., Toll, A., and Hueto, J.A. (2017). Targeting metastasis-initiating cells through the fatty acid receptor CD36. Nature *541*, 41.
- Pasternak, N.D., and Dzikowski, R. (2009). PfEMP1: an antigen that plays a key role in the pathogenicity and immune evasion of the malaria parasite Plasmodium falciparum. The international journal of biochemistry & cell biology *41*, 1463-1466.
- Patel, S., Di Bartolo, B.A., Nakhla, S., Heather, A.K., Mitchell, T.W., Jessup, W., Celermajer, D.S., Barter, P.J., and Rye, K.-A. (2010). Anti-inflammatory effects of apolipoprotein AI in the rabbit. Atherosclerosis *212*, 392-397.
- Patel, S.N., Serghides, L., Smith, T.G., Febbraio, M., Silverstein, R.L., Kurtz, T.W., Pravenec, M., and Kain, K.C. (2004). CD36 mediates the phagocytosis of Plasmodium falciparum–infected erythrocytes by rodent macrophages. The Journal of infectious diseases *189*, 204-213.
- Patel, S.S., and Siddiqui, M.S. (2018). Current and Emerging Therapies for Non-alcoholic Fatty Liver Disease. Drugs, 1-10.
- Pearce, S.F.A., Wu, J., and Silverstein, R.L. (1995). Recombinant GST/CD36 Fusion Proteins Define a Thrombospondin Binding Domain EVIDENCE FOR A SINGLE CALCIUM-DEPENDENT BINDING SITE ON CD36. Journal of Biological Chemistry *270*, 2981-2986.
- Peck, R. (1985). A one-plate assay for macrophage bactericidal activity. Journal of immunological methods *82*, 131-140.
- Penberthy, K.K., and Ravichandran, K.S. (2016). Apoptotic cell recognition receptors and scavenger receptors. Immunological reviews *269*, 44-59.
- Pennathur, S., Pasichnyk, K., Bahrami, N.M., Zeng, L., Febbraio, M., Yamaguchi, I., and Okamura, D.M. (2015). The macrophage phagocytic receptor CD36 promotes fibrogenic pathways on removal of apoptotic cells during chronic kidney injury. The American journal of pathology *185*, 2232-2245.
- Pepino, M.Y., Kuda, O., Samovski, D., and Abumrad, N.A. (2014). Structure-function of CD36 and importance of fatty acid signal transduction in fat metabolism. Annual review of nutrition *34*, 281-303.
- Perera, M., Herath, N., Pathirana, S., Phone-Kyaw, M., Alles, H., Mendis, K., Premawansa, S., and Handunnetti, S. (2013). Association of high plasma TNF-alpha levels and TNF-alpha/IL-10 ratios with TNF2 allele in severe P. falciparum malaria patients in Sri Lanka. Pathogens and global health *107*, 21-29.

- Piao, L., Chen, Z., Li, Q., Liu, R., Song, W., Kong, R., and Chang, S. (2019). Molecular dynamics simulations of wild type and mutants of SAPAP in complexed with Shank3. International journal of molecular sciences *20*, 224.
- Pillaiyar, T., Meenakshisundaram, S., Manickam, M., and Sankaranarayanan, M. (2020). A medicinal chemistry perspective of drug repositioning: Recent advances and challenges in drug discovery. European Journal of Medicinal Chemistry, 112275.
- Podrez, E.A., Poliakov, E., Shen, Z., Zhang, R., Deng, Y., Sun, M., Finton, P.J., Shan, L., Febbraio, M., and Hajjar, D.P. (2002a). A novel family of atherogenic oxidized phospholipids promotes macrophage foam cell formation via the scavenger receptor CD36 and is enriched in atherosclerotic lesions. Journal of Biological Chemistry *277*, 38517-38523.
- Podrez, E.A., Poliakov, E., Shen, Z., Zhang, R., Deng, Y., Sun, M., Finton, P.J., Shan, L., Gugiu, B., and Fox, P.L. (2002b). Identification of a novel family of oxidized phospholipids that serve as ligands for the macrophage scavenger receptor CD36. Journal of Biological Chemistry *277*, 38503-38516.
- Poghosyan, G., Melkonyan, V., Mikaelyan, M., and Gasparyan, V. (2003). A simplified method for purification of annexin V from human placenta. Preparative Biochemistry and Biotechnology *33*, 209-215.
- Porto, B.N., Alves, L.S., Fernández, P.L., Dutra, T.P., Figueiredo, R.T., Graça-Souza, A.V., and Bozza, M.T. (2007). Heme induces neutrophil migration and reactive oxygen species generation through signaling pathways characteristic of chemotactic receptors. Journal of Biological Chemistry *282*, 24430-24436.
- PrabhuDas, M., Bowdish, D., Drickamer, K., Febbraio, M., Herz, J., Kobzik, L., Krieger, M., Loike, J., Means, T.K., and Moestrup, S.K. (2014). Standardizing scavenger receptor nomenclature. The Journal of Immunology *192*, 1997-2006.
- PrabhuDas, M.R., Baldwin, C.L., Bollyky, P.L., Bowdish, D.M., Drickamer, K., Febbraio, M., Herz, J., Kobzik, L., Krieger, M., and Loike, J. (2017). A consensus definitive classification of scavenger receptors and their roles in health and disease. The Journal of Immunology *198*, 3775-3789.
- Prada, J., Malinowski, J., Muller, S., Bienzle, U., and Kremsner, P.G. (1996). Effects of Plasmodium vinckei hemozoin on the production of oxygen radicals and nitrogen oxides in murine macrophages. The American journal of tropical medicine and hygiene *54*, 620-624.
- Prasad, G.K., Dhar, V., and Mukhopadhaya, A. (2019). Vibrio cholerae OmpU mediates CD36-dependent reactive oxygen species generation triggering an additional pathway of MAPK activation in macrophages. The Journal of Immunology *202*, 2431-2450.
- Price, R.N., Simpson, J.A., Nosten, F., Luxemburger, C., Hkirjaroen, L., ter Kuile, F., Chongsuphajaisiddhi, T., and White, N.J. (2001). Factors contributing to anemia after uncomplicated falciparum malaria. The American journal of tropical medicine and hygiene *65*, 614-622.
- Primo, L., Ferrandi, C., Roca, C., Marchiò, S., Di Blasio, L., Alessio, M., and Bussolino, F. (2005). Identification of CD36 molecular features required for its in vitro angiostatic activity. The FASEB journal *19*, 1713-1715.
- Pushpakom, S., Iorio, F., Eyers, P.A., Escott, K.J., Hopper, S., Wells, A., Doig, A., Guilliams, T., Latimer, J., and McNamee, C. (2019). Drug repurposing: progress, challenges and recommendations. Nature reviews Drug discovery *18*, 41-58.
- Qiao, J., Arthur, J.F., Gardiner, E.E., Andrews, R.K., Zeng, L., and Xu, K. (2018). Regulation of platelet activation and thrombus formation by reactive oxygen species. Redox biology *14*, 126-130.
- Qiao, L., Koutsos, M., Tsai, L.-L., Kozoni, V., Guzman, J., Shiff, S.J., and Rigas, B. (1996). Staurosporine inhibits the proliferation, alters the cell cycle distribution and induces apoptosis in HT-29 human colon adenocarcinoma cells. Cancer letters *107*, 83-89.
- Rać, M.E., Safranow, K., and Poncyljusz, W. (2007). Molecular basis of human CD36 gene mutations. Molecular Medicine *13*, 288-296.
- Rada, P., González-Rodríguez, Á., García-Monzón, C., and Valverde, Á.M. (2020). Understanding lipotoxicity in NAFLD pathogenesis: is CD36 a key driver? Cell Death & Disease *11*, 1-15.

- Radoshevich, L., and Dussurget, O. (2016). Cytosolic innate immune sensing and signaling upon infection. Frontiers in microbiology *7*, 313.
- Rahaman, S.O., Lennon, D.J., Febbraio, M., Podrez, E.A., Hazen, S.L., and Silverstein, R.L. (2006). A CD36-dependent signaling cascade is necessary for macrophage foam cell formation. Cell metabolism *4*, 211-221.
- Rahaman, S.O., Zhou, G., and Silverstein, R.L. (2011). Vav protein guanine nucleotide exchange factor regulates CD36 protein-mediated macrophage foam cell formation via calcium and dynamin-dependent processes. Journal of Biological Chemistry *286*, 36011-36019.
- Rajagopalan, S., Mckay, I., Ford, I., Bachoo, P., Greaves, M., and Brittenden, J. (2007). Platelet activation increases with the severity of peripheral arterial disease: implications for clinical management. Journal of vascular surgery *46*, 485-490.
- Ramakrishnan, D.P., Hajj-Ali, R.A., Chen, Y., and Silverstein, R.L. (2016). Extracellular vesicles activate a CD36-dependent signaling pathway to inhibit microvascular endothelial cell migration and tube formation. Arteriosclerosis, thrombosis, and vascular biology *36*, 534-544.
- Ramasamy, R., Yan, S.F., and Schmidt, A.M. (2012). The diverse ligand repertoire of the receptor for advanced glycation endproducts and pathways to the complications of diabetes. Vascular pharmacology *57*, 160-167.
- Reichert, J.M. (2003). Trends in development and approval times for new therapeutics in the United States. Nature Reviews Drug Discovery *2*, 695-702.
- Ren, Y. (2012). Peroxisome Proliferator-Activator Receptor: A Link between Macrophage CD36 and Inflammation in Malaria Infection. PPAR research *2012*.
- Ren, Y., Tang, J., Mok, M., Chan, A.W., Wu, A., and Lau, C. (2003). Increased apoptotic neutrophils and macrophages and impaired macrophage phagocytic clearance of apoptotic neutrophils in systemic lupus erythematosus. Arthritis & Rheumatism *48*, 2888-2897.
- Ricciarelli, R., d'Abramo, C., Zingg, J.-M., Giliberto, L., Markesbery, W., Azzi, A., Marinari, U.M., Pronzato, M.A., and Tabaton, M. (2004). CD36 overexpression in human brain correlates with β-amyloid deposition but not with Alzheimer's disease. Free Radical Biology and Medicine *36*, 1018-1024.
- Ricciarelli, R., Zingg, J.-M., and Azzi, A. (2000). Vitamin E reduces the uptake of oxidized LDL by inhibiting CD36 scavenger receptor expression in cultured aortic smooth muscle cells. Circulation *102*, 82-87.
- Rigotti, A., Acton, S.L., and Krieger, M. (1995). The class B scavenger receptors SR-BI and CD36 are receptors for anionic phospholipids. Journal of Biological Chemistry *270*, 16221-16224.
- Robinson, S.R., Dang, T.N., Dringen, R., and Bishop, G.M. (2009). Hemin toxicity: a preventable source of brain damage following hemorrhagic stroke. Redox Report *14*, 228-235.
- Rodrigue-Way, A. (2011). Regulation of lipid metabolism in adipocytes and hepatocytes by hexarelin through scavenger receptor CD36.
- Rodrigue-Way, A., Caron, V., Bilodeau, S., Keil, S., Hassan, M., Lévy, E., Mitchell, G.A., and Tremblay, A. (2014). Scavenger receptor CD36 mediates inhibition of cholesterol synthesis via activation of the PPARγ/PGC-1α pathway and Insig1/2 expression in hepatocytes. The FASEB Journal *28*, 1910-1923.
- Rodríguez, M.a.E., Van der Pol, W.-L., and Van de Winkel, J.G. (2001). Flow cytometry-based phagocytosis assay for sensitive detection of opsonic activity of pneumococcal capsular polysaccharide antibodies in human sera. Journal of immunological methods *252*, 33-44.
- Rogerson, S.J., Van den Broek, N., Chaluluka, E., Qongwane, C., Mhango, C., and Molyneux, M.E. (2000). Malaria and anemia in antenatal women in Blantyre, Malawi: a twelve-month survey. The American journal of tropical medicine and hygiene *62*, 335-340.
- Rosano, G.L., and Ceccarelli, E.A. (2014). Recombinant protein expression in Escherichia coli: advances and challenges. Frontiers in microbiology *5*, 172.
- Royo, J., Rahabi, M., Kamaliddin, C., Ezinmegnon, S., Olagnier, D., Authier, H., Massougbodji, A., Alao, J., Ladipo, Y., and Deloron, P. (2019). Changes in monocyte subsets are associated with clinical outcomes in severe malarial anaemia and cerebral malaria. Scientific reports *9*, 1-13.

- Rudd, P.M., Wormald, M.R., Stanfield, R.L., Huang, M., Mattsson, N., Speir, J.A., DiGennaro, J.A., Fetrow, J.S., Dwek, R.A., and Wilson, I.A. (1999). Roles for glycosylation of cell surface receptors involved in cellular immune recognition. Journal of molecular biology *293*, 351-366.
- Ryeom, S.W., Silverstein, R.L., Scotto, A., and Sparrow, J.R. (1996). Binding of anionic phospholipids to retinal pigment epithelium may be mediated by the scavenger receptor CD36. Journal of Biological Chemistry *271*, 20536-20539.
- Rysavy, N.M., Shimoda, L.M., Dixon, A.M., Speck, M., Stokes, A.J., Turner, H., and Umemoto, E.Y. (2014). Beyond apoptosis: the mechanism and function of phosphatidylserine asymmetry in the membrane of activating mast cells. BioArchitecture *4*, 127-137.
- Sabatino, D., Proulx, C., Pohankova, P., Ong, H., and Lubell, W.D. (2011). Structure–activity relationships of GHRP-6 azapeptide ligands of the CD36 scavenger receptor by solid-phase submonomer azapeptide synthesis. Journal of the American Chemical Society *133*, 12493-12506.
- San-Miguel, T., Pérez-Bermúdez, P., and Gavidia, I. (2013). Production of soluble eukaryotic recombinant proteins in E. coli is favoured in early log-phase cultures induced at low temperature. SpringerPlus *2*, 89.
- Sayed, A., Šerý, O., Plesnik, J., Daoudi, H., Rouabah, A., Rouabah, L., and Khan, N.A. (2015). CD36 AA genotype is associated with decreased lipid taste perception in young obese, but not lean, children. International journal of obesity *39*, 920-924.
- Scaccabarozzi, D., Deroost, K., Corbett, Y., Lays, N., Corsetto, P., Salè, F.O., Van den Steen, P.E., and Taramelli, D. (2018). Differential induction of malaria liver pathology in mice infected with Plasmodium chabaudi AS or Plasmodium berghei NK65. Malaria Journal *17*, 18.
- Scherf, A., Lopez-Rubio, J.J., and Riviere, L. (2008). Antigenic variation in Plasmodium falciparum. Annu Rev Microbiol *62*, 445-470.
- Schlessinger, J. (2000). Cell signaling by receptor tyrosine kinases. Cell *103*, 211-225.
- Schmitt, T.H., Frezzatti, W., and Schreier, S. (1993). Hemin-induced lipid membrane disorder and increased permeability: a molecular model for the mechanism of cell lysis. Archives of biochemistry and biophysics *307*, 96-103.
- Schutte, B., Nuydens, R., Geerts, H., and Ramaekers, F. (1998). Annexin V binding assay as a tool to measure apoptosis in differentiated neuronal cells. Journal of neuroscience methods *86*, 63-69.
- Schwenk, R., Dirkx, E., Coumans, W., Bonen, A., Klip, A., Glatz, J., and Luiken, J. (2010). Requirement for distinct vesicle-associated membrane proteins in insulin-and AMP-activated protein kinase (AMPK)-induced translocation of GLUT4 and CD36 in cultured cardiomyocytes. Diabetologia *53*, 2209-2219.
- Scorza, T., Magez, S., Brys, L., and De Baetselier, P. (1999). Hemozoin is a key factor in the induction of malaria-associated immunosuppression. Parasite immunology *21*, 545-554.
- Serghides, L., and Kain, K.C. (2001). Peroxisome proliferator-activated receptor γ-retinoid X receptor agonists increase CD36-dependent phagocytosis of Plasmodium falciparum-parasitized erythrocytes and decrease malaria-induced TNF-α secretion by monocytes/macrophages. The Journal of Immunology *166*, 6742-6748.
- Serghides, L., Smith, T.G., Patel, S.N., and Kain, K.C. (2003). CD36 and malaria: friends or foes? Trends in parasitology *19*, 461-469.
- Serrano-Pozo, A., Frosch, M.P., Masliah, E., and Hyman, B.T. (2011). Neuropathological alterations in Alzheimer disease. Cold Spring Harbor perspectives in medicine *1*, a006189.
- Serrano, M.R. (1998). Relationship between obesity and the increased risk of major complications in non-insulin-dependent diabetes mellitus. European journal of clinical investigation *28*, 14-17, discussion 17-18.
- Shaklai, N., Shviro, Y., Rabizadeh, E., and Kirschner-Zilber, I. (1985). Accumulation and drainage of hemin in the red cell membrane. Biochimica et Biophysica Acta (BBA)-Biomembranes *821*, 355-366.
- Shalygina, N., Kanshina, O., and Kanshin, N. (1989). Involvement of the appendix in the inflammatory process in severe nonspecific chronic ulcerative colitis in children. Arkhiv patologii *51*, 24-26.

- Sharif, O., Matt, U., Saluzzo, S., Lakovits, K., Haslinger, I., Furtner, T., Doninger, B., and Knapp, S. (2013). The scavenger receptor CD36 downmodulates the early inflammatory response while enhancing bacterial phagocytosis during pneumococcal pneumonia. The Journal of Immunology *190*, 5640-5648.
- SHARMA, G., SHE, Z.-G., VALENTA, D.T., STALLCUP, W.B., and SMITH, J.W. (2010). Targeting of macrophage foam cells in atherosclerotic plaque using oligonucleotide-functionalized nanoparticles. Nano Life *1*, 207.
- Shayakhmetov, D.M., Di Paolo, N.C., and Mossman, K.L. (2010). Recognition of virus infection and innate host responses to viral gene therapy vectors. Molecular Therapy *18*, 1422-1429.
- Shiono, H., Yagi, Y., Chikayama, Y., Miyazaki, S., and Nakamura, I. (2003). Oxidative damage and phosphatidylserine expression of red blood cells in cattle experimentally infected with Theileriasergenti. Parasitology Research *89*, 228-234.
- Shiratsuchi, A., Kaido, M., Takizawa, T., and Nakanishi, Y. (2000). Phosphatidylserine-mediated phagocytosis of influenza A virus-infected cells by mouse peritoneal macrophages. Journal of Virology *74*, 9240-9244.
- Shiratsuchi, A., Osada, S., Kanazawa, S., and Nakanishi, Y. (1998). Essential role of phosphatidylserine externalization in apoptosing cell phagocytosis by macrophages. Biochemical and biophysical research communications *246*, 549-555.
- Shirsath, N.R., and Goswami, A.K. (2020). Natural Phytochemicals and Their Therapeutic Role in Management of Several Diseases: A Review. Current Traditional Medicine *6*, 43-53.
- SILVERSTEIN, R.L. (2009). Inflammation, atherosclerosis, and arterial thrombosis: role of the scavenger receptor CD36. Cleveland Clinic journal of medicine *76*, S27.
- Silverstein, R.L., and Febbraio, M. (2009). CD36, a scavenger receptor involved in immunity, metabolism, angiogenesis, and behavior. Science signaling *2*, re3-re3.
- Silverstein, R.L., Li, W., Park, Y.M., and Rahaman, S.O. (2010). Mechanisms of cell signaling by the scavenger receptor CD36: implications in atherosclerosis and thrombosis. Transactions of the American Clinical and Climatological Association *121*, 206.
- Singh, V.P., Bali, A., Singh, N., and Jaggi, A.S. (2014). Advanced glycation end products and diabetic complications. The Korean Journal of Physiology & Pharmacology *18*, 1-14.
- Sivandzade, F., Bhalerao, A., and Cucullo, L. (2019). Analysis of the Mitochondrial Membrane Potential Using the Cationic JC-1 Dye as a Sensitive Fluorescent Probe. Bio-protocol *9*.
- Smith, T.G., Serghides, L., Patel, S.N., Febbraio, M., Silverstein, R.L., and Kain, K.C. (2003). CD36-mediated nonopsonic phagocytosis of erythrocytes infected with stage I and IIA gametocytes of Plasmodium falciparum. Infection and immunity *71*, 393-400.
- Sordet, O., Khan, Q.A., Plo, I., Pourquier, P., Urasaki, Y., Yoshida, A., Antony, S., Kohlhagen, G., Solary, E., and Saparbaev, M. (2004). Apoptotic topoisomerase I-DNA complexes induced by staurosporine-mediated oxygen radicals. Journal of Biological Chemistry *279*, 50499-50504.
- Soulard, V., Bosson-Vanga, H., Lorthiois, A., Roucher, C., Franetich, J.-F., Zanghi, G., Bordessoulles, M., Tefit, M., Thellier, M., and Morosan, S. (2015). Plasmodium falciparum full life cycle and Plasmodium ovale liver stages in humanized mice. Nature communications *6*, 7690.
- Souza, A.C.P., Bocharov, A.V., Baranova, I.N., Vishnyakova, T.G., Huang, Y.G., Wilkins, K.J., Hu, X., Street, J.M., Alvarez-Prats, A., and Mullick, A.E. (2016). Antagonism of scavenger receptor CD36 by 5A peptide prevents chronic kidney disease progression in mice independent of blood pressure regulation. Kidney international *89*, 809-822.
- Sp, N., Kang, D., Kim, D., Park, J., Lee, H., Kim, H., Darvin, P., Park, Y.-M., and Yang, Y. (2018). Nobiletin Inhibits CD36-Dependent Tumor Angiogenesis, Migration, Invasion, and Sphere Formation Through the Cd36/Stat3/Nf-Kb Signaling Axis. Nutrients *10*, 772.
- Spence, J. (1989). Pathogenesis of atherosclerosis and its complications: effects of antihypertensive drugs. Journal of human hypertension *3*, 63-68.
- St George-Hyslop, P.H., and Petit, A. (2005). Molecular biology and genetics of Alzheimer's disease. Comptes rendus biologies *328*, 119-130.

- Staples, K.J., Pounce, Z., Wallington, J.C., Spalluto, C.M., Morris, D., Nicholas, B., Djukanovic, R., and Wilkinson, T.M. (2015). Viral infection of macrophages reduces CD36 expression: Implications for phagocytosis of non-typeable haemophilus influenzae (Eur Respiratory Soc).
- Steinbusch, L.K., Schwenk, R.W., Ouwens, D.M., Diamant, M., Glatz, J.F., and Luiken, J.J. (2011). Subcellular trafficking of the substrate transporters GLUT4 and CD36 in cardiomyocytes. Cellular and Molecular Life Sciences *68*, 2525-2538.
- Stewart, C.R., Stuart, L.M., Wilkinson, K., Van Gils, J.M., Deng, J., Halle, A., Rayner, K.J., Boyer, L., Zhong, R., and Frazier, W.A. (2010). CD36 ligands promote sterile inflammation through assembly of a Toll-like receptor 4 and 6 heterodimer. Nature immunology *11*, 155.
- Stuart, L.M., Deng, J., Silver, J.M., Takahashi, K., Tseng, A.A., Hennessy, E.J., Ezekowitz, R.A.B., and Moore, K.J. (2005a). Response to Staphylococcus aureus requires CD36-mediated phagocytosis triggered by the COOH-terminal cytoplasmic domain. J Cell Biol *170*, 477-485.
- Stuart, L.M., Deng, J., Silver, J.M., Takahashi, K., Tseng, A.A., Hennessy, E.J., Ezekowitz, R.A.B., and Moore, K.J. (2005b). Response to Staphylococcus aureus requires CD36-mediated phagocytosis triggered by the COOH-terminal cytoplasmic domain. The Journal of cell biology *170*, 477-485.
- Su, H.P., Nakada-Tsukui, K., Tosello-Trampont, A.-C., Li, Y., Bu, G., Henson, P.M., and Ravichandran, K.S. (2002). Interaction of CED-6/GULP, an adapter protein involved in engulfment of apoptotic cells with CED-1 and CD91/low density lipoprotein receptor-related protein (LRP). Journal of Biological Chemistry *277*, 11772-11779.
- Sudhakar, A. (2009). History of cancer, ancient and modern treatment methods. Journal of cancer science & therapy *1*, 1.
- Swerdlow, R.H. (2007). Pathogenesis of Alzheimer's disease. Clinical Interventions in Aging *2*, 347.
- Tabet, F., Remaley, A.T., Segaliny, A.I., Millet, J., Yan, L., Nakhla, S., Barter, P.J., Rye, K.-A., and Lambert, G. (2010). The 5A apolipoprotein AI mimetic peptide displays antiinflammatory and antioxidant properties in vivo and in vitro. Arteriosclerosis, thrombosis, and vascular biology *30*, 246-252.
- Tabeta, K., Georgel, P., Janssen, E., Du, X., Hoebe, K., Crozat, K., Mudd, S., Shamel, L., Sovath, S., and Goode, J. (2004). Toll-like receptors 9 and 3 as essential components of innate immune defense against mouse cytomegalovirus infection. Proceedings of the National Academy of Sciences *101*, 3516-3521.
- Tait, J.F., and Smith, C. (1999). Phosphatidylserine receptors: role of CD36 in binding of anionic phospholipid vesicles to monocytic cells. Journal of Biological Chemistry *274*, 3048-3054.
- Takeuchi, O., and Akira, S. (2010). Pattern recognition receptors and inflammation. Cell *140*, 805-820.
- Tamura, Y., Adachi, H., Osuga, J.-i., Ohashi, K., Yahagi, N., Sekiya, M., Okazaki, H., Tomita, S., Iizuka, Y., and Shimano, H. (2003). FEEL-1 and FEEL-2 are endocytic receptors for advanced glycation end products. Journal of Biological Chemistry *278*, 12613-12617.
- Tanaka, Y., and Schroit, A. (1983). Insertion of fluorescent phosphatidylserine into the plasma membrane of red blood cells. Recognition by autologous macrophages. Journal of Biological Chemistry *258*, 11335-11343.
- Thorne, R.F., Meldrum, C.J., Harris, S.J., Dorahy, D.J., Shafren, D.R., Berndt, M.C., Burns, G.F., and Gibson, P.G. (1997). CD36 forms covalently associated dimers and multimers in platelets and transfected COS-7 cells. Biochemical and biophysical research communications *240*, 812-818.
- Thrisnadia, S. (2019). EFEK EKSTRAKAIR DAUN SIRSAK (Annona muricataL.) TERHADAP KADAR Superoxide Dismutase (SOD) DAN Malondialdehida (MDA) JARINGAN GINJAL KANAN TIKUS WISTARYANG DIINDUKSIDIET TINGGI LEMAK DAN TINGGI FRUKTOSA. Jurnal Bio Komplementer Medicine *6*.
- Thylur, R.P., Wu, X., Gowda, N.M., Punnath, K., Neelgund, S.E., Febbraio, M., and Gowda, D.C. (2017). CD36 receptor regulates malaria-induced immune responses primarily at early blood stage infection contributing to parasitemia control and resistance to mortality. Journal of Biological Chemistry *292*, 9394-9408.

- Torre, D., Giola, M., Speranza, F., Matteelli, A., Basilico, C., and Biondi, G. (2001). Serum levels of interleukin-18 in patients with uncomplicated Plasmodium falciparum malaria. European cytokine network *12*, 361-364.
- Toure, Y., and Oduola, A. (2004). Focus: malaria. Nature Reviews Microbiology *2*, 276-277.
- Tralau-Stewart, C.J., Wyatt, C.A., Kleyn, D.E., and Ayad, A. (2009). Drug discovery: new models for industry–academic partnerships. Drug discovery today *14*, 95-101.
- Tran, D.H.-Y., Tran, D.H.-N., Mattai, S.A., Sallam, T., Ortiz, C., Lee, E.C., Robbins, L., Ho, S., Lee, J.E., and Fisseha, E. (2016). Cathelicidin suppresses lipid accumulation and hepatic steatosis by inhibition of the CD36 receptor. International journal of obesity *40*, 1424.
- Trang, T.T.M., Phu, N.H., Vinh, H., Hien, T.T., Cuong, B.M., Chau, T.T.H., Mai, N.T.H., Waller, D.J., and White, N.J. (1992). Acute renal failure in patients with severe falciparum malaria. Clinical Infectious Diseases *15*, 874-880.
- Trivedi, V., Boire, A., Tchernychev, B., Kaneider, N.C., Leger, A.J., O'Callaghan, K., Covic, L., and Kuliopulos, A. (2009). Platelet matrix metalloprotease-1 mediates thrombogenesis by activating PAR1 at a cryptic ligand site. Cell *137*, 332-343.
- Trivedi, V., Zhang, S.C., Castoreno, A.B., Stockinger, W., Shieh, E.C., Vyas, J.M., Frickel, E.-M., and Nohturfft, A. (2006). Immunoglobulin G signaling activates lysosome/phagosome docking. Proceedings of the National Academy of Sciences *103*, 18226-18231.
- Trosko, J.E., and Ruch, R.J. (1998). Cell-cell communication in carcinogenesis. Front Biosci *3*, d208-236.
- Tserentsoodol, N., Gordiyenko, N.V., Pascual, I., Lee, J.W., Fliesler, S.J., and Rodriguez, I.R. (2006). Intraretinal lipid transport is dependent on high density lipoprotein-like particles and class B scavenger receptors. Mol Vis *12*, e33.
- Turcotte, L., Raney, M., and Todd, M. (2005). ERK1/2 inhibition prevents contraction-induced increase in plasma membrane FAT/CD36 content and FA uptake in rodent muscle. Acta Physiologica *184*, 131-139.
- Turner, L., Lavstsen, T., Berger, S.S., Wang, C.W., Petersen, J.E., Avril, M., Brazier, A.J., Freeth, J., Jespersen, J.S., and Nielsen, M.A. (2013). Severe malaria is associated with parasite binding to endothelial protein C receptor. Nature *498*, 502-505.
- van der Vorst, E.P., Döring, Y., and Weber, C. (2015). Chemokines and their receptors in Atherosclerosis. Journal of molecular medicine *93*, 963-971.
- Varin, A., and Gordon, S. (2009). Alternative activation of macrophages: immune function and cellular biology. Immunobiology *214*, 630-641.
- Verkleij, A., Zwaal, R., Roelofsen, B., Comfurius, P., Kastelijn, D., and Van Deenen, L. (1973). The asymmetric distribution of phospholipids in the human red cell membrane. A combined study using phospholipases and freeze-etch electron microscopy. Biochimica et Biophysica Acta (BBA)-Biomembranes *323*, 178-193.
- Vermes, I., Haanen, C., Steffens-Nakken, H., and Reutellingsperger, C. (1995). A novel assay for apoptosis flow cytometric detection of phosphatidylserine expression on early apoptotic cells using fluorescein labelled annexin V. Journal of immunological methods *184*, 39-51.
- Viriyavejakul, P., Khachonsaksumet, V., and Punsawad, C. (2014). Liver changes in severe Plasmodium falciparum malaria: histopathology, apoptosis and nuclear factor kappa B expression. Malaria journal *13*, 1-10.
- Vlassara, H. (1996). Advanced glycation end-products and atherosclerosis. Annals of medicine *28*, 419-426.
- Vlassara, H., and Uribarri, J. (2014). Advanced glycation end products (AGE) and diabetes: cause, effect, or both? Current diabetes reports *14*, 453.
- Vo, N.T., Moore, L.C., Leis, E., and DeWitte-Orr, S.J. (2019). Class A scavenger receptors mediate extracellular dsRNA sensing, leading to downstream antiviral gene expression in a novel American toad cell line, BufoTad. Developmental & Comparative Immunology *92*, 140-149.

- Walker, F., and Burgess, A.W. (1987). Internalisation and recycling of the granulocyte-macrophage colony-stimulating factor (GM-CSF) receptor on a murine myelomonocytic leukemia. Journal of cellular physiology *130*, 255-261.
- Wang, J.-G., and Aikawa, M. (2015). Toll-Like Receptors and Src-Family Kinases in Atherosclerosis–Focus on Macrophages–. Circulation Journal, CJ-15-1039.
- Wang, J., and Li, Y. (2019). CD36 tango in cancer: signaling pathways and functions. Theranostics *9*, 4893.
- Wang, J., Wang, S., Zhang, X., Hu, L., and Shi, P. (2017). Artemisinin Reduces Lipid Accumulation in Hepatocytes by Inhibition of CD36 Expression. INDIAN JOURNAL OF PHARMACEUTICAL EDUCATION AND RESEARCH *51*, 393-400.
- Wang, L., Bao, Y., Yang, Y., Wu, Y., Chen, X., Si, S., and Hong, B. (2010). Discovery of antagonists for human scavenger receptor CD36 via an ELISA-like high-throughput screening assay. Journal of biomolecular screening *15*, 239-250.
- Wang, Y., Yang, R., Chen, X., Zhang, X., He, S., Feng, J., Wan, S., Wang, S., and Chen, X. (2014). Intermedin inhibits uptake of oxidized LDL via CD36 pathway in RAW264. 7 cells. Die Pharmazie-An International Journal of Pharmaceutical Sciences *69*, 473-476.
- Wilkinson, K., Boyd, J.D., Glicksman, M., Moore, K.J., and El Khoury, J. (2011). A high content drug screen identifies ursolic acid as an inhibitor of amyloid β protein interactions with its receptor CD36. Journal of Biological Chemistry *286*, 34914-34922.
- Wilkinson, K., and El Khoury, J. (2012). Microglial scavenger receptors and their roles in the pathogenesis of Alzheimer's disease. International journal of Alzheimer's disease *2012*.
- Wilson, C.G., Tran, J.L., Erion, D.M., Vera, N.B., Febbraio, M., and Weiss, E.J. (2016). Hepatocyte-specific disruption of CD36 attenuates fatty liver and improves insulin sensitivity in HFD-fed mice. Endocrinology *157*, 570-585.
- Wilson, N.O., Jain, V., Roberts, C.E., Lucchi, N., Joel, P.K., Singh, M.P., Nagpal, A.C., Dash, A.P., Udhayakumar, V., and Singh, N. (2011). CXCL4 and CXCL10 predict risk of fatal cerebral malaria. Disease markers *30*, 39-49.
- Wlodkowic, D., Skommer, J., and Darzynkiewicz, Z. (2009). Flow cytometry-based apoptosis detection. In Apoptosis (Springer), pp. 19-32.
- Wrenger, C., Eschbach, M.-L., Müller, I.B., Warnecke, D., and Walter, R.D. (2005). Analysis of the vitamin B6 biosynthesis pathway in the human malaria parasite Plasmodium falciparum. Journal of Biological Chemistry *280*, 5242-5248.
- Wu, Y., Singh, S., Georgescu, M.-M., and Birge, R.B. (2005). A role for Mer tyrosine kinase in αvβ5 integrin-mediated phagocytosis of apoptotic cells. Journal of cell science *118*, 539-553.
- Wyler, D., Quinn, T.C., and Chen, L.-T. (1981). Relationship of alterations in splenic clearance function and microcirculation to host defense in acute rodent malaria. The Journal of clinical investigation *67*, 1400-1404.
- Xu, C., Zhang, C., Ji, J., Wang, C., Yang, J., Geng, B., Zhao, T., Zhou, H., Mu, X., and Pan, J. (2018a). CD36 deficiency attenuates immune-mediated hepatitis in mice by modulating the proapoptotic effects of CXC chemokine ligand 10. Hepatology *67*, 1943-1955.
- Xu, S., Li, L., Yan, J., Ye, F., Shao, C., Sun, Z., Bao, Z., Dai, Z., Zhu, J., and Jing, L. (2018b). CML/CD36 accelerates atherosclerotic progression via inhibiting foam cell migration. Biomedicine & Pharmacotherapy *97*, 1020-1031.
- Xu, X., Ding, F., Pang, J., Gao, X., Xu, R.-K., Hao, W., Cao, J.-M., and Chen, C. (2012). Chronic administration of hexarelin attenuates cardiac fibrosis in the spontaneously hypertensive rat. American Journal of Physiology-Heart and Circulatory Physiology *303*, H703-H711.
- Xu, Y., Wang, J., Bao, Y., Jiang, W., Zuo, L., Song, D., Hong, B., and Si, S. (2010). Identification of two antagonists of the scavenger receptor CD36 using a high-throughput screening model. Analytical biochemistry *400*, 207-212.

- Yamanaka, M., Ishikawa, T., Griep, A., Axt, D., Kummer, M.P., and Heneka, M.T. (2012). PPARγ/RXRα-induced and CD36-mediated microglial amyloid-β phagocytosis results in cognitive improvement in amyloid precursor protein/presenilin 1 mice. Journal of Neuroscience *32*, 17321-17331.
- Yamashita, S., Hirano, K.-I., Kuwasako, T., Janabi, M., Toyama, Y., Ishigami, M., and Sakai, N. (2007). Physiological and pathological roles of a multi-ligand receptor CD36 in atherogenesis; insights from CD36-deficient patients. Molecular and cellular biochemistry *299*, 19-22.
- Yang, J., Park, K.W., and Cho, S. (2018). Inhibition of the CD36 receptor reduces visceral fat accumulation and improves insulin resistance in obese mice carrying the BDNF-Val66Met variant. Journal of Biological Chemistry *293*, 13338-13348.
- Yang, M., and Silverstein, R.L. (2019). CD36 signaling in vascular redox stress. Free Radical Biology and Medicine *136*, 159-171.
- Yesner, L.M., Huh, H.Y., Pearce, S.F., and Silverstein, R.L. (1996). Regulation of monocyte CD36 and thrombospondin-1 expression by soluble mediators. Arteriosclerosis, thrombosis, and vascular biology *16*, 1019-1025.
- Yipp, B.G., Baruch, D.I., Brady, C., Murray, A.G., Looareesuwan, S., Kubes, P., and Ho, M. (2003a). Recombinant PfEMP1 peptide inhibits and reverses cytoadherence of clinical Plasmodium falciparum isolates in vivo. Blood *101*, 331-337.
- Yipp, B.G., Robbins, S.M., Resek, M.E., Baruch, D.I., Looareesuwan, S., and Ho, M. (2003b). Src-family kinase signaling modulates the adhesion of Plasmodium falciparum on human microvascular endothelium under flow. Blood, The Journal of the American Society of Hematology *101*, 2850-2857.
- Yipp, B.G., Robbins, S.M., Resek, M.E., Baruch, D.I., Looareesuwan, S., and Ho, M. (2003c). Src-family kinase signaling modulates the adhesion ofPlasmodium falciparum on human microvascular endothelium under flow. Blood *101*, 2850-2857.
- Yokoi, H., and Yanagita, M. (2016). Targeting the fatty acid transport protein CD36, a class B scavenger receptor, in the treatment of renal disease. Kidney international *89*, 740-742.
- Yu, M., Jiang, M., Chen, Y., Zhang, S., Zhang, W., Yang, X., Li, X., Li, Y., Duan, S., and Han, J. (2016). Inhibition of Macrophage CD36 Expression and Cellular Oxidized Low Density Lipoprotein (oxLDL) Accumulation by Tamoxifen A PEROXISOME PROLIFERATOR-ACTIVATED RECEPTOR (PPAR) γ-DEPENDENT MECHANISM. Journal of Biological Chemistry *291*, 16977-16989.
- Yu, P., Chao, W., and Ling, Y. (2015a). Mitochondria-targeted antioxidant SS-31 is a potential novel ophthalmic medication for neuroprotection in glaucoma. Medical hypothesis, discovery and innovation in ophthalmology *4*, 120.
- Yu, X., Guo, C., Fisher, P.B., Subjeck, J.R., and Wang, X.-Y. (2015b). Scavenger receptors: emerging roles in cancer biology and immunology. In Advances in cancer research (Elsevier), pp. 309-364.
- Yun, M.R., Im, D.S., Lee, S.J., Park, H.M., Bae, S.S., Lee, W.S., and Kim, C.D. (2009a). 4-Hydroxynonenal enhances CD36 expression on murine macrophages via p38 MAPK-mediated activation of 5-lipoxygenase. Free Radical Biology and Medicine *46*, 692-698.
- Yun, M.R., Park, H.M., Seo, K.W., Kim, C.E., Yoon, J.W., and Kim, C.D. (2009b). Cilostazol attenuates 4-hydroxynonenal-enhanced CD36 expression on murine macrophages via inhibition of NADPH oxidase-derived reactive oxygen species production. The Korean Journal of Physiology & Pharmacology *13*, 99-106.
- Zang, R., Li, D., Tang, I.-C., Wang, J., and Yang, S.-T. (2012). Cell-based assays in high-throughput screening for drug discovery. International Journal of Biotechnology for Wellness Industries *1*, 31-51.
- Zani, I.A., Stephen, S.L., Mughal, N.A., Russell, D., Homer-Vanniasinkam, S., Wheatcroft, S.B., and Ponnambalam, S. (2015). Scavenger receptor structure and function in health and disease. Cells *4*, 178-201.
- Zaynab, M., Fatima, M., Abbas, S., Sharif, Y., Umair, M., Zafar, M.H., and Bahadar, K. (2018). Role of secondary metabolites in plant defense against pathogens. Microbial pathogenesis *124*, 198-202.
- Zhang, G., Gurtu, V., Kain, S.R., and Yan, G. (1997). Early detection of apoptosis using a fluorescent conjugate of annexin V. Biotechniques *23*, 525-531.

- Zhang, X., Qu, L., Chen, L., and Chen, C. (2018). Improvement of cardiomyocyte function by in vivo hexarelin treatment in streptozotocin-induced diabetic rats. Physiological reports *6*.
- Zhao, J., Zhi, Z., Wang, C., Xing, H., Song, G., Yu, X., Zhu, Y., Wang, X., Zhang, X., and Di, Y. (2017). Exogenous lipids promote the growth of breast cancer cells via CD36. Oncology reports *38*, 2105-2115.
- Zhao, L., Varghese, Z., Moorhead, J., Chen, Y., and Ruan, X.Z. (2018a). CD36 and lipid metabolism in the evolution of atherosclerosis. British medical bulletin *126*, 101-112.
- Zhao, L., Varghese, Z., Moorhead, J., Chen, Y., and Ruan, X.Z. (2018b). CD36 and lipid metabolism in the evolution of atherosclerosis. British medical bulletin.
- Zhou, J., Ludlow, L.E., Hasang, W., Rogerson, S.J., and Jaworowski, A. (2012). Opsonization of malaria-infected erythrocytes activates the inflammasome and enhances inflammatory cytokine secretion by human macrophages. Malaria journal *11*, 343.
- Zhu, W., Li, W., and Silverstein, R.L. (2012). Advanced glycation end products induce a prothrombotic phenotype in mice via interaction with platelet CD36. Blood *119*, 6136-6144.
- Zingg, J.M., Azzi, A., and Meydani, M. (2017a). α-Tocopheryl Phosphate Induces VEGF Expression via CD36/PI3Kγ in THP-1 Monocytes. Journal of cellular biochemistry *118*, 1855-1867.
- Zingg, J.M., Hasan, S.T., Nakagawa, K., Canepa, E., Ricciarelli, R., Villacorta, L., Azzi, A., and Meydani, M. (2017b). Modulation of cAMP levels by high-fat diet and curcumin and regulatory effects on CD36/FAT scavenger receptor/fatty acids transporter gene expression. Biofactors *43*, 42-53.
- Zoccal, K.F., Gardinassi, L.G., Sorgi, C.A., Meirelles, A.F., Bordon, K.C., Glezer, I., Cupo, P., Matsuno, A.K., Bollela, V.R., and Arantes, E.C. (2018). CD36 shunts eicosanoid metabolism to repress CD14 licensed interleukin-1β release and inflammation. Frontiers in immunology *9*, 890.

TH-2507_156106009

List of publications:

1. **Sooram Banesh**, Vishal Trivedi: *Therapeutic potentials of Scavenger receptor CD36 mediated innate immune responses against infectious and non-infectious diseases*. Current Drug Discovery Technologies 08/2019; 16. DOI: 10.2174/1570163816666190802153319

2. **Sooram Banesh**, Vibin Ramakrishnan, and Vishal Trivedi: *Mapping of phosphatidylserine recognition region on CD36 ectodomain*. Archives of Biochemistry and Biophysics 10/2018; 660. DOI:10.1016/j.abb.2018.10.005

3. Mostakim SK, **Sooram Banesh**, Vishal Trivedi, Shyam Biswas: *Selective and Sensitive Sensing of Hydrogen Peroxide by a Boronic Acid Functionalized Metal–Organic Framework and Its Application in Live-Cell Imaging*. Inorganic Chemistry 11/2018; 57(23)., DOI:10.1021/acs.inorgchem.8b02240

4. Soutick Nandi, **Sooram Banesh**, Vishal Trivedi, Shyam Biswas: *A dinitro-functionalized metal-organic framework featuring visual and fluorogenic sensing of H2S in living cells, human blood plasma and environmental samples*. The Analyst 02/2018; 143(6). DOI: 10.1039/C7AN01964E

5. Aniruddha Das, **Sooram Banesh**, Vishal Trivedi, Shyam Biswas: *Extraordinary Sensitivity for H2S and Fe(III) Sensing in Aqueous Medium by Al-MIL-53-N3 Metal-Organic Framework: In Vitro and In Vivo Applications of H2S Sensing*. Dalton Transactions 01/2018; 47(8). DOI: 10.1039/C7DT04009A

6. Soutick Nandi, Helge Reinsch, **Sooram Banesh**, Norbert Stock, Vishal Trivedi, Shyam Biswas: *Rapid and highly sensitive detection of extracellular and intracellular H2S by an azide-functionalized Al(III)-based metal-organic framework*. Dalton Transactions 09/2017; 46(38). DOI: 10.1039/C7DT02293J

7. Sooram Banesh, Visal Trivedi*: CD36 ectodomain based method for detection of apoptotic Cells*. Analytical Biochemistry (Submitted).

8. Sooram Banesh, Sourav Layek, Vishal Trivedi: *Role of CD36 in hemin mediated immune Dysfunction and its relevance in malaria pathology* (Manuscript under preparation).

List of conferences:

1. Attended 11th International conference of ISHR on: Changing Trends on Cardiovascular Drug Discovery and Development (2014).
2. Presented poster in 26thNational parasitology Congress on "Addressing New Challenges and Emerging Issues in Parasitology and Disease Biology" held at BHU, Varanasi between21st to 23rdJanuary, 2016.
3. Presented poster in Research conclave 2016 an annual conglomeration of scientific community organized by Indian Institute of Technology-Guwahati held during 17thto 20thMarch 2016.
4. Presented poster entitles "Biochemical and molecular modeling study to understand CD36-PS interaction: potentials in downstream applications" in the scientific session in the "85thAnnual Meeting of Society of Biological chemists (India)" held during 21stto 24thNovember, 2016 at CSIR-CFTRI, Mysuru, India.
5. Presented poster entitles "Probing the interactions of phosphatidylserine with scavenger receptor CD36 using in-silico tools and its implications in understanding the non-opsonic phagocytosis mechanism" in Research Conclave 2017, organized by Indian Institute of Technology-Guwahati held during 16th-19thMarch 2017.
6. Participated in the International conference on Drug Design, held during 7-9 April, 2017 organized by Schrodinger.

TH-2507_156106009